



Donohue, Penelope J. C. (2015) *The effects of acidification and warming on marine calcifying biota*. PhD thesis.

<https://theses.gla.ac.uk/6175/>

Copyright and moral rights for this work are retained by the author

A copy can be downloaded for personal non-commercial research or study, without prior permission or charge

This work cannot be reproduced or quoted extensively from without first obtaining permission in writing from the author

The content must not be changed in any way or sold commercially in any format or medium without the formal permission of the author

When referring to this work, full bibliographic details including the author, title, awarding institution and date of the thesis must be given

Enlighten: Theses

<https://theses.gla.ac.uk/>
research-enlighten@glasgow.ac.uk

The effects of acidification and warming on marine calcifying biota

Penelope J C Donohue

BA (hons) Coventry University
BSc (hons) University of Plymouth

Submitted in fulfilment of the requirement for the
degree of Doctor of Philosophy

School of Geographical and Earth Sciences
College of Science and Engineering
University of Glasgow

March 2015

© Penelope J C Donohue, 2015

Dedication

To my beautiful niece Emily and gorgeous nephew Jacob

You are both at the very beginning of your lives, and right at this moment you have the potential to be anything you want to be and do anything you want to do

Work hard, play hard and live happy

I hope this serves as an inspiration for you both in the future

Abstract

The Earth's climate is changing at an unprecedented rate due to increasing use of fossil fuels and widespread deforestation. This means that the concentration of atmospheric carbon dioxide is increasing, elevating mean global temperatures. In addition, the oceans act as a huge carbon sink and are absorbing more carbon dioxide than they have in the last 650, 000 years causing the oceans to become more acidic. At the beginning of this study the guidelines stated that the control $p\text{CO}_2$ concentration for laboratory studies should be 380 μatm (Meehl et al., 2007), concordant with the then current atmospheric $p\text{CO}_2$. Four years later, the most recent literature reports that current concentrations of atmospheric $p\text{CO}_2$ have now risen to 400 μatm (IPCC, 2013). This demonstrates the unprecedented speed at which our climate is changing and highlights the urgency for research into the potential implications that this change may have on marine systems. In many coastal marine systems calcifying organisms construct biogenic formations that can underpin the ecosystem and form biodiversity hotspots. Calcifying algae and cold water corals are two such organisms. These habitats are economically, politically and socially important. However our knowledge of how these keystone marine organisms may respond in the future is still ambiguous. In general marine calcifiers are likely to be negatively affected, although within some taxa there is considerable variability in their response during climate change studies (e.g. coralline algae and corals). Furthermore, natural variability will overlay the environmental changes associated with anthropogenic global climate change, and as such is likely to significantly influence the response of marine biota to the projected environmental changes. Currently, there are few studies that consider global climate change in the context of natural variability and/ or run long enough to assess acclimatisation potential. Thus, this research aims to provide a better understanding of the impact global climate change may have on key marine calcifiers in the context of natural variability and acclimatisation. This was achieved through a number of laboratory- and field-based studies, utilising well established and adapted techniques.

This research focused primarily on red coralline algae. Projected changes in seawater carbonate chemistry mean that marine organisms that utilise dissolved

inorganic carbon species as a substrate for multiple physiological processes (i.e. photosynthesis and calcification) are likely to be amongst those most greatly impacted by environmental change. Chapter 3 is the longest laboratory study (24 months), to date, investigating the effects of global climate change on a marine calcifier. Results suggest that seasonal variability in environmental conditions will greatly impact the response of coralline algae to elevated temperature and $p\text{CO}_2$. In addition, while calcification may be maintained or increase in response to elevated temperature and/ or $p\text{CO}_2$ (chapter 3 and 5) and despite evidence of acclimatisation potential, overall growth was significantly hampered by elevated temperature in the long term. This supports the hypothesis that dissolution may in fact be the primary threat to marine calcifiers, as opposed to impaired calcification.

Irradiance is key in coralline algal photosynthesis yet the role of light availability on mediating coralline algal responses to multiple stressors remains scant. The present study examined net photosynthesis and photosynthetic characteristics in the free-living coralline algae, *Lithothamnion glaciale* in response to sub-diel changes in irradiance in algae exposed to elevated temperature and $p\text{CO}_2$ (chapter 4). Observations suggest that light availability will mediate the response of coralline algae to global climate change in the future, as optimal light for photosynthesis increases with increasing temperature and $p\text{CO}_2$ (chapter 3, 4 and 5).

Cold-water corals make up some of the most heterogeneous, biologically diverse, three-dimensional ecosystems known in the deep sea. However, due to the difficulty in accessing these habitats, to date there is little information about how these organisms may respond to global climate change. The present study provides evidence of intraspecific variability in the response of cold water corals to global climate change that may be dependent upon their prior environmental experience (chapter 7). *In situ* acclimatisation to variable and low pH may provide cold water corals with the physiological flexibility to acclimatise and adapt to global climate change in the future. Evidence of intraspecific differences in physiology and morphology were also observed *in situ* in the brown partially calcifying alga, *Padina gymnospora* between algae located on the reef crest and more environmentally variable reef flat (chapter 6).

Climate change is one of the most-studied topics in marine science in recent times; however our knowledge of how marine organisms may respond in the future is still ambiguous. The unprecedented rate of change means that there is an urgent need for robust experimentation to assess the response of keystone species to changing climatic conditions. This research focused on improving our understanding of the impact of warming and acidification on key marine calcifiers in the context of (1) natural variability and the role that it may play in influencing a species response to global climate change (2) acclimatisation, including; the potential scope for acclimatisation to elevated temperature and $p\text{CO}_2$; and the role acclimatisation to *in situ* variable and low pH may play in influencing a species response to global climate change.

Contents

Dedication.....	i
Abstract.....	ii
List of Figures.....	xv
List of Tables.....	xvii
Publications arising from research.....	xix
Acknowledgements.....	xxi
Author's declaration.....	xxiv
Definitions and abbreviations.....	xxv
Chapter 1: Introduction	27
1.1 Anthropogenic global climate change	29
1.1.1 Anthropogenic global warming.....	29
1.1.1.1 Past warming	29
1.1.1.2 Projected warming.....	30
1.1.2 Anthropogenic ocean acidification	32
1.1.2.1 Chemistry	32
1.1.2.2 Past changes in ocean chemistry.....	35
1.1.2.3 Projected ocean acidification	36
1.2 Natural variability, coastal systems and climate change.....	37
1.2.1 Fine-scale natural variability	38
1.2.2 Large-scale natural variability	39
1.3 Importance of marine calcifiers	40
1.3.1 Ecosystem services and biodiversity.....	40
1.3.2 Carbon sequestration and storage.....	41
1.3.3 Palaeoclimatic archives.....	41
1.3.4 Maerl beds	42
1.3.4.1 Lithothamnion glaciale	44
1.3.4.2 Photosynthesis and red coralline algae	45
1.3.4.2.1 Light and dark reactions of photosynthesis.....	45
1.3.4.2.2 Chloroplasts.....	46
1.3.4.2.3 Pigments and light harvesting.....	47
1.3.4.2.4 Rubisco	49
1.3.4.3 Biomineralisation and red coralline algae	49
1.3.4.3.1 Carbonic anhydrase.....	50
1.3.5 Cold water coral reefs	51
1.3.5.1 Lophelia pertusa	52
1.4 Threats to biogenic reefs	53

1.4.1	Global climate change and coastal marine calcifiers	53
1.4.1.1	Calcification and climate change	53
1.4.1.2	Photosynthesis and climate change	54
1.5	Acclimatisation and adaptation to climate change	56
1.6	Aims of this research	57

Chapter 2: Methods and Techniques..... 58

2.1	The ocean acidification mesocosm set-up	58
2.1.1	Seawater acidification	60
2.1.2	Long-term set-up.....	60
2.1.3	Short-term set-up.....	61
2.2	Pulse Amplitude Modulation fluorometry	61
2.2.1	Chlorophyll fluorescence	62
2.2.2	Modulated fluorometry	62
2.2.3	Fluorescence notation	62
2.2.4	Dark adaptation	64
2.2.4.1	Quasi-dark adaptation	65
2.2.5	Rapid light Curves.....	65
2.2.6	The diving-PAM	66
2.2.7	Photosynthetic parameters	68
2.3	Proteins.....	68
2.3.1	Protein extraction	69
2.3.1.1	Extraction: Method 1	69
2.3.1.1.1	Concentrating: Option 1.....	70
2.3.1.1.2	Concentrating: Option 2.....	71
2.3.1.2	Extraction: Method 2	72
2.3.1.3	Extraction: Method 3	73
2.3.1.3.1	Automated sample grinding	74
2.3.2	Polyacrylamide gel electrophoresis of proteins.....	74
2.3.2.1	Staining	75
2.3.2.2	Gel image analysis.....	75
2.3.2.3	Protein identification	76
2.4	Total protein quantitation	77
2.4.1	Different methods for protein quantitation	77
2.4.2	The Bradford Method for protein quantitation.....	78
2.4.2.1	Effects of Sodium dodecyl sulfate (SDS) on the Bradford Assay	79
2.4.3	Bradford method for quantitation of proteins in calcifying algae and coral.....	79

2.4.3.1	Calculation of total protein.....	80
2.5	Seawater sample collection	80
2.6	Total alkalinity titrations	81
2.6.1	Different methods for determining total alkalinity	81
2.6.2	Automated, closed-cell, potentiometric titration procedure.....	82
2.6.2.1	General principle.....	82
2.6.2.2	Analysis of seawater reference material	83
2.6.3	Modified spectrophotometric procedure to determine total alkalinity in seawater.....	83
2.6.3.1	General principle.....	83
2.6.3.2	Calculation of results	84
2.6.3.3	Analysis of seawater reference material	85
2.7	Dissolved inorganic carbon determination	85
2.7.1	Different methods for determining dissolved inorganic carbon	86
2.7.2	Coulometric determination of dissolved organic carbon	87
2.7.2.1	General principle.....	87
2.7.2.2	Analysis of seawater reference material	88
2.8	Other environmental factors	88
2.8.1	Partial pressure of CO ₂ (<i>p</i> CO ₂)	88
2.8.2	Temperature, salinity and dissolved oxygen	88
2.8.3	Photosynthetically active radiation	88
2.9	CO ₂ SYs	88

Chapter 3: Natural Variability and the long term effects of climate change on the free living red coralline alga, *Lithothamnion glaciale* 89

3.1	Long term vs. short term studies.....	89
3.2	Seasonal variability and coralline algae physiology.....	90
3.3	Growth, breakage and repair	92
3.4	Aims of the chapter	93
3.5	Methods	94
3.5.1	Study site.....	94
3.5.2	Sampling points.....	94
3.5.3	Environmental parameters	95
3.5.3.1	Carbonate chemistry	95
3.5.3.2	Other environmental parameters	96
3.5.4	Photosynthesis	96
3.5.4.1	Chlorophyll-a fluorescence (PAM fluorometry)	96
3.5.5	Proteins	96

3.5.5.1	Protein extraction and solubilisation.....	96
3.5.6	Calcification	96
3.5.7	Statistical analysis	97
3.6	Results	97
3.6.1	Environmental parameters	97
3.6.2	Photosynthesis	100
3.6.2.1	Chlorophyll-a fluorescence (PAM fluorometry)	100
3.6.2.1.1	Calculated photosynthetic characteristics (Fq' / Fm'_{max} , E_k , α , $rETR_{max}$).....	100
3.6.2.1.2	Measured photochemical parameters (photochemical quenching) (Fq' / Fm' , qP and $rETR$)	100
3.6.2.1.3	Photoprotective parameters (non-photochemical quenching) (qN).....	100
3.6.3	Proteins	103
3.6.3.1	Field: Total Protein.....	103
3.6.3.2	Field: Rubisco and phycoerythrin	104
3.6.4	Calcification	105
3.7	Discussion	106
3.7.1	Natural environmental variability	106
3.7.2	Natural biological variability	106
3.7.3	Conclusions	107
3.8	Methods	107
3.8.1	Experimental set-up	107
3.8.2	Sampling regime.....	109
3.8.3	Environmental parameters	109
3.8.3.1	Carbonate chemistry	109
3.8.3.2	Other environmental parameters	109
3.8.4	Photosynthesis	110
3.8.4.1	Chlorophyll-a fluorescence (PAM fluorometry)	110
3.8.5	Proteins	110
3.8.5.1	Protein extraction and solubilisation.....	110
3.8.6	Calcification	110
3.8.7	Growth and repair	110
3.8.7.1	Growth	110
3.8.7.2	Branch breakage and repair	111
3.8.8	Statistical analysis	112
3.9	Results	113
3.9.1	Environmental parameters	113

3.9.2	Photosynthesis	115
3.9.2.1	Chlorophyll-a fluorescence (PAM fluorometry)	115
3.9.2.1.1	Calculated photosynthetic characteristics (Fq'/Fm'_{max} , E_k , α , $rETR_{max}$); between months within treatments	115
3.9.2.1.2	Calculated photosynthetic characteristics (Fq'/Fm'_{max} , E_k , α , $rETR_{max}$); between treatments within each month	115
3.9.2.1.3	Measured photochemical parameters (photochemical quenching) (Fq'/Fm' , qP and $rETR$)	120
3.9.2.1.4	Photoprotective parameters (non-photochemical quenching) (qN).....	120
3.9.3	Proteins	123
3.9.3.1	Total protein	123
3.9.3.2	Rubisco.....	123
3.9.3.3	Phycoerythrin.....	123
3.9.4	Calcification	127
3.9.4.1	Between months within treatments	127
3.9.4.2	Between treatments within months	127
3.9.5	Growth and repair	130
3.9.5.1	Growth	130
3.9.5.2	Re-growth and repair.....	130
3.9.6	Scope for acclimatisation	131
3.9.6.1	Photosynthetic characteristics	131
3.9.6.2	Proteins.....	132
3.9.6.2.1	Total Protein.....	132
3.9.6.2.2	Rubisco	132
3.9.6.2.3	Phycoerythrin.....	132
3.9.6.3	Calcification.....	133
3.10	Discussion	135
3.10.1	Environmental parameters	135
3.10.2	Photosynthesis	135
3.10.2.1	Light	136
3.10.2.2	Temperature and photosynthesis	137
3.10.2.3	Photoprotective mechanisms.....	138
3.10.2.4	PAR.....	139
3.10.3	Protein	139
3.10.3.1	Total protein	139
3.10.3.2	Phycoerythrin.....	140
3.10.3.3	Rubisco.....	141

3.10.4	Calcification, growth and repair	142
3.10.4.1	Calcification.....	142
3.10.4.2	Growth	143
3.10.4.3	Branch repair	144
3.10.5	Scope for acclimatisation	145
3.10.5.1	Calcification.....	146
3.10.5.2	Proteins.....	146
3.10.5.3	Photosynthesis.....	147
3.10.6	Wider implications	148
3.10.7	Conclusions.....	149

Chapter 4: Short-term experiment: Light availability mediates coralline algae responses to multiple stressors 150

4.1	Light-saturated photosynthesis and temperature	150
4.2	Light-limited photosynthesis and temperature	151
4.3	$p\text{CO}_2$, temperature, photosynthesis and irradiance	151
4.4	Aims of this chapter	152
4.5	Methods	153
4.5.1	Experimental set-up.....	153
4.5.2	Environmental parameters	153
4.5.2.1	Carbonate chemistry	153
4.5.2.2	Photosynthetically active radiation	154
4.5.3	Photosynthesis	154
4.5.3.1	Net photosynthesis (light response curves)	154
4.5.3.2	Chlorophyll- α fluorescence (PAM fluorometry)	154
4.5.4	Statistical analysis	155
4.6	Results	155
4.6.1	Environmental parameters	155
4.6.1.1	Carbonate chemistry	155
4.6.2	Photosynthetic characteristics.....	156
4.6.2.1	Net photosynthesis and photosynthetic light response curves	156
4.6.2.2	PAM fluorometry	157
4.7	Discussion	158
4.7.1	Photosynthesis	159
4.7.2	Wider implications	159
4.7.3	Conclusions	161

Chapter 5: Short-term experiment: seasonal differences in the effects of climate change on light limited photosynthesis and calcification in red coralline algae	162
5.1 Global climate change and coralline algae	163
5.2 <i>In situ</i> irradiance	163
5.3 Aims of the chapter	164
5.4 Methods	165
5.4.1 Experimental set-up	165
5.4.2 Environmental parameters	165
5.4.2.1 Carbonate chemistry	165
5.4.2.2 Photosynthetically active radiation	166
5.4.3 Photosynthesis	166
5.4.3.1 Chlorophyll- α fluorescence (PAM fluorometry)	166
5.4.3.2 Chlorophyll-a concentration	166
5.4.3.3 Total protein, Rubisco and phycoerythrin concentration	167
5.4.4 Calcification	167
5.4.5 Statistical analysis	167
5.5 Results	168
5.5.1 Environmental parameters	168
5.5.2 Photosynthetic characteristics	168
5.5.2.1 Chlorophyll- α fluorescence (PAM fluorometry)	168
5.5.2.2 Chlorophyll concentration	171
5.5.2.3 Total protein	172
5.5.2.4 Rubisco concentration	173
5.5.2.5 Phycoerythrin.....	173
5.5.3 Calcification	173
5.6 Discussion	174
5.6.1 Photosynthetic characteristics	174
5.6.2 Proteins	176
5.6.3 Pigments.....	176
5.6.4 Calcification	177
5.6.5 Wider implications	178
5.6.6 Conclusions	178

Chapter 6: Coral reef calcifying algae persist in naturally variable environment, but at what cost?.....	180
6.1 Natural variability, climate change and coral reefs	180
6.2 Global climate change and marine calcifying algae	182
6.3 Tropical calcifying algae	183
6.4 Aims of this chapter	184
6.5 Methods	185
6.5.1 Sample site	185
6.5.2 Sampling points	185
6.5.3 Environmental parameters	186
6.5.3.1 <i>Physico-chemical seawater parameters and depth</i>	186
6.5.3.2 <i>Net community photosynthesis (dissolved oxygen)</i>	187
6.5.3.3 <i>Photosynthetically active radiation</i>	187
6.5.4 Determination of thallus size and abundance	187
6.5.5 Photosynthetic characteristics	187
6.5.5.1 <i>Rubisco concentration</i>	187
6.5.5.2 <i>Photosynthetic characteristics</i>	188
6.5.5.3 <i>Night time samples</i>	188
6.5.6 Statistical analysis	189
6.6 Results	189
6.6.1 Environmental parameters	189
6.6.1.1 <i>Physico-chemical seawater parameters and depth</i>	189
6.6.1.2 <i>Net community photosynthesis and physico-chemical seawater parameters</i>	189
6.6.1.3 <i>Photosynthetically active radiation during the day</i>	192
6.6.2 Thallus size and abundance	192
6.6.3 Photosynthetic characteristics	193
6.6.3.1 <i>Intracellular Rubisco concentration</i>	193
6.6.3.2 <i>Photochemical parameters</i>	194
6.6.3.2.1 <i>Calculated photosynthetic characteristics ($F_q'/F_m'_{max}$, E_k, α, $rETR_{max}$): temporal changes</i>	194
6.6.3.2.2 <i>Calculated photosynthetic characteristics ($F_q'/F_m'_{max}$, E_k, α, $rETR_{max}$): spatial differences</i>	194
6.6.3.2.3 <i>Measured photochemical (photochemical quenching) parameters (F_q'/F_m' (and F_v/F_m), qP and $rETR$): spatial and temporal differences</i>	195
6.6.3.3 <i>Photo-protection (qN)</i>	197
6.7 Discussion	198

6.7.1	Biological and Physical Control of physico-chemical seawater parameters.....	198
6.7.2	Phenotypic variation in algal photo-physiology.....	199
6.7.3	Growth and abundance	201
6.7.4	Conclusions	202

Chapter 7: Intraspecific differences in the response of cold water corals to climate change 203

7.1	Global climate change and cold-water corals	203
7.1.1	Calcification and carbonate chemistry.....	204
7.1.2	Calcification response to climate change	204
7.2	Cold-water coral reefs and contemporary environmental conditions	205
7.2.1	Mingulay Reef Complex	205
7.2.2	Logachev coral carbonate mounds	206
7.2.3	Environmental conditions	206
7.3	Aims of this chapter	209
7.4	Methods	209
7.4.1	Sample collection	209
7.4.2	Experimental set-up	210
7.4.3	Experimental carbonate chemistry.....	211
7.4.4	Protein extraction and solubilisation	211
7.4.4.1	Protein identification and visualisation	212
7.4.5	Total protein.....	212
7.4.6	Statistical analysis	212
7.5	Results	212
7.5.1	Environmental parameters	212
7.5.2	Total protein.....	213
7.5.2.1	Mingulay Reef Complex.....	213
7.5.2.2	Logachev coral carbonate mounds.....	214
7.5.3	Protein identification and visualisation	215
7.5.3.1	Protein profile	215
7.5.3.1.1	Mingulay Reef Complex	216
7.5.3.1.2	Logachev coral carbonate mounds	216
7.6	Discussion	218
7.6.1	Protein concentration	218
7.6.2	Proteins and physiological functions	219

7.6.3	<i>In situ</i> environment and response of coral to elevated temperature and $p\text{CO}_2$	222
7.6.4	Conclusions	223

Chapter 8: Discussion and conclusions..... 225

8.1	Natural variability and global climate change.....	227
8.1.1	Seasonal environmental variability.....	227
8.1.2	Calcification and dissolution	229
8.1.3	The importance of light.....	229
8.1.4	Prior environmental experience	230
8.2	Acclimatisation	230
8.3	Future work and research direction	231
8.3.1	Natural variability.....	231
8.3.1.1	Implications for empirical studies.....	231
8.3.1.2	In situ studies	232
8.3.1.3	The importance of light	233
8.3.1.4	Multiple stressors	233
8.3.2	Acclimatisation.....	234
8.3.2.1	Rate of change	234
8.3.2.2	Mechanisms that promote acclimatisation.....	234
8.3.3	Growth, breakage and repair.....	235
8.4	Wider implications of this research	235
8.4.1	Impact of global climate change on marine systems.....	235
8.4.2	Biodiversity and ecosystem services.....	235
8.4.3	Policy and management strategies.....	236
8.5	Conclusions	236

Figures

	Page
Figure 1.1 Thesis structure and the links between each chapter.....	28
Figure 1.2 Depth-averaged 0 to 700 m temperature trend for 1971–2010 (taken from (IPCC, 2013))	31
Figure 1.3 Multi-model simulated time series from 1950 to 2100 (CMIP5; IPCC, 2013) for change in global annual mean surface temperature relative to 1986-2005.....	32
Figure 1.4 The projected change in carbon chemistry relative to preindustrial carbon dioxide.....	34
Figure 1.5 Bjerrum Plot showing the change in the carbonate system of seawater due to ocean acidification	34
Figure 1.6 Long term trends of surface pCO ₂ , pH and carbonate ion concentration at three subtropical ocean time series in the North Atlantic and North Pacific oceans (Taken from IPCC, 2013).	35
Figure 1.7 Maps of multi-model mean results of changes in surface ocean pH in 2081–2100.	37
Figure 1.8 Climate change, large scale natural variability and the coastal system.	40
Figure 1.9 Maerl bed and Lithothamnion glaciale thallus.....	43
Figure 1.10 The global distribution of free-living red coralline algae.	43
Figure 1.11 Distribution of red coralline algae species within Europe.....	45
Figure 1.12 The reactions of photosynthesis.....	46
Figure 1.13 The basic structure of a chloroplast.	47
Figure 1.14 Possible mode of organisation of the thylakoid membrane in algae.	47
Figure 1.15 Schematic representation of phycobilisomes structure	49
Figure 1.16 Current global distribution of reef framework-forming cold-water corals....	51
Figure 1.17 Lophelia pertusa, scleractinian reef framework forming cold water coral....	52
Figure 2.1 University of Glasgow Ocean Acidification Mesocosm Facility; Long-term experimental set-up (i.e. years).	59
Figure 2.2 University of Glasgow Ocean Acidification Mesocosm Facility; Short-term experimental set-up (i.e. weeks and months).....	60
Figure 2.3 Example of a typical Pulse Amplitude Modulated (PAM) fluorescence trace. ..	63
Figure 2.4 An example of chlorophyll-a fluorescence signals during a rapid light curve (RLC) in the seagrass Zostera marina.	66
Figure 2.5 The Walz Diving-PAM underwater fluorometer	67
Figure 2.6 Use of the Diving-PAM in the field.....	67
Figure 2.7 Examples of a SDS polyacrylamide gels showing extracted Lithothamnion glaciale proteins using method 1 (described in section 2.3.1.1).....	70
Figure 2.8 Example of a SDS polyacrylamide gel showing extracted Lithothamnion glaciale proteins using method 1, concentrating option 1 (described in section 2.3.1.1 and 0).	71
Figure 2.9 Example of a SDS polyacrylamide gel showing extracted Lithothamnion glaciale proteins using method 1, concentrating option 2 (described in sections 2.3.1.1 and 2.3.1.1.2).	72
Figure 2.10 Example of a SDS polyacrylamide gel showing extracted Lithothamnion glaciale proteins using method 2 (described in section 2.3.1.2).....	73
Figure 2.11 Example of a SDS polyacrylamide gel showing extracted Lithothamnion glaciale proteins using method 3 (described in section 2.3.1.3).....	74

Figure 2.12	Polyacrylamide gel electrophoresis gel apparatus.	75
Figure 2.13	Example of gel image analysis.	76
Figure 2.14	An example of a Bradford assay standard curve using bovine γ -globulin.	80
Figure 3.1	Lithothamnion glaciale: an example of a broken branch and a cross section showing growth bands.....	93
Figure 3.2	Field site in Loch Sween, Scotland.....	95
Figure 3.3	Changes in temperature, salinity, irradiance and photoperiod in the field.....	99
Figure 3.4	Calculated photosynthetic characteristics of <i>L. glaciale</i> collected in situ in Loch Sween (field site) over a 12 month period.	101
Figure 3.5	Photochemical response of <i>Lithothamnion glaciale</i> in Loch Sween during summer, spring, autumn and winter.	102
Figure 3.6	<i>Lithothamnion glaciale</i> photoprotective response (1-qN) during summer, autumn, winter and spring in Loch Sween (field site).....	103
Figure 3.7	Protein concentrations (mg g^{-1} (fresh weight) FW^{-1}) in <i>L. glaciale</i> collected from Loch Sween (field site) over a 12 month period.	104
Figure 3.8	Rate of calcification (CaCO_3 (whole mass) $\mu\text{mol g}^{-1} \text{h}^{-1}$) in <i>Lithothamnion glaciale</i> in Loch Sween over a 12 month sampling period.	105
Figure 3.9	An example of a transverse section of an <i>L. glaciale</i> branch showing the Calcein stain laid down at the beginning of the 24 month experimental period and new growth thereafter.	111
Figure 3.10	An example of a broken <i>Lithothamnion glaciale</i> branch before and after re-growth of the photosynthetic cells.	112
Figure 3.11	Changes in temperature, salinity, irradiance and photoperiod in the field and laboratory	114
Figure 3.12	Effect of elevated temperature and pCO_2 on the calculated photosynthetic characteristics of <i>Lithothamnion glaciale</i> over a two year experimental period. .	117
Figure 3.13	The effect of elevated temperature and pCO_2 on the photochemical response of <i>Lithothamnion glaciale</i> during summer, autumn, winter and spring.	121
Figure 3.14	The effect of elevated temperature and pCO_2 on the photoprotective response of <i>Lithothamnion glaciale</i> during summer, autumn, winter and spring.	122
Figure 3.15	The effect of elevated temperature and pCO_2 on Rubisco, Phycoerythrin and total protein concentration ($\text{mg g}^{-1} \text{FW}^{-1}$) in <i>L. glaciale</i> over the two year laboratory experimental period.....	125
Figure 3.16	Effect of elevated temperature and pCO_2 on calcification rate (CaCO_3 (whole mass) $\mu\text{mol g}^{-1} \text{h}^{-1}$) in <i>Lithothamnion glaciale</i> over a two year experimental period.	128
Figure 3.17	Mean \pm SE of growth (mm) of <i>Lithothamnion glaciale</i> after 24 months exposure to elevated pCO_2 and temperature.	130
Figure 3.18	Mean \pm SE of re-growth of photosynthetic material on <i>Lithothamnion glaciale</i> after branch breakage after four months exposure to elevated pCO_2 and temperature.....	131
Figure 4.1	Net photosynthetic light response curves (oxygen $\mu\text{mol g}^{-1} \text{h}^{-1}$, MEAN \pm SD) of <i>Lithothamnion glaciale</i> exposed to elevated temperature and pCO_2 ($n = 6$). .	157
Figure 4.2	MEAN \pm SE effect of elevated temperature and pCO_2 on the photosynthetic yield parameters of <i>L. glaciale</i>	158
Figure 4.3	The effect of elevated temperature and pCO_2 on the relative and calculated maximum photochemical efficiency of PSII in <i>Lithothamnion glaciale</i>	158

Figure 5.1 Irradiance recorded in Loch Sween, Scotland (collection site of <i>L. glaciale</i>)....	164
Figure 5.2 Short-term effect of elevated temperature and pCO ₂ on the photosynthetic yield parameters of <i>L. glaciale</i> calculated from RLCs during the summer and winter.....	170
Figure 5.3 rETR ($\mu\text{mol electrons m}^{-2} \text{s}^{-1}$) curve responses of <i>Lithothamnion glaciale</i> in response to elevated temperature and pCO ₂ during the summer and the winter.....	171
Figure 5.4 The effect of elevated temperature and pCO ₂ on the relative and calculated maximum photochemical efficiency of PSII in <i>Lithothamnion glaciale</i> during the summer and the winter.....	171
Figure 5.5 Short-term effect of elevated temperature and pCO ₂ on total protein, Rubisco and phycoerythrin concentration in <i>L. glaciale</i> during the summer and winter.	172
Figure 5.6 Short-term effect of elevated temperature and pCO ₂ on calcification rate ($\mu\text{mol g}^{-1}$ (live tissue) h ⁻¹) in <i>Lithothamnion glaciale</i> during summer and winter.....	174
Figure 6.1 <i>Padina gymnospora</i>	184
Figure 6.2 Suleman reef transect location and examples of the benthic community within each sample zone.	186
Figure 6.3 Yield measurements of <i>Padina gymnospora</i> in the light (0-10 mins) and in dark (15-100 mins).	188
Figure 6.4 Physico-chemical parameters on the Suleman reef.	191
Figure 6.5 Net community photosynthesis on the Suleman reef flat and crest.	192
Figure 6.6 Rubisco concentration in <i>Padina gymnospora</i>	193
Figure 6.7 Diel pattern of calculated photosynthetic yield parameters of <i>P. gymnospora</i> located on the reef crest and flat.	196
Figure 6.8 Photochemical response of <i>Padina gymnospora</i> located on the Suleman reef.	197
Figure 6.9 <i>Padina gymnospora</i> photo-protective response (1-qN) in different locations.	198
Figure 7.1 Map and example habitats of the sites from which <i>Lophelia pertusa</i> was sampled in the northeast Atlantic during the 'changing oceans' expedition 2012	208
Figure 7.2 The Holland-1 remote operated vehicle (ROV).....	210
Figure 7.3 Experimental tanks and potted coral fragments on board the RRS James Cook (cruise 073) during the Changing Oceans Expedition 2012.	210
Figure 7.4 The effect of elevated temperature and pCO ₂ on total protein ($\mu\text{g g}^{-1}$ (fresh weight) FW ⁻¹) in <i>Lophelia pertusa</i> collected from the Mingulay Reef Complex over 21 days.....	214
Figure 7.5 The effect of elevated temperature and pCO ₂ on total protein ($\mu\text{g g}^{-1}$ (fresh weight) FW ⁻¹) in <i>Lophelia pertusa</i> collected from the Logachev coral carbonate mounds over 14 days.	215
Figure 7.6 The effect of elevated pCO ₂ and temperature on the protein profile of one colony from the Mingulay Reef Complex and one colony from the Logachev coral carbonate mounds over 21 days and 14 days, respectively.	217
Figure 7.7 Schematic of the calcification process in azooxanthellate cold-water corals	221

Tables

	Page
Table 1.1 Average changes in carbonate chemistry of surface seawater 1766 to 2100 (Gattuso and Lavigne, 2009).....	36
Table 2.1 Fluorescence parameters and definitions.....	64
Table 3.1 Parameters of the carbonate system in Loch Sween in each season.	98
Table 3.2 pCO ₂ (ppm) values for the high-CO ₂ treatments during the four week ramping period.	108
Table 3.3 Parameters of the carbonate system in the laboratory experiment in each treatment and season.....	113
Table 3.4 Summary of two-way nested ANOVAs followed by Tukey HSD post hoc tests testing the effects of elevated temperature and pCO ₂ on <i>Lithothamnion glaciale</i> photochemical characteristics (E_k and $rETR_{max}$) during each month of a two year experiment.	118
Table 3.5 Summary of two-way nested ANOVAs (or Scheirer-ray-hare) followed by Tukey HSD post hoc tests testing the effects of elevated temperature and pCO ₂ on <i>Lithothamnion glaciale</i> photochemical characteristics ($F_q'/F_{m'_{max}}$ and α) during each month of a two year experiment.....	119
Table 3.6 Summary of two-way nested ANOVAs (or Scheirer-ray-hare test) followed by Tukey HSD post hoc tests testing the effects of elevated temperature and pCO ₂ on <i>Lithothamnion glaciale</i> protein concentration during each month of a two year experiment.	126
Table 3.7 Summary Scheirer-ray-hare tests followed by Tukey HSD post hoc tests testing the effects of elevated temperature and pCO ₂ on rate of calcification (CaCO ₃ (whole mass) $\mu\text{mol g}^{-1} \text{h}^{-1}$) in <i>Lithothamnion glaciale</i> during each month of a two year experiment.	129
Table 3.8 Summary of one way ANOVAs testing the difference between physiological parameters in May and February 2013 with May and February 2014 for evidence of acclimatisation to elevated temperature and pCO ₂	134
Table 4.1 Mean \pm SD seawater physico-chemical parameters measured or calculated for the aquaria during the experimental period.	156
Table 5.1 Mean \pm SD of seawater physico-chemical parameters measured or calculated for the aquaria during the experimental periods in summer and winter.....	168
Table 7.1 Environmental conditions in the surface water and reef-top water above the Mingulay Reef Complex and the Logachev coral carbonate mounds in May 2012.	207
Table 7.2 Environmental conditions in experimental tanks on board the RRS James Cook (cruise 073) during the Changing Oceans Expedition 2012.	213

Publications arising from this research

Under review:

Chapter 4: Donohue, PJC., Hennige, S., Cusack, M., Roberts, JM., Kamenos, N., Light availability mediates coralline algal responses to multiple stressors. *PLoS One*.

Chapter 6: Donohue, PJC., Burdett, HL., Cusack, M., Roberts, JM., Kamenos, N., Coral reef calcifying algae persist in naturally variable environments, but at what cost? *Ecology and Evolution*.

In preparation:

Chapter 3: Donohue, PJC., Cusack, M., Roberts, JM., Kamenos, N., Natural variability and long term effects of climate change on free living red coralline algae, *Lithothamnion glaciale*

Chapter 7: Donohue, PJC., Cusack, M., Roberts, JM., Kamenos, N., Intraspecific differences in the response of cold water corals to climate change.

Associated publications not directly contributing to this research:

Pauly M., Kamenos N.A., Donohue P.J.C., LeDrew E. (2015) Coralline algal Mg-O bond strength as a marine $p\text{CO}_2$ proxy. *Geology*. doi:10.1130/G36386.1

Brodie J., Williamson C., Smale D., Kamenos N., Mieszkowska N., Santo R., Cunliffe M., Steinke M., Yesson, C., Anderson K., Asnaghi V., Brownlee C., Burdett H., Burrows M., Collins S., Donohue P., Harvey B., Foggo A., Noisette F., Nunes J., Ragazzola F., Raven J A., Schmidt D., Suggett D., Teichberg M., Hall-Spencer J. (2014) The future of the NE Atlantic benthic flora in a high CO_2 world. *Ecology and Evolution*. DOI: 10.1002/ece3.1105

Burdett H., Carruthers M., Donohue P., et al. (2014) Effects of high temperature and CO₂ on intracellular DMSP in the cold-water coral *Lophelia pertusa*. *Marine Biology*. 161(7): 1499-1506

Burdett H., Donohue P. et al. (2013) Spatiotemporal Variability of Dimethylsulphoniopropionate on a Fringing Coral Reef: The Role of Reefal Carbonate Chemistry and Environmental Variability. *PLoS ONE* 8(5): e64651.
doi:10.1371/journal.pone.0064651

Acknowledgements

Firstly, I would like to thank the Marine Alliance for Science and Technology Scotland (MASTS) for awarding me with a Prize Studentship and the funding for this research. Funding was also gratefully received from the University of Glasgow, College of Science and Engineering Mobility Fund for work carried out in Egypt and NERC for a place on the Changing Oceans Expedition 2012. Thank you also to my supervisors Nicholas Kamenos, Maggie Cusack (Glasgow University) and Murray Roberts (Heriot-Watt University). Murray, the Changing Oceans Expedition 2012 was by far the most enjoyable part of my PhD!

An enormous thank you goes to Axel Miller, without whom I would not have got through this process. Your support, encouragement and advice were greatly received and for that I will be eternally grateful. I sincerely hope we remain friends. I would also like to thank the rest of the MASTS Graduate School. In no particular order, special mention goes to Ewan Edwards, Sally Rouse, Flora Kent, Thomas Linley, Jennifer Loxton, Anna Kintner, Amy Scott-Murray, James Thorburn, Enrique Pirotta, Adam Chivers, and Niki Lacey. Also, Ashleigh Currie, Nikki Khanna, Rachel (Hale) Jacques, I am so happy we met. The timing of meeting you all was perfect and I was greatly encouraged by our oddly similar personalities, love of gin, and general outlook on life. I love you all and this process would have been significantly worse without you. I hope our lives continue to collide long into the future.

Scott, Ewan, Gregor and Rory Steel, you were all an unexpected but welcome addition to my life. There is not much that would have kept me in the frozen north, but you have convinced me! Thank you Scott for the emotional (and financial!) support, you are amazing and awesome. Thank you Rory, Ewan and Gregor for all the fun, no matter how stressful work was you never failed to put a smile on my face. I love you all and thank you for reminding me what is important in life and giving me a place to finally call my home.

My longest and dearest friend Juliette Cornish, you are an incredible person. Although we are opposite in so many ways we have formed an unyielding friendship, you

are my constant. I am not sure if you are aware of how much your, sometimes daily, morning phone calls were appreciated but they definitely played a significant role in me finishing this PhD. I love you dearly and I look forward to the next 24 years and beyond!

Piero Calosi, you have been my inspiration and a fantastic friend. I most certainly would not have got to this point without your support and encouragement;

"...association renders men stronger and brings out each person's best gifts, and gives a joy which is rarely to be had by keeping to oneself, the joy of realising how many honest decent capable people there are for whom it is worth giving one's best (while living just for oneself very often the opposite happens, of seeing people's other side, the side which makes one keep one's hand always on the hilt of one's sword)."

Italo Calvino, *The Baron in the Trees*

To my mum, I know you love me dearly and will be proud. To my dad, I am glad we met and I have appreciated your words of encouragement. To my wee sister Jennifer and husband Mathew, my beautiful niece Emily, and gorgeous nephew Jacob, even though you are on the other side of the world you have always been there when I have needed you. You are all my family and I love you all dearly.

To everyone in the Gregory building with whom I have shared many laughs, tears and coffee, in no particular order; Jill McColl, Eric Portenga, Heather Rawcliffe, Crystal Smiley, Mark Wildman, Callum Graham, Caroline Miller, Emma Lyons Horton Fairley. Also, Heidi Burdett thank you for all your help and advice during the last four years.

Last but not least, thanks Bob Plant, you have been by my side for the last 8 years.

“It is a curious situation that the sea, from which life first arose should now be threatened by the activities of one form of that life. But the sea, though changed in a sinister way, will continue to exist; the threat is rather to life itself.”

Rachel Carson, *The Sea Around Us*

Author's declaration

I declare that this thesis, except where acknowledged to others, represents my own work carried out in the School of Geographical and Earth Sciences, University of Glasgow. The research presented here has not been submitted for any other degree at the University of Glasgow, nor at any other institution. Any published or unpublished work by other authors has been given full acknowledgement in the text.



Penelope J C Donohue

Definitions and abbreviations

AL	Actinic light
ANOVA	Analysis of variance
A_T	Total alkalinity
ATP	Adenosine triphosphate
BSA	Bovine serum albumin
Ca^{2+}	Calcium ion
$CaCO_3$	Calcium carbonate
Chl- α	Chlorophyll- α
CMIP5	Coupled Model Intercomparison Project 5 (part of IPCC Report 2013)
CO_2	Carbon dioxide
CO_3^{2-}	Carbonate ion
DIC	Dissolved inorganic carbon
DO	Dissolved oxygen
E	<i>See PAR</i>
E_k	Light saturation coefficient ($\mu\text{mol photons m}^{-2} \text{s}^{-1}$)
ENSO	El Nino Southern Oscillation
F'	Fluorescence under actinic light
F_m	Maximum fluorescence (dark acclimated)
F_m'	Maximum fluorescence (light acclimated)
F_o	Minimum fluorescence (dark acclimated)
F_o'	Minimum fluorescence (light acclimated)
F_q	Fluorescence quenched ($F_m - F'$)
F_q' / F_m'	Effective photochemical efficiency yield of PSII under actinic light
$F_q' / F_m'_{\text{max}}$	Calculated photochemical efficiency of PSII
F_q' / F_v'	Photochemical quenching (qP) under actinic light
F_v	Variable fluorescence (dark acclimated)
F_v'	Variable fluorescence under actinic light
F_v / F_m	Maximum photochemical efficiency or yield of PSII (dark acclimated)
F_v' / F_m'	Maximum photochemical quenching (qN) under actinic light
H^+	Hydrogen ions
H_2CO_3	Carbonic acid
H_2O	Water
HCl	Hydrochloric acid
HCO_3^-	bicarbonate ion
$HgCl_2$	Mercuric chloride
IPCC	Intergovernmental panel on Climate Change
LN_2	Liquid nitrogen
NADP	Nicotinamide adenine dinucleotide phosphate
NOAA	National Oceanographic and Atmospheric Administration (USA)
NPQ	Non-photochemical quenching
O_2	Oxygen
OA	Ocean acidification
PAM	Pulse Amplitude Modulation
PAR	Photosynthetically Active Radiation ($\mu\text{mol photons m}^{-2} \text{s}^{-1}$)
pCO_2	Partial pressure of CO_2
PS I	Photosystem I
PS II	Photosystem II

qN	Non photochemical quenching
qP	Photochemical quenching
RCP	Representative Concentration Pathways are four greenhouse gas concentration (not emissions) trajectories adopted by the IPCC for its fifth Assessment Report (IPCC 2013).
$rETR$	Relative electron transport rate ($\mu\text{mol electrons m}^{-2} \text{s}^{-1}$)
$rETR_{\text{max}}$	Maximum relative electron transport rate ($\mu\text{mol electrons m}^{-2} \text{s}^{-1}$)
RLC	Rapid light curve
SCUBA	Self-contained underwater breathing apparatus
SDS	sodium dodecyl sulfate
SST	Sea surface temperature
S	Salinity
t	<i>in situ</i> water temperature
$t, 380$	Experimental control treatment (t with $p\text{CO}_2$ 380 μatm)
$t, 750$	Elevated $p\text{CO}_2$ experimental treatment; t with $p\text{CO}_2$ 750 μatm
$t, 1000$	Elevated $p\text{CO}_2$ experimental treatment; t with $p\text{CO}_2$ 1000 μatm
$t+2, 380$	Elevated temperature experimental treatment; $t + 2^\circ\text{C}$ with $p\text{CO}_2$ 380 μatm
$t+2, 750$	Combined elevated temperature and $p\text{CO}_2$ experimental treatment; $t + 2^\circ\text{C}$ with $p\text{CO}_2$ 750 μatm
$t+2, 1000$	Combined elevated temperature and $p\text{CO}_2$ experimental treatment; $t + 2^\circ\text{C}$ with $p\text{CO}_2$ 1000 μatm
UV	Ultra violet
α	Initial slope of the light dependent part of a Rapid Light Curve
Ω	Saturation state
$\Omega_{\text{aragonite}}$	Aragonite saturation
Ω_{calcite}	Calcite saturation
1D SDS	1D sodium dodecyl sulfate polyacrylamide gel

1

Introduction

The Earth's climate is changing at an unprecedented rate due to increasing use of fossil fuels and widespread deforestation. Anthropogenically accelerated climate change includes multiple simultaneously changing factors, of which ocean acidification and global warming are the two greatest concerns for coastal marine systems. In many coastal marine systems, calcifying organisms construct biogenic formations that can underpin the ecosystem and form biodiversity hotspots. Calcifying algae and cold water corals are two such organisms. These habitats are economically, politically and socially important. However our knowledge of how these keystone marine organisms may respond in the future is still ambiguous. In general marine calcifiers are likely to be negatively affected, although within some taxa there is considerable variability in their response during climate change studies (e.g. coralline algae and corals). Natural variability will overlay the environmental changes associated with anthropogenic global climate change, and as such is likely to significantly influence the response of marine biota to the projected environmental changes. Currently, there are few studies that consider global climate change in the context of natural variability and run long enough to assess acclimatisation potential. Thus, through several separate, yet related, studies (Figure 1.1) this research, with a focus on marine calcifying algae, aimed to provide a better understanding of the impact that global climate change may have on key marine calcifiers in the context of natural variability and acclimatisation.

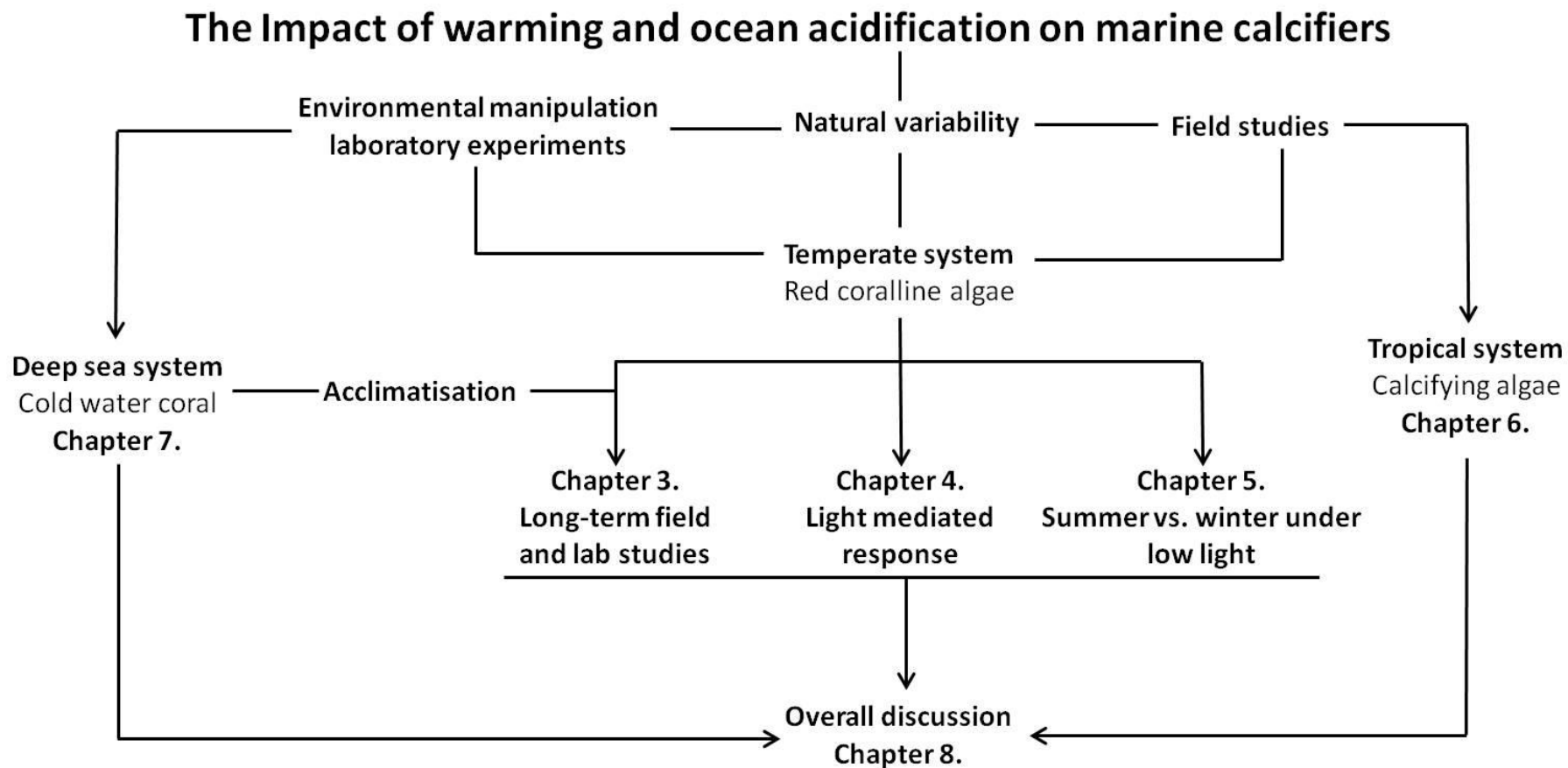


Figure 1.1 Thesis structure and the links between each chapter.

1.1 Anthropogenic global climate change

Anthropogenically accelerated global climate change is a widely accepted phenomenon. It refers to the changes that have occurred to the Earth's climate over the last 200 years in response to the increased anthropogenic use of fossil fuels. It is acknowledged that the Earth's climate is a dynamic entity, however the precipitous increase in the anthropogenic use of fossil fuels and land-use change over the last 200 years has led to a marked increase in concentrations of carbon dioxide (CO₂), methane and nitrous oxide (collectively; greenhouse gases) (Meehl et al., 2007). CO₂ is the most important anthropogenic greenhouse gas and atmospheric concentrations have ranged between 172-300 μatm over the last 800 000 years (Luthi et al., 2008). In the last 200 years atmospheric CO₂ has increased from a pre-industrial value of 280 μatm to the present day value of 400 μatm (IPCC, 2013). Furthermore, atmospheric CO₂ levels are projected to increase to 428 μatm by 2025, 1000 μatm around the year 2100 and exceed 1900 μatm by the year 2300 (Caldeira and Wickett, 2003, Raven et al., 2005, IPCC, 2013). The rate of increase in atmospheric CO₂ was $\sim 1.0\% \text{ yr}^{-1}$ in the 1990s and reached $\sim 3.4\% \text{ yr}^{-1}$ between 2000-2008 (Le Quere et al., 2009) and this extreme rate of change to the Earth's atmosphere has major implications for the world's oceans. Climate change includes multiple simultaneously changing environmental factors (Solomon et al., 2007), of which ocean acidification (decreasing ocean pH as a result of increasing seawater $p\text{CO}_2$) (Caldeira and Wickett, 2003) and rising global sea surface temperatures are two of the most widespread concerns for coastal marine systems.

1.1.1 Anthropogenic global warming

1.1.1.1 Past warming

Warming of the Earth's climate is unequivocal, since the start of the industrial revolution (circa 1750) the overall effect of human activities has been a warming influence in the earth's climate (Meehl et al., 2007). Global warming is evident from observations of increases in global average air and ocean temperatures (Forster et al., 2007, IPCC, 2013), widespread melting of snow and ice, and rising global average sea level (Solomon et al., 2007). Increasing greenhouse gases affect the Earth's temperature by altering incoming solar radiation and out-going infrared (thermal) radiation that are part of the Earth's energy balance (IPCC, 2013). In terms of warming, the anthropogenic influence on the global climate during the last 200 years far exceeds that due to known

changes in natural processes, such as solar changes and volcanic eruptions (Forster et al., 2007). The oceans have the ability to store vast amounts of heat echoing the size (surface area and depth) and heat capacity compared to the Earth's surface and atmosphere (IPCC, 2013, Levitus et al., 2012, Murphy et al., 2009). In the last 50 years the oceans have stored almost 93% of all the Earth's excess heat energy (Levitus et al., 2012). The increase in the amount of heat in the oceans amounts to 17×10^{22} Joules over the last 30 years (IPCC, 2013). Throughout most of the Earth's oceans at depth 0-700 m ocean temperature trends increase from 1971 to 2010 (Levitus et al., 2009) (Figure 1.2). In the Northern Hemisphere warming is more prominent, although the greater volume of oceans in the Southern Hemisphere increases the contribution of their warming to global heat content (IPCC, 2013) (Figure 1.2). The global average ocean warming between 1971 and 2010 is 0.11°C per decade in the upper 75 m, decreasing to 0.015°C per decade at 700 m (IPCC, 2013) (Figure 1.2). However, warming of the oceans is likely to have started earlier than 1971; Gouretski et al. (2012) present evidence of ocean warming between 1900-1945.

1.1.1.2 Projected warming

Global temperature is predicted to rise further (Figure 1.3). A temperature increase in average surface ocean temperature of between $0.6\text{-}2^\circ\text{C}$, and $0.3\text{-}0.6^\circ\text{C}$ at a depth of ~ 1000 m, is predicted by the end of the century (Solomon et al., 2007, IPCC, 2013). Heat will penetrate from the surface of the ocean to the deep ocean, eventually affecting ocean circulation (IPCC, 2013). Warming is projected to be greater in the surface ocean in the tropical and Northern Hemisphere subtropical regions, while warming at a greater depth will be greater in the Southern Ocean (IPCC, 2013).

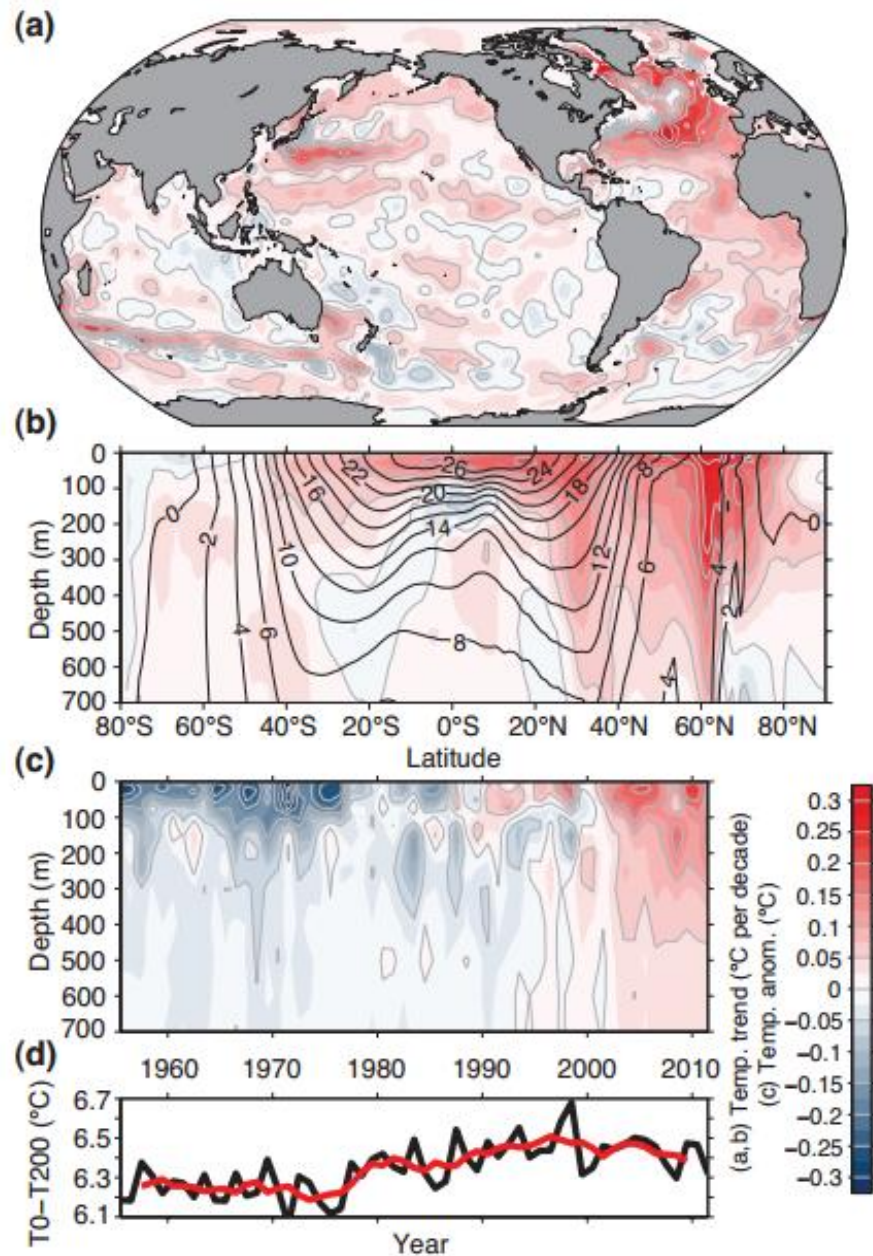


Figure 1.2 Depth-averaged 0 to 700 m temperature trend for 1971–2010 (taken from (IPCC, 2013))

Depth-averaged 0 to 700 m temperature trend for 1971–2010 (longitude vs. latitude, colours and grey contours in degrees Celsius per decade). (b) Zonally averaged temperature trends (latitude vs. depth, colours and grey contours in degrees Celsius per decade) for 1971–2010 with zonally averaged mean temperature over-plotted (black contours in degrees Celsius). (c) Globally averaged temperature anomaly (time vs. depth, colours and grey contours in degrees Celsius) relative to the 1971–2010 mean. (d) Globally averaged temperature difference between the ocean surface and 200 m depth (black: annual values, red: 5-year running mean). All panels are constructed from an update of the annual analysis of (Levitus et al., 2009) and the figure was taken from (IPCC, 2013).

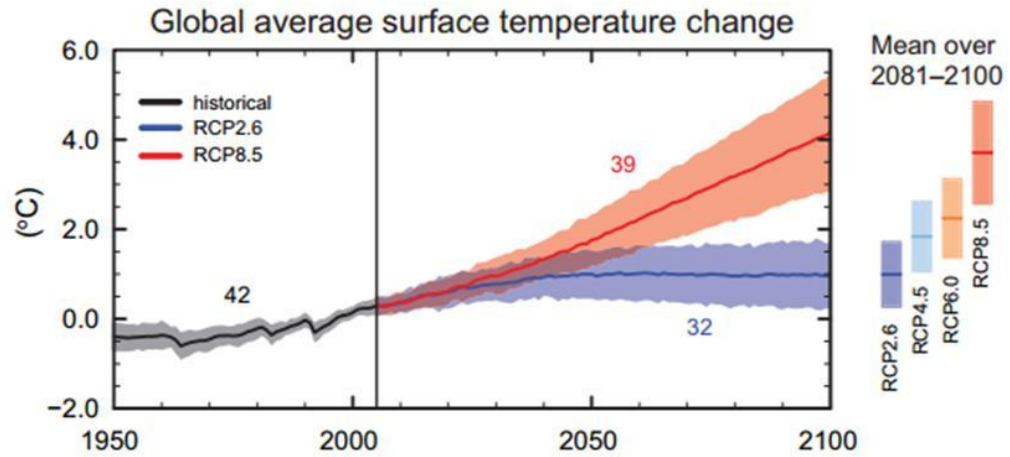


Figure 1.3 Multi-model simulated time series from 1950 to 2100 (CMIP5; IPCC, 2013) for change in global annual mean surface temperature relative to 1986–2005. Time series of projections and a measure of uncertainty (shading) are shown for scenarios RCP2.6 (representative concentration pathways; (IPCC, 2013)) (blue) and RCP8.5 (red). Black (grey shading) is the modeled historical evolution using historical reconstructed forcings. The mean and associated uncertainties averaged over 2081–2100 are given for all RCP scenarios as colored vertical bars. The numbers of CMIP5 models used to calculate the multi-model mean is indicated. Source: (IPCC, 2013).

1.1.2 Anthropogenic ocean acidification

1.1.2.1 Chemistry

Ocean uptake of increasing atmospheric CO_2 results in a gradual acidification of seawater; this process is termed ocean acidification (IPCC, 2013, Broecker and Clark, 2001, Caldeira and Wickett, 2003). Ocean acidification refers to the reduction in pH over decades, and describes the direction of pH change as opposed to the end point. Whereby, ocean pH is decreasing but is not expected to become acidic (i.e. $\text{pH} < 7$) (IPCC, 2013). Acidification of the oceans can be caused by natural activity (e.g. volcanic activity), however anthropogenic ocean acidification refers to a reduction in ocean pH as a result of human activities, namely; increasing atmospheric CO_2 as a result of an increased anthropogenic use of fossil fuels. Rising levels of atmospheric CO_2 means more is dissolved into the oceans. It is estimated that the surface waters of the oceans have taken up $\sim 25\%$ of the carbon generated by anthropogenic activities since 1800 (Sabine et al., 2004, Khatiwala et al., 2013). Atmospheric CO_2 reacts with seawater through a series of four chemical reactions once it exchanges across the air-sea interface (IPCC, 2013) (Figure 1.4). These reactions increase the concentration of carbon species; dissolved CO_2 ($\text{CO}_{2(\text{aq})}$), carbonic acid (H_2CO_3) and bicarbonate (HCO_3^-). Once dissolved in seawater (Figure 1.4i), CO_2 reacts with water (H_2O) to form carbonic acid ($\text{CO}_2 + \text{H}_2\text{O} = \text{H}_2\text{CO}_3$).

H_2CO_3 is a weak acid and dissolves rapidly to form bicarbonate (HCO_3^- ; a base) and hydrogen ions (H^+ ; an acid) (Figure 1.4iii). The percentage increase in H^+ is greater than the percentage increase of HCO_3^- . Seawater is naturally saturated with carbonate ions (CO_3^{2-} ; a base). Therefore, to maintain chemical equilibrium, CO_3^{2-} reacts with H^+ to form more bicarbonate (Figure 1.4iv). Collectively, these four reactions result in an increase in the concentration of bicarbonate ions [HCO_3^-] and a decrease in the availability of carbonate ions [CO_3^{2-}] (Gattuso and Hansson, 2011) ($\text{CO}_2 + \text{H}_2\text{O} + \text{CO}_3^{2-} = 2\text{HCO}_3^-$) (Figure 1.5). The decrease in [CO_3^{2-}] means a decrease in the saturation state (Ω) with respect to calcium carbonate (aragonite and calcite) (Feely et al. 2004), because carbonate is required to form calcium carbonate ($\text{Ca}^{2+} + \text{CO}_3^{2-} = \text{CaCO}_3$). Seawater is in equilibrium with calcium carbonate when $\Omega = 1$, supersaturation (i.e. $\Omega > 1$) promotes inorganic precipitation, and undersaturation (i.e. $\Omega < 1$) promotes inorganic dissolution (Gattuso and Hansson, 2011). The concentration of protons [H^+] also increases, as it is directly proportional to the ratio [CO_3^{2-}] / [2HCO_3^-]. Thus, seawater pH decreases resulting in ocean acidification (Gattuso and Hansson, 2011). The pH scale is logarithmic, so a change of 1 unit corresponds to a 10-fold change in hydrogen ion concentration (Figure 1.4). If calcium carbonate dissolves in large enough quantities, with enough time it could return the oceans' pH to its natural state, which may explain why pH in the past did not decrease as dramatically as the high CO_2 levels in the past may suggest (Orr et al., 2005). It is suggested that [CO_3^{2-}] may increase in the future as the oceans warm, however models suggest that this is likely to only compensate for 10% of the [CO_3^{2-}] lost due to ocean acidification (Orr et al., 2005).

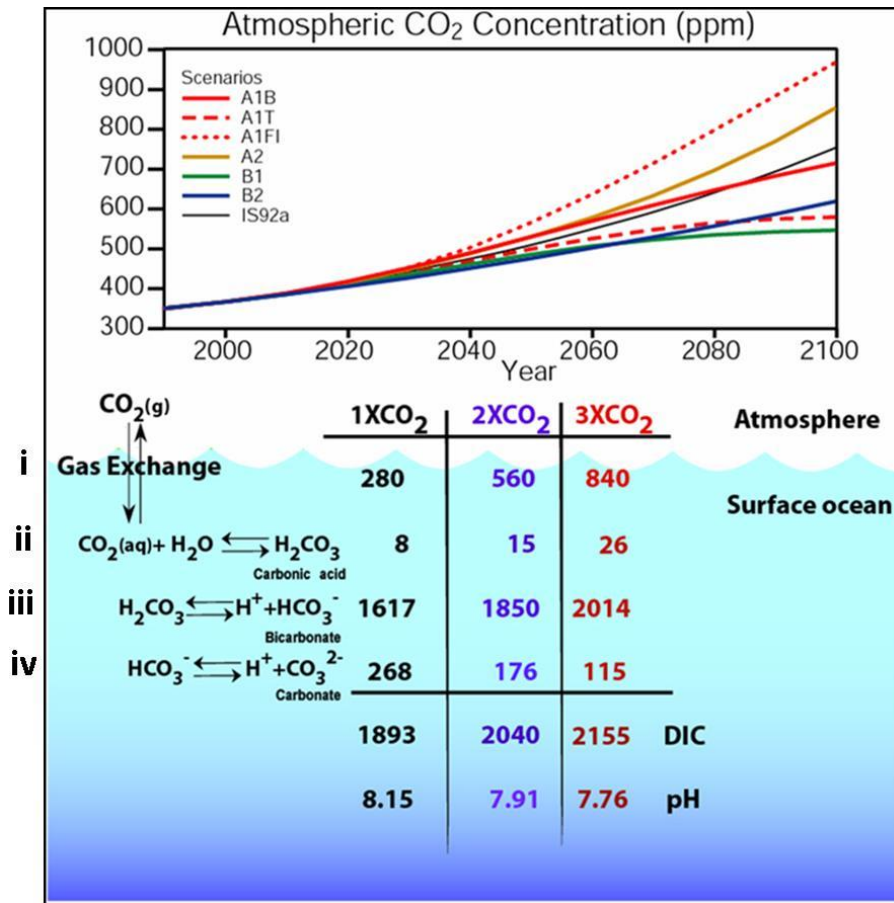


Figure 1.4 The projected change in carbon chemistry relative to preindustrial carbon dioxide Scenarios relate to models described in (IPCC, 2013). i-iv; the four equations that take place when carbon dioxide reacts with seawater.

Source: NOAA; <http://www.pmel.noaa.gov/co2/story/Ocean+Carbon+Uptake>

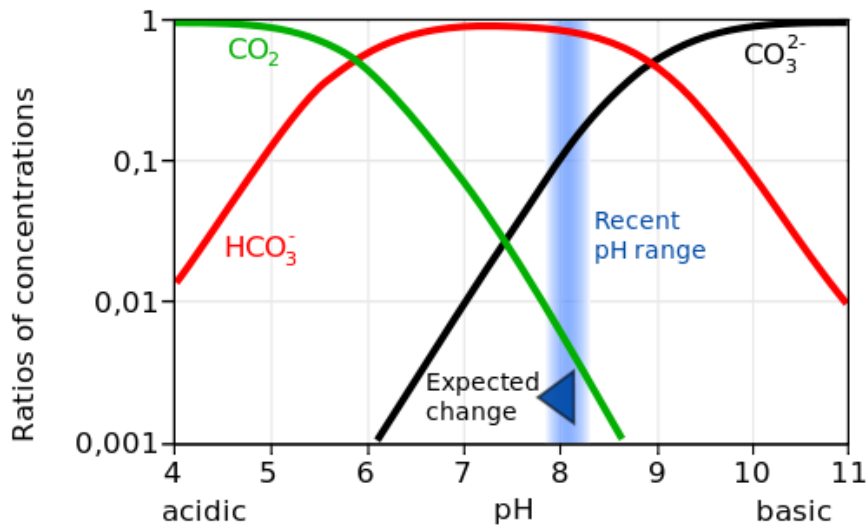


Figure 1.5 Bjerrum Plot showing the change in the carbonate system of seawater due to ocean acidification carbon dioxide (CO₂), bicarbonate (HCO₃⁻) and carbonate (CO₃²⁻). Source: (Gattuso and Hansson, 2011)

1.1.2.2 Past changes in ocean chemistry

The capacity of the oceans to absorb CO_2 away from the atmosphere has assisted greatly in the mitigation of climatic changes by decreasing greenhouse gas levels in the atmosphere and reducing some of the impacts of global warming (IPCC, 2013). Since the beginning of the industrial revolution era ocean acidification has led to a reduction in ocean pH by 0.1 unit (IPCC, 2013), this corresponds to a 26% increase in $[\text{H}^+]$ concentration of seawater (Orr et al., 2005, Feely et al., 2009) (Figure 1.6, Table 1.1). The decrease in pH with increasing atmospheric $p\text{CO}_2$ is demonstrated by direct measurements on ocean time-series stations in the North Pacific and North Atlantic, records show decreasing ocean pH ranging between -0.0014 and -0.0024 yr^{-1} (Figure 1.6; Bates, 2007, 2010, Santana-Casiano et al., 2007, Dore et al., 2009, Olafsson et al., 2009, Gonzalez-Davila et al., 2010, IPCC, 2013).

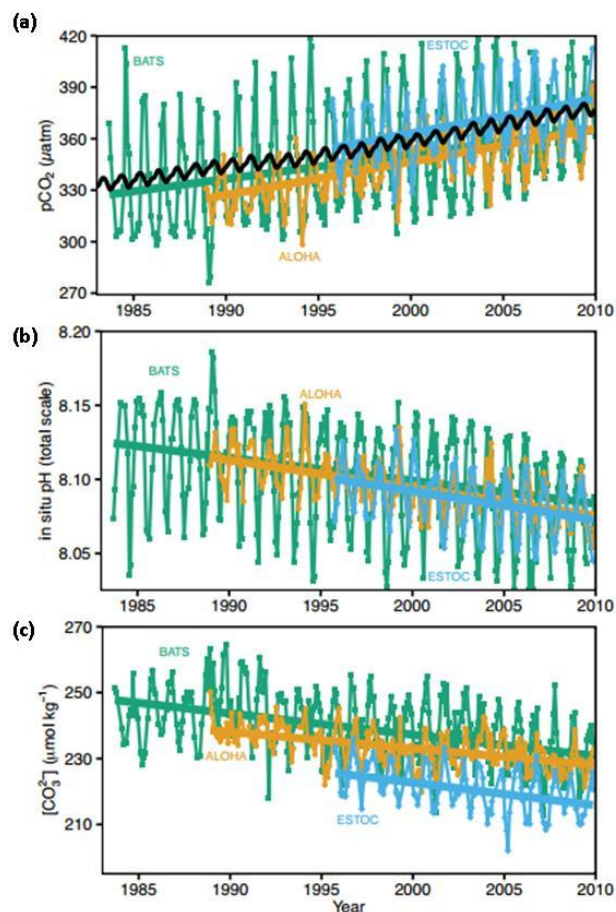


Figure 1.6 Long term trends of surface $p\text{CO}_2$, pH and carbonate ion concentration at three subtropical ocean time series in the North Atlantic and North Pacific oceans (Taken from IPCC, 2013). (a) $p\text{CO}_2$; (b) pH (c) carbonate ion concentration. Sites Include; Bermuda Atlantic Time-series Study (BATS, $31^\circ 40' \text{N}$, $64^\circ 10' \text{W}$; green) and Hydrostation S ($32^\circ 10' \text{N}$, $64^\circ 30' \text{W}$) from 1983 to present (updated from (Bates, 2007)); Hawaii Ocean Time-series (HOT) at Station ALOHA (A Long-term Oligotrophic Habitat Assessment; $22^\circ 45' \text{N}$, $158^\circ 00' \text{W}$; orange) from 1988 to present (updated from Dore et al., 2009); European Station for Time series in the Ocean (ESTOC, $29^\circ 10' \text{N}$, $15^\circ 30' \text{W}$; blue) from 1994 to present (updated from (Gonzalez-Davila et al., 2010)). Atmospheric $p\text{CO}_2$ (black) from the Mauna Loa Observatory Hawaii is shown in the top panel.

Table 1.1 Average changes in carbonate chemistry of surface seawater 1766 to 2100 (Gattuso and Lavigne, 2009)

Parameter	Unit	LGM	1766	2007	2100
Temperature	°C	17.2	18.3	18.9	21.4
Salinity	–	36	34.9	34.9	34.7
Total phosphate	10 ⁻⁶ mol kg ⁻¹	0.66	0.66	0.63	0.55
Total silicate	10 ⁻⁶ mol kg ⁻¹	7.35	7.35	7.35	7.35
Total alkalinity	10 ⁻⁶ mol kg ⁻¹	2399	2326	2325	2310
CO ₂ partial pressure (seawater)	µatm	180	267	384	793
[CO ₂]	10 ⁻⁶ mol kg ⁻¹	6.26	9.05	12.8	24.7
[HCO ₃ ⁻]	10 ⁻⁶ mol kg ⁻¹	1660	1754	1865	2020
[CO ₃ ²⁻]	10 ⁻⁶ mol kg ⁻¹	299	231	186	118
Dissolved inorganic carbon	10 ⁻⁶ mol kg ⁻¹	1966	1994	2064	2162
pH _T	–	8.33	8.20	8.07	7.79
[H ⁺]	10 ⁻⁹ mol kg ⁻¹	4.589	6.379	8.600	16.13
Calcite saturation	–	7.1	5.5	4.5	2.8
Aragonite saturation	–	4.6	3.6	2.9	1.8

LGM = last glacial maximum. Total alkalinity, CO₂ partial pressure (*p*CO₂), salinity and temperature were fixed and used to drive the other parameters using Seacarb software using the seacarb software (Lavigne et al., 2008) and the dissociation constant of carbonic acid of (Lueker et al., 2000). It is assumed that the ocean and atmosphere are in equilibrium with respect to CO₂. Values of temperature, salinity, total alkalinity and total phosphate in 1766, 2007 and 2100 are from (Plattner et al., 2001) prescribing historical CO₂ records and non-CO₂ radiative forcing from 1766 to 1990 and using the A2 IPCC SRES emissions scenario (Nakicenovic, 2000) thereafter. Temperature during the LGM was set 1.9_C colder than in 2007 (MARGO Project Members, 2009). The LGM salinity was set 1.07 higher than during pre-industrial time (Paul and Schafer-Neth, 2003). Total alkalinity in the LGM was scaled to salinity while the total phosphate concentration was assumed to be the same as in 1766. *p*CO₂ in 1766 and 2100 are from (Plattner et al., 2001), while values in the LGM and 2007 are from (Petit, 2001) and (Keeling et al., 2008), respectively. The concentration of total silicate is assumed to have remained constant from the LGM to 2100. It was calculated using the gridded data reported by (Garcia et al., 2006) between 0 and 10m and weighing the averages using the surface area of each grid cell. pH is expressed on the total scale.

1.1.2.3 Projected ocean acidification

The current period of ocean acidification is in stark contrast to the last 25 million years, where ocean pH remained between pH 8.3 and 8.0 (Caldeira and Wickett, 2003). Currently, 30% of the total anthropogenic emissions of CO₂ are accumulating in the atmosphere (Le Quere, 2010, Le Quere et al., 2010). Estimates of future atmospheric and oceanic carbon dioxide concentrations suggest this will equate to a further reduction of best case 0.06-0.07 pH units, to worst case 0.2 to 0.21 pH units by the end of the 21st century (IPCC, 2013) (Figure 1.7). This will mean that by 2100, average surface ocean pH could be lower than it has been in more than 50 million years (Caldeira and Wickett, 2003).

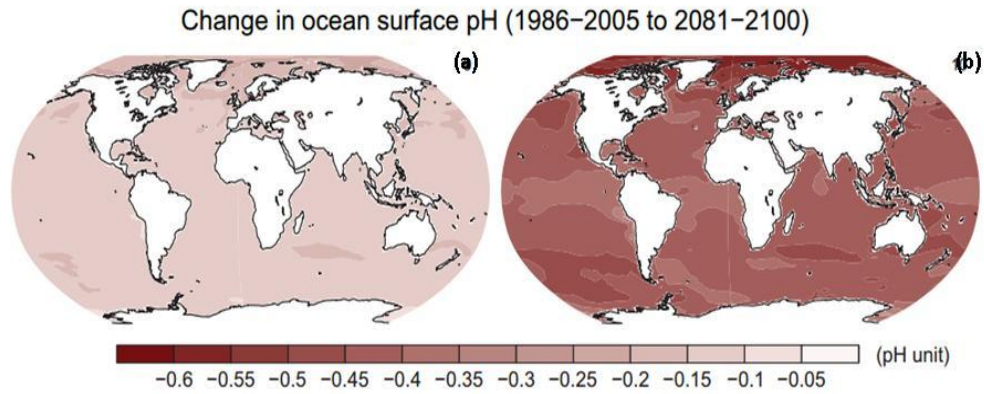


Figure 1.7 Maps of multi-model mean results of changes in surface ocean pH in 2081–2100. (CMIP5; scenarios RCP2.6 and RCP8.5, IPCC, 2013). (a) Past changes in ocean pH; 1986–2005 (b) Projected changes in ocean pH; 2081–2100. Source: (IPCC, 2013).

1.2 Natural variability, coastal systems and climate change

Coastal marine systems are among the most ecologically and socio-economically important systems in the world (Costanza et al., 1997). Coastal marine habitats are estimated to provide over £10 trillion worth of ecosystem goods (e.g. food and raw materials) and services (e.g. disturbance regulation and nutrient cycling) per year (Costanza et al., 1997). The production of many of these goods and services are controlled directly or indirectly by the *in situ* environmental conditions which are influenced by natural variability. Natural variability of the ocean's environment includes variability across a range of temporal and spatial scales; seasonal/ diurnal cycles, latitudinal differences in climate, hydrological processes (e.g. upwelling), inter-annual patterns (e.g. El Niño Southern Oscillation ; ENSO), inter-decadal cycles (e.g. North Atlantic and Pacific Decadal oscillations), and changes in a multi-millennial scale (e.g. glacial and inter-glacial transitions) (Harley et al., 2006). Evolutionary adaptations and biogeographical patterns of species are often reflective of this natural variability (Harley et al., 2006). However, over the past several hundred years' anthropogenic activities have become an additional, and significant, component to the Earth's climatic system. Thus in the long term (a century), anthropogenic variability will play a significant role in shaping the future of marine systems. However, in the short term (decades) natural variability will overlay the environmental changes associated with anthropogenic global climate change, and as such are likely to significantly influence the response of marine

biota to the projected environmental changes (e.g. warming and ocean acidification). In addition to large scale temporal variability (e.g. seasonal changes), experience of fine-scale localised variability is also likely to influence the response of marine organisms to acidification and warming (e.g. Johnson et al., 2014). Findlay et al. (2014) suggest that while there is now considerable nutrient and carbonate system data, generally this data is only available from global studies (e.g. World Ocean Atlas (WOA) or the Global Ocean Data Analysis Project (GLODAP) (Key et al., 2004)). While this data is useful for global assessments (i.e. IPCC, 2013), knowledge of fine-scale spatial and temporal dynamics would provide a baseline of the physicochemical environment associated with specific marine organisms (Findlay et al., 2014). Furthermore, in conjunction with more information about the localised environment, knowledge of the response of marine organisms to natural variability will help predict how they might respond in the future.

1.2.1 Fine-scale natural variability

The dominant cause of the observed changes in carbonate chemistry in surface seawater over the past several centuries are as a result of the uptake of anthropogenic CO₂ (Doney et al., 2009, Feely et al., 2009). However, changes in carbonate chemistry in surface waters can also mirror local physical (i.e. hydrography) and biological (i.e. photosynthesis and calcification) variability that is not associated with global climate change. Carbon and nutrient conditions are be highly variable on tropical coral reefs (Silverman et al., 2007b, 2007a, Manzello, 2010, Albright et al., 2013, Burdett et al., 2013), but the presence of the reef themselves can also directly contribute to the variability in carbon and nutrients over diel and seasonal patterns (Gray et al., 2012, Anthony et al., 2013, Maier et al., 2012). On both temporal and spatial scales the seawater carbonate system is highly variable on tropical reef systems in the Eastern Pacific (Panamá and the Galápagos Islands) (Manzello, 2010). This variability is explained by physical forcing from seasonal rainfall and hydrographical (upwelling and tides) processes interacting with the diurnal reef metabolism (Manzello, 2010). Similarly, Findlay et al. (2014) attributed the increased diel variability in fine-scale carbonate and nutrient conditions to localised hydrodynamics (e.g. upwelling) on cold water coral reefs in the North Atlantic. Fine-scale diel natural variability in carbonate chemistry has also been shown to influence the physiology of tropical macroalgae (e.g. Burdett et al., 2013). Maximum intracellular dimethylsulphoniopropionate (DMS/P) and water column DMS/P concentrations were

observed at night, a response suggested to maintain metabolic function during the time of lowest carbonate saturation state (Burdett et al., 2013). Red coralline algae have also demonstrated variability in their photosynthetic characteristics in response to changes in irradiance that allow them to tolerate the naturally high light regimes experienced on tropical coral reefs (Burdett et al., 2014). This type of research could have significant implications for the management of marine ecosystems under current conditions and in the future (Burdett et al., 2013). It also provides important information for future empirical studies and may help predict how organisms may respond in the future. For example, changes in DMS/P production by algae can impact larval settlement and the sulfur cycle (Burdett et al., 2014). Therefore, changes in DMS/P concentration in response to low carbonate conditions are important information for the management of tropical marine systems under both naturally variable contemporary conditions and in the future.

1.2.2 Large-scale natural variability

The large scale natural environmental variability and human interaction experienced on the coasts can make it difficult to identify the impacts of climate change (IPCC, 2013) (Figure 1.8). There have been long term ecological studies on the rocky shore that attribute changes in the community to anthropogenic climate change trends (Hawkins et al., 2003). Thus far, the clearest evidence of the impact of climate change comes from coastal ecosystems at high (poles; e.g. Wassmann et al., 2011) and low (tropics, e.g. Johnson and Holbrook, 2014) latitudes (Nicholls et al., 2007, Doney et al., 2012). Mid-latitudinal coastal ecosystems (e.g. temperate zones) have a great deal of natural variability (because of their position between the tropics and the poles) that often make it difficult to distinguish between changes due to natural variability and those due to climate change (Nicholls et al., 2007). Byrne et al. (2010) attributed declines in pH in the mid-latitude North Pacific Ocean between 800 m and the mixed layer, from 1991-2006, equally to natural and anthropogenic variability, while changes in surface pH were as a direct effect of the changes in atmospheric CO₂. Large-scale natural variability has also been shown to influence the physiology of marine organisms. Coral bleaching and mortality in the Indo-Pacific region has been linked to the frequency and intensity of ENSO events (Buddemeier et al., 2004). ENSO events are likely to alter as a component of climate change (Nicholls et al., 2007), becoming more widespread in the future because

of global warming (Stone et al., 1999). This suggests that global climate change is likely to exacerbate the negative effects that contemporary natural variability can have on marine ecosystems. In addition, understanding adaptation of marine organisms to global climate change requires an insight into processes at decadal to century scales, at which understanding is least developed (de Groot and Orford, 1999, Nicholls et al., 2007).

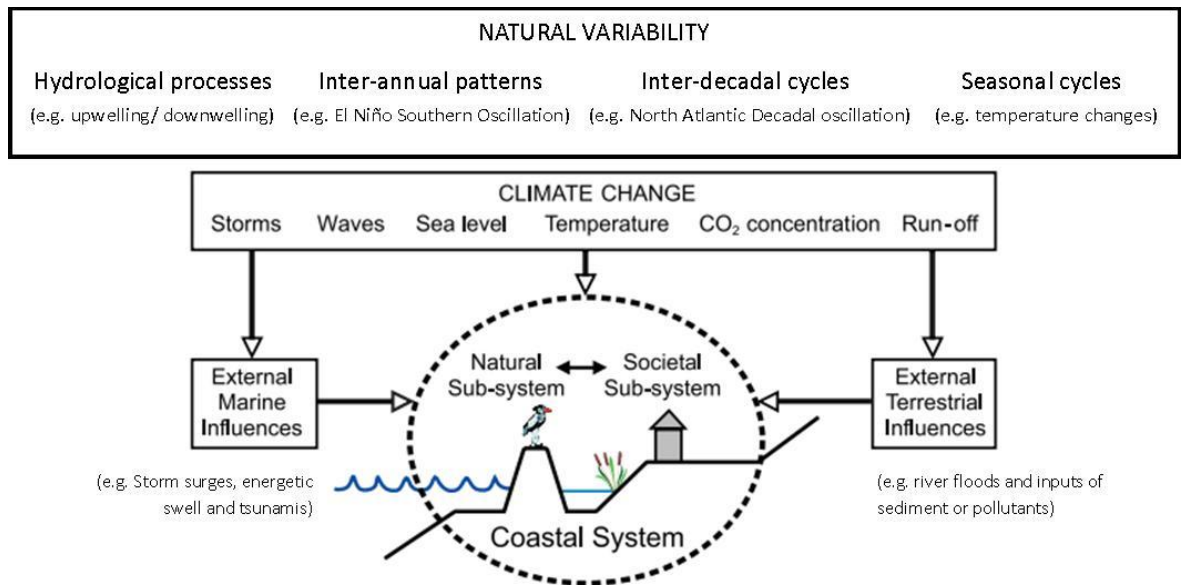


Figure 1.8 Climate change, large scale natural variability and the coastal system. Adapted from (Nicholls et al., 2007). Showing the major climate change and large scale natural variability factors.

1.3 Importance of marine calcifiers

In many marine coastal ecosystems marine calcifiers form an integral part of the community; often responsible for the construction of biogenic structures that can underpin the ecosystem and create habitat for many associated species. These biogenic reefs are defined as a solid massive structures which are created by accumulations of organisms, usually arising from the seabed, or at least clearly forming a substantial, discrete community or habitat which is very different from the surrounding seabed (Holt et al., 1998). Biogenic reefs do not have a uniform structure and can vary dramatically in scale and extent. Their associated community and structure will depend on their geographic location and species of reef builder (Hendrick et al., 2011).

1.3.1 Ecosystem services and biodiversity

Biogenic reefs perform a number of important ecological roles; stabilisation of substrate, provision of hard substratum for the attachment of sessile organisms,

heterogeneous habitat for colonisation and the accumulation of faeces, pseudofaeces and other sediments that are important food sources for marine organisms (Holt et al., 1998). Thus, biogenic reefs are significant contributors to biodiversity. In addition, biogenic reefs can also provide nursery grounds for many species, making them particularly important to commercial fisheries and shellfish industries (Hall-Spencer and Stehfest, 2009, Husebo et al., 2002, Costello et al., 2005, Kamenos et al., 2004a, Kamenos et al., 2004b, Pena and Barbara, 2008, Holt et al., 1998, Hendrick et al., 2011). Furthermore, coralline algae, which can form large free-living aggregations (maerl beds), can impact on the climate system including cloud nucleation and ozone stability (Ohsawa et al., 2001) and contribute to the sulfur cycle (Kamenos et al., 2008a).

1.3.2 Carbon sequestration and storage

Marine calcifiers, particularly reef forming species, significantly contribute to the global carbon cycle (Burrows et al., 2014, BIOMAERL et al., 2003). In particular, highly productive reef systems (e.g. coral reefs) and photosynthesising reef builders (e.g. free living coralline algae aggregations; maerl beds) may significantly contribute to carbon storage in coastal waters (Burrows et al., 2014) over geological time scales (Bensoussan and Gattuso, 2007). For example, maerl beds provide the most carbonate of all coastal habitats in Europe (BIOMAERL et al., 2003) and are significant calcifiers in many coastal ecosystems (e.g. coral reefs, Tierney and Johnson, 2012). Furthermore, biogenic reefs can promote the stabilisation and accumulation of carbon-loaded sediments (i.e. pseudofaeces / faeces) (Holt et al., 1998). Along with high primary productivity (i.e. maerl beds), these sediments can provide a direct and indirect carbon source to macrofauna, microbes and plankton associated with the biogenic reef (i.e. Krumhansl and Scheibling, 2012).

1.3.3 Palaeoclimatic archives

The longevity and slow growth rates associated with some biogenic reef builders means that they can contain important palaeoclimatic information. In particular, the cosmopolitan distribution of free-living coralline algae (Figure 1.10) and cold water corals (Figure 1.16) means that they may have the potential to provide more information compared to other biogenic palaeoclimatic proxies such as tropical corals (Roberts et al., 2006). The distribution of tropical corals is generally limited to the tropics and subtropics (0-30°N and S) because of their physiology. In addition, cold-water corals and free-living

red coralline algae both have a banded skeletal structure (Figure 3.1; chapter 3 details more information about the growth of coralline algae) that means that high resolution palaeoclimatic data can be contained within the structure (Roberts et al., 2006, Kamenos et al., 2008b, Halfar et al., 2008). For example, bi-weekly resolution of sea surface temperature was obtained from free-living red coralline algae by analysing concentrations of MgCO_3 and SrCO_3 (mol %) deposited in the growth bands (Kamenos et al., 2008b). Calcification and isotopic ratios (^{18}O and ^{14}C) have also been used to reconstruct Holocene temperature (Kamenos and Law, 2010, Halfar et al., 2009, Halfar et al., 2008, Hetzinger et al., 2009), historic cloud cover (Burdett et al., 2011) and relative salinity changes (Kamenos et al., 2012). Similarly, temperature can also be reconstructed from cold water coral skeletons (Smith et al., 2000, Sherwood et al., 2005a, Thresher et al., 2004). However, interpreting chronologies can be more challenging compared to coralline algae because of the cryptic banding and complex skeletal structures associated with some cold water corals (Roberts et al., 2006). Despite this complexity Adkins et al. (2004) were able to interpret an annual chronology using ^{210}Pb as a time proxy in *Enallopsammia rostrata*. Furthermore, there is evidence to suggest banding in deep sea octocorals is annual (Sherwood et al., 2005b).

1.3.4 Maerl beds

Free-living red coralline algae can occur in aggregations forming large biogenic reefs commonly called maerl beds (Figure 1.9a). In terms of global area covered (Figure 1.10), maerl beds may be one of the Earth's largest and most widespread benthic communities, on a par with kelp forests, tropical coral reefs and seagrass beds (Foster, 2001). Free-living coralline algae have the largest depth range of any photosynthetic organism and can be found from the intertidal to greater than 250 m depth (Pena and Barbara, 2008, BIOMAERL et al., 2003). Nonetheless, a major constraint on the distribution of red coralline algae is their requirement for light, restricting them to depths shallower than 32m in northern Europe (Hall-Spencer, 1998). In addition, maerl requires water motion (i.e. current or wave action) in order to prevent fouling, burial by sediment, overgrowth by other algae and invertebrates, and to maintain them in a free living, unattached state (Foster, 2001, Steller et al., 2003). Maerl are among the slowest growing algal species and are very long-lived and, with growth rates as low as 0.1 to 2 mm

yr^{-1} it can take thousands of years for maerl beds to accumulate (Blake and Maggs, 2003, Bosenice and Wilson, 2003).

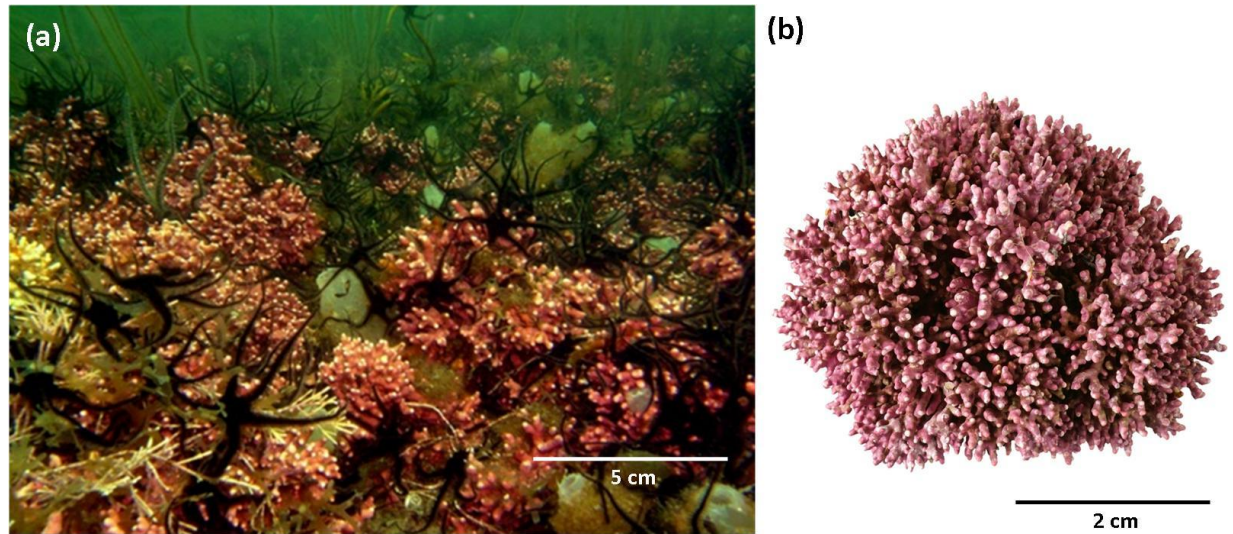


Figure 1.9 Maerl bed and *Lithothamnion glaciale* thallus
 (a) Aggregation of free-living red coralline algae in Loch Sween, Scotland (b) *Lithothamnion glaciale* ; an example of a free-living coralline red algae thallus. Photo: N. Kamenos and L. Hill.



Figure 1.10 The global distribution of free-living red coralline algae.
 Black dots indicate the recorded locations. Picture source: (Burdett, 2013) adapted and updated from (Foster, 2001).

1.3.4.1 *Lithothamnion glaciale*

Temperature appears to drive the geographical distribution of individual species (Foster, 2001). For example there are several species associated with European waters, each with distinct distributions associated with temperature (Figure 1.11). *L. glaciale* (Figure 1.9b) contributes significantly to maerl beds in Scotland, with its distribution continuing north to the Arctic (Teichert et al., 2012). Within Europe *L. glaciale* occurs at shallow depths (6-~35 m) dependent on irradiance (Hall-Spencer, 1998). Although, at higher latitudes, when irradiance and temperature in deep water are comparable to those of shallower water, *L. glaciale* can be found at depths of 50-250 m (Foster et al., 2013).

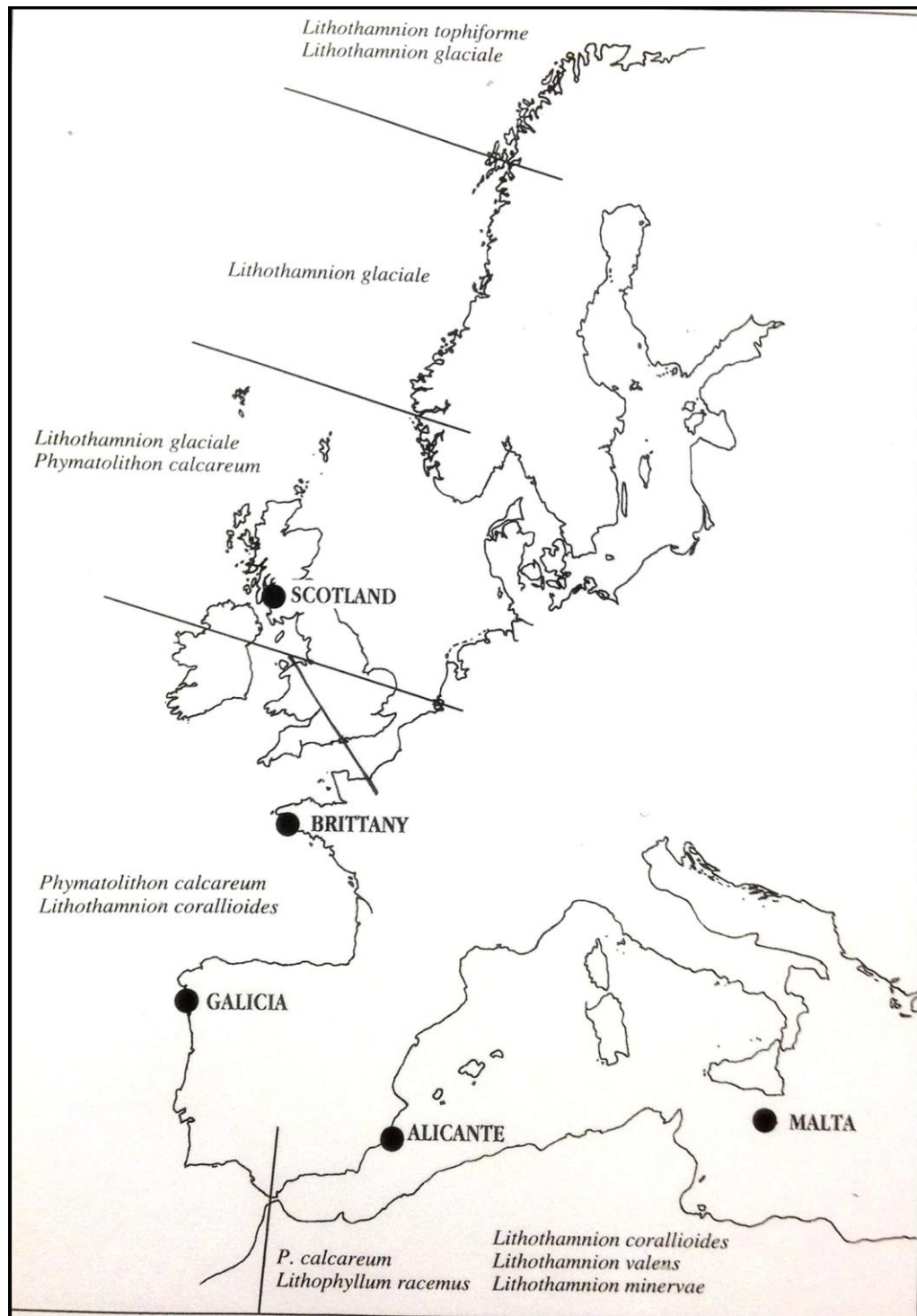


Figure 1.11 Distribution of red coralline algae species within Europe
 Picture source: (BIOMAERL et al., 2003)

1.3.4.2 Photosynthesis and red coralline algae

1.3.4.2.1 Light and dark reactions of photosynthesis

The photosynthetic process can be split into two sections; light and dark reaction (Figure 1.12). Light reactions take place in the thylakoid membranes (Figure 1.14) in photosystems I (PSI) and II (PSII) and require light energy to proceed (Kirk, 2011) (Figure

1.12). The dark reactions take place in the stroma (Figure 1.13) and use nicotinamide adenine dinucleotide phosphate dehydrogenase (NADPH_2) from the light reactions to reduce CO_2 to carbohydrate (the Calvin cycle) (Figure 1.12).

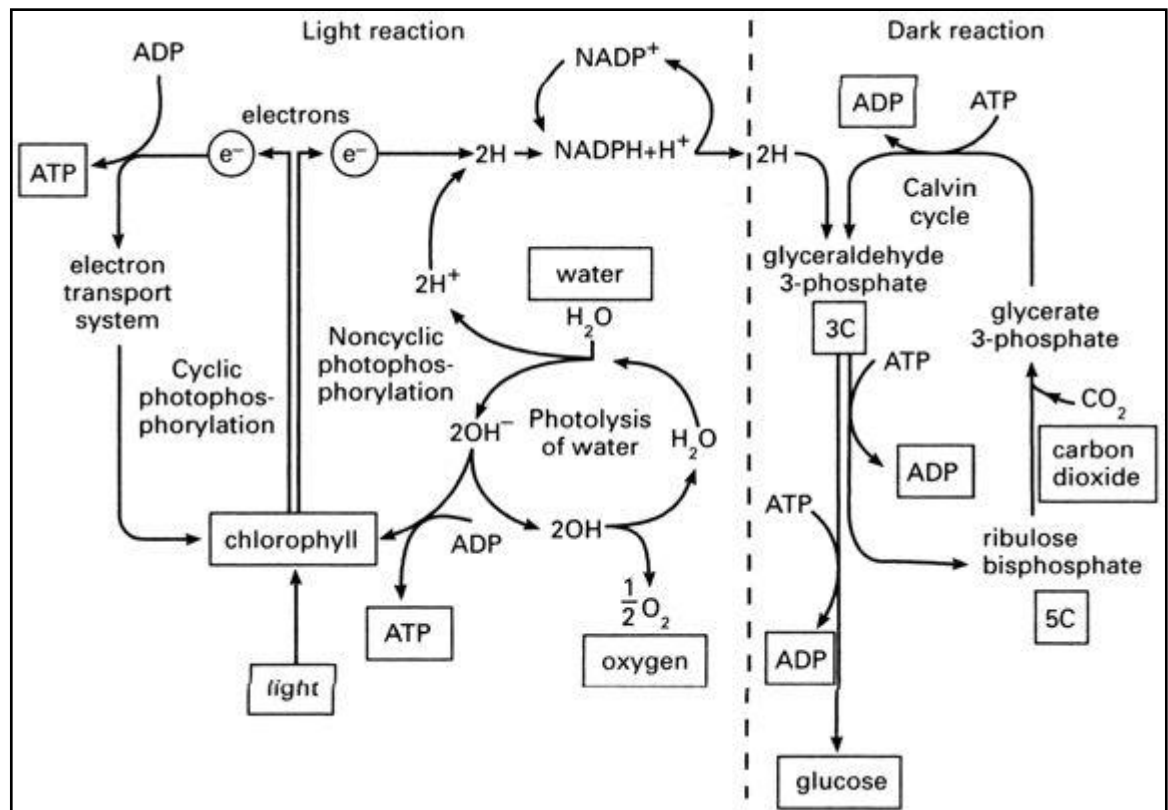


Figure 1.12 The reactions of photosynthesis
Source: Oxford Dictionary of Chemistry (Daintith, 2004)

1.3.4.2.2 Chloroplasts

In eukaryotic plants and algae photosynthesis is carried out in organelles known as chloroplasts (Figure 1.13) (Falkowski and Raven, 2013). Chloroplasts contain the light capturing pigments, electron carriers that utilise the absorbed energy to generate reducing power in the form of NADPH_2 and biochemical energy in the form of adenosine triphosphate (ATP), and enzymes that use NADPH_2 and ATP to convert carbon dioxide (CO_2) and water to carbohydrate (Kirk, 2011). Red coralline algae are in the Florideophycidae group; one of the two groups of Rhodopyta, the other being Bangiophycidae (Kirk, 2011). Algae in the Florideophycidae group normally contain numerous small lens-shaped chloroplasts around the periphery of the cell (Kirk, 2011).

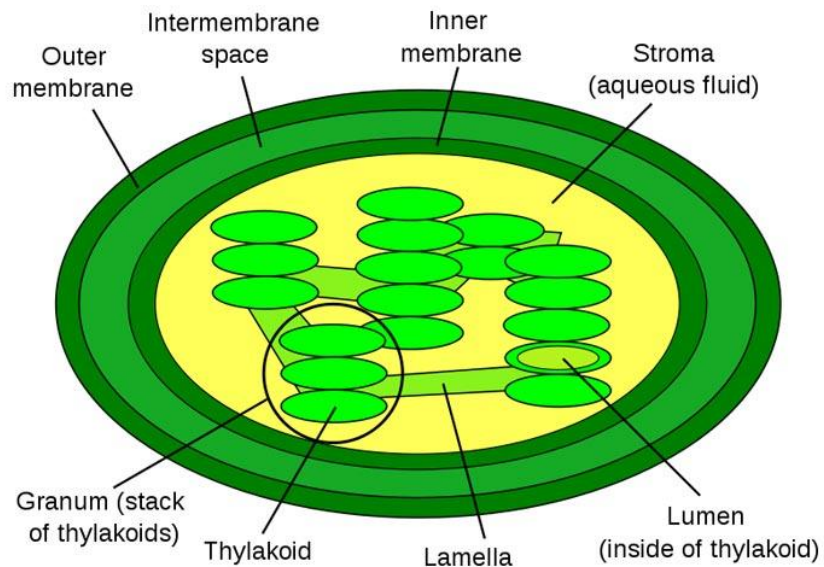


Figure 1.13 The basic structure of a chloroplast.

The chloroplast features an inner membrane, outer membrane, intermembrane, stroma (aqueous fluid), lamella, lumen. Pigments and electron carriers are contained within the thylakoid (Figure 1.14). Enzymes for CO₂ fixation are distributed throughout the stroma.

Picture source: www.sciencekids.co.nz/pictures/plants/chloroplastdiagram

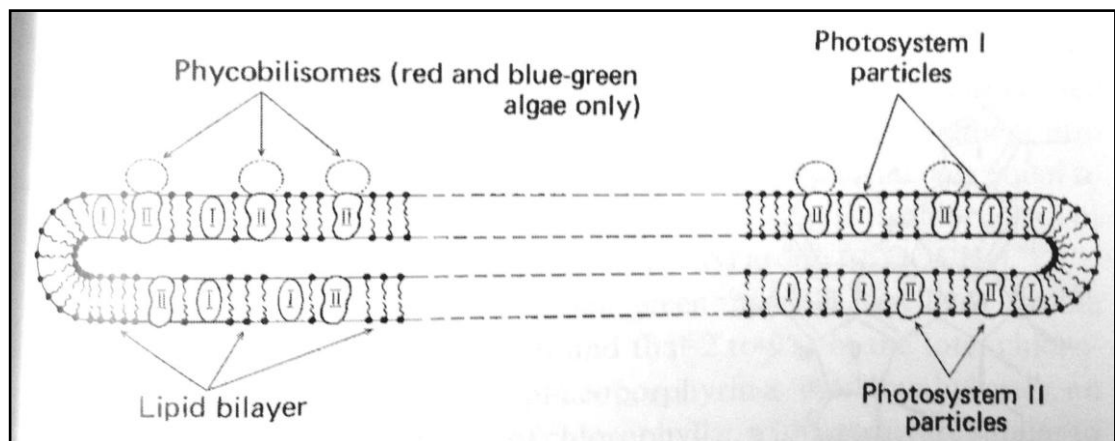


Figure 1.14 Possible mode of organisation of the thylakoid membrane in algae.

Attached to the outside of the thylakoid membranes are particles 30-40 nm in diameter known as phycobilisomes, which are unique to red algae and cyanobacteria. Source: (Kirk, 2011)

1.3.4.2.3 Pigments and light harvesting

Light is collected from the aquatic environment using photosynthetic pigments; the structures of these molecules allow them to efficiently absorb light between 700-400 nm (Kirk, 2011). There are three chemically distinct types of pigments; chlorophylls, carotenoids, and biliproteins (Kirk, 2011). All algae contain chlorophylls and carotenoids, but only red algae (and blue-green algae and the cryptophytes) contain biliproteins (Figure 1.14) (Rowan, 1989).

Chlorophyll

Rhodophyta contain only chlorophyll-*a*, the content of which varies greatly between species. The light absorption properties of the chlorophylls are interpreted in terms of two excited singlet states (i.e. upper and lower) of the electrons. Absorbance peaks of chlorophyll-*a* are at 435 nm (red region of the light spectrum) and between 670-680 nm (blue region of the light spectrum) (Kirk, 2011). In contrast, carotenoids (α and β) have three distinct absorption peaks ranging between 423-475 nm (Kirk, 2011, Hedley and Mumby, 2002).

Biliproteins

Biliproteins are the primary component of Phycobilisomes (i.e. the light harvesting pigments found in red algae). There are three biliprotein pigments found in red algae; phycoerythrin (red), phycocyanin and allophycocyanin (blue) (Kursar and Alberte, 1983, Mimuro and Kikuchi, 2003). The absorption peaks of phycocyanin and allophycocyanin are 618 and 654, respectively (Hedley and Mumby, 2002). Phycoerythrin is generally the dominant biliprotein and has three distinct absorption peaks; 490 nm, 545, and 576 nm (Hedley and Mumby, 2002). Generally, the lower the wavelength of an absorption peak, the higher the energy of photons that are absorbed (Kirk, 2011). Thus, the higher the energy level to which the electrons in the molecule are excited (Kirk, 2011). This suggests that a range of pigments with a range of absorbance peaks may be advantageous. *In vivo*, phycobiliproteins aggregate to form structured phycobilisome particles (Figure 1.15) located on the surface of the thylakoids (Figure 1.14). Allophycocyanin is located at the base of the particle, next to the membrane. Phycocyanin and phycoerythrin then form a shell around allophycocyanin. It is allophycocyanin that transfers the energy harvested by the phycobilisome particle to the chlorophyll (Kirk, 2011) (Figure 1.15).

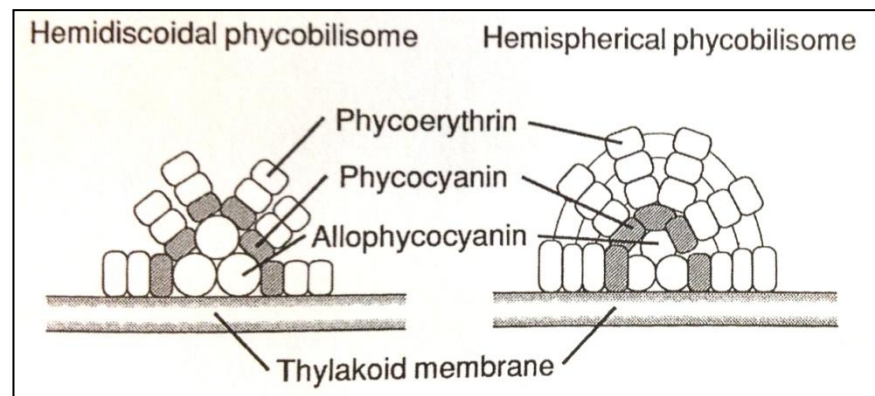


Figure 1.15 Schematic representation of phycobilisomes structure
 Source: (Kirk, 2011), after (Gantt et al., 1986, Glazer and Melis, 1987, Glazer, 1985)

1.3.4.2.4 Rubisco

Ribulose-1, 5-biphosphate carboxylase/ oxygenase (Rubisco) catalyses the incorporation of CO₂ into biological compounds in photosynthetic organisms (Andersson and Backlund, 2008). It has been suggested this may be the most abundant protein on Earth, comprising up to 50 % of the total soluble protein in some plant leaves (Andersson and Backlund, 2008). During the Calvin cycle, Rubisco catalyses the CO₂ reduction reaction; binding CO₂ to the acceptor molecule Ribulose-1, 5-biphosphate (RuBP) to form two molecules of 3-phosphoglycerate (Figure 1.12). However, Rubisco is an extremely slow catalyst and, in addition, competing side-reactions can compromise its carboxylation activity (Andersson and Backlund, 2008). Oxygen can bind to the same active site on RuBP as CO₂, resulting in opposing oxygenase activity of Rubisco, leading to the release of previously fixed CO₂ (and NH₃ and energy) (Lin et al., 2014) and a reduction in the efficiency of CO₂ fixation by up to 50% (Andersson and Backlund, 2008). These catalytic imperfections have been well documented (Morell et al., 1992) and cannot easily be avoided by photosynthetic organisms, thus Rubisco is the major rate limiting factor in photosynthesis.

1.3.4.3 Biomineralisation and red coralline algae

Coralline algae is long lived and growth is extremely slow (< 1mm yr⁻¹) (Kamenos et al., 2008b). A high-magnesium (high-Mg) calcite skeleton is deposited around each cell as the algae grow. However, a great deal remains unknown about exactly how the CaCO₃ skeleton is formed and the specific mechanism for growth in red coralline algae (Rahman and Halfar, 2014). A recent study on the biomineralisation process in the subarctic coralline alga *Clathromorphum compactum* indicated that the protein-polysaccharide of

the organic matrices such as chitin and collagen play a key role in stabilising the calcite crystals (Rahman and Halfar, 2014). Chitin is involved in biomineralisation in many marine invertebrates (Mann, 1988, Mikkelsen et al., 1997, Hall et al., 2002) and is regarded as the substrate that binds other macromolecules, which in turn induce nucleation in the mineral phase (Weiss and Schonitzer, 2006). Chitin is considered to contribute the framework at the base of the biological hierarchy for calcification in many marine organisms (Feng et al., 2013). An alignment between the orientation of chitin fibres and the crystallographic axes of the mineral phase has been observed (Banks et al., 2005) and, in some cases, the chitin matrix is the sole template in the calcification system (Hall et al., 2002). However, there is also substantial evidence to suggest that proteins and other organic components may control biomineralisation in marine calcifiers, providing preferential sites for nucleation and controlling the orientation of the resulting crystals (Rahman et al., 2011).

1.3.4.3.1 Carbonic anhydrase

Carbonic anhydrase is ubiquitously distributed in nature and is involved in fundamental biological processes such as photosynthesis, respiration, pH homeostasis, and ion transport (Tashian et al., 1990) and in the case of marine calcifying algae, it is also likely to play a significant role in calcification (Hofmann et al., 2013). The carbonic anhydrases form a family of enzymes that catalyse the interconversion of CO_2 and H_2O to bicarbonate and protons (H^+). The bicarbonate can then be combined with calcium ions to form calcium carbonate which in turn associates with organic matrices to form unique, often species-specific, biomineralized structures (Rahman et al., 2008). The active site of most carbonic anhydrases contains a zinc ion, although a cadmium containing carbonic anhydrase was found in marine diatoms, thought to be associated with low concentrations of zinc in the open ocean (Lane et al., 2005). Hofmann et al. (2012a) demonstrated that calcification rates in *Corallina officinalis* had a parabolic relationship to CO_2 concentration, and Hofmann et al. (2012b) showed that external carbonic anhydrase activity increased with elevated $p\text{CO}_2$ in the same species. The studies hypothesise that as photosynthesis was not stimulated by CO_2 in *C. officinalis* despite an increase in external carbonic anhydrase activity, it is likely external carbonic anhydrase activity is related to calcification and that its activity may be up-regulated under elevated $p\text{CO}_2$ (Hofmann et al., 2012a, Hofmann et al., 2012b). This hypothesis is supported by the

observed relationship between external carbonic anhydrase activity and skeletal inorganic carbon content of *C. officinalis*, which only became apparent after long term exposure to elevated $p\text{CO}_2$ (Hofmann et al., 2012b).

1.3.5 Cold water coral reefs

Cold-water corals are azooxanthellate (i.e. lacking in the symbiotic dinoflagellates associated with tropical shallow water corals) and do not require light. Their habitat ranges from close to the surface to beyond 2 km, and this group of cnidarians includes Scleractinia (stony corals), Octocorallina (soft corals), Anitpatharia (black corals), and Stylasteridae (hydrocorals). Cold-water corals can occur as individual isolated colonies, in small patch reefs or coral gardens, measuring several metres across or they can form vast reefs and huge carbonate mounds measuring up to 300 m high and several kilometers in diameter (Roberts et al., 2006). The largest reefs and carbonate mounds are formed by the scleractinian reef framework forming cold-water corals and are key contributors to biodiversity and habitat provision in the deep sea (Jonsson et al., 2004, Henry and Roberts, 2007). These giant reefs can take many thousands to millions of years to form and their age, coupled with slow growth rates, means that in addition to containing high-resolution palaeoclimatic information, reefs may also be key speciation centres in the deep sea (Roberts et al., 2005). Reef forming cold-water corals have been known since the 18th century, however concordant with the advancement of technology and exploration of deeper waters, only recently have they been the subject of ecological research (Roberts et al., 2006) and their global scale and abundance realised (Roberts et al., 2005, Freiwald et al., 2004) (Figure 1.16).

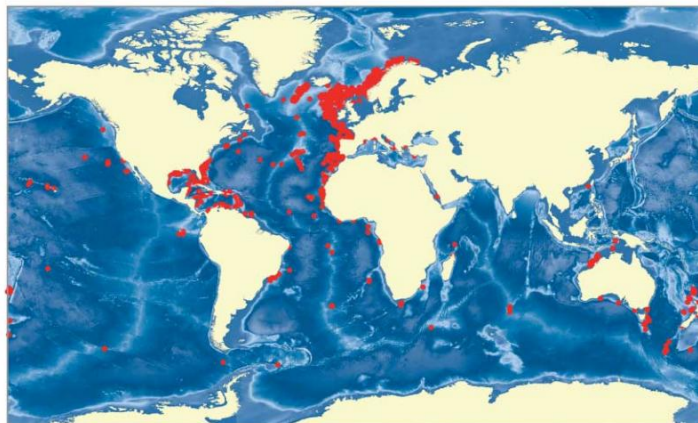


Figure 1.16 Current global distribution of reef framework-forming cold-water corals (taken from Roberts et al., 2006). Reef Locations are indicated by red dots.

1.3.5.1 *Lophelia pertusa*

Lophelia pertusa is widely distributed across the Atlantic, Pacific and Indian Oceans, and the Mediterranean (Cairns, 1994), and due to its complex three-dimensional structure forms biodiversity hotspots in the deep-ocean worldwide. *L. pertusa* is the predominant cold-water reef framework forming coral in the north-east Atlantic (Fossa et al., 2002, Cairns, 1994) and forms from single polyps to form colonies (Figure 1.17) which then merge to form patch reefs and, if conditions are favorable, the process continues to form vast reefs, some of which are the largest known on Earth (e.g. Rost Reef, off Norway, 35 km long). There is an increasing catalogue of species associated with *L. pertusa* reefs, with the current tally more than 1300 species, many of which are new to science (Myers and Hall-Spencer, 2004, Henry and Roberts, 2007), including; sessile suspension feeders, grazers, scavenging and predatory invertebrates (inc. molluscs, crustaceans, echiurans, echinoderms) (Roberts et al., 2006, Hall-Spencer and Stehfest, 2009, Freiwald et al., 2004). Due to their longevity and high biodiversity *L. pertusa* reefs have long been recognised for their conservation importance, however, more recently their benefits to commercial fisheries (Hall-Spencer and Stehfest, 2009, Husebo et al., 2002, Costello et al., 2005) and recreational activities (Henry et al., 2013) has been acknowledged. The high biodiversity, benefit to commercial fisheries and value as paleoclimatic resources means that these reefs have significant implications for local and global economic, political and social development and sustainability.

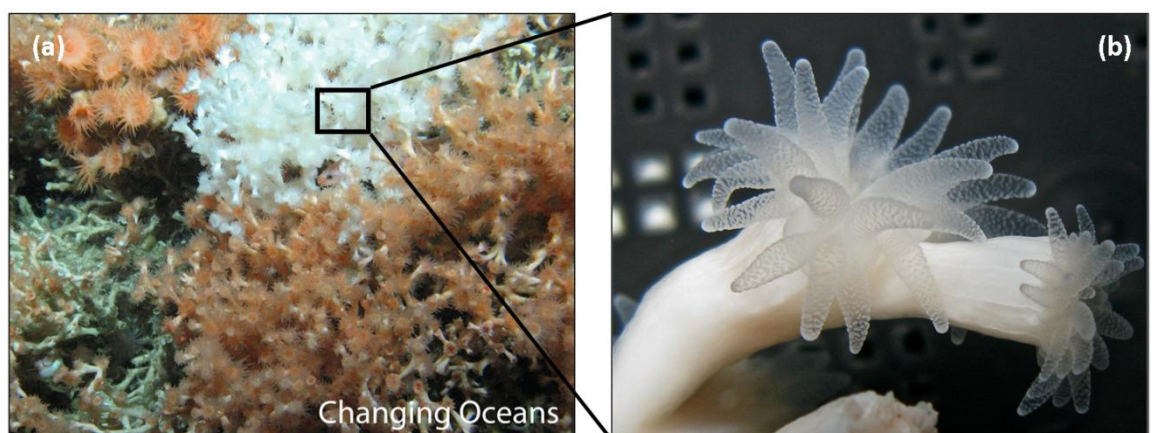


Figure 1.17 *Lophelia pertusa*, scleractinian reef framework forming cold water coral
(a) Example of *Lophelia pertusa* structures (b) Close up of a single *L. pertusa* polyp. Photographic images were taken during the Changing Oceans Expedition 2012 (RRS James Cook cruise 073).

1.4 Threats to biogenic reefs

A complex interplay of factors governs the presence and scale of biogenic reefs. Environmental conditions largely determine their development, whilst 'disturbance' of varying degrees and sources is the principle threat to their survival (Hendrick et al., 2011). The potential sources for disturbance are both natural and anthropogenic. In terms of natural disturbance this can include; storms, changes in turbidity and burial, biological competition, and predation. Anthropogenic threats include; pollution, human commercial (e.g. fishing) and recreational activity, and anthropogenically accelerated global climate change. It is likely that anthropogenic climate change is the greatest threat to marine systems in modern times, in particular elevated temperature and $p\text{CO}_2$ are of most concern for coastal systems and marine calcifiers (Harley et al., 2012).

1.4.1 Global climate change and coastal marine calcifiers

Due to its shallow depth and continental proximity, the coastal zone is likely to be more affected by global climate change than its open ocean counterpart (Scavia et al., 2002), suggesting that many biogenic reef forming organisms may be under considerable threat in the future. Projected changes in ocean chemistry have a wide range of implications for marine organisms. Temperature and pH play a crucial role in many physiological processes such as ion transport, enzyme activity and protein function (Madhus, 1988). Changes to these processes can directly impact other key functions associated with biogenic reef forming organisms (e.g. maerl and cold water corals) including, calcification, photosynthesis, acid-base homeostasis, respiration and gas exchange, and metabolic rate (GATTUSO et al., 1999, Fabry et al., 2008).

1.4.1.1 *Calcification and climate change*

The effect of global climate change on marine calcifiers is currently, and has been, the subject of significant scientific investigation with regards to the immediate future (e.g. Gattuso et al., 1998, Gattuso and Hansson, 2011, Kroeker et al., 2013b, Maier et al., 2009, Maier et al., 2013b, Martin et al., 2013b, Ries, 2011, Ries et al., 2009) and the geological past (Knoll et al., 2007). Ocean acidification is considered to be the primary threat to calcification, and thought to be responsible for a two-sided attack on marine calcifiers; reduction in their ability to calcify, and enhancing dissolution of calcium carbonate (CaCO_3) skeletal structures. This prediction has been endorsed due to the high level of confidence and robust evidence that underpins what we know about ocean acidification

(Roleda et al., 2012). Increasing ocean acidification (with increasing $p\text{CO}_2$) will lead to a decrease in the availability of carbonate ions (CO_3^{2-}) in the oceans (Gattuso and Hansson, 2011). This is important for species that combine carbonate ions with calcium to form their biogenic calcium carbonate skeletons or shells (Wicks and Roberts, 2012). These carbonate structures are composed predominantly of the most common calcium carbonate polymorphs in the biosphere (Falini et al., 1996) (calcite and aragonite). Critically, calcium carbonate minerals dissolve at low pH, with aragonite and high-Mg calcite being more susceptible than calcite (Bischoff et al., 1987). However, the response of calcification in marine organisms to elevated $p\text{CO}_2$ has been varied (Ries et al., 2009) suggesting a requirement for more understanding about the mechanisms underlying the biological responses of marine calcifiers to ocean acidification (Gattuso and Hansson, 2011). Most recently, several studies have re-evaluated the origin of the carbonate ion used in calcification (Jokiel, 2011), and how some marine calcifiers are able to modify seawater chemistry close to the site of calcification (Venn et al., 2013, McCulloch et al., 2012a). Suggesting that bicarbonate (HCO_3^-) may be the substrate for calcification (as opposed to CO_3^{2-}), derived either directly from the seawater or mitochondrial CO_2 that is converted by carbonic anhydrase (Jokiel, 2011, Roleda et al., 2012). Therefore, the primary threat to marine calcifiers under acidified conditions may in fact be dissolution rather than impaired calcification (Roleda et al., 2012). Nonetheless, evidence suggests that under acidified conditions, calcification by marine organisms is likely to be impacted, both an increase and a decrease in calcification has been observed (Ries et al., 2009). A decrease in calcification rates has implications for growth, development, and competitive interactions but, equally, an increase in calcification may require energetic trade-offs that reduce overall performance (Wood et al., 2008, Hennige et al., 2014).

1.4.1.2 Photosynthesis and climate change

Elevated temperature and $p\text{CO}_2$ is likely to impact marine primary producers in different ways (Koch et al., 2013, Harley et al., 2012). For taxa that are currently carbon-limited under elevated $p\text{CO}_2$ a benefit may be observed because CO_2 is the substrate used in photosynthesis. In calcifying photosynthesisers (e.g. red coralline algae), any benefit of increased availability of CO_2 for photosynthesis may be negated by the increased metabolic cost of calcification, and dissolution of calcified skeletons as carbonate becomes undersaturated in seawater (Nelson, 2009, Brodie et al., 2014). In a recent meta analysis photosynthesis in calcified marine algae was highly variable and reduced by an

average of 28% in response to exposure to high-CO₂ (Kroeker et al., 2013b). In general, the response of photosynthesis to acidification in non-calcified algae (i.e. fleshy algae) varied little, with generally no change or an increase observed, and growth increased by an average of 22% (Kroeker et al., 2013b). Although this apparent benefit of increased substrate for photosynthesis is only likely to occur if waters remain sufficiently cool (Brodie et al., 2014). It is suggested that the greatest threat to non-calcified algal physiology will be increasing temperature, that will ultimately lead to a significant decrease in productivity and widespread mortality (Brodie et al., 2014). Indeed, there has already been a detracting of kelp beds at their low latitudinal limits (Tuya et al., 2012, Wernberg et al., 2013). The successes of primary producers in the future will be a balance between their competitive ability for resources, resistance to herbivores, and ability to acclimatise to environmental change (Connell et al., 2013). Carbon concentrating mechanisms (CCMs) are used in some marine algae (Giordano et al., 2005) and could impact the ability of algae to utilise resources and acclimatise in the future. Thought to have evolved as a coping mechanism in response to the competition between O₂ and CO₂ for the active site on Rubisco, CCMs use energy to increase CO₂ concentration in the vicinity of Rubisco for carbon fixation (Giordano et al., 2005). Some of these mechanisms involve the primary use of HCO₃⁻, while others involve CO₂ uptake (Giordano et al., 2005). The influence of various environmental factors on CCM expression were examined in marine algae; increased photosynthetically active radiation (PAR) increased CCM expression in terms of CO₂ affinity, whilst there is little information available about the impact of temperature on CCM expression in algae (Raven et al., 2011). Decreased nitrogen and iron supply generally increased CO₂ affinity, whilst changes in phosphorous supply had varying affects (Raven et al., 2011). There is little known about the role of CCMs in red coralline algae, and currently CCMs are not part of models as to how climate change may impact algae physiology in the future (Raven et al., 2011). However, controlling CCMs may be crucial in the energetic and nutritional budgets of a cell, and may be significant in terms of maintaining primary productivity in algae in the future (Giordano et al., 2005).

1.5 Acclimatisation and adaptation to climate change

Organisms and species faced with global climate change have four options; migration, acclimatisation (i.e. tolerance), adaptation, or extinction (Gattuso and Hansson, 2011). The global extent of anthropogenic climate change and the multiple factors involved means that although migration by some species or populations may be possible, the migration due to one changing factor (i.e. acidification and changes in carbonate saturation) may be limited by another (i.e. temperature). Acclimatisation is defined as a process by which individuals adjust (i.e. a physiological adjustment) to environmental change to tolerate the new conditions (Gattuso and Hansson, 2011). Adaptation is the adjustment of species to environmental change between generations as a result of natural selection (Gattuso and Hansson, 2011). Acclimatisation by some individuals within a population allows for adaptation (Gattuso and Hansson, 2011), thus, evidence of acclimatisation potential in marine organisms will be key in predicting the 'winners' and 'losers' of the future. Prior environmental experience may influence the ability of marine organisms to adapt to climate change. Although, to date there are few studies that consider the response of marine organism to global climate change in the context of their contemporary environment. Carilli et al. (2012) demonstrated that tropical corals subjected to larger year-to-year fluctuations in maximum ocean temperature were more resistant to warming events. Johnson et al. (2014) observed that individuals existing in dynamic $p\text{CO}_2$ habitats may be acclimatised to ocean acidification, at least within the scope of *in situ* variability. These types of studies provide an insight into the potential for plasticity in habitat and species-specific responses to changing ocean chemistry (Johnson et al., 2014). Organisms have adapted to climatic changes in the past, for example hermatypic corals have survived for many millennia (Stanley, 1981), however, this period of greatly accelerated change may mean that there simply is not enough time for organisms to adapt. If organisms are not able to acclimatise or adapt to global climate change than this may result in large scale local and global extinctions, changes to geographical species distribution (Parmesan and Yohe, 2003) and widespread ecological disturbance (Portner et al., 2004).

1.6 Aims of this research

Our knowledge of how marine organisms may respond to global climate change in the future is still ambiguous, despite a considerable research effort in the last decade. Although, in general, marine calcifiers are likely to be negatively affected, within some taxa, there is considerable variability (e.g. coralline algae and corals). In addition, there are few studies that consider global climate change in the context of natural variability and run long enough to assess acclimatisation potential. Continuing research to improve our understanding of the consequences of climate change on keystone marine calcifiers should be a priority. Thus, though several separate, yet related, studies (Figure 1.1) presented in chapters 3-7 this research, with a focus on marine calcifying algae, aimed to provide a better understanding of the impact global climate change may have on key marine calcifiers, in the context of:

1. Natural variability and the role that it may play in influencing a species response to global climate change: Temporal differences in environmental conditions (i.e. seasonal and sub diel changes) and the impact that this has on the response of marine organisms to global climate change (chapter 3, 4 and 5); the influence of *in situ* environmental variability on the response of marine organisms to elevated temperature and $p\text{CO}_2$ (chapter 7), and expressed phenotypes (chapter 6).
2. Acclimatisation: provide an insight into the scope for acclimatisation to elevated temperature and $p\text{CO}_2$ (chapter 3); and the role acclimatisation to *in situ* environmental variables (e.g. low and variable pH) may play in influencing a species response to global climate change (Chapter 7).

2

Methods and techniques

This research established the effects of global climate change (i.e. increasing temperature and ocean acidification) on the physiology of marine calcifiers using Pulse Amplitude Modulation (PAM) fluorometry, SDS polacrylamide gel electrophoresis of proteins, Bradford Assay to determine total protein and mass spectrometry for protein identification. Furthermore, various techniques were employed to determine the environmental parameters associated with each study. This chapter discusses these general techniques and methodologies employed. Details of sample collections and chapter-specific methods are described in the relevant chapters.

2.1 The ocean acidification mesocosm set-up

The Ocean Acidification Mesocosm Facility was purpose built to host environmental manipulation experiments. The environmental parameters chosen to focus on in the laboratory studies performed in the present research were temperature and $p\text{CO}_2$. The temperature and $p\text{CO}_2$ levels were chosen to simulate values that may be encountered by benthic marine organisms under predicted climate change scenarios in the future and the specific levels are detailed within the appropriate chapters. The mesocosm facility houses two set-ups; (1) a set-up for performing long-term studies (i.e. years, see Figure 2.1) and, (2) a set-up for performing shorter term experiments (i.e. weeks or months, see Figure 2.2).

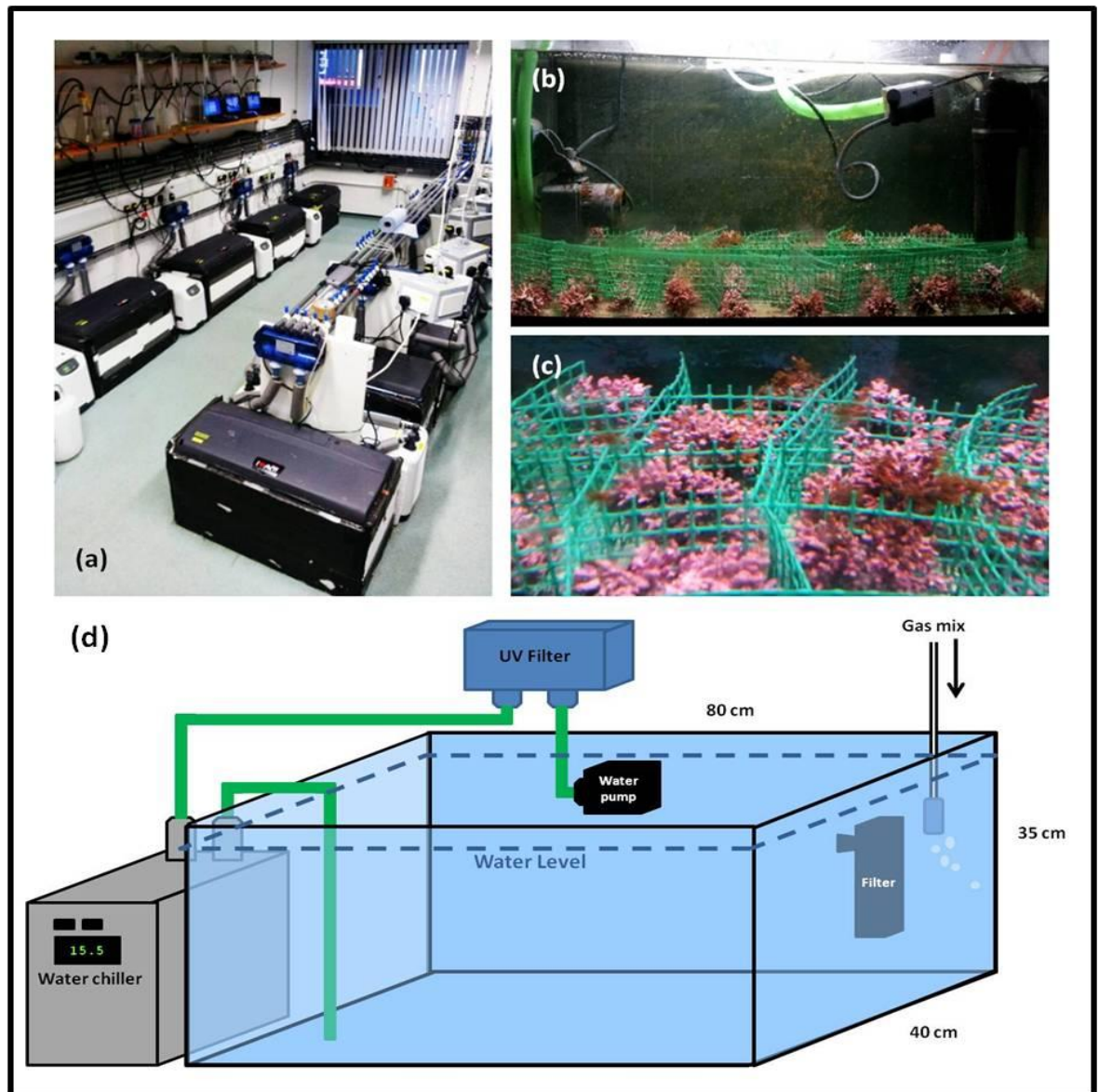


Figure 2.1 University of Glasgow Ocean Acidification Mesocosm Facility; Long-term experimental set-up (i.e. years).

(a) Overall set-up; 12 x 120 l tanks in which temperature and $p\text{CO}_2$ can be manipulated (b) The view inside one of the tanks, showing the pump system and *Lithothamnion glaciale* (c) *Lithothamnion glaciale* in individual baskets (d) schematic diagram of the long-term tank set up (this is repeated in 12 individual tanks). Photos: P. Donohue.

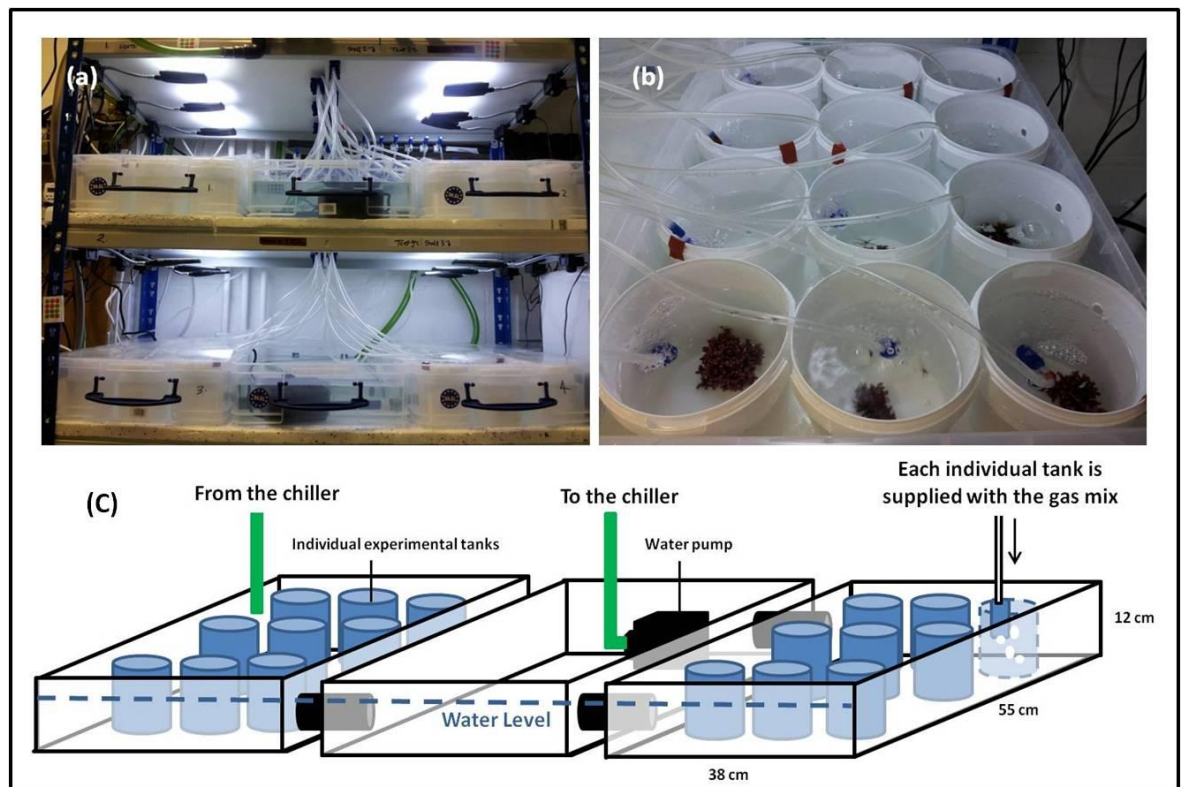


Figure 2.2 University of Glasgow Ocean Acidification Mesocosm Facility; Short-term experimental set-up (i.e. weeks and months).

(a) Overall set-up; 48 x 2 l tanks in which temperature and $p\text{CO}_2$ can be manipulated (b) Aerial view of the tanks, each containing a *Lithothamnion glaciale* thallus, with an air-line bubbling the gas mix (c) schematic of the short-term aquarium set-up (this set-up is repeated on two shelves to enable two temperature regimes). Photos: P. Donohue.

2.1.1 Seawater acidification

The $p\text{CO}_2$ level for each treatment was mixed separately. CO_2 gas was mixed with air supplied via an air pump (Resun 150L/min Air piston pump ACO-012) to produce the required treatment levels. The gas mix was then bubbled directly into each of the tank via an air-stone to produce very fine bubbles, enabling the gas mix to pass rapidly into the seawater. The gas mix was monitored continuously using a LI-COR system and computer software (LI-820 CO_2 Analyzer, LI-COR Environmental – GmbH, Bad Homburg, Germany) and $p\text{CO}_2$ was logged every five minutes (see also Riebesell et al., 2010, Widdicombe and Needham, 2007).

2.1.2 Long-term set-up

The long term set-up consisted of 12x120 L tanks (Figure 2.1). Each of the twelve tanks was filled with natural seawater and the $p\text{CO}_2$ level was controlled as described (2.1.1). Treatments were randomly assigned to each of the tanks. Seawater temperature was maintained in each tank with a water chiller (Teco Seachill TR15 Aquarium Chiller, Sterner, UK) and circulated through the chiller using an internal power head filter (Rio400

Aqua pump, TAAM 250 L water hr⁻¹), *via* an ultra violet filter (Vecton² 120 Nana UV Aquarium Sterilizer). To maintain water circulation within each tank there was also an internal jet pump (7Seio™ 620 G.P.H., 2400 LPH) and a filter (Aquael Fan2plus filter 200 L water hr⁻¹) (see Figure 2.1). Lighting was supplied to each set-up *via* one bulb attached to the centre of the lid of each tank and the photo-period was controlled with a timer (24 Hour 7 Day Digital Mains Timer, Maplin, UK) set to follow the ambient photo-period for the time of year. Photosynthetically active radiation (PAR) was maintained at 90 μmol photons m⁻² s⁻¹, an average light level recorded in Loch Sween (*in situ* maerl bed and field site) A 1/4 water change was performed every 2-3 weeks throughout the duration of the experimental period. Samples were placed in the bottom of the tank in individual baskets (Figure 2.1b, c).

2.1.3 Short-term set-up

The short-term set-up consisted of 48x1 L tanks on two shelves. A temperature treatment was assigned to each shelf, and the acidification regime was then randomly assigned to each mini tank on each shelf. Each of the forty-eight mini-tanks was filled with natural seawater and the acidified conditions in each mesocosm were controlled as described (2.1.1). Each of the tanks was placed into a water-bath, the temperature of which is maintained using a water chiller (Teco Seachill TR15 Aquarium Chiller, Sterner, UK). Water from the water-bath was circulated through the chiller using an internal power-head pump (Rio400 Aqua pump, TAAM 250 L water hr⁻¹) (see Figure 2.2). Lighting was supplied via LED lamps (48 LED clip light, 27.4 x 15.4 x 7 cm) suspended above the set-up (Figure 2.2a) to provide even lighting to all tanks and photo-period was controlled using a timer (24 Hour 7 Day Digital Mains Timer, Maplin, UK) set to follow the ambient photo-period for the time of year. Average PAR was 12 μmol photons m⁻² s⁻¹.

2.2 Pulse Amplitude Modulation fluorometry

Pulse Amplitude Modulation (PAM) fluorometry is a method used to quantify the induction and quenching of chlorophyll-*a* fluorescence in physiological studies of plants and algae. Measurement of chlorophyll-*a* fluorescence provides information about the state of photosystem II, and thus the efficiency of the photosynthetic apparatus. Other methods for assessing photosynthesis in algae include measurement of oxygen evolution (Emerson and Arnold, 1932) and stable isotope analysis (e.g. ¹⁴C (Steemann Nielsen, 1975) or ¹³C (Hama et al., 1983)), although these methods do not lend themselves well to

in situ measurements. As a noninvasive and efficient way to determine *in vivo* photosynthetic performance in algae, *in situ* and within the laboratory, PAM fluorometry was chosen for use in the present study, although measurement of oxygen evolution was used in conjunction with PAM fluorometry in Chapter 4 to directly measure net photosynthesis.

2.2.1 Chlorophyll fluorescence

The three fates of light energy absorbed by chlorophyll molecules in algae are (1) used to power photosynthesis (photochemical quenching of chlorophyll fluorescence) (2) dissipated as heat (non-photochemical quenching of chlorophyll fluorescence) (3) re-emitted as light (chlorophyll fluorescence) (Maxwell and Johnson, 2000). There is a competitive interaction between these three processes; an increase in the efficiency of one, will lead to a decrease in the yield of the other two (Maxwell and Johnson, 2000). Thus by measuring chlorophyll-*a* fluorescence, information about photochemical efficiency and photoprotective mechanisms (i.e. heat dissipation) can be acquired.

2.2.2 Modulated fluorometry

Three distinct light sources are used in PAM fluorometry; (1) a weak ($<1.0 \mu\text{mol photons m}^{-2} \text{s}^{-1}$) pulsed measuring light, (2) actinic light (light used to drive photosynthesis; $0\text{-}300 \mu\text{mol photons m}^{-2} \text{s}^{-1}$) (3) a saturating light of high intensity (up to $18,000 \mu\text{mol photons m}^{-2} \text{s}^{-1}$) (Brooks and Niyogi, 2011). The advantages of the system employed in PAM fluorometry, compared to that of conventional fluorometry, is that changes in the fluorescence yield excited by the pulsed measuring light can be isolated and quantified in a background of fluorescence intensity changes originating from the actinic and saturating lights (Brooks and Niyogi, 2011). This allows accurate determination of chlorophyll fluorescence (and photosynthetic efficiency) while in the presence of background illumination (i.e. ambient sunlight). A typical PAM trace is given in Figure 2.3 and descriptions of the parameters used in this research are given in Table 2.1.

2.2.3 Fluorescence notation

PSII reaction centres are progressively closed when algae is transferred from darkness into light, resulting in an increase in the yield of chlorophyll-*a* fluorescence. Decreasing fluorescence yield is termed fluorescence quenching. Fluorescence quenching

can be explained in two ways; (1) photochemical quenching: an increase in the rate at which electrons are transported away from PSII (due to light induced activation of enzymes involved in carbon fixation), (2) non-photochemical quenching (NPQ): an increase in the efficiency with which energy is converted into heat (Maxwell and Johnson, 2000).

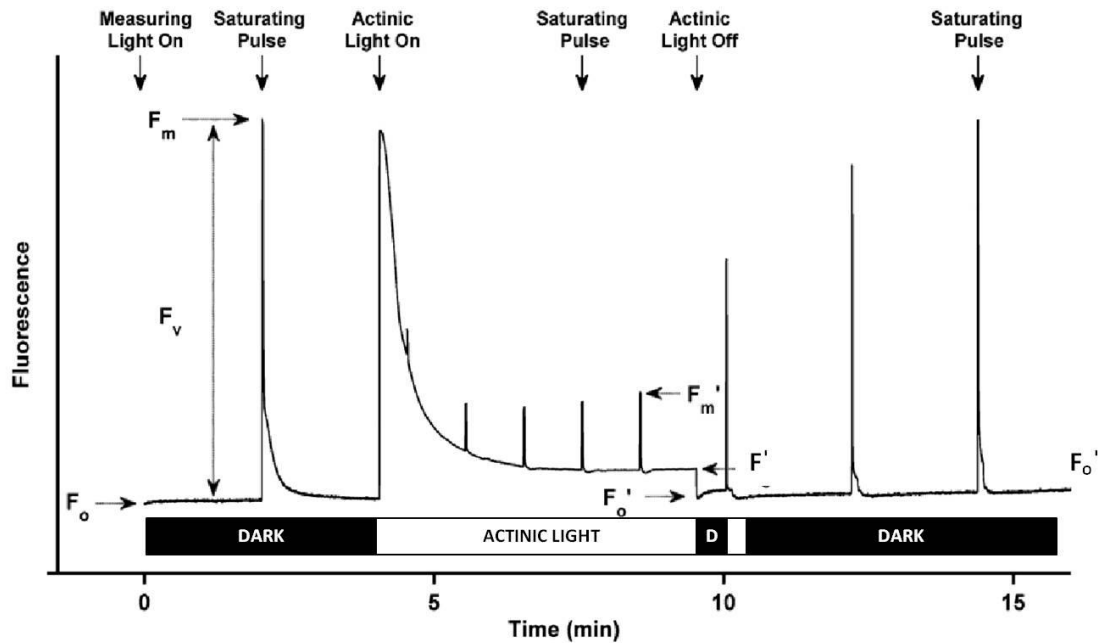


Figure 2.3 Example of a typical Pulse Amplitude Modulated (PAM) fluorescence trace. F_0 is the dark-acclimated fluorescence yield; F_m is the maximum fluorescence yield in the dark; F_v is the difference between F_m and F_0 ; F' is the fluorescence yield under actinic light; F_0' is the light-acclimated fluorescence yield; and F_m' is the maximum fluorescence yield under actinic light. Note that not all saturating pulses are labeled. All parameters and notations used in this research are detailed in Table 2.1. Source: adapted from Brooks and Niyogi (2011).

It is necessary to distinguish between photochemical and non-photochemical quenching in order to gain useful information about the photochemical efficiency of algae from measurements of chlorophyll fluorescence. This can be achieved by 'switching off' the photochemical quenching using a high intensity, short duration flash of light (i.e. saturating pulse) to momentarily close all PS II reaction centres (Quick and Horton, 1984). Allowing fluorescence yield to reach a value that would be obtained in the absence of photochemical quenching, F_m . F_m can then be compared with fluorescence under actinic light (F') and fluorescence yield in the absence of actinic light (F_0) to provide information about the efficiency of photochemical quenching and, thus the performance of PS II (Maxwell and Johnson, 2000) (Figure 2.3).

There have been attempts to normalise fluorescence notation (Kromkamp and Forster, 2003), however it still remains varied. The present research will use the notation detailed in Table 2.1.

Table 2.1 Fluorescence parameters and definitions
Fluorescence notation used in this research is consistent with this table. Fluorescence yields have instrument specific units, ratios are dimensionless.

Parameter	Definition
F_o	Minimum fluorescence (dark acclimated)
F_o'	Minimum fluorescence (light acclimated)
F_m	Maximum fluorescence (dark acclimated)
F_m'	Maximum fluorescence (light acclimated)
F'	Fluorescence under actinic light
F_v	Variable fluorescence (dark acclimated); $(F_m - F_o)$
F_v'	Variable fluorescence yield under actinic light; $(F_m' - F_o')$
F_q'	Fluorescence quenched $(F_m - F')$
F_v/F_m	Maximum photochemical efficiency or quantum yield of PSII (dark acclimated)
F_q'/F_m'	Effective photochemical efficiency or quantum yield of PSII under actinic light; $(F_m - F')/F_m'$
$F_q'/F_{m' \max}$	Calculated maximum photochemical efficiency of PSII
F_v'/F_m'	Non photochemical quenching, qN, under actinic light
F_q'/F_v'	Photochemical quenching, qP, under actinic light
NPQ	Non-photochemical quenching; $(F_m - F_m')/F_m'$
α	Initial slope of the light dependant part of a Rapid Light Curve
$rETR$	Relative electron transport rate ($\mu\text{mol photons m}^{-2} \text{s}^{-1}$)
$rETR_{\max}$	Calculated maximum relative electron transport rate ($\mu\text{mol photons m}^{-2} \text{s}^{-1}$)
E_k	Light saturation coefficient ($\mu\text{mol photons m}^{-2} \text{s}^{-1}$)

2.2.4 Dark adaptation

It is not possible to inhibit non-photochemical quenching completely; consequently it is not possible to measure chlorophyll-*a* fluorescence in the absence of non-photochemical quenching. Therefore, all estimates of non-photochemical quenching are relative to a dark-adapted point. The dark-adaptation point is determined by the time

taken to fully relax PSII, open all reaction centres, and achieve F_v/F_m . This is an essential baseline measurement upon which all other measurements were based. Dark adaptation is species specific and has already been determined for *Lithothamnion glaciale* by Burdett et al. (2012b).

2.2.4.1 Quasi-dark adaptation

Quasi-darkness can be used as a substitute to dark adaptation enabling assessment of minimal fluorescence yield (F_o) and F_v/F_m , in algae under circumstances when complete darkness is difficult to accomplish (i.e. in the field) (Hennige et al., 2008, Burdett et al., 2012b). In the present research, quasi-dark adaptation was achieved by using the Diving-SH (surface holder; see Figure 2.6b) to shade the photosynthetic tissue of the algae for 10 seconds prior to performing fluorescence measurements (Figure 2.6b). This method has been shown to cause the quantum yield to rise to >95% of the maximum quantum yield achieved after full dark adaptation for *Lithothamnion glaciale* (Burdett et al., 2012c, Hennige et al., 2008) (also see chapter 4, Figure 4.3 for demonstration of the effectiveness of quasi-dark adaptation in *Padina gymnospora*, the tropical calcifying brown algae also studied as part of this research).

2.2.5 Rapid light Curves

Rapid light curves (RLCs) provide detailed information on the saturation characteristics of electron transport and the overall photosynthetic characteristics of algae (Ralph and Gademann, 2005). Traditional light curves can assess the present photosynthetic capacity of an alga and the potential activity, over a wide range of ambient light intensities (Ralph and Gademann, 2005, Falkowski and Raven, 1997). Comparatively, RLCs measure the effective quantum yield (F_q'/F_m') as a function of irradiance (Ralph and Gademann, 2005). A single F_q'/F_m' measurement is highly dependent on the light environment immediately prior to the saturating pulse (i.e. closure of PS II reaction centres) (Rascher et al., 2000, Schreiber, 2004). RLCs assess photosynthetic activity by integrating the alga's ability to tolerate light fluctuation, in addition to reflecting its immediate short term light history (White and Critchley, 1999), particularly useful in situations where the light field is rapidly fluctuating (i.e. *in situ*) (Ralph and Gademann, 2005). The RLC takes approximately 90 seconds and records F_o , F_m' , F_q'/F_m' , and ETR. The first saturating pulse occurs after a period of quasi-darkness, and the following 8 measurements occur at 10 second intervals after stepped increasing

actinic irradiance, the levels of which are species dependent and described within the relevant chapter (see Figure 2.4 for an example RLCs).

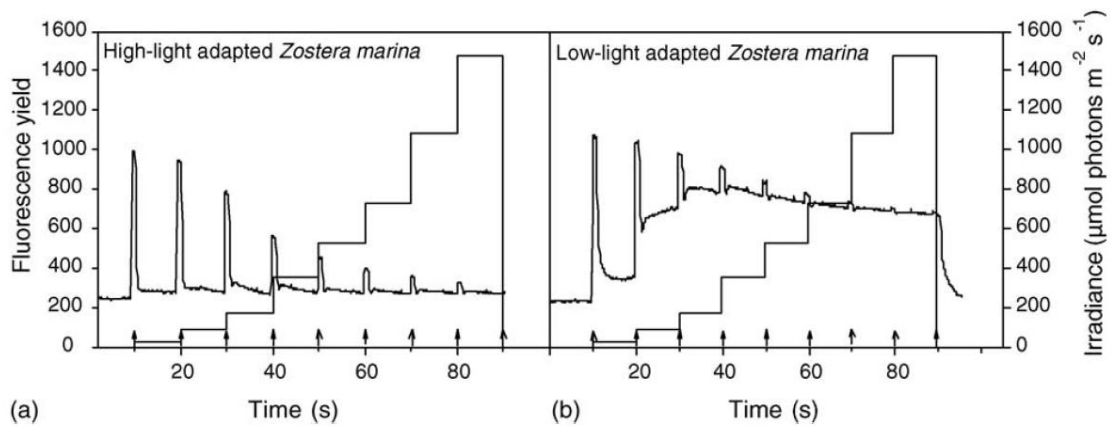


Figure 2.4 An example of chlorophyll-*a* fluorescence signals during a rapid light curve (RLC) in the seagrass *Zostera marina*. (a) High-light adapted *Z. marina* leaf (b) Low-light adapted *Z. marina* leaf. Time response curve of fluorescence yield (F_0'), showing maximum fluorescence (F_m') peaks after each saturating pulse plotted against time. The actual irradiance of the RLC is super imposed (stepped curve) and the arrows indicate the saturating pulses. Source: Ralph and Gademann (2005).

2.2.6 The diving-PAM

A Diving-Pulse Amplitude Modulation (Diving-PAM) fluorometer and Wincontrol software (Walz GmbH, Germany) (Figure 2.3) were used to make all discrete measurements of chlorophyll-*a* fluorescence during this research. The Diving-PAM has been specifically designed to operate underwater.

The Diving-PAM was used to perform rapid light curves (RLCs), set to employ a measuring-light; a pulse modulated red light emitted from a light-emitting diode (LED 650 nm), delivered to the algal thallus via a fibre optic cable (5 mm) (Figure 2.6). A surface holder (Diving-SH) (Walz GmbH, Germany) was fitted to the free end of the fibre optic cable to standardise the distance between the fibre optic tip and the surface of the algal blade (10 mm), the Diving-SH was then positioned in the centre of the algal thallus while RLCs were performed (Figure 2.6). The pulse modulated light stimulated chlorophyll-*a* fluorescence which was then detected at wavelengths above 700 nm by a PIN-photodiode (type BYP 12, Siemens) via a long-pass filter (type RG 9, Schott). This measuring-light determined the minimal fluorescence yield (F_0) for a quasi-dark adapted sample. Following quasi-darkness the thalli were exposed to a series of rapidly (10 s) changing light climates; nine increments of increasing actinic light intensity of photosynthetically

active radiation (PAR), from 2 to 1455 $\mu\text{mol m}^{-2} \text{s}^{-1}$ (specific details for each algae are given in the respective chapter), each of which was followed by a saturating light pulse. Other key Diving-PAM operational settings were: measuring intensity = 12, pulse frequency = 0.6kHz, actinic light intensity = 5, actinic width = 30 seconds, actinic light factor = 1, light curve intensity = 4, saturation width = 0.8 μm , saturation intensity = 3, gain = 9 and signal damping = 2, light offset = 0, light gain = 1, induction delay = 40 seconds, induction width = 20 seconds.



Figure 2.5 The Walz Diving-PAM underwater fluorometer
Source: Walz (2014)

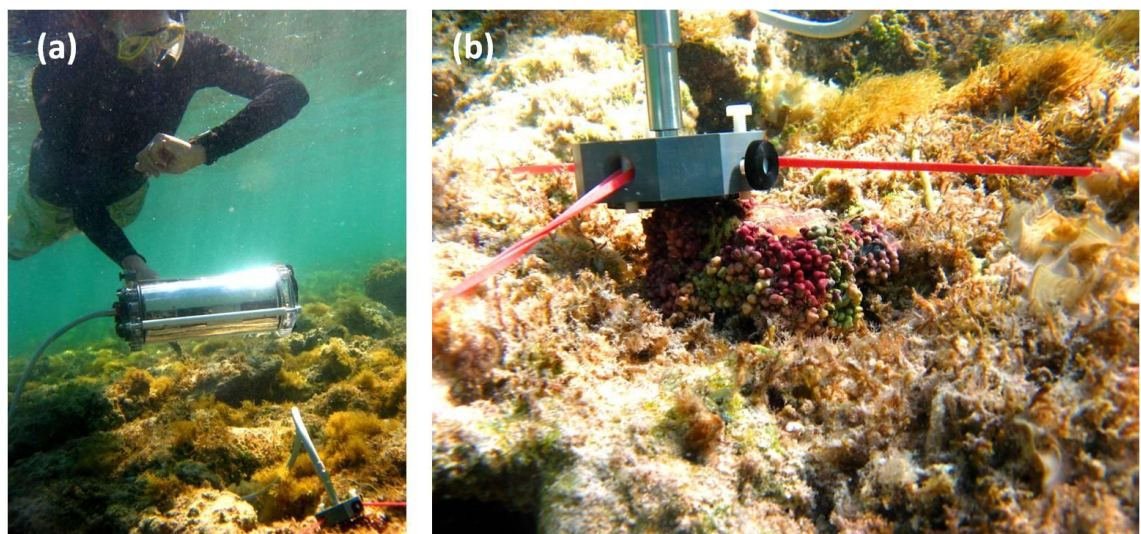


Figure 2.6 Use of the Diving-PAM in the field.
The Diving-PAM in use on a coral reef flat in Egypt, performing Rapid Light Curves on calcifying algae. (a) Snorkeler holding the Diving-PAM whilst RLCs are carried out (b) End of the fibre optic cable attached to the surface holder which is clamped in place on a free-living calcifying algae thallus. Photo: P. Donohue

2.2.7 Photosynthetic parameters

To describe the light-response of quantum efficiency the quantum yield measurements from each RLC were fitted against the following model using non-linear least squares regression (Suggett et al., 2007, Hennige et al., 2008):

$$F_q'/F_m' = [(F_q'/F_{m'_{\max}} \times E_k)(1 - \exp(-E/E_k))] / \text{PAR}$$

Equation 2.1

where, E_k ($\mu\text{mol photons m}^{-2} \text{s}^{-1}$) is the minimum saturation intensity (Hill et al., 2004), the light level at which photochemical efficiency shifts from light limitation to light saturation. PAR ($\mu\text{mol photons m}^{-2} \text{s}^{-1}$) is the photosynthetically active radiation used during the RLCs. The maximum effective quantum yield ($F_q'/F_{m'_{\max}}$) is also calculated from Equation 2.1 (Hennige et al. 2008). Using F_q'/F_m' values, the relative electron transport rate ($r\text{ETR } \mu\text{mol electrons m}^{-2} \text{s}^{-1}$) was calculated for each actinic light intensity (PAR) used in the RLCs:

$$r\text{ETR} = F_q'/F_m' * \text{PAR} * 0.5$$

Equation 2.2

$r\text{ETR}$ values were then fitted against the following model to describe the light-dependent and light-saturated $r\text{ETR}$ (α (dimensionless) and $r\text{ETR}_{\max}$ ($\mu\text{mol electrons m}^{-2} \text{s}^{-1}$), respectively) using non-linear least squares regression (Hennige et al. 2008) modified from Jassby and Platt (1976):

$$r\text{ETR} = r\text{ETR}_{\max} * [1 - \exp(-\alpha * E/r\text{ETR}_{\max})]$$

Equation 2.3

2.3 Proteins

Proteins are central to the functioning of cells and, consequently, whole organisms. The proteome refers to the entire set of protein associated with an organism, and can change over time depending on the requirements of an organisms (i.e. reproduction or growth), or stresses the organism may undergo (i.e. environmental change or pollution). Understanding how environmental change may impact the algal

proteome may be central to our understanding of the response of marine organism to global climate change in the future. The present research required a relatively rapid and efficient method for assessing changes to the algal proteome in response to changing environmental conditions. After extraction and solubilisation of proteins, 1D sodium dodecyl sulfate (SDS) polyacrylamide gel electrophoresis was used to view the proteome and interrogation by mass spectrometry was used to identify proteins.

2.3.1 Protein extraction

During the present research several methods were trialled to extract the intercellular proteins from *Lithothamnion glaciale*. The high level of calcification within each cell presented challenges for the protein extraction methodology. During all extraction methods samples were kept at 4°C.

2.3.1.1 Extraction: Method 1

The whole *L. glaciale* thallus was placed in deionised water (dH_2O) over 48 hours whilst stirring to remove any salt from the cells. Once rinsed, the sample was air dried for 72hrs. The sample was then crushed into a fine powder using an agate pestle and mortar. 1.0g of the crushed algae sample was added to 23ml of buffer (20g EDTA + 100ml dH_2O + 0.4ml of 100mM DTT) in a falcon tube (50ml). The solution was then mixed on an electronic shaker for 72 hours (EDTA (Ethylenediaminetetraacetic acid): Ca binding 1:1 ratio and DTT (Dithiothreitol) breaks sulphide-sulphide bonds). The sample was then centrifuged to separate undissolved matter and protein solution (4000 x g for 30 minutes, 4°C). Gel electrophoresis (see section 2.3.2) was then used to separate and view the extracted proteins (Figure 2.7). Improvement was required to increase the concentration of protein in solution to yield better gel electrophoresis results as the protein bands were very faint and proved difficult to use for analysis (Figure 2.7).

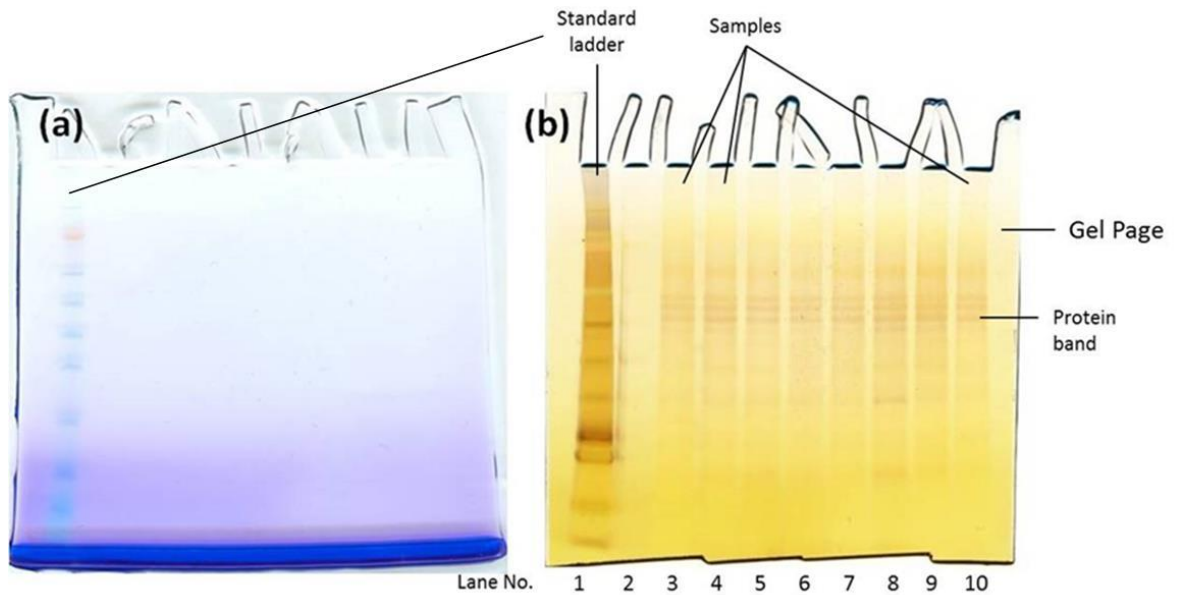


Figure 2.7 Examples of a SDS polyacrylamide gels showing extracted *Lithothamnion glaciale* proteins using method 1 (described in section 2.3.1.1). Bis-tris 4-12% SDS gel. (a) Coomassie stained (b) Silver stained. For details on electrophoresis and staining refer to section 2.3.2. The standard ladder contains a mix of proteins of known molecular weight.

2.3.1.1.1 Concentrating: Option 1

The protein solution (generated in extraction method 1, section 2.3.1.1) was transferred into centrifugal concentrator tubes (Vivaspin 20 MWCO (PES) 5,000 polyethersulfone membrane 5-20ml sample). The solution was transferred using a syringe with a syringe filter (Minisart, single use filter unit, 0.2 μ m) to remove any further particles from the solution. The solution was then concentrated down 20 x fold using a centrifuge (4000 x g, 4 °C).

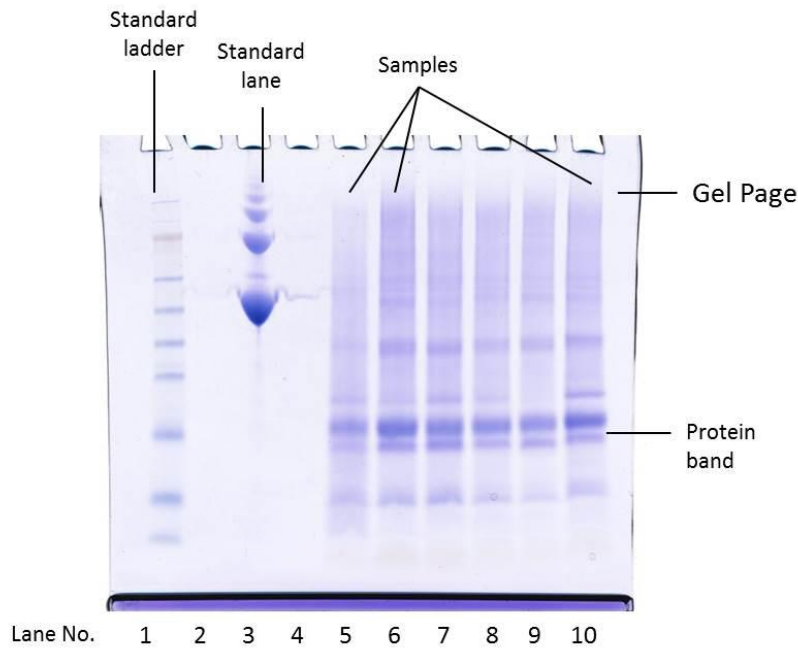


Figure 2.8 Example of a SDS polyacrylamide gel showing extracted *Lithothamnion glaciale* proteins using method 1, concentrating option 1 (described in section 2.3.1.1 and 0). Bis-tris 4-12% SDS gel, Coomassie stained. For details on electrophoresis and staining refer to section 2.3.2. The standard ladder contains a mix of proteins of known molecular weight. The standard is a known concentration of protein (bovine serum albumin, BSA).

2.3.1.1.2 Concentrating: Option 2

The protein solution (generated in extraction method 1, section 2.3.1.1) was transferred into a glass beaker (50ml) using a syringe. A syringe filter (Minisart, single use filter unit, 0.2 μ m) was attached to remove any further particles from the solution. The sample was then freeze dried for 24 h or until a powder. The protein powder was then re-solubilised in sample buffer (LDS Sample Buffer, Invitrogen, UK).

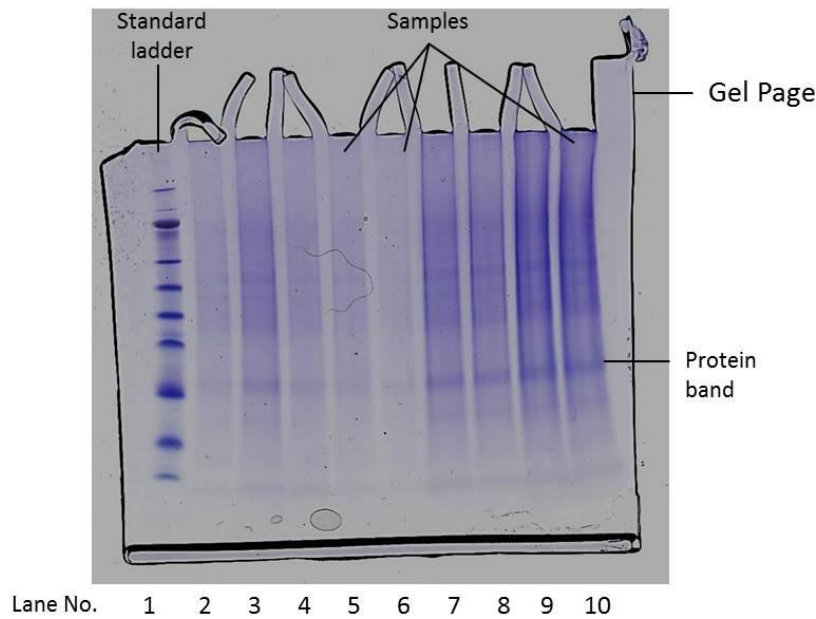


Figure 2.9 Example of a SDS polyacrylamide gel showing extracted *Lithothamnion glaciale* proteins using method 1, concentrating option 2 (described in sections 2.3.1.1 and 2.3.1.1.2). Bis-tris 4-12% SDS gel, Coomassie stained. For details on electrophoresis and staining refer to section 2.3.2. The standard ladder contains a mix of proteins of known molecular weight.

2.3.1.2 Extraction: Method 2

To improve the extraction method and increase efficiency method 2 was trialled. A known amount of sample (dependant on species/ experiment/ availability; details of which are described in the respective chapters) was ground directly in sodium dodecyl sulphate (SDS) pre-stained buffer (Invitrogen, UK, 0.5 ml) using liquid nitrogen and a pestle and mortar to produce a paste. The paste was then transferred to a microcentrifuge tube (Eppendorf, 1.5 ml), boiled for 5 min, and centrifuged at 14 000 x g. for 1 – 2 min to yield a cell-free protein extract. Protein extracts were analysed by 1D-gel electrophoresis (refer to section 2.3.2).

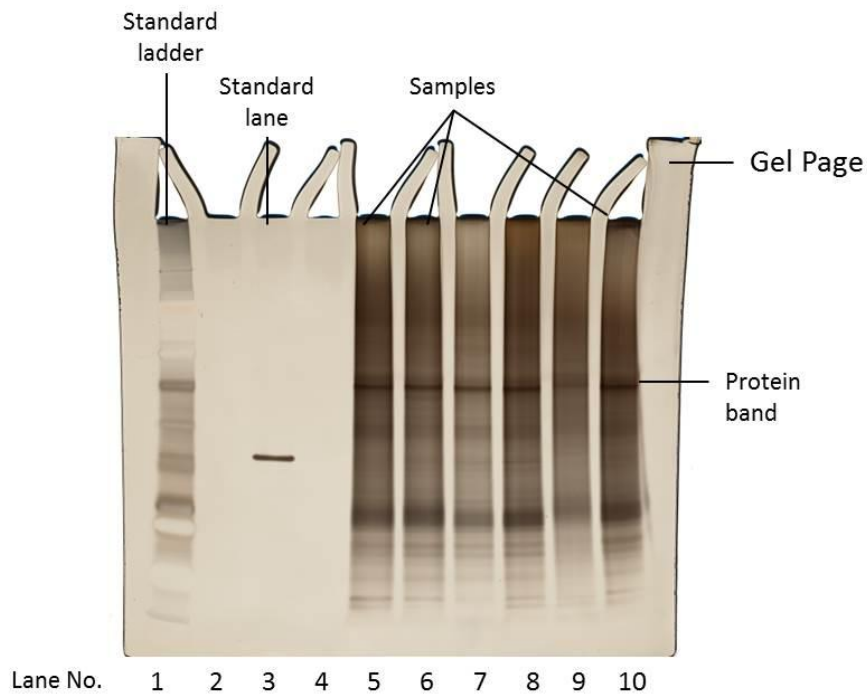


Figure 2.10 Example of a SDS polyacrylamide gel showing extracted *Lithothamnion glaciale* proteins using method 2 (described in section 2.3.1.2). Bis-tris 4-12% SDS gel, silver stained. For details on electrophoresis and staining refer to section 2.3.2. The standard ladder contains a mix of proteins of known molecular weight. The standard is a known concentration of protein (carbonic anhydrase).

2.3.1.3 Extraction: Method 3

To perform the total protein assay, solubilisation of the proteins into a clear buffer was required. The SDS buffer used in extraction method 2 was pre-stained and therefore required a slight modification. The extraction buffer was made without a stain; 0.125M Tris-HCl pH 6.8, 2% sodium dodecyl sulphate (SDS) and algae samples were ground directly into this using liquid nitrogen and a pestle and mortar to produce a paste. The paste was then transferred to a centrifuge tube (50 ml) and the slurry was centrifuged to yield a cell-free protein extract. In addition, to yield a greater concentration of proteins ml^{-1} , proteins were precipitated out of solution and then resuspended. Cold acetone was added to a sub-sample of the protein extract (4x volume acetone: protein extract). The sample was vortexed (SA8, Stuart, Staffordshire, UK) and then incubated at -20°C for > 1 hour. The sample was then centrifuged (10 mins at 13 000 x g) and supernatant was decanted. The pellet was then washed with 80% acetone and centrifuged briefly (2 mins at 13 000 x g) before supernatant was decanted and residual supernatant removed with a pipette. The pellet was then air dried for ~5 mins and resuspended in SDS sample buffer (0.125M Tris-HCl, pH 6.8, 2% SDS, 20% glycerol, 100mM DTT).

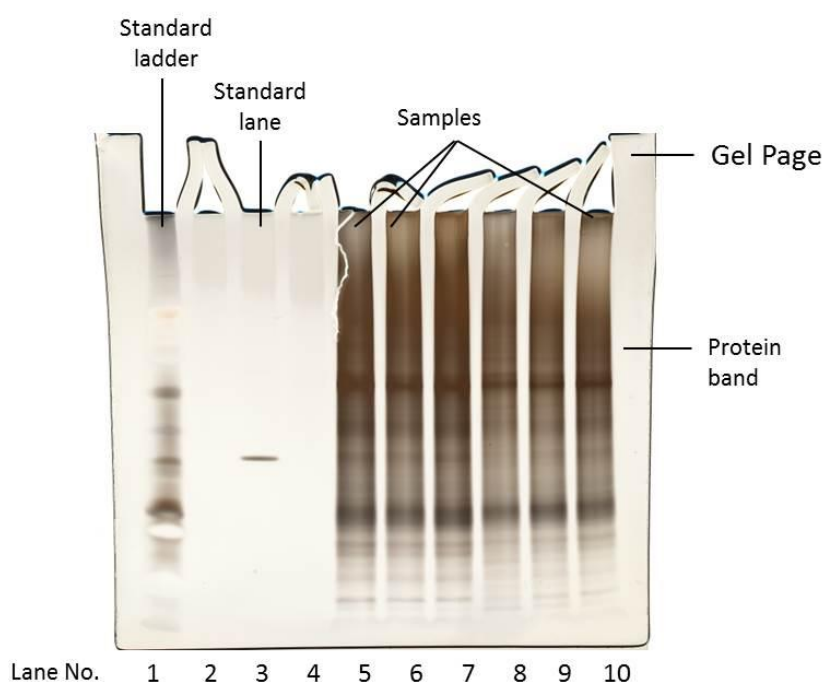


Figure 2.11 Example of a SDS polyacrylamide gel showing extracted *Lithothamnion glaciale* proteins using method 3 (described in section 2.3.1.3). Bis-tris 4-12% SDS gel, silver stained. For details on electrophoresis and staining refer to section 2.3.2. The standard ladder contains a mix of proteins of known molecular weight. The standard is a known concentration of protein (carbonic anhydrase).

2.3.1.3.1 Automated sample grinding

To further speed up the extraction process and improve consistency between samples another modification to the method was added. Algae were ground using an electronic shaker mill with agate grinding jars and balls at 30 shakes/seconds (Retsch MM400, Haan, Germany) in preference to the hand-operated pestle and mortar.

2.3.2 Polyacrylamide gel electrophoresis of proteins

For analytical separation of proteins, gel electrophoresis is often used. During electrophoresis, molecules with a net charge migrate in an electrical field. A polyacrylamide gel is used as the stationary phase because a solid gel is more easily handled than a solution, and mixing due to heating effects are minimised in the gel (Elliot and Elliot, 2005). NuPAGE Bis-Tris precast gels (4-12%, Life Technologies) were used throughout the research. The gel was such that as the proteins migrated in the electrical field towards the anode, proteins were separated by molecular sieving (i.e. the smaller proteins move faster through the gel). The proteins can be visualised in the gel as bands after staining. The benefits of using gels include; multiple samples can be run on the same gel in different tracks and if a standard mixture of proteins of known molecular

weights is included, the molecular weight of proteins in the sample can be estimated. Furthermore, the variation in the amount of different proteins within a sample can be semi-quantified and compared.

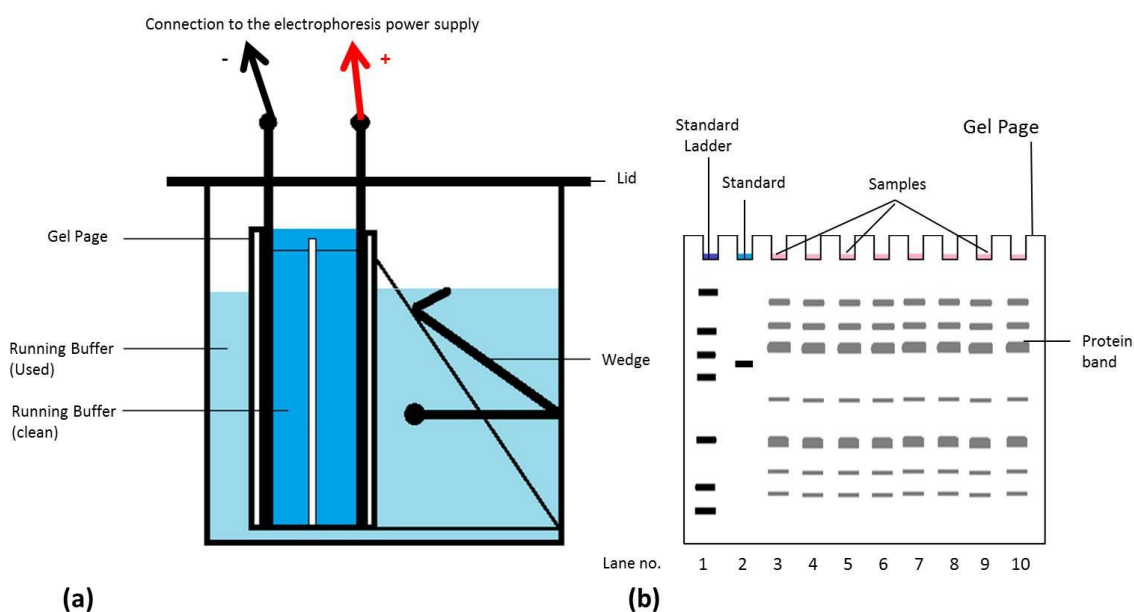


Figure 2.12 Polyacrylamide gel electrophoresis gel apparatus.

(a) The electrophoresis running apparatus including the precast polyacrylamide gel page. **(b)** A view of the gel page after electrophoresis and staining. The samples are injected into the wells through the buffer solution using a syringe. To prevent mixing of the sample with buffer, the sample buffer contains glycerol to make them dense. The standard ladder contains a mix of proteins of known molecular weight. The standard is a known concentration of protein.

2.3.2.1 Staining

To visualise the protein bands within the gels, gels were either Coomassie stained (0.1% Coomassie Brilliant Blue R250, 40% MeOH, 10% Acetic Acid) or silver stained (Life Technologies, NOVEX SilverQuest Silver Staining Kit). Silver staining is 30-fold faster and more sensitive than Coomassie staining, the greater sensitivity allowing for the detection of most proteins. However, Coomassie staining is more compatible with mass spectrometry (MS) analysis, although the SilverQuest kit mitigates the problems associated with traditional silver staining because the reagents used do not modify protein side chains and do not interfere with the trypsin digestion (required prior to MS analysis). In the present study, where possible Coomassie staining was used when MS analysis was required.

2.3.2.2 Gel image analysis

After staining, the intensity and width of the band (protein) was relative to its concentration (i.e. the wider and more intense the band the greater the protein

concentration). Intensity of the selected protein band was compared between different gel lanes using Image J analysis software to provide a semi-quantitative assessment of intracellular protein concentration (e.g. Lombardi et al., 2011) (see Figure 2.13).

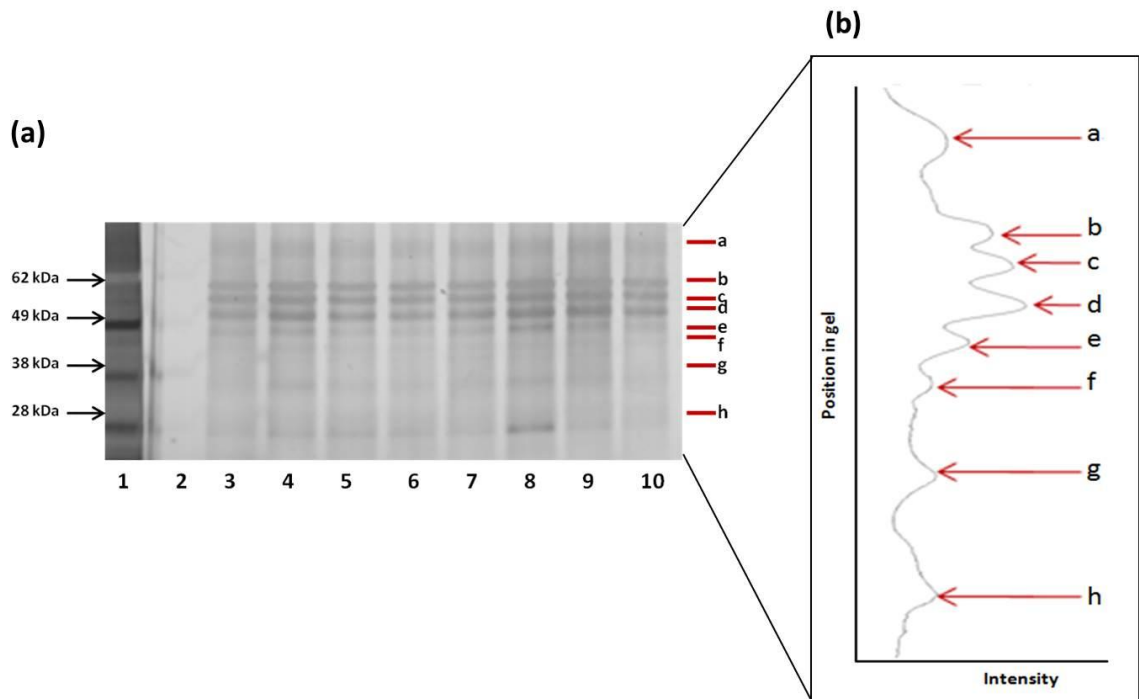


Figure 2.13 Example of gel image analysis.

(a) Polyacrylamide Bis-Tris 4-12% Gel of *L. glaciale* proteome stained with silver staining. Lane 1: prestained standard of approximate molecular weight as indicated by arrows. Lane 2: blank lane with no protein. Lane 3-10: treatments. Letter (a-h) indicate protein bands. (b) Protein intensities from *L. glaciale*. Protein intensities which are indicative of relative protein concentration are from lane 2a, scanning from top to bottom. Peaks labelled a-h correspond with labelled bands a-h in (a). Images were scanned using ImageJ software. Intensities are arbitrary units scaled to the highest intensity.

2.3.2.3 Protein identification

Proteins of known molecular weights were excised from the gel and subjected to in-gel trypsin digest, as previously described (Daneshvar et al., 2012). Peptides were solubilized in 0.5 % formic acid and fractionated on a nanoflow uHPLC system (Thermo RSLCnano), before online analysis by electrospray ionisation (ESI) mass spectrometry on an Amazon ion trap MS/MS (Bruker Daltonics). Peptide separation was performed on a Pepmap C18 reversed phase column (LC Packings), using a 5 - 85% v/v acetonitrile gradient (in 0.5% v/v formic acid) run over 45 min at a flow rate of 0.2 $\mu\text{l min}^{-1}$. Mass spectrometric (MS) analysis was performed using a continuous duty cycle of survey MS scan followed by up to ten MS/MS analyses of the most abundant peptides, choosing the most intense multiply charged ions with dynamic exclusion for 120s. MS data was processed using Data Analysis software (Bruker) and the automated Matrix Science

Mascot Daemon server (v2.1.06). Protein identifications were assigned using the Mascot search engine to interrogate protein sequences in the NCBI Genbank database, allowing a mass tolerance of 0.4 Da for both MS and MS/MS. All MS analysis was performed by the MS facility in the Institute of Infection, Immunity and Inflammation at the University of Glasgow.

2.4 Total protein quantitation

A rapid and sensitive method of the quantitation of protein is essential in many areas of biology and biochemistry. Generally, protein quantitation is a necessary step required for before isolation and/ or characterisation of proteins, and prior to submitting protein samples for chromatographic, electrophoretic and other separation analysis. In terms of relevance to environmental research and the present research, changes in total protein concentration can be indicative of physiological stress and can be used for bio-monitoring.

2.4.1 Different methods for protein quantitation

There are a variety of methods for protein quantitation. The objective of this research was to select a rapid and sensitive method, requiring the least manipulation or pre-treatment of the protein sample. The most common methods for protein quantitation are outlined below:

- Protein determination by UV absorption (Kirschenbaum, 1975, Aitken and Learmonth, 2009).
- The Lowry method (Lowry et al., 1951).
- The bicinchoninic Acid (BCA) Assay (Smith et al., 1985)
- The Bradford method (Bradford, 1976)
- Protein determinations using microwave enhancement (Akins and Tuan, 1992)
- The nitric acid method (Boerner et al., 2009)
- Kinetic silver staining of proteins (Root and Wang, 2009)

- Quantitation of cellular proteins by flow cytometry (Friedrich et al., 2009a)
- Quantitation of cellular proteins by laser scanning cytometry (Friedrich et al., 2009b)

The Bradford method, first described by Bradford (1976), is a widely used method for protein quantitation, is rapid and accurate, and has a proven track record in the literature. Therefore, this method was employed for protein quantitation of algal and coral samples throughout this research.

2.4.2 The Bradford Method for protein quantitation

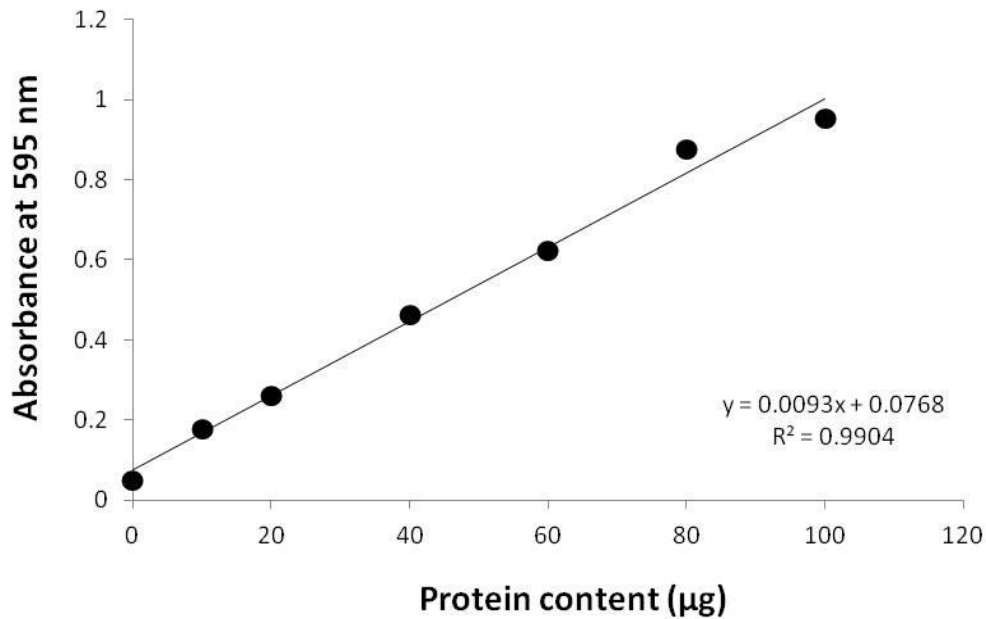
The Bradford method was used in the present study because compared to other methods (i.e. Lowry Method (Lowry et al., 1951)) the Bradford assay is simpler, faster, more sensitive, and subject to less interference by common reagents and non-protein components of biological samples (Kruger, 2009). The Bradford assay relies on a change in absorbance on the binding of the dye Coomassie Blue G250 to basic and aromatic amino acids (protein) under acidic conditions (Compton and Jones, 1985). The free dye can exist in four different ionic forms, of which the more cationic red and green forms have an absorbance maxima at 470 nm and 650 nm, respectively, in the acidic reagent solution (Chial and Splittgerber, 1993). Comparatively, the more anionic blue form of the dye, which binds to protein, has an absorbance maximum at 590 nm (Chial and Splittgerber, 1993, Kruger, 2009). Therefore, protein concentration can be estimated by determining the amount of dye in the blue ionic form (Kruger, 2009). This is achieved through measuring the absorbance of the solution at 595 nm. The absorbance maximum of the blue ionic form of the dye Coomassie Blue G250 shifts from 590 nm to 620 nm with the binding of the protein (Chial and Splittgerber, 1993), suggesting absorbance measurements at the higher wavelength would yield the best results. However, the pH of the assay means a large proportion of the dye is in the green form ($\lambda_{\text{max}} = 650 \text{ nm}$) and subsequently interferes with the absorbance measurement of the protein-dye complex at 620 nm (Kruger, 2009). Therefore, it is suggested measurement at 595 nm represents a compromise between maximising the absorbance due to the protein-dye complex while minimising the contribution from the green form of the dye (Kruger, 2009, Chial and Splittgerber, 1993, Compton and Jones, 1985, Congdon et al., 1993).

2.4.2.1 Effects of Sodium dodecyl sulfate (SDS) on the Bradford Assay

The Bradford assay is relatively free from interference by the most commonly used biochemical reagents (Kruger, 2009), however, SDS (used during protein extraction in the present study) can alter the absorbance leading to over- or under-estimations of the protein concentrations (Bradford, 1976, Stoscheck, 1990). To account for the interference caused by SDS during the Bradford assay, SDS was included in the reagent blank and calibration standards at the same concentration as that found in the samples analysed throughout this research.

2.4.3 Bradford method for quantitation of proteins in calcifying algae and coral

Proteins were extracted using the method described in section 2.2. 5 ml of the assay reagent (100 mg Coomassie Blue G250, 50 ml of 95% ethanol, 100 ml 85% phosphoric acid, and 850 ml of distilled water) was added to 30 μl of the protein solution and 70 μl of distilled water and gently vortexed. Once prepared the assay reagent was filtered through Whatman No. 1 filter paper and stored in an amber bottle at room temperature. Prior to each set of assays a calibration curve was produced (Figure 2.14). Duplicate volumes ($n = 3$) of 10, 20, 40, 60, 80 and 100 μl of bovine γ -globulin standard solution (bovine γ -globulin at a concentration of 1 mg ml^{-1} in sample buffer described in section 2.2) made up to 100 μl with distilled water and gently vortexed avoiding foaming. Absorbance at 595 nm (A_{595}) was measured in samples and standards against the reagent blank 5 minutes after vortexing.



2.14 An example of a Bradford assay standard curve using bovine γ -globulin. Values mean \pm SD.

2.4.3.1 Calculation of total protein

Using the standard curve the concentration of total protein can be calculated in each sample using the following equation:

$$\text{Total protein concentration } (\mu\text{g}) = (y - 0.0768) / 0.0093$$

Equation 2.4

where y is the absorbance at 595 nm.

2.5 Seawater sample collection

Seawater samples in both the laboratory and the field were collected as described by Dickson et al. (2007) in the 'Guide for Best Practices for Ocean CO₂ Measurements'. Seawater samples were collected using a glass syringe with a valve, and in manner which minimised gas exchange with the atmosphere. On collection, seawater samples were poisoned with mercuric chloride (50 μ l of a 100% saturated solution), and stored in 12 ml screw top borosilicate glass vials (Exetainer, Labco Ltd., UK). The samples were treated with mercuric chloride solution to prevent biological activity that may alter the carbon distributions in the sample container before analysis. The samples were stored in a cool, dark location until use.

2.6 Total alkalinity titrations

Total alkalinity (A_T) of seawater is related to the charge balance in seawater and is defined as a difference between the excess concentration of proton acceptors over proton donors in 1 kg of seawater (DOE, 1994). A_T describes the quantitative capacity of the solutes within the seawater to buffer changes in acidity (Gattuso and Hansson, 2011):

$$A_T = [\text{HCO}_3^-] + 2[\text{CO}_3^{2-}] + [\text{B(OH)}_4^-] + [\text{OH}^-] - [\text{H}^+] + \text{minor compounds}$$

Equation 2.5

A_T is a key measurement in the analytical assessment of carbon dioxide (CO_2) cycling of the ocean. In contrast to other CO_2 system measurements (e.g. dissolved inorganic carbon (DIC), pH and $p\text{CO}_2$) A_T stays constant even when CO_2 increases in seawater (i.e. via gas exchange with the atmosphere) because the charge balance of the solution stays the same (i.e. the number of proton donors generated equals the number of proton acceptors generated by these reactions). For complete CO_2 system characterisation, and for determination of the environmental conditions during experiments conducted within the present research, at least two CO_2 system measurements were required in addition to temperature (T) and salinity (S). The present research characterised A_T and $p\text{CO}_2$ (see 2.8.1) or DIC (see 2.7) for determination of experimental conditions.

2.6.1 Different methods for determining total alkalinity

A_T of a solution is defined as the capacity for solutes it contains to react with and neutralise acid, as such A_T has always been measured by some form of titrimetric procedure (Dickson, 1981). Generally the differences between the various methods relates to the location of the endpoint. The objective of this research was to select a method based on those most widely used in the literature, to enable A_T analysis to be carried out accurately, and cost- and time-effectively. Various methods for the determination of A_T are detailed below:

- Back titration method (Gripenberg, 1936, Almgren and Fonselius, 1976).
- Back titration with colorimetric determination of excess acid (Thompson and Bonnar, 1931).

- Single-step acid addition with potentiometric determination of excess acid (Culberson et al., 1970, Anderson and Robinson, 1946).
- Stepwise addition of acid to a closed titration cell and use of chemical algorithms (gran function) to determine equivalence points on the titration curve (Edmond, 1970, Hansson and Jagner, 1973, Dyrssen and Sillen, 1967).
- A non-linear least squares procedure/ modified Gran Functions to estimate the A_T potentiometric titration data using an automated, closed-cell titrator (Dickson, 1981, Riebesell et al., 2010, Dickson et al., 2007).
- Single-step acid addition with spectrophotometric pH determinations (Breland and Byrne, 1993).
- Modified spectrophotometric procedure using rapid scan linear array spectrometers (Yao and Byrne, 1998a, Yao and Byrne, 1998b).

The non-linear least squares procedure to estimate A_T from potentiometric titration method proposed by Dickson (1981), and the modified spectrophotometric procedure proposed by Yao and Byrne (1998b, 1998a) are the most widely used methods for the determination of seawater A_T and have a proven track records in the literature. Both techniques were employed during this research.

2.6.2 Automated, closed-cell, potentiometric titration procedure

The non-linear least squares method described by Dickson (1981) is the most widely used method for the determination of A_T , particularly within ocean acidification research, and is one of the recommended methods for measurement of A_T in seawater outlined in by Dickson et al. (2007) in the Guide to the best practices for ocean CO_2 measurements.

2.6.2.1 General principle

Seawater samples to be titrated were brought to 25°C using a thermostat bath (Jalabo ED, Labortechnik GmbH, Germany) capable of maintaining the temperature to within ± 0.05 °C. A known volume of sample (10 ml) was placed in a closed thermostated, titration vessel (848 Titrino plus, Metrohm, UK) where a solution of hydrochloric acid (HCl

0.1M) was automatically added in small increments (0.1-0.2 cm³) into the solution *via* a motor driven-piston burette. After each addition of acid, the total volume of acid added and the pH of the solution was recorded (913 pH Meter, Metrohm, UK). The HCl was made up in a sodium chloride background to the approximate ionic strength of seawater to maintain activity coefficients approximately constant during the titration. In addition a closed cell was used, meaning that during the analysis of the data it could be assumed total DIC remained constant throughout the titration, apart from the effect of the dilution during the titration (see Riebesell et al., 2010, Dickson et al., 2007). Once the solution had been titrated to ~pH 3 the titration is ended and the titration data was used to compute the A_T of the sample, using modified Gran Functions (where equations are rearranged to a linear form and then fitted iteratively by the method of least squares) (see Dickson et al., 2007).

2.6.2.2 Analysis of seawater reference material

A stable reference material (Certified Reference Material, A. Dickson, University of California, USA) was analysed regularly during both methods for determining A_T in seawater samples.

2.6.3 Modified spectrophotometric procedure to determine total alkalinity in seawater

The spectrophotometric procedure described by Yao and Byrne (1998a, 1998b) was selected as it allowed A_T to be determined rapidly and accurately utilising the facilities available at the University of Glasgow.

2.6.3.1 General principle

A volume of seawater (10 ml) was placed in a closed titration vessel where it was automatically titrated (848 Titrino Plus Automated Titrator, Metrohm, UK) in a single step to pH 3.9 with a solution of hydrochloric acid (HCl 0.1M). The HCl was made up in a sodium chloride background to the approximate ionic strength of seawater. The sodium chloride background of the HCl maintained activity coefficients approximately constant during the titration. The use of a closed cell meant following analysis of the data could assume total DIC remained constant throughout the titration, apart from the effect of the dilution during the titration (see Riebesell et al., 2010, Dickson et al., 2007). Acid was added to the sample during the titration via a piston burette, the titration progression

was monitored using a glass electrode, and the volume of acid added was recorded on the automated titrator. Following titration, the acidified sample was decanted into a pre-stained 10 ml cuvette (bromocresol green (BCG) SMART cuvette, Ocean Optics) and absorbance was measured at λ_{666} and λ_{414} using a spectrophotometer (Lange DR 5000™ UV-Vis Laboratory Spectrophotometer, HACH, USA) against a seawater blank. A thermostat water bath was used to bring the samples to 25 ± 0.05 °C prior to analysis.

2.6.3.2 Calculation of results

A_T of a seawater sample that has been acidified and purged of CO_2 can be written as follows (Yao and Byrne, 1998b):

$$A_T M_{sw} = N_A M_A - [\text{H}^+]_{ASW} M_{ASW} - [\text{HI}]_{\text{total}} \Delta(\text{HI}) M_{ASW}$$

Equation 2.6

where A_T is the alkalinity (mol kg^{-1} (seawater)) of a seawater sample, M_{sw} is the mass of the seawater sample (kg), N_A is the concentration of acid added (mol kg^{-1} (solution)), M_A is the mass of the acid added, $[\text{H}^+]_{ASW}$ is the excess hydrogen ion concentration in the acidified seawater (mol kg^{-1} (seawater)), M_{ASW} is the mass of acidified seawater calculated as $M_{sw} + M_A$. The final part of the equation, $[\text{HI}]_{\text{total}}$ which is the total concentration of indicator in both the protonated and unprotonated forms (mol kg^{-1} (acidified seawater)) and $\Delta(\text{HI})$ which is a term that accounts for the moles of H^+ lost or gained by the indicator in the final acidified seawater relative to the stock solution from which it is added, is not required as no indicator solution is added to the acidified seawater due the use of the SMART cuvette (Yao and Byrne, 1998b).

To take into account the temperature and salinity dependence of pH measurements, using bromocresol green as an indicator, solution pH_T is calculated as follows (Breland and Byrne, 1993):

$$\text{pH}_T = 4.2699 + 0.002578(35 - S) + \log((R(25) - 0.00131)/(2.3148 - 0.1299 R(25))) - \log(1 - 0.001005 S)$$

Equation 2.7

and

$$R(25) = R(t) \{1 + 0.00909(25 - t)\}$$

Equation 2.8

where $29 \leq S \leq 37$ and $13^\circ\text{C} \leq t \leq 32^\circ\text{C}$. The bromocresol green dissociation constant $K(\text{BCG})$ in Equation 2.7 ($-\log K(\text{BCG}) = 4.2699$ at $S = 35$ and $t = 25^\circ\text{C}$) was originally measured on the molal concentration scale. The final term in Equation 2.8 is added to provide total excess acid concentration ($[\text{H}^+]_{\text{ASW}}$) in moles per kg of solution ($\text{pHT} = -\log[\text{H}^+]_{\text{ASW}}$). The salinity dependence of the BCG dissociation constant in seawater is given at the second term in Equation 2.7 ($0.002578(35 - S)$). The absorbance ratio at 25°C in Equation 2.7 is calculated from BCG absorbance at temperature t using Equation 2.8 with $R(t) = A_{616}/A_{444}$. Equation 2.6 represents the a redetermination of the original equation (Breland and Byrne, 1993) by Yao and Byrne (1998b) to extend the determination to lower temperatures.

2.6.3.3 Analysis of seawater reference material

A stable reference material (Certified Reference Material, A. Dickson, University of California, USA) was analysed regularly during both methods for determining A_T in seawater samples.

2.7 Dissolved inorganic carbon determination

Characterisation of total dissolved inorganic carbon (DIC) is key to the analytical assessment of carbon dioxide (CO_2) cycling of the ocean and was required for complete CO_2 system characterisation of the environmental conditions during experiments. DIC content of sea water is defined as (Dickson et al., 2007):

$$\text{DIC} = [\text{CO}_2^*] + [\text{HCO}_3^-] + [\text{CO}_3^{2-}]$$

Equation 2.9

where brackets represent total concentrations of these constituents in solution (in mol kg^{-1}) and $[\text{CO}_2^*]$ represents the total concentration of all ionised carbon dioxide, whether present as H_2CO_3 or CO_2 . The concentration of the different DIC species depends on the

pH of the solution and they are related by the following chemical equilibria (Riebesell et al., 2010):



Equation 2.10

2.7.1 Different methods for determining dissolved inorganic carbon

DIC can be measured directly by acidifying the seawater sample, extracting the resulting unionised CO_2 , and measuring its amount (Riebesell et al., 2010). The objective of this research was to select a method with a proven track record, accurate, and cost- and time-effectively. Various methods for the determination of DIC are detailed below:

- Acidification/ vacuum extraction/ manometric determination (Dickson, 2010)
- Acidification/ gas stripping/ coulometric determination (Dickson et al., 2007). Coulometry is the process of determining the amount of matter transformed during an electrophoresis reaction by measuring the amount of electricity (in coulombs) consumed or produced.
- Acidification/ gas stripping/ infrared detection (Goyet and Snover, 1993)
- Closed-cell acidimetric titration (Muller and Bleie, 2008, Yao and Byrne, 1998a), although this method is not recommended for determination of DIC in this context because if the electrode used is non-Nernstian a significant error is introduced in its estimation (Riebesell et al., 2010).

Coulometric determination of DIC proposed by Dickson (2007) is one of the widely applied methods in ocean acidification research, recommended by Riebesell et al. (2010) in the 'guide to best practices for ocean acidification research and data reporting', and was employed throughout the present research.

2.7.2 Coulometric determination of dissolved organic carbon

2.7.2.1 General principle

The following method is described by Dickson et al. (2007) and carried out at the Scottish Association for Marine Science, UK. A known volume of seawater (10 ml) was transferred into the stripping chamber of a CO₂ Coulometer (with acidification module; CM5014 (version 3), UIC Ltd.) using a glass syringe. In the stripping chamber the sample was acidified with 2M HCl (~3 ml) and purged with nitrogen gas. The volume of CO₂ in the resulting gas stream was determined by trapping the CO₂ in an absorbent containing ethanolamine¹ and titrating the hydroxyethylcarbamic acid that is formed coulometrically² (see Johnson et al., 1985). The pH of the solution is monitored by measuring the transmittance of thymolphthalein indicator at ~610 nm. The relevant chemical reactions occurring in the solution are (Dickson et al., 2007):



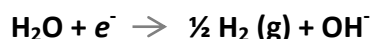
Equation 2.11

and



Equation 2.12

The hydroxide ions used are generated at the cathode by electrolysis of water:



Equation 2.13

while silver is dissolved at the anode:



Equation 2.14

¹ Ethanolamine (ETA); an organic chemical compound used for gas stream scrubbing (see JOHNSON, K. M., KING, A. E. & SIEBURTH, J. M. 1985. Coulometric TCO₂ analyses for marine studies; an introduction. *Marine Chemistry*, 16, 61-82.)

² An analytical method for determining the amount of a substance released during electrolysis in which the number of coulombs used is measured.

The overall efficiency of the coulometric procedure was calibrated using known amounts of sodium bicarbonate solution (NaHCO_3 2mM). Results were then calculated using the method described by Dickson et al. (2007).

2.7.2.2 Analysis of seawater reference material

A stable reference material (Certified Reference Material, A. Dickson, University of California, USA) was analysed regularly during this method for determining DIC in seawater samples.

2.8 Other environmental factors

2.8.1 Partial pressure of CO_2 ($p\text{CO}_2$)

$p\text{CO}_2$ was determined was monitored continuously and recorded every 5 minutes throughout laboratory experiments using a LI-COR and computer software (LI-820 CO_2 Analyzer, LI-COR Environmental – GmbH, Bad Homburg, Germany).

2.8.2 Temperature, salinity and dissolved oxygen

Temperature (t), salinity (S), and dissolved oxygen (DO) in seawater both in the field and laboratory were measured using a temperature and salinity corrected handheld meter (Pro 2030, YSI, Ohio, USA).

2.8.3 Photosynthetically active radiation

Photosynthetically active radiation (PAR, $\mu\text{mol photons m}^{-2} \text{ s}^{-1}$) was determined using PAR meters (Apogee QSO-E underwater quantum sensor connected to a Gemini voltage data logger).

2.9 CO2SYS

Additional carbonate system parameters ($p\text{CO}_2$, calcite and aragonite saturation, $[\text{HCO}_3^-]$ and $[\text{CO}_3^{2-}]$ and pH) were calculated from TA, DIC, salinity and temperature using the software program CO2SYS (Pierrot et al., 2006) with dissociation constants from Mehrbach et al. (1973) refit by Dickson and Millero (1987) and $[\text{KSO}_4]$ using Dickson (1990). Sampling depth (m) was recorded at the time of sampling using a tape measure or diving depth gauge.

3

Natural variability and the long term effects of climate change on the free living red coralline algae, *Lithothamnion glaciale*

Projected changes in seawater carbonate chemistry mean marine organisms that utilise dissolved inorganic carbon species as a substrate for physiological processes (i.e. photosynthesis and calcification) are likely to be amongst those most greatly impacted by environmental change. Long experiments can provide an important insight into the long term effects of exposure to multiple stressors. The present study is the longest laboratory study, to date, investigating the effects of global climate change on a marine calcifier.

3.1 Long term vs. short term studies

The present-day marine environment is experiencing environmental change processes. Driven by anthropogenic CO₂ emissions, these changes are unprecedented in their speed and scope. It is likely climate change will produce ‘winners’, species that are best able to cope with the changes and gain from a selective advantage, and ‘losers’, species that decline or become extinct (Brodie et al., 2014). However, there is very little

known at present about the long-term responses of most marine organisms to global climate change (Tatters et al., 2013). In particular, the response of coralline marine algae to global climate change has been varied (Brodie et al., 2014, Ries et al., 2009). The majority of studies have reported negative impacts on growth, calcification, ultrastructure, recruitment, photosynthesis and abundance (Diaz-Pulido et al., 2012, Martin and Gattuso, 2009, Hall-Spencer et al., 2008, Ragazzola et al., 2012, Kuffner et al., 2008, Kroeker et al., 2013b). In contrast, a few studies suggest calcification or photosynthesis may increase or be maintained under ocean acidification in some macroalgae (Martin et al., 2013a, Ries, 2011, Semesi et al., 2009, Burdett et al., 2012a). Furthermore, coralline algal structure may be more sensitive to rate, as opposed to the magnitude, of ocean acidification (Kamenos et al., 2013), and seasonal patterns in irradiance and temperature may alter the response of photosynthesis and calcification in algae exposed to elevated temperature and $p\text{CO}_2$ (Martin et al., 2013b). Thus, the variability in the response of coralline algae to global climate change makes prediction of their long-term response and / or trade-offs between these physiological responses difficult to predict (Ragazzola et al., 2013). The majority of studies investigating the response of calcifying marine algae to elevated temperature and $p\text{CO}_2$ have used a short-term experimental approach (i.e. weeks-months for macroalgae). Short-term studies can serve as an efficient way to gather information, and have been demonstrated to provide a reasonable proxy to predict the longer term effects of global climate change in some marine microalgae (Tatters et al., 2013). However, short-term experiments cannot assess physiological acclimation (Martin et al., 2013b) and results may be indicative of a reaction to sudden stress (Ragazzola et al., 2013). The ability and / or opportunity to acclimate has been suggested to contribute to an organism's ability to cope with global climate change (Stillman, 2003). Long-term studies (i.e. years for macroalgae) also provide the opportunity to include other environmental changes related to seasonal patterns (e.g. irradiance, day length, temperature), and assess how these may interact with global climate change (Martin et al., 2013b).

3.2 Seasonal variability and coralline algae physiology

Coralline algae abundance, size, shape, and species contribution in maerl bed varies dramatically dependent on local environmental conditions (Martin et al., 2006).

On the northwest coast of Scotland, maerl beds are primarily composed of *Phymatolithon calcareum* and *Lithothamnion glaciale*. The latter is used in this study, and it is a cold temperate species spreading from Arctic Russia to its southern distribution limit on the west coast of Scotland close to the field site examined here (Loch Sween). *L. glaciale* physiology is strongly influenced by temperature. Generally, growth rates of corallines increase with water temperature (Adey, 1970), with maximum growth rates in *Lithothamnion corallioides*, *L. glaciale* and *P. calcareum* in the summer (Adey and McKibbin, 1970, Martin et al., 2006, Potin et al., 1990, Kamenos and Law, 2010).

Temperature and irradiance are tightly correlated to seasons and have considerable influence over coralline algae metabolism (Payri, 2000, Martin et al., 2006, Martin et al., 2013b). Both photosynthesis and calcification rates in *Lithophyllum cabiochae* are strongly related to irradiance (Martin et al., 2013a). Primary productivity, respiration and calcification in *L. corallioides* also show a strong link to seasonal changes, with maximal rates reported during the summer (Martin et al., 2006). In fact, under contemporary conditions, a direct link between photosynthetic rate and calcification in coralline algae has been described (Pentecost, 1978).

Carbonate chemistry also varies seasonally in marine systems, although this variability is poorly characterised in the majority of coastal systems, with the majority of focus on tropical reef systems (Bates et al., 2010, Shaw et al., 2012, Albright et al., 2013) and more recently a temperate fjord estuary, in Puget Sound, USA (Reum et al., 2014). Carbonate chemistry covaried with temperature and oxygen depending primarily on season, and secondly on region in the fjord (Reum et al., 2014). $p\text{CO}_2$ exceeded 392 μatm during summer, winter and autumn, with widespread undersaturation of the biogenic carbonate mineral aragonite (Reum et al., 2014). During the winter $p\text{CO}_2$ values were fairly uniform throughout the water column, enriched in subsurface waters in summer, and in the autumn some values exceeded 2500 μatm (Reum et al., 2014). Variability will be different regionally dependent on; benthic community composition, biological activity (which can vary with temperature, light and nutrients), physical forcing (e.g. temperature and salinity), tidal regime, water depth and residence time (Albright et al., 2013, Anthony et al., 2011, Falter et al., 2013, Zhang et al., 2013). However, the study by Reum et al. (2014) suggests that there is seasonal variability in carbonate chemistry in coastal systems similar to sea loch systems found in Scotland. Seasonal change in seawater carbonate

chemistry is also likely to be linked to seasonal patterns in algae physiological processes, particularly those that rely on dissolved inorganic carbon (DIC; HCO_3^- , CO_3^{2-} , CO_2) as a substrate for photosynthesis and calcification. In the future, global climate change may present additional challenges to corallines further to those presented by natural seasonal change.

Salinity varied a little, in the fjord system in Puget Sound, and weakly covaried with carbonate chemistry (Reum et al., 2014). Salinity has also been shown to have a dramatic influence on Corallinacea growth rate (Adey and Mc Kibbin, 1970), although this parameter has less seasonal variation in temperate systems compared to other environmental factors (Reum et al., 2014). However, with environmental changes in precipitation patterns predicted with global climate change (Trenberth et al., 2003, Trenberth and Jones, 2007) salinity may become more significant in the future.

3.3 Growth, breakage and repair

Maerl-forming coralline algae are long-lived (up to 700 years, Frantz et al., 2005) and the growth of *L. glaciale* is extremely slow ($<1\text{mm yr}^{-1}$) (Kamenos et al., 2008b, Freiwald and Henrich, 1994). Branches of free living *L. glaciale* generally have a radial core, around which extensively calcified cells divide simultaneously to form regular growth bands (Figure 3.1 and Figure 3.9), with each subsequent band overgrowing the previous. A high-magnesium (high-Mg) calcite skeleton is deposited around each cell as the algae grow (Kamenos et al., 2008b). Growth is faster in the summer, resulting in larger, less calcified cells, and slower during the winter, leading to smaller, more calcified cells (Kamenos and Law, 2010). Growth in this manner creates internal growth bands similar to tree rings, with the live tissue (active photosynthetic cells) associated with the top few layers of cells on the surface of the algal thallus (Figure 3.1).

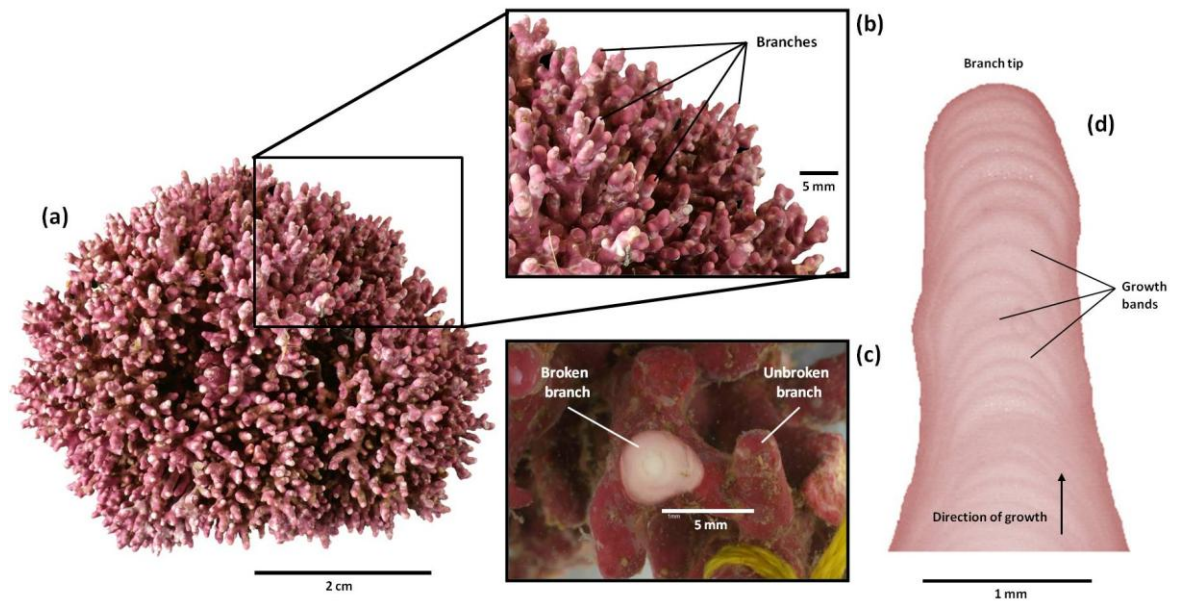


Figure 3.1 *Lithothamnion glaciale*: an example of a broken branch and a cross section showing growth bands.
 (a) *L. glaciale* thallus (b) Individual branches highlighted on an *L. glaciale* thallus (c) A broken branch exposing the calcium carbonate skeleton (d) a transverse section of an *L. glaciale* branch showing growth bands. Photo: N. Kamenos and L. Hill.

Marine organisms inhabiting coastal environments are often subject to regular hydrodynamic forces capable of causing dislodgement and / or damage. Subtidal maerl beds may not be exposed to the dramatic hydrodynamic forces experienced by their intertidal counterparts, however, wave movement and tidal flow above the maerl bed can cause thalli to roll and move. Since thalli lack flexibility, this process can cause branches to break. Furthermore, repeated insults from hydrodynamic forces may cause structural materials to fatigue and eventually fail (Denny et al., 2013). Branch breakage on free living *L. glaciale* thalli results in a reduction in the surface area of live tissue, and exposure of calcium carbonate skeleton (Figure 3.1). The ability of the algae to repair damage may have significant implications for algae survival.

3.4 Aims of the chapter

This chapter aims to investigate the differences in photophysiological characteristics, growth and repair, and calcification of *Lithothamnion glaciale* in response to elevated temperature and $p\text{CO}_2$ over a two year laboratory experiment. In addition, a field study was conducted to investigate natural seasonal changes in environmental conditions (temperature, irradiance, carbonate chemistry) and algal physiology over twelve months. The inclusion of a field study, alongside the laboratory experiment, will

help to distinguish between changes in algae physiological processes that occur naturally and those changes that may happen in response to anthropogenic change. In addition, identification of natural seasonal patterns in the environmental conditions experienced by coralline algae will provide a basis for identifying control conditions during climate change experiments and highlight the range of conditions organisms may currently experience in this, and similar coastal ecosystems. Comparison of the response of the algae in the field with the control treatment in the laboratory will also provide information about stress caused by laboratory conditions and handling.

It was hypothesised that exposure to multiple stressors would have a negative impact on *L. glaciale* physiology and growth, and *in situ*, algae physiology would follow seasonal patterns in temperature and irradiance, and day length.

Herein this chapter will be divided into two sections (a) field study (b) laboratory study with an overall discussion at the end.

Part a: field study

3.5 Methods

3.5.1 Study site

The field site was a free-living coralline algal aggregation (a maerl bed) located in Loch Sween on the west coast of Scotland, UK (56°01.99'N, 05°36.13'W). This is a typical maerl bed composed of primarily *Lithothamnion glaciale*. The maerl bed is at ~4-6 m depth and ~2 km in length and lies in the centre of an 80 m wide channel (Figure 3.2). Tidal currents are greatest in the centre of the channel which reduces sedimentation on the maerl bed. This site is undisturbed from trawling, fish farming and other anthropogenic perturbations.

3.5.2 Sampling points

To determine temporal (monthly) changes and spatial variation (above the maerl bed vs. above the sandy bedside) in seawater chemistry, and temporal (monthly) changes in the physiology of *L. glaciale* a time series was conducted over a 13 month period between February 2012 and March 2013 at 1-2 monthly intervals (average time between sampling was 7 weeks): T2, T3, T4, T7, T8, T10, T12, T13, and T14 (where T0 (month) was

January in year 1). Samples of seawater and algae were collected at irregular intervals to avoid inadvertently following algal circadian rhythms. Seawater samples were collected from two locations (1) above (10 cm) the maerl bed and, (2) above (10 cm) the sandy bedside (see Figure 3.2). *L. glaciale* samples were collected randomly from the maerl bed, and photosynthetic efficiency and calcification rate were determined *in situ* using PAM fluorometry and *in situ* incubations, respectively.

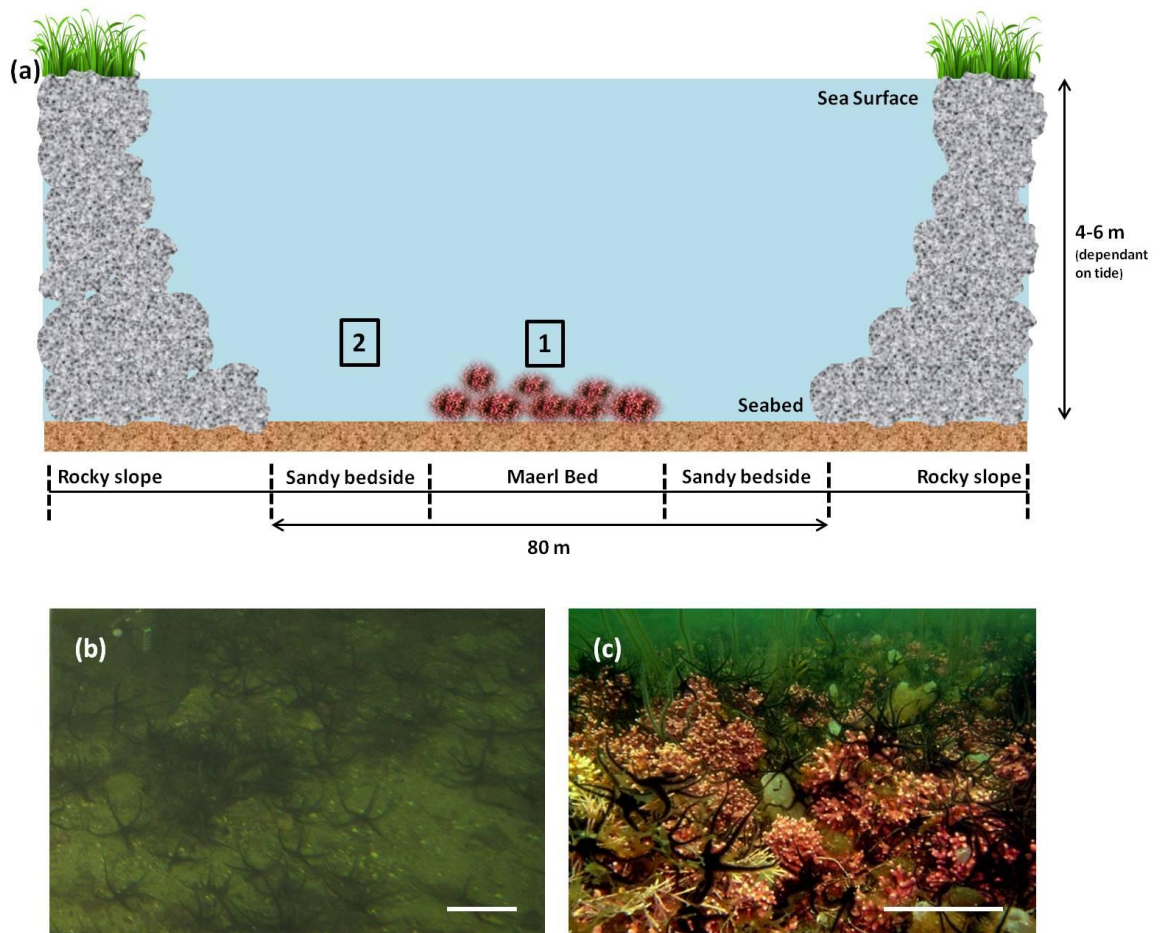


Figure 3.2 Field site in Loch Sween, Scotland. (a) Schematic cross-section of Loch Sween and the two locations for seawater sampling (not to scale). 1: above (10 cm) the maerl bed, 2: above (10 cm) the sandy bedside (b) Sandy bedside (c) Aggregation of free-living coralline algae (maerl bed). Scale bars: 5 cm. Photos: N. Kamenos.

3.5.3 Environmental parameters

3.5.3.1 Carbonate chemistry

Total alkalinity (A_T) and dissolved inorganic carbon (DIC) were determined from seawater samples as described in Chapter 2 (section 2.6) and salinity and temperature were recorded *in situ* using a handheld conductivity meter (Pro 2030, YSI, Ohio, USA). Additional carbonate system parameters were then calculated using the software program CO2SYS as described in Chapter 2 (section 2.9).

3.5.3.2 Other environmental parameters

Photosynthetically active radiation (PAR, $\mu\text{mol m}^{-2} \text{s}^{-1}$) was recorded *in situ* on the day of sampling using a PAR meter placed on the maerl bed (Apogee QSO-E underwater quantum sensor connected to a Gemini voltage data logger). Depth was recorded on a dive computer (Suunto Zoop dive computer, Faversham, UK). Dissolved oxygen (% DO) was measured *in situ* using a temperature and salinity corrected handheld meter (Pro 2030, YSI, Ohio, USA) operated from the seawater surface on a 10m cable.

3.5.4 Photosynthesis

3.5.4.1 Chlorophyll-a fluorescence (PAM fluorometry)

Rapid light curves (RLCs) were used to determine photochemical efficiency of *L. glaciale* at each sampling time point in the field ($n = 10$). Maerl thalli were randomly selected and a diving-PAM was used to carry out RLCs in accordance with methods detailed in Chapter 2 (section 2.2).

3.5.5 Proteins

3.5.5.1 Protein extraction and solubilisation

Samples of *L. glaciale* were collected by hand using SCUBA. Samples were frozen immediately in liquid N_2 upon collection and kept frozen (-20°C) until analysis to ensure that the proteins were preserved. *L. glaciale* samples were processed in accordance with methods described in Chapter 2 for quantification of total protein (section 2.4), Rubisco and phycoerythrin concentration (section 2.3.2).

3.5.6 Calcification

The total alkalinity anomaly technique (Smith and Key 1975; Ohde and Hossain 2004) was used to determine calcification rate in *L. glaciale*. In the field this analysis was performed *in situ* at each sampling time point: individual maerl thalli ($n = 5$) were randomly selected and incubated in 1 litre glass chambers for ~ 2 h on the seabed in Loch Sween. Samples of the incubation water were taken at the beginning and end of the incubation period. A_T was then determined using the methods described by Yao & Byrne (1998) (described in Chapter 2) and calcification ($\mu\text{mol CaCO}_3 \text{ g h}^{-1}$) was calculated using the following equation:

$$\text{Calcification} = 0.5(\Delta A_T) \cdot V / \Delta T / \text{TDW}$$

where ΔA_T is the change of total alkalinity (mol/kg), W is the weight of experimental seawater (kg) and ΔT is the experimental period (h).

3.5.7 Statistical analysis

One-way ANOVAs were used to investigate differences in calcification, photosynthetic characteristics, and protein concentration in algae between each time point. Where assumptions of ANOVA could not be met, data were either \log^{10} transformed or a non-parametric Kruskal- wallis test was used. Differences between means/ medians were considered to be significant when $p \leq 0.05$. All analysis were conducted using SPSS v10.0.

3.6 Results

3.6.1 Environmental parameters

The carbonate chemistry parameters recorded in both the laboratory and the field over the experimental period are summarised in Table 3.1. Temperature, salinity, irradiance and photoperiod are summarised in Figure 3.3.

Table 3.1 Parameters of the carbonate system in Loch Sween in each season.

	pH	A_T ($\mu\text{mol kg}^{-1}$)	$p\text{CO}_2$ (μatm)	HCO_3^-	CO_3^{2-} ($\mu\text{mol kg}^{-1}$)	DIC	Ω_{cal}	Ω_{ara}
<i>Above maerl bed</i>								
Summer	8.33±0.04	2367.02±11.1	104.43±3.34	1765.10±6.67	241.99±6.1	2013.71±5.3	5.85±0.1	3.66±0.1
Autumn	8.3±0.05	2433.54±21.5	118.58±7.62	1853.37±8.95	234.68±12.3	2095.57±3.4	5.68±0.3	3.55±0.1
Winter	8.42±0.01	2399.12±19.22	108.12±11.65	1796.29±26.34	243.57±19.1	2046.73±7.9	5.91±0.4	3.69±0.2
Spring	8.43±0.09	2525.17±7.22	85.74±26.66	1730.20±120.7	304.25±25.14	1939.61±37.5	7.33±0.60	4.59±0.38
<i>Above sandy bedside</i>								
Summer	8.25±0.01	2364.73±2.29	112.08±2.64	1787.68±8.15	231.71±3.23	2026.47±5.28	5.60±0.07	3.51±0.04
Autumn	8.23±0.03	2386.85±21.84	144.24±11.96	1889.37±11.98	200.38±14.10	2098.91±1.36	4.86±0.34	3.09±0.21
Winter	8.39±0.01	2372.21±8.09	113.71±1.79	1804.01±10.23	228.98±0.78	2040.85±9.57	5.56±0.02	3.47±0.01
Spring	8.34±0.01	2401.82±13.87	115.45±3.54	1811.37±3.75	236.74±6.72	2055.34±5.09	5.69±0.16	3.57±0.10

The values reported are means±SE. Total alkalinity (A_T) and DIC (dissolved inorganic carbon) were measured; pH, $p\text{CO}_2$, HCO_3^- , CO_3^{2-} , calcite saturation (Ω_{cal}), aragonite saturation (Ω_{ara}) were calculated using CO2SYS. Summer: July and August 2012; Autumn: October and December 2012; Winter: January and February 2013; Spring: April and May 2013.

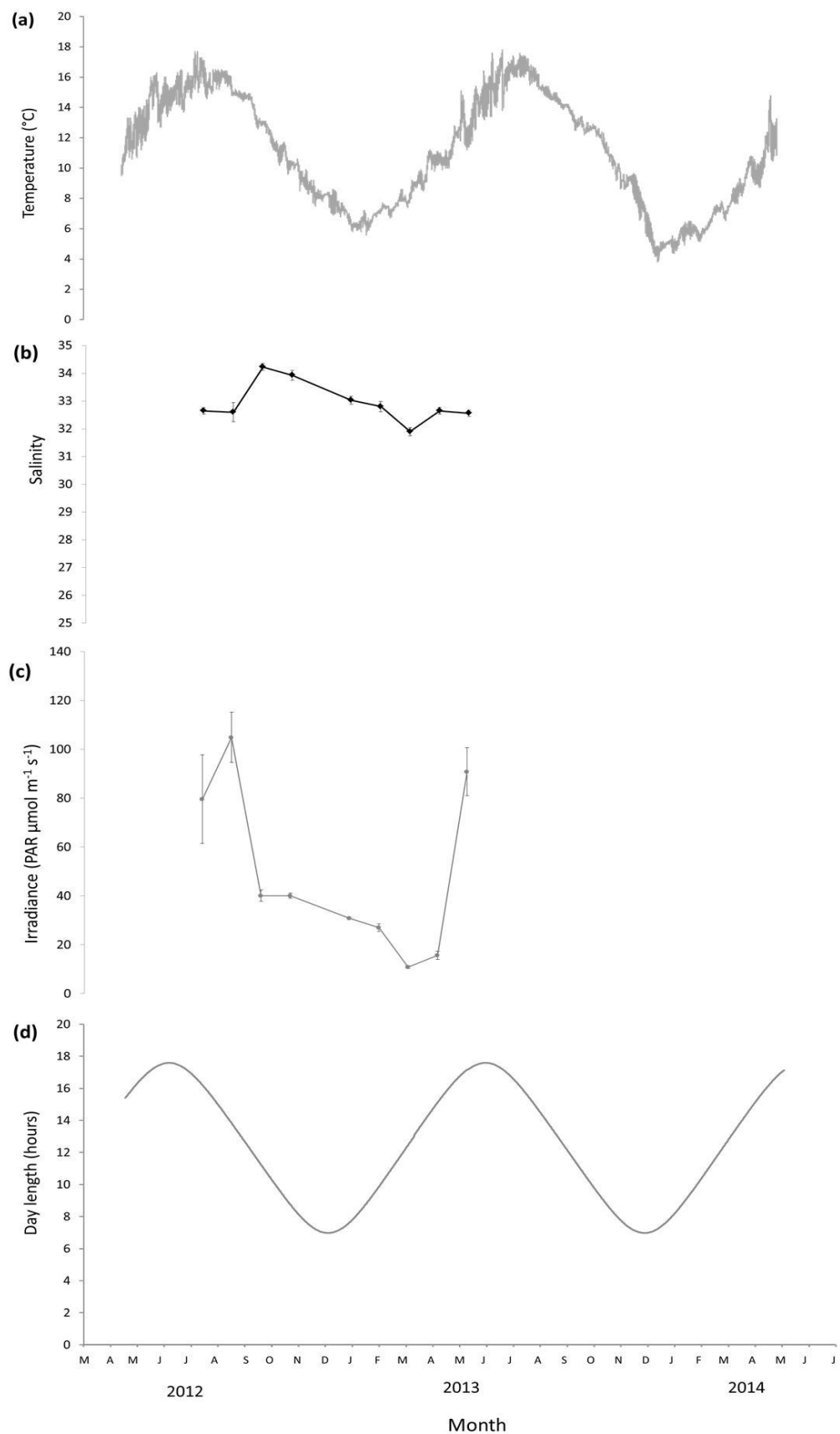


Figure 3.3 Changes in temperature, salinity, irradiance and photoperiod in the field. (a) Temperature (°C) (b) Salinity (c) Irradiance ($\mu\text{mol m}^{-2} \text{s}^{-1}$) (d) day length (hours). Temperature and PAR (photosynthetically active radiation) measurements in Loch Sween were made on the maerl bed (depth = 5-6 m, depending on tide).

3.6.2 Photosynthesis

3.6.2.1 Chlorophyll-a fluorescence (PAM fluorometry)

3.6.2.1.1 Calculated photosynthetic characteristics (Fq' / Fm'_{max} , E_k , α , $rETR_{max}$)

The calculated photosynthetic characteristics of *L. glaciale* significantly changed dependent on the month in which samples were collected (Figure 3.4). In months where irradiance and temperature were highest, $rETR_{max}$ and E_k were greater compared to months where temperature and irradiance were lowest ($F_{1, 71} = 8.494$, $p < 0.001$ and $F_{1, 71} = 9.147$ and $P < 0.001$, respectively). Fq' / Fm'_{max} and α were significantly greater during October 2012, with the lowest values reported during July/ August 2012 and February/ March 2012 ($F_{1, 71} = 3.058$, $p = 0.007$ and $F_{1, 71} = 3.157$ and $P = 0.048$, respectively) (Figure 3.4).

3.6.2.1.2 Measured photochemical parameters (photochemical quenching) (Fq' / Fm' , qP and $rETR$)

Photochemical quenching parameters differed between seasons. Photochemical data from months in each season were pooled to produce light-response curves of photochemical quenching parameters (described by Fq' / Fm' , qP and $rETR$); summer: July and August; autumn: October and December; winter: January and February; Spring: May and June. Fq' / Fm' , qP and $rETR$ were greatest during spring and autumn compared to the winter and the summer (Figure 3.5).

3.6.2.1.3 Photoprotective parameters (non-photochemical quenching) (qN)

Non-photochemical quenching data were pooled to produce light-response curves of photochemical quenching parameters (described by $1-qN$); summer: July and August; autumn: October and December; winter: January and February; Spring: May and June. qN (plotted as $1-qN$, Figure 3.6) was greatest in *L. glaciale* during the summer and spring and lowest during the autumn and winter. qN is a calculation of the decrease in fluorescence due to non-photochemical quenching, therefore by plotting the reciprocal ($1-qN$) a decrease in the qN number represents an increase in non-photochemical quenching.

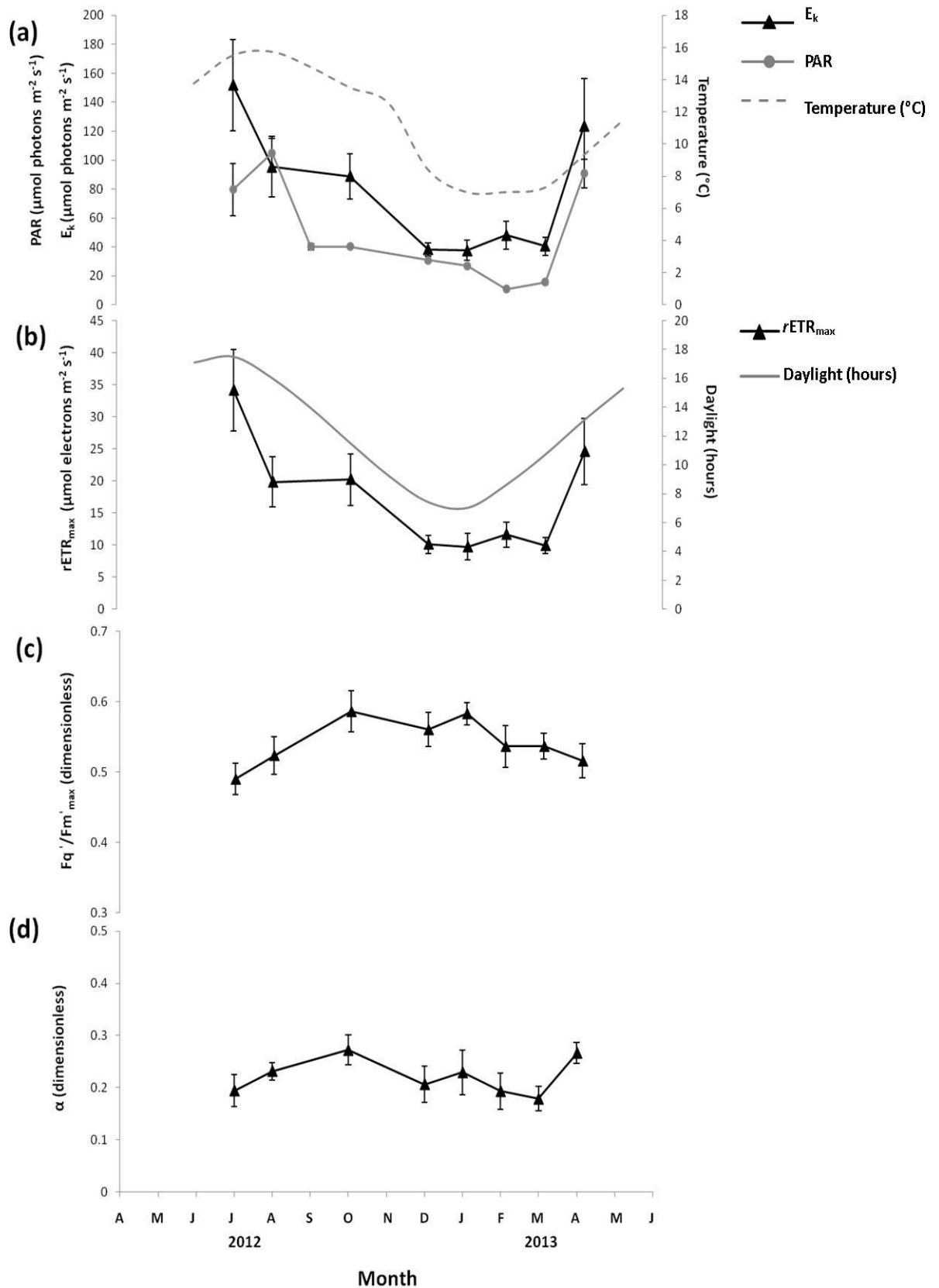


Figure 3.4 Calculated photosynthetic characteristics of *L. glaciale* collected *in situ* in Loch Sween (field site) over a 12 month period.

mean \pm SE. (a) $rETR_{\text{max}}$ ($\mu\text{mol electrons m}^{-2} \text{s}^{-1}$) and environmental parameters recorded in Loch Sween (b) E_k ($\mu\text{mol photons m}^{-2} \text{s}^{-1}$) (c) $F_q' / F_m'_{\text{max}}$ (dimensionless) (d) α (dimensionless). Solid black triangles = calculated parameters; grey dotted line = temperature ($^{\circ}\text{C}$) measured *in situ*; grey circles = photosynthetically active radiation (PAR) ($\mu\text{mol photons m}^{-2} \text{s}^{-1}$) measured *in situ*; solid grey line = daylight (hours) measured *in situ*.

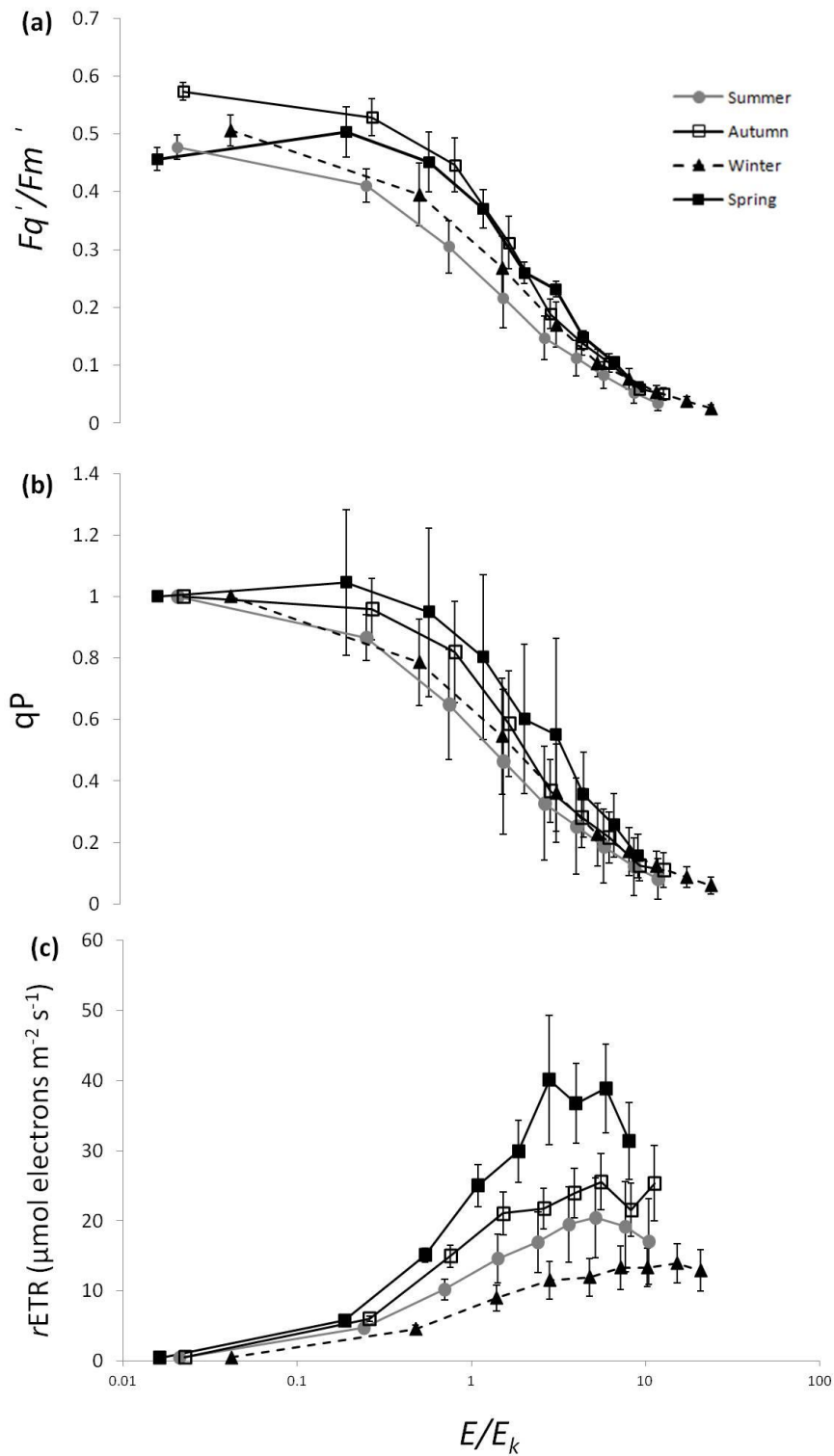


Figure 3.5 Photochemical response of *Lithothamnion glaciale* in Loch Sween during summer, spring, autumn and winter. Mean \pm SE. Data normalised to E/E_k . (a) Fq' / Fm' (dimensionless) (b) qP (dimensionless) (c) $rETR$ ($\mu\text{mol electrons m}^{-2} \text{s}^{-1}$). Summer: July/ August; Autumn: October/ December; Winter: January/ February; Spring: May/ June. $E = \text{PAR}$; $E_k = \text{optimum light level for efficient photosynthesis}$. E/E_k is used to allow for comparison between treatments when E_k is different between samples (1= optimum light level)

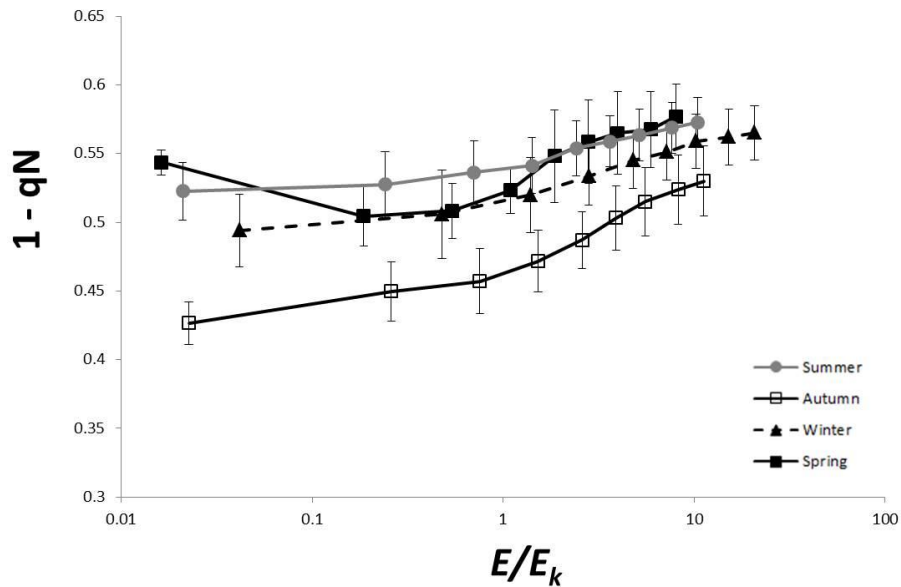


Figure 3.6 *Lithothamnion glaciale* photoprotective response ($1-qN$) during summer, autumn, winter and spring in Loch Sween (field site). Data normalized to E/E_k . Values reported are mean \pm SE. E/E_k is used to allow for comparison between treatments when E_k is different between samples (1= optimum light level)

3.6.3 Proteins

3.6.3.1 Field: Total Protein

Total protein concentration in *L. glaciale* in Loch Sween did not differ significantly in between months ($F_{8, 52} = 0.34$, $P = 0.625$) (Figure 3.7). Although there is a seasonal pattern; lowest values observed during summer (August) and the greatest values observed during the autumn (December).

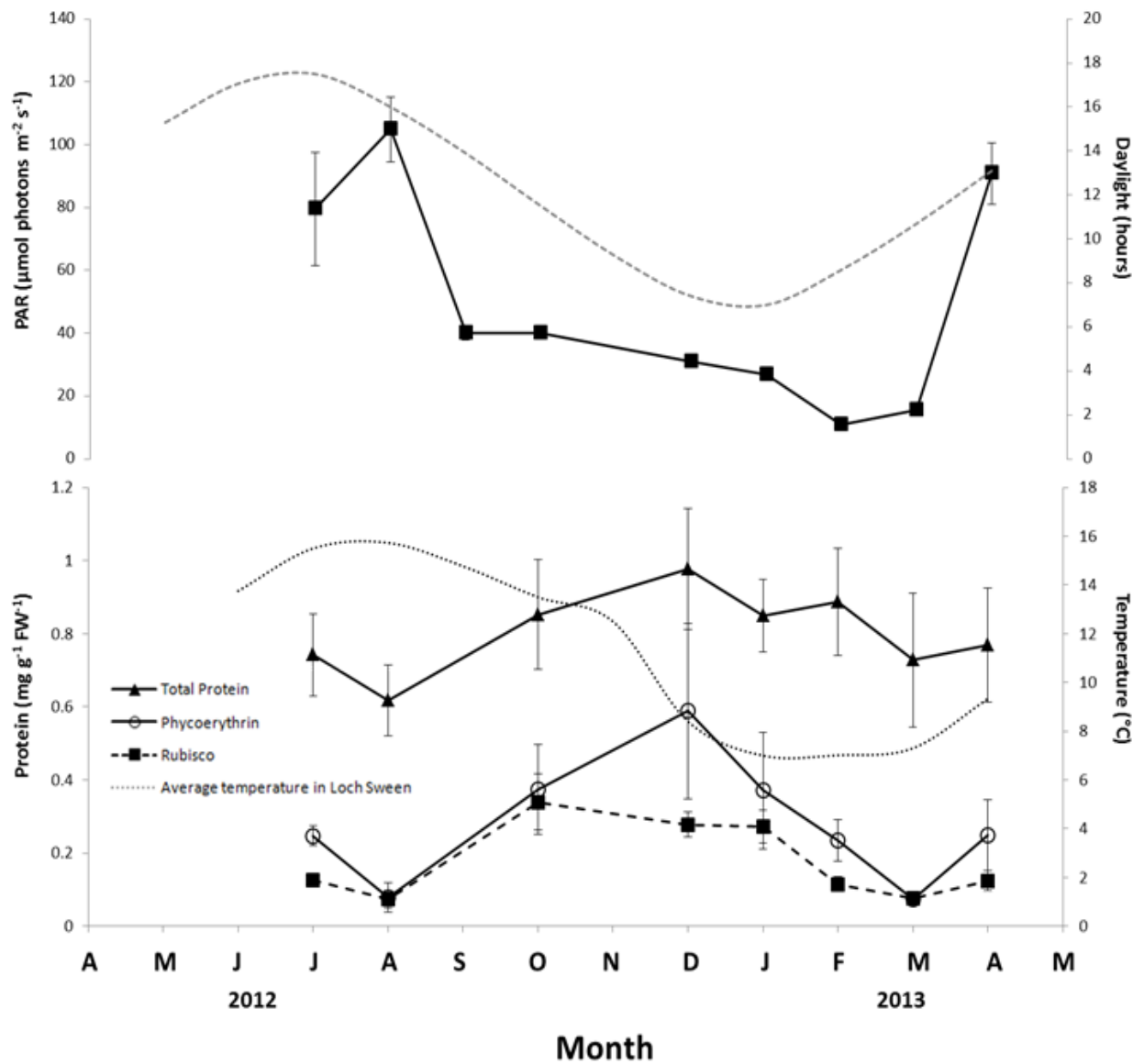


Figure 3.7 Protein concentrations (mg g^{-1} (fresh weight) FW^{-1}) in *L. glaciale* collected from Loch Sween (field site) over a 12 month period. mean \pm SE. Solid grey line: Mean temperature ($^{\circ}\text{C}$) in Loch Sween over 12 month sampling period; Dashed grey line: Day length (hours of light); Black squares: mean PAR (photosynthetically active radiation) $\mu\text{mol m}^{-2} \text{s}^{-1}$. NB. Where error bars are not visible, the error is so small that view of the error bar is obstructed by the symbol on the graph.

3.6.3.2 Field: Rubisco and phycoerythrin

Rubisco and phycoerythrin concentration in *L. glaciale* differed significantly between each month in samples collected from Loch Sween (field site) over a 12 month period ($H_{8,52} = 28.47$, $p < 0.001$, $H_{8,52} = 35.62$, $p < 0.001$, respectively). In general, Rubisco and phycoerythrin concentration was greatest during autumn (December) and lowest during summer (August) and spring (May) when *in situ* PAR was close to its lowest (Figure 3.7).

3.6.4 Calcification

Rate of calcification observed in *L. glaciale in situ* in Loch Sween differed significantly between months ($F_{8,52} = 23.58$, $p = 0.004$) (Figure 3.8). In general calcification increased during the months where temperature, irradiance and day length were greatest.

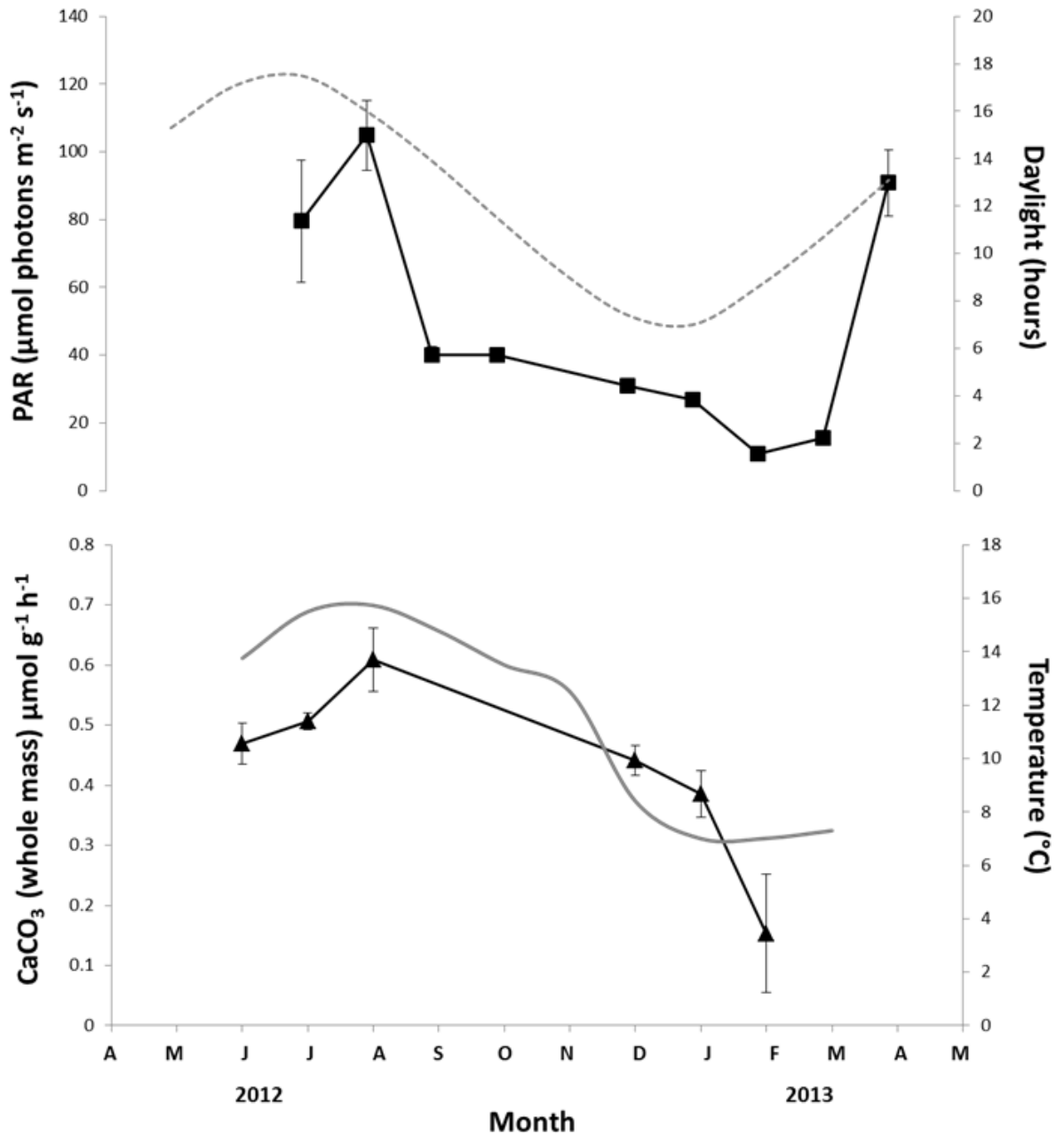


Figure 3.8 Rate of calcification (CaCO_3 (whole mass) $\mu\text{mol g}^{-1} \text{h}^{-1}$) in *Lithothamnion glaciale* in Loch Sween over a 12 month sampling period. Mean \pm SE. Solid black triangles: rate of calcification (CaCO_3 (whole mass) $\mu\text{mol g}^{-1} \text{h}^{-1}$), solid grey line: Mean temperature ($^{\circ}\text{C}$) in Loch Sween over 12 month sampling period; Dashed grey line: Day length (hours of light); Black squares: mean PAR (photosynthetically active radiation) $\mu\text{mol m}^{-2} \text{s}^{-1}$. NB. Where error bars are not visible, the error is so small that view of the error bar is obstructed by the symbol on the graph.

3.7 Discussion

3.7.1 Natural environmental variability

Temperature, irradiance and day length followed strong seasonal patterns in the field, and salinity was stable throughout the year with no discernible seasonal pattern (Figure 3.3). The highest temperatures coincided with the highest PAR, although there was a noticeable lag between these parameters and maximum day length. Maximum day length was observed during July, while maximum temperature and PAR were observed in August. Carbonate chemistry parameters across all seasons were similar, as were the carbonate chemistry parameters measured above the maerl bed compared to the sandy bedside. The field site is a shallow maerl bed (4-6 m) and is situated in the centre of an 80 m wide channel, and it is likely the water within the channel is well mixed due to the tidal currents. Although in other sites there is evidence that large maerl beds can impact the local water chemistry (Burrows et al., 2014). Similarly, changes in reef-water carbonate chemistry depend primarily on a ratio between benthic metabolism of the coral reef community and local hydrodynamics (Falter et al., 2013). Diurnal changes in pH, $p\text{CO}_2$ and $\Omega_{\text{aragonite}}$ were primarily dependent on changes in net productivity and were relatively insensitive to changes in net calcification, while net changes in the same parameters were more strongly influenced by net calcification when averaged over 24 hours (Falter et al., 2013). In the present study, pH in the field was between 8.2-8.4 units, slightly above the present day average for marine waters of 8.0-8.2 pH units (IPCC, 2013). It is likely that the observed pH in Loch Sween was slightly higher because all seawater samples for carbonate chemistry analysis were collected close to the seabed during midday when the algae were photosynthesising and algal metabolism was likely to be relatively high. In the present study pH values above the sandy bedside were slightly higher than those observed above the maerl bed, indicating that algae may be removing CO_2 from the surrounding water for photosynthesis and lowering pH. Similarly, Mediterranean seagrass meadows are able to modify pH in the water column by as much as 0.06-0.7 pH units through photosynthetic activity (Frankignoulle and Bouquegneau, 1990, Hendriks et al., 2014).

3.7.2 Natural biological variability

Strong seasonal patterns in photophysiology and calcification were observed in *L. glaciale*. Although total protein did not change significantly between months there was a

detectable seasonal pattern which was similar to that of Rubisco and phycoerythrin. Highest calcification rates coincided with highest *in situ* PAR and temperature during August, suggesting that these two parameters are key for controlling calcification while $rETR_{\max}$ was greatest during July, coinciding with maximum day length. During July PAR was below E_k (optimal light for efficient photosynthesis), suggesting algae were operating under suboptimal light conditions, therefore day length is likely to be important in terms of energy availability at this time. Maximum total protein was observed during December, when PAR was close to its minimum, and Rubisco and Phycoerythrin followed a similar pattern. It is likely that total protein concentration is driven by the concentration of Rubisco and phycoerythrin, which have been shown to increase under decreased irradiance (Cole and Sheath, 1990), presumably to increase light harvesting efficiency under low irradiance. Changes in Rubisco concentration may also be linked to a resource optimisation involving the reallocation of resources including nitrogen, a major component of Rubisco (Leakey et al., 2009).

3.7.3 Conclusions

Photosynthesis, protein concentration and calcification all followed strong seasonal patterns, most likely linked to seasonal changes in PAR, day length and temperature. It is also likely that algal metabolism locally influences the carbonate chemistry over a diurnal time scale, although the present study did not detect seasonal difference despite seasonal changes in photosynthesis and calcification.

The field study results will be discussed in more detail below, alongside the laboratory discussion in order to put the response of *L. glaciale* to climate change in the context of natural variability.

Part b: Laboratory study

3.8 Methods

3.8.1 Experimental set-up

L. glaciale thalli were collected by hand using SCUBA from Loch Sween in March 2012 from a depth of 6 m. Thalli were maintained in ambient conditions ($t = 7.7^{\circ}\text{C}$, $S = 32.6$) and transported to the University of Glasgow Marine Mesocosm Facility where thalli

were transferred to one of twelve 120 litre experimental seawater tanks (see Figure 2.1). Thalli were maintained at ambient conditions ($t = 7.67 \pm 0.05$, $S = 32.62 \pm 0.05$, PAR = 90 $\mu\text{mol photons m}^{-2} \text{s}^{-1}$, $p\text{CO}_2 = 387.06 \pm 23.33$, MEAN \pm SD) and acclimated to laboratory conditions for 6 weeks prior to commencement of the experiment. After the acclimation period, one of six experimental conditions was randomly assigned to each of the twelve experimental tanks:

- (1) ambient temperature, $p\text{CO}_2$ 380 ppm (t , 380)
- (2) ambient temperature + 2°C, $p\text{CO}_2$ 380 ppm ($t + 2$, 380)
- (3) ambient temperature, $p\text{CO}_2$ 750 ppm (t , 750)
- (4) ambient temperature + 2°C, $p\text{CO}_2$ 750 ppm ($t + 2$, 750)
- (5) ambient temperature, $p\text{CO}_2$ 1000 ppm (t , 1000)
- (6) ambient temperature + 2°C, $p\text{CO}_2$ 1000 ppm ($t + 2$, 1000)

Treatments were chosen to be representative of the IPCC year 2050 and 2100 climate change scenarios (IPCC, 2013). The $p\text{CO}_2$ (750 and 1000 ppm) was increased in the treatments tanks gradually over a four week period (Table 3.2) to allow algae to acclimatise to the elevated $p\text{CO}_2$.

Table 3.2 $p\text{CO}_2$ (ppm) values for the high- CO_2 treatments during the four week ramping period. During the four week ramping period the $p\text{CO}_2$ was gradually increased to the required experimental level in treatments: t , 750; $t + 3$, 750; t , 1000; $t + 3$, 1000. MEAN \pm SE.

Week	$p\text{CO}_2$	
	Treatment: 750 ppm	Treatment: 1000 ppm
1	453.69 \pm 0.95	454.14 \pm 0.96
2	585.42 \pm 0.58	655.31 \pm 1.69
3	663.06 \pm 3.92	832.11 \pm 1.75
4	739.43 \pm 0.63	1109.62 \pm 10.81

During the two year lab experimental period the photo-period was adjusted monthly to follow the natural daylight hours; taken as the time between sunrise and sunset in Glasgow, UK (the latitude of which is the same as the field site, Loch Sween). Data were obtained from the *Astronomical Almanac*, published annually by the UK Hydrographic Office and the United States Naval Observatory. Photosynthetically active radiation (PAR) was set at $90 \mu\text{mol photons m}^{-2} \text{s}^{-1}$ (the annual average for Loch Sween, (Rix et al., 2012)) for the duration of the experiment.

3.8.2 Sampling regime

The laboratory experiment was run over a two year period between May 2012 and May 2014. *L. glaciale* samples were collected at time points throughout the experiment to assess the physiological response of *L. glaciale* to elevated temperature and $p\text{CO}_2$: T6, T7, T8, T12, T14, T17, T26, T29 (where T0 (month) was January in year one). At each sampling time point maerl thalli were randomly chosen for collection using a random number generator. The same numbered thalli were collected from each of the twelve tanks.

3.8.3 Environmental parameters

3.8.3.1 Carbonate chemistry

Total alkalinity (A_T) was determined at set time points from seawater samples as described in Chapter 2 (section 2.6). $p\text{CO}_2$ was measured and recorded every five minutes (LiCor-820, see chapter 2, 2.1.1). Salinity and temperature were recorded daily using a handheld conductivity meter (Pro 2030, YSI, Ohio, USA). Additional carbonate system parameters were then calculated using the software program CO2SYS as described in Chapter 2 (section 2.9).

3.8.3.2 Other environmental parameters

Photosynthetically active radiation (PAR, $\mu\text{mol m}^{-2} \text{s}^{-1}$) was recorded in each tank using a PAR meter (Apogee QSO-E underwater quantum sensor connected to a Gemini voltage data logger). Dissolved oxygen (% DO) was measured daily using a temperature and salinity corrected handheld meter (Pro 2030, YSI, Ohio, USA).

3.8.4 Photosynthesis

3.8.4.1 Chlorophyll-a fluorescence (PAM fluorometry)

Rapid light curves (RLCs) were used to determine photochemical efficiency of *L. glaciale* at each sampling time point (n = 6). Maerl thalli were randomly selected and a diving-PAM was used to carry out RLCs in accordance with methods detailed in Chapter 2 (Section 2.2).

3.8.5 Proteins

3.8.5.1 Protein extraction and solubilisation

Samples collected at set time points and were frozen immediately in liquid N₂ upon collection to ensure no degradation of the proteins. Samples were kept frozen (-20°C) until analysis. *L. glaciale* samples were processed in accordance with methods described in Chapter 2 (section 2.3) for quantification of total protein, Rubisco and phycoerythrin concentration.

3.8.6 Calcification

The total alkalinity anomaly technique (Smith and Key 1975; Ohde and Hossain 2004) was used to determine calcification rate in *L. glaciale*. Analysis was performed in each of the experimental tanks: individual maerl thalli (n = 6) were randomly selected and incubated in 1 litre glass chambers for ~ 2 h. Samples of the incubation water were taken at the beginning and end of the incubation period. A_T was then determined using the methods described by Yao & Byrne (1998) (described in Chapter 2) and calcification (μmol CaCO₃ g h⁻¹) was calculated using the following equation:

$$\text{Calcification} = 0.5(\Delta A_T) \bullet V / \Delta T / \text{TDW}$$

where ΔA_T is the change of total alkalinity (mol/kg), W is the weight of experimental seawater (kg) and ΔT is the experimental period (h).

3.8.7 Growth and repair

3.8.7.1 Growth

To monitor the growth of *L. glaciale* over the 24 month experimental period, algal thalli were stained with Calcein, a fluorescent dye (24h at 50μM concentration, as per Brahma et al. (2010)), to enable identification of skeletal material deposited during the

experimental period (Figure 3.9). Following staining, thalli were grown for 24 months in the Marine Mesocosm Facility at the University of Glasgow (see section 2.1.2). Following the 24 month experimental period branches from different *L. glaciale* individuals ($n = 5$) from each treatment were transverse sectioned and polished in resin blocks (Buehler Epoxy cure). Growth after treatment was identified by determining the position of the Calcein stain using fluorescence microscopy (Olympus BH-2 microscope) and quantified using image analysis software (Image J).

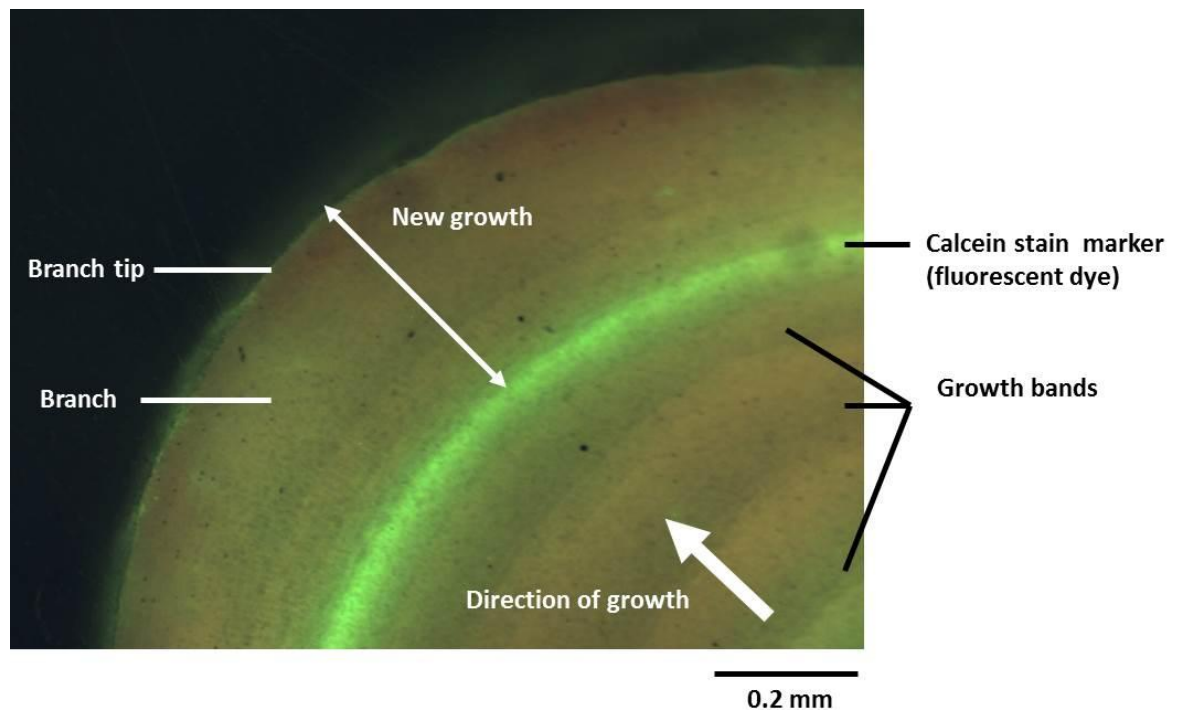


Figure 3.9 An example of a transverse section of an *L. glaciale* branch showing the Calcein stain laid down at the beginning of the 24 month experimental period and new growth thereafter.

3.8.7.2 Branch breakage and repair

The re-growth of algal photosynthetic cells after branch breakage on *L. glaciale* thalli was determined using image analysis. Thalli were randomly selected from each laboratory treatment ($n = 6$) and re-growth was measured over a period of 4 months between June and October 2013. A single branch from each thallus was removed and the exposed area of calcium carbonate skeleton was photographed (Figure 3.1). *L. glaciale* thalli were then placed back in their respective treatments with the broken area upright towards the light. After four months the thalli were removed from each of the treatments and the broken area was re-photographed (Figure 3.10). Using image software (Image J) the percentage area of re-growth from the total break area was

calculated to assess the effect of elevated $p\text{CO}_2$ and temperature on re-growth of the photosynthetic cells of *L. glaciale*.

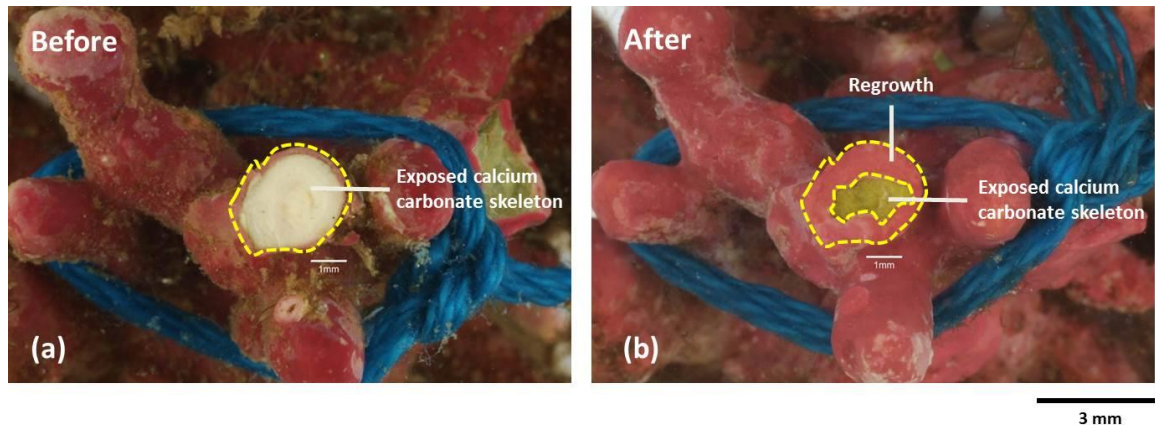


Figure 3.10 An example of a broken *Lithothamnion glaciale* branch before and after re-growth of the photosynthetic cells. (a) Broken branch immediately after break, prior to re-growth, exposing the calcium carbonate skeleton. (b) Broken branch after four months of re-growth of the photosynthetic cells. The % coverage of photosynthetic material on the total area of exposed calcium carbonate skeleton after branch breakage was calculated after four months and compared between treatments. The blue string in the photograph was used to identify different replicates. Photo: Les Hill.

3.8.8 Statistical analysis

One-way ANOVAs were used to investigate differences in photochemical characteristics, calcification and protein concentrations in algae between each month. One-way ANOVAs were also used to investigate differences in growth and repair of algae and between treatments. Two-way nested ANOVAs were used to investigate differences in photochemical characteristics, protein concentrations, and calcification between algae exposed to a control treatment (t , 380), elevated temperature ($t+2$, 380), elevated $p\text{CO}_2$ (t , 750 or 1000), and a combined treatment ($t+2$, 750 or 1000) and tank effect, at each time point. ANOVAs were followed by Tukey HSD post hoc tests. Independent two-way nested ANOVAs were performed at each month as measurements were not repeated on the same algae. Where the assumptions of ANOVA could not be met data were either \log^{10} transformed or a non-parametric Scheirer-Ray-Hare test (non-parametric two-way ANOVA) or Kruskal-Wallis test (non-parametric one-way ANOVA) were used. Differences between means/ medians were considered to be significant when $p \leq 0.05$. All analysis were conducted with SPSS v18.0.

3.9 Results

3.9.1 Environmental parameters

The carbonate chemistry parameters recorded in both the laboratory and the field over the experimental period are summarised in Table 3.3. Temperature, salinity, irradiance and photoperiod are summarised in Figure 3.11.

Table 3.3 Parameters of the carbonate system in the laboratory experiment in each treatment and season.

	pH	A_T ($\mu\text{mol kg}^{-1}$)	$p\text{CO}_2$ (μatm)	HCO_3^-	CO_3^{2-}	DIC	Ω_{cal}	Ω_{ara}
				($\mu\text{mol kg}^{-1}$)				
t, 380								
Summer	8.0±0.1	1195.1±108.5	383.1±25.1	1048.4±44.2	48.6±8.5	1108.6±96.1	1.2±0.2	0.7±0.1
Autumn	8.1±0.02	1672.5±53.1	390.7±30.01	1488.2±52.1	67.3±1.9	1572.7±54.1	1.6±0.06	1.01±0.03
Winter	8.1±0.09	2028.9±458.7	367.1±3.4	1758.9±351.2	103.9±46.7	1879.5±397.2	2.5±1.1	1.5±0.7
Spring	8.1±0.09	1432.2±365.2	364.4±3.5	1243.4±298.5	66.2±28.1	1322.4±327.0	1.6±0.6	0.9±0.4
t+2, 380								
Summer	8.1±0.1	1390.4±64.5	383.08±12.5	1186.5±48.1	69.3±6.1	1266.92±54.3	1.6±0.2	1.1±0.1
Autumn	8.1±0.01	1851.2±187.3	390.7±30.01	1614.4±150.1	88.7±16.3	1718.74±166.4	2.1±0.3	1.3±0.2
Winter	8.1±0.1	2203.6±604.9	367.1±3.4	1867.4±453.7	131.7±66.1	2014.4±519.5	3.1±1.5	1.9±0.9
Spring	8.2±0.1	1959.9±844.6	364.4±3.5	1605.9±619.3	137.1±99.3	1754.4±718.1	3.2±2.3	2.0±1.4
t, 750								
Summer	7.8±0.1	1532.9±198.7	747.6±13.5	1413.4±170.6	42.8±11.4	1480.7±182.2	1.1±0.3	0.64±0.2
Autumn	7.8±0.01	1753.0±194.6	759.6±39.01	1644.7±174.6	40.3±8.4	1719.6±183.7	0.9±0.2	0.6±0.1
Winter	7.8±0.02	2049.3±112.8	755.8±73.9	1907.8±104.7	54.3±3.8	1997.3±110.5	1.3±0.08	0.8±0.05
Spring	7.8±0.06	1627.6±279.1	758.1±0.7	1509.8±247.8	43.1±13.3	1580.7±247.8	1.0±0.3	0.7±0.2
t+2, 750								
Summer	7.8±0.1	1473.6±89.7	747.6±6.7	1352.2±75.1	24.6±5.7	1417.5±40.3	1.1±0.1	0.64±0.1
Autumn	7.8±0.01	1850.4±9.5	759.6±39.01	1722.7±7.3	48.2±0.9	1802.4±7.8	1.2±0.02	0.7±0.01
Winter	7.9±0.02	2197.6±146.1	755.9±73.9	2022.3±135.0	68.1±4.7	2122.3±135.0	1.6±0.09	1.02±0.06
Spring	8.2±0.1	1959.9±844.6	758.1±0.7	1509.8±247.8	43.1±13.3	1580.7±247.8	1.0±0.3	0.7±0.2
t, 1000								
Summer	7.6±0.1	1533.5±219.7	1138.7±119.8	1449.6±193.5	30.0±10.9	1518.1±200.3	0.7±0.2	0.4±0.1
Autumn	7.7±0.05	1978.4±165.2	1054.8±29.01	1877.5±155.3	38.5±5.0	1963.98±159.8	0.9±0.1	0.6±0.08
Winter	7.7±0.03	2555.8±205.9	1186.8±4.1	2414.7±182.3	56.6±10.3	2526.7±191.7	1.4±0.2	0.8±0.2
Spring	7.8±0.08	2086.1±544.5	1041.9±21.2	1949.8±490.2	53.1±24.1	2041.4±516.7	1.3±0.6	0.8±0.4
t+2, 1000								
Summer	7.7±0.1	1591.5±132.2	1138.7±119.9	1497.2±104.9	34.1±10.2	1566.93±110.3	0.8±0.2	0.5±0.1
Autumn	7.7±0.06	1934.6±266.6	1054.8±29.01	1831.4±239.3	39.5±11.5	1914.8±249.9	0.9±0.2	0.6±0.2
Winter	7.8±0.02	2533.3±189.2	1186.8±4.1	2383.5±163.2	60.1±10.7	2494.3±174.1	1.4±0.2	0.9±0.1
Spring	7.9±0.09	2109.3±499.9	1041.9±21.2	1954.5±443.5	60.4±24.9	2049.0±469.1	1.5±0.5	0.9±0.2

The values reported are means±SE. Total alkalinity (A_T) and $p\text{CO}_2$ were measured; pH, dissolved inorganic carbon (DIC), HCO_3^- , CO_3^{2-} , calcite saturation (Ω_{cal}), aragonite saturation (Ω_{ara}) were calculated using CO2SYS. Summer: July and August 2012/2013; Autumn: November and December 2012/2013; Winter: January and February 2013/ 2014; Spring: May and June 2013/ 2014.

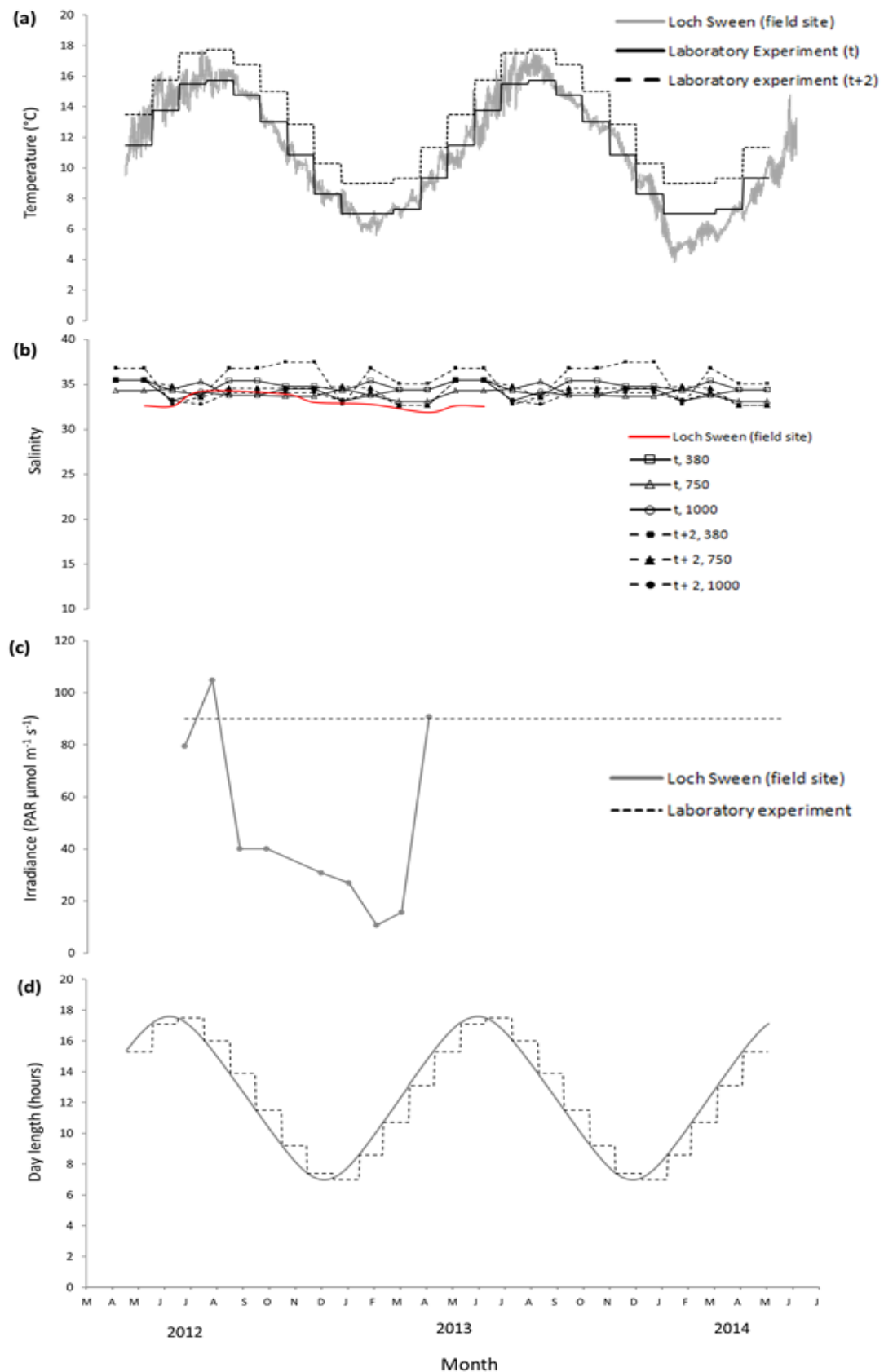


Figure 3.11 Changes in temperature, salinity, irradiance and photoperiod in the field and laboratory
 (a) Temperature ($^{\circ}\text{C}$) (b) Salinity (c) PAR (photosynthetically active radiation) ($\mu\text{mol m}^{-2} \text{s}^{-1}$) (d) day length (hours). t = ambient temperature; $t+2$ = ambient temperature + 2°C ; at $p\text{CO}_2$ 380, 750 or 1000 ppm (c) Photoperiod (h). Temperature and irradiance measurements in Loch Sween were made on the maerl bed (depth = 5-6 m, depending on tide).

3.9.2 Photosynthesis

3.9.2.1 Chlorophyll-a fluorescence (PAM fluorometry)

3.9.2.1.1 Calculated photosynthetic characteristics ($F_q'/F_{m'_{max}}$, E_k , α , $rETR_{max}$); between months within treatments

The calculated photosynthetic characteristics of *Lithothamnion glaciale* significantly differed between months within each treatment (Figure 3.12). $F_q'/F_{m'_{max}}$ differed significantly between months in treatments: t, 380: $F_{6,42} = 6.157$, $P < 0.001$; t+2, 380: $F_{6,42} = 6.576$, $P < 0.001$; t, 750: $H_{6,42} = 18.960$, $P = 0.004$; t+2, 750: $F_{6,42} = 4.791$, $P = 0.001$. However, in treatments t, 1000 and t+2, 1000, $F_q'/F_{m'_{max}}$ did not respond differently between months ($F_{6,42} = 1.969$, $P = 0.097$; $F_{6,42} = 1.111$, $P = 0.376$, respectively). α differed between months in treatments: t, 380: $H_{6,42} = 15.220$, $P < 0.001$; t+2, 380: $F_{6,42} = 2.599$, $P = 0.034$; t+2, 750: $F_{6,42} = 2.787$, $P = 0.025$; t+2, 1000: $F_{6,42} = 2.935$, $P = 0.02$. However, in treatments t, 750 and t, 1000 α did not differ between months ($F_{6,42} = 1.692$, $P = 0.153$, $F_{6,42} = 0.510$, $P = 0.797$, respectively). E_k differed significantly between months in all treatments: t, 380: $F_{6,42} = 17.813$, $P < 0.001$; t+2, 380: $F_{6,42} = 4.765$, $P < 0.001$; t, 750: $H_{6,42} = 30.264$, $P < 0.001$; t+2, 750: $H_{6,42} = 29.001$, $P < 0.001$; t, 1000: $H_{6,42} = 26.689$, $P < 0.001$; t+2, 1000: $H_{6,42} = 23.218$, $P < 0.001$. $rETR_{max}$ also differed significantly between months in all treatments: t, 380: $F_{6,42} = 52.109$, $P < 0.001$; t+2, 380: $F_{6,42} = 5.702$, $P < 0.001$; t, 750: $H_{6,42} = 31.051$, $P < 0.001$; t+2, 750: $H_{6,42} = 29.298$, $P < 0.001$; t, 1000: $H_{6,42} = 27.190$, $P < 0.001$; t+2, 1000: $H_{6,42} = 23.218$, $P < 0.001$ (Figure 3.12). In general, $rETR_{max}$ and E_k increased during months where temperature were greatest (summer; July and August), and $F_q'/F_{m'_{max}}$ and α increased during December and May/June (autumn and spring) (Figure 3.12).

3.9.2.1.2 Calculated photosynthetic characteristics ($F_q'/F_{m'_{max}}$, E_k , α , $rETR_{max}$); between treatments within each month

Within each month sampled the calculated photosynthetic characteristics differed in response to exposure to elevated pCO_2 and temperature (p values are summarised in Table 3.4 and Table 3.5). E_k did not differ significantly among treatments in summer and winter but did increase significantly in response to elevated pCO_2 (750 μatm) during spring (June 2012), and increased in response to elevated temperature during autumn (December 2012). α increased in response to combined elevated temperature and pCO_2 during spring (June 2012), and increased during the summer (August 2012) in response to elevated temperature (Figure 3.12). $rETR_{max}$ significantly increased in response to

elevated temperature when combined with elevated $p\text{CO}_2$ in summer (August 2012) and Spring (June 2012) (Figure 3.12). Fq'/Fm'_{max} decreased in response to elevated temperature at ambient $p\text{CO}_2$, but increased in response to elevated temperature when combined with elevated $p\text{CO}_2$ (1000 μatm) during the summer (July 2012) (Figure 3.12). Fq'/Fm'_{max} also decreased in response to elevated temperature in both August 2012 and December 2012 (Figure 3.12).

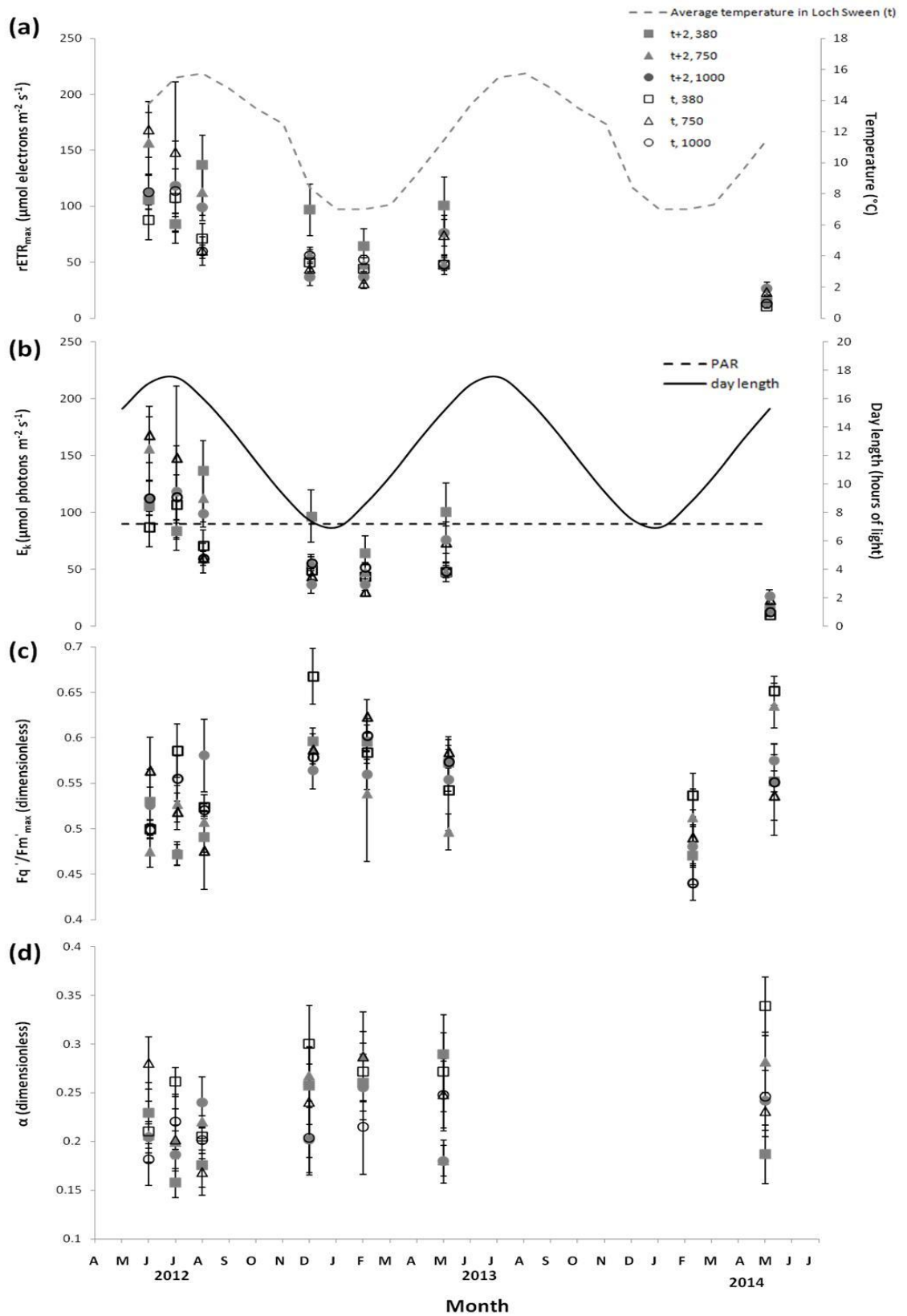


Figure 3.12 Effect of elevated temperature and $p\text{CO}_2$ on the calculated photosynthetic characteristics of *Lithothamnion glaciale* over a two year experimental period. mean \pm SE. (a) $rETR_{max}$ ($\mu\text{mol electrons m}^{-2} \text{s}^{-1}$) (b) E_k ($\mu\text{mol photons m}^{-2} \text{s}^{-1}$) (c) $F_q'/F_m'_{max}$ (dimensionless) (d) α (dimensionless). t = ambient temperature; $t+2$ = ambient temperature + 2 $^{\circ}\text{C}$ at 380, 750 or 1000 ppm $p\text{CO}_2$. Plots also include; Day length (hours of light), experimental PAR (photosynthetically active radiation) $\mu\text{mol m}^{-2} \text{s}^{-1}$ and temperature ($^{\circ}\text{C}$) (t). In February 2014 data plotted in $F_q'/F_m'_{max}$, I was unable to perform rapid light curves during this month therefore $F_q'/F_m'_{max}$ and other parameters could not be calculated.

Table 3.4 Summary of two-way nested ANOVAs followed by Tukey HSD post hoc tests testing the effects of elevated temperature and pCO₂ on *Lithothamnion glaciale* photochemical characteristics (E_k and $rETR_{max}$) during each month of a two year experiment.

		Statistical data										Tukey HSD Test											
		Source of variation				Nested factor																	
		pCO ₂		Temperature		pCO ₂ *temperature		(tank number)				t, 380		t+2, 380		t, 750		t+2, 750		t, 1000		t+2, 1000	
		df	F	p	Test statistic	p	Test statistic	p	Test statistic	p	Test statistic	p											
E_k																							
Spring	June 2012	(2, 36)	18.385	0.05	0.028	0.895	2.202	0.312	0.072	0.821			a	a	b	b	ab	ab					
Summer	July 2012	(2, 36)	0.094	0.914	0.125	0.783	0.54	0.948	0.221	0.688			nd										
Summer	August 2012	(2, 36)	0.755	0.570	97.523	0.06	0.567	0.638	0.084	0.802			nd										
Autumn	December 2012	(2, 36)	2.196	0.313	59.234	0.02	1.013	0.498	3.432	0.172			a	b	a	a	a	a					
Winter	February 2013	(2, 36)	2.698	0.270	5.732	0.252	2.313	0.302	0.486	0.673			nd										
Spring	May 2013	(2, 36)	0.212	0.825	4.496	0.281	6.787	0.128	1.363	0.649			nd										
Spring	May 2014	(2, 36)	2.028	0.330	29.663	0.116	3.932	0.203	1.090	0.758			nd										
$rETR_{max}$																							
Spring	June 2012	(2, 36)	7.098	0.123	1.105	0.484	16.346	0.05	0.865	0.476			nd										
Summer	July 2012	(2, 36)	0.065	0.939	0.479	0.615	0.139	0.878	0.265	0.650			nd										
Summer	August 2012	(2, 36)	1.059	0.486	82.406	0.07	1822.178	<0.01	0.307	0.626			a	b	a	b	a	b					
Autumn	December 2012	(2, 36)	1.605	0.384	0.097	0.808	9.252	0.098	3.593	0.230			nd										
Winter	February 2013	(2, 36)	1.795	0.358	1.620	0.424	0.223	0.818	5.646	0.958			nd										
Spring	May 2013	(2, 36)	0.593	0.628	2.721	0.347	6.693	0.130	1.926	0.819			nd										
Spring	May 2014	(2, 36)	0.606	0.623	1.120	0.482	4.804	0.172	0.006	0.947			a	b	b	b	a	b					

t = ambient temperature; t+2 = ambient temperature + 2°C at 380, 750 or 1000 ppm pCO₂. Different letters (a-b) indicate a significant difference between treatments. nd = no difference. RLCs were not performed during February 2014, measurements of Fq' / Fm' were taken instead. The difference is considered significant when p < 0.05 (indicated by the red values).

Table 3.5 Summary of two-way nested ANOVAs (or Scheirer-ray-hare) followed by Tukey HSD post hoc tests testing the effects of elevated temperature and $p\text{CO}_2$ on *Lithothamnion glaciale* photochemical characteristics ($F_q'/F_{m'_{\max}}$ and α) during each month of a two year experiment.

		Statistical data										Tukey HSD Test					
		Source of variation				Nested factor											
		$p\text{CO}_2$		Temperature		$p\text{CO}_2$ *temperature		(tank number)									
		Test statistic	<i>p</i>	Test statistic	<i>p</i>	Test statistic	<i>p</i>	Test statistic	<i>p</i>	<i>t</i> , 380	<i>t</i> +2, 380	<i>t</i> , 750	<i>t</i> +2, 750	<i>t</i> , 1000	<i>t</i> +2, 1000		
SS	df																
<i>F_q'/f_m'_{max}</i>																	
Spring	June 2012		(2, 36)	F = 0.04	0.965	F = 0.27	0.658	F = 13.012	0.071	F = 0.88	0.425	nd					
Summer	July 2012		(2, 36)	F = 0.295	0.772	F = 461.100	0.03	F = 93.064	0.01	F = 0.512	0.551	a	b	c	c	ac	b
Summer	August 2012	16206	2	H = 0.436	0.20	H = 0.016	0.01	H = 0.298	0.14	H = 0.324	0.19	a	b	ab	ab	a	c
Autumn	December 2012		(2, 36)	F = 1.076	0.482	F = 2884336.11	<0.01	F = 0.774	0.564	F = 0.590	0.698	c	a	ab	ab	ab	b
Winter	February 2013	16206	2	H = 0.380	0.17	H = 0.285	0.13	H = 105.366	0.99	H = 0.453	0.21	nd					
Spring	May 2013		(2, 36)	F = 1.729	0.366	F = 3.149	0.327	F = 1.651	0.377	F = 0.155	0.865	nd					
Winter	February 2014 (<i>F_q'/F_m'</i>)		(2, 36)	F = 0.998	0.500	F = 6.059	0.246	F = 4.827	0.172	F = 2.807	0.990	nd					
Spring	May 2014		(2, 36)	F = 1.909	0.344	F = 0.061	0.845	F = 5.951	0.144	F = 2.283	0.569	nd					
α																	
Spring	June 2012		(2, 36)	F = 1.151	0.465	F = 0.156	0.761	F = 18.255	0.05	F = 0.091	0.78	a	ab	b	a	a	a
Summer	July 2012		(2, 36)	F = 2.125	0.320	F = 2.902	0.338	F = 1.468	0.405	F = 0.038	0.963	nd					
Summer	August 2012		(2, 36)	F = 2.626	0.276	F = 176.131	0.04	F = 3.285	0.233	F = 0.737	0.576	ab	b	b	a	b	b
Autumn	December 2012		(2, 36)	F = 0.743	0.574	F = 36.618	0.106	F = 0.154	0.773	F = 0.460	0.685	nd					
Winter	February 2013		(2, 36)	F = 2.294	0.304	F = 4.416	0.283	F = 0.090	0.918	F = 0.148	0.918	nd					
Spring	May 2013	16206	2	H = 0.960	0.38	H = 1.075	0.42	H = 0.024	0.01	H = 0.856	0.26	nd					
Spring	May 2014		(2, 36)	F = 1.183	0.458	F = 17.261	0.150	F = 15.739	0.06	F = 0.457	0.687	nd					

t = ambient temperature; **t+2** = ambient temperature + 2°C at 380, 750 or 1000 ppm $p\text{CO}_2$. Different letters (a-c) indicate a significant difference between treatments. nd = no difference. RLCs were not performed during February 2014, measurements of $F_q'/F_{m'}$ were taken instead. The difference is considered significant when $p < 0.05$ (indicated by the red values).

3.9.2.1.3 Measured photochemical parameters (photochemical quenching) (F_q'/F_m' , qP and $rETR$)

Photochemical data from months were pooled to produce light-response curves of photochemical quenching parameters for each season (described by F_q'/F_m' , qP and $rETR$); summer: July and August; autumn: December; winter: February; Spring: May and June. Photochemical parameters differed between seasons and between treatments (Figure 3.13). $rETR$ decreased with decreasing temperature and/ or day length, and was lowest during winter. During each season, $rETR$ increased in response to elevated temperature, compared to algae in ambient temperature (Figure 3.13i-j). During the summer F_q'/F_m' was greatest in algae exposed to the combined treatment (t+3, 1000), with F_q'/F_m' similar in algae exposed to ambient temperature at all pCO_2 levels. During autumn F_q'/F_m' was generally greater in algae exposed to ambient temperature compared to elevated temperature treatments (Figure 3.13). F_q'/F_m' was lowest during winter and similar between all treatments during the spring (Figure 3.13). Data were normalised to E/E_k (E = PAR photosynthetically active radiation; E_k = optimum light level for efficient photosynthesis. E/E_k is used to allow for comparison between treatments when E_k is different between samples (1= optimum light level). Generally each response observed during each season was the same above and below optimum light level ($E/E_k = 1$), with exception to F_q'/F_m' during autumn. In this instance the control was more efficient below optimum light level, while a combined treatment (t+2, 750) was more efficient above optimal light level (Figure 3.13).

3.9.2.1.4 Photoprotective parameters (non-photochemical quenching) (qN)

Non-photochemical data from months were pooled to produce light-response curves of photochemical quenching parameters for each season (described by $1-qN$); summer: July and August; autumn: December; winter: February; Spring: May and June. qN (plotted as $1-qN$) was greatest during the summer and the winter. During summer, autumn and winter qN increased in response to elevated temperature and pCO_2 compared to the control (Figure 3.14), although during the summer decreased in algae exposed to elevated temperature and pCO_2 1000 μatm . During the spring qN was similar in all treatments (Figure 3.14).

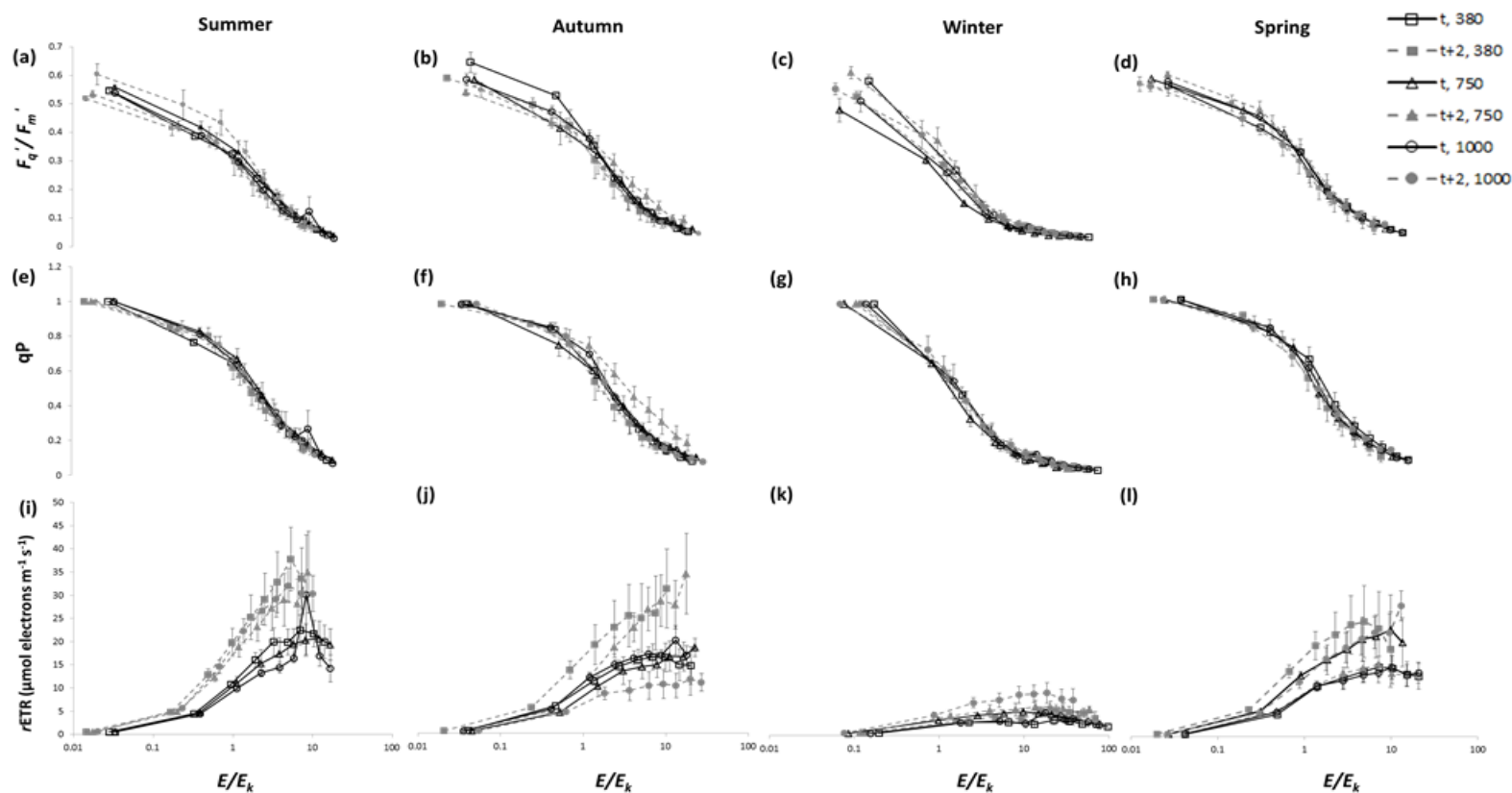


Figure 3.13 The effect of elevated temperature and $p\text{CO}_2$ on the photochemical response of *Lithothamnion glaciale* during summer, autumn, winter and spring. (a-d) F_q'/F_m' (e-h) qP (i-l) $rETR$ ($\mu\text{mol electrons m}^{-2} \text{s}^{-1}$). Summer: July and August; Autumn: December; Winter: February; Spring: May and June. Data normalised to E/E_k ; values are mean \pm SE. t = ambient temperature; $t+2$ = ambient temperature + 2°C at 380, 750 or 1000 ppm $p\text{CO}_2$.

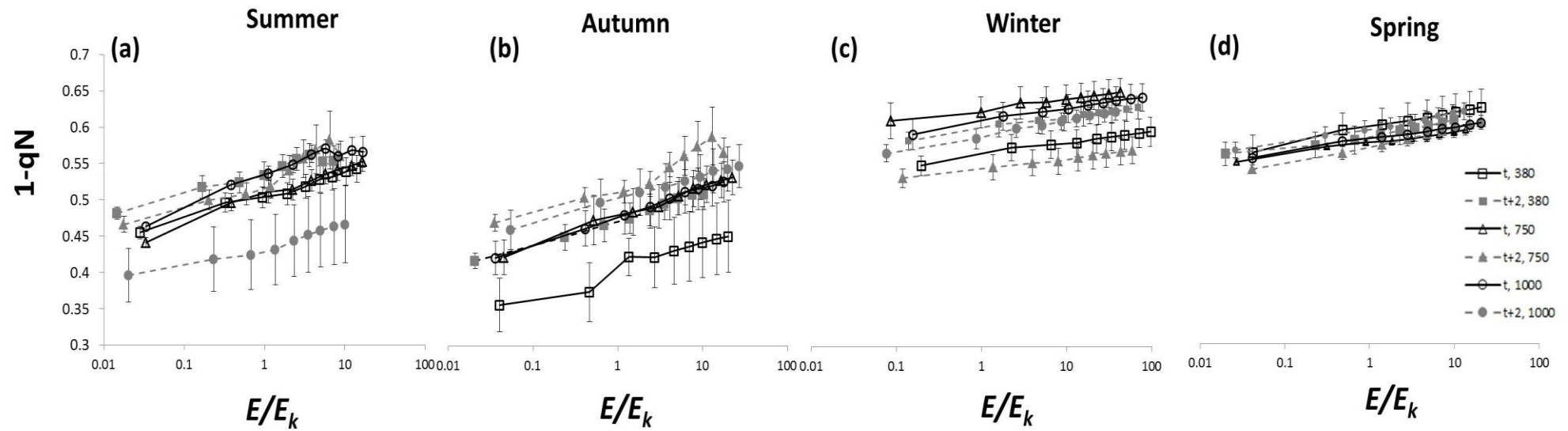


Figure 3.14 The effect of elevated temperature and $p\text{CO}_2$ on the photoprotective response of *Lithothamnion glaciale* during summer, autumn, winter and spring. (a) Summer: July and August (b) Autumn: December (c) Winter: February (d) Spring: May and June. Data normalised to E/E_k ; values are mean \pm SE. t = ambient temperature; $t+2$ = ambient temperature + 2°C at 380, 750 or 1000 ppm $p\text{CO}_2$

3.9.3 Proteins

3.9.3.1 Total protein

Total protein in *Lithothamnion glaciale* differed significantly between month within treatments: $t+2$, 380: $H = 16.40$, $p = 0.02$; t , 750: $H = 43.16$, $p < 0.001$; t , 1000: $H = 17.15$, $p = 0.02$; $t+2$, 1000: $H = 19.85$, $p = 0.006$. Total protein did not differ between months in treatments; $t+2$, 750: $H = 7.37$, $p = 0.39$ and t , 380: $H = 7.85$, $p = 0.34$. Generally, total protein was greatest during the summer (June – August), and lowest during the winter (Figure 3.15). The response of total protein concentration to elevated temperature and $p\text{CO}_2$ differed within each month and was variable (p values are summarised in Table 3.6).

3.9.3.2 Rubisco

Rubisco concentration in *Lithothamnion glaciale* differed significantly between months within all treatments; t , 380: $H = 30.214$, $p < 0.001$; $t+2$, 380: $H = 30.515$, $p < 0.001$; t , 750: $H = 39.138$, $p < 0.001$; $t+2$, 750: $H = 34.299$, $p < 0.001$; t , 1000: $H = 29.867$, $p < 0.001$; $t+2$, 1000: $H = 33.699$, $p < 0.001$ (Figure 3.7). Generally, Rubisco concentration was greatest during the summer (June – August), and lowest during the winter (Figure 3.15). The response of Rubisco concentration to elevated temperature and $p\text{CO}_2$ differed dependent on the month (p values are summarised in Table 3.6). During summer (August 2012) Rubisco concentration increased in response to elevated $p\text{CO}_2$ and during autumn (December 2012) Rubisco concentration increased in response to elevated $p\text{CO}_2$. Rubisco concentration was affected by an interaction between temperature and $p\text{CO}_2$ during the winter and spring (May and February 2013, respectively), increasing in winter ($t+2$, 750) and in spring ($t+2$, 1000).

3.9.3.3 Phycoerythrin

Phycoerythrin concentration in *Lithothamnion glaciale* differed significantly between months within all treatments; t , 380: $H = 31.629$, $p < 0.001$; $t+2$, 380: $H = 34.248$, $p < 0.001$; t , 750: $H = 43.167$, $p < 0.001$; $t+2$, 750: $H = 38.587$, $p < 0.001$; t , 1000: $H = 36.915$, $p < 0.001$; $t+2$, 1000: $H = 40.081$, $p < 0.001$ (Figure 3.15). Generally, phycoerythrin concentration was greatest during the summer (June – August), and lowest during the winter (Figure 3.15). The response of phycoerythrin concentration to elevated temperature and $p\text{CO}_2$ differed dependent on the month (p values are summarised in Table 3.6). During spring and summer (June 2012/ May 2013 and August 2012)

phycoerythrin concentration mirrored seasonal changes in temperature and day length (Figure 3.15), increasing with increasing temperature and day length in all three months. In addition, the interaction between elevated temperature and $p\text{CO}_2$ caused a further increase in phycoerythrin concentration during May 2013.

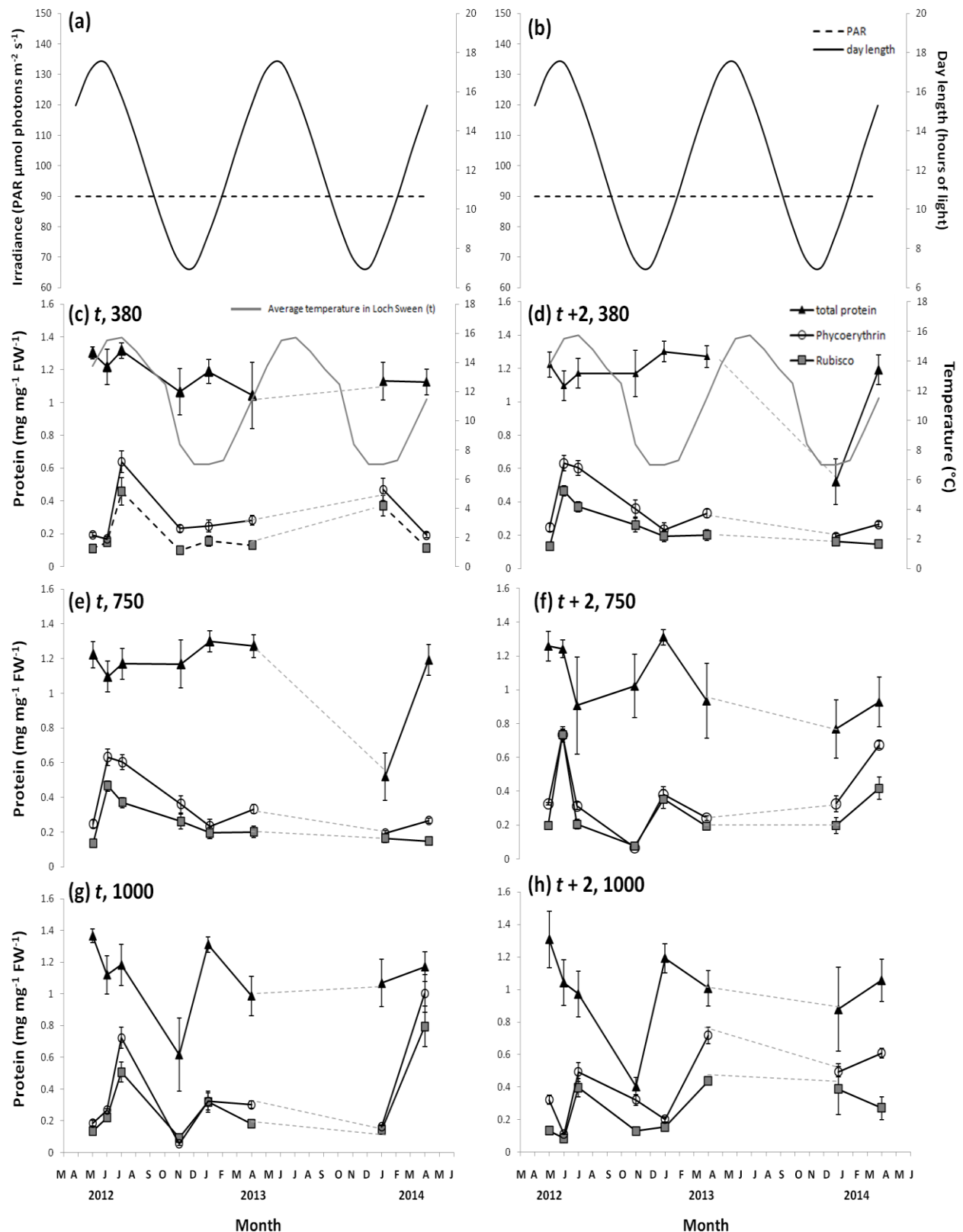


Figure 3.15 The effect of elevated temperature and $p\text{CO}_2$ on Rubisco, Phycoerythrin and total protein concentration ($\text{mg g}^{-1} \text{FW}^{-1}$) in *L. glaciale* over the two year laboratory experimental period. mean \pm SE. (a and b) Day length (hours of light) and experimental PAR (photosynthetically active radiation) $\mu\text{mol m}^{-2} \text{s}^{-1}$ (c) t , 380 (d) $t+2^{\circ}\text{C}$, 380 (e) t , 750 (f) $t+2^{\circ}\text{C}$, 750 (g) t , 1000 (h) $t+2^{\circ}\text{C}$, 1000; where t = ambient temperature for the time of year; $t+2^{\circ}\text{C}$ = ambient temperature + 2°C ; at 380, 750 or 1000 $\mu\text{atm } p\text{CO}_2$. NB. Where error bars are not visible, the error is so small that view of the error bar is obstructed by the symbol on the graph.

Table 3.6 Summary of two-way nested ANOVAs (or Scheirer-ray-hare test) followed by Tukey HSD post hoc tests testing the effects of elevated temperature and pCO_2 on *Lithothamnion glaciale* protein concentration during each month of a two year experiment.

		Statistical data										Tukey HSD Test					
		Source of variation				Source of variation				Source of variation							
		pCO_2		Temperature		pCO_2 *temperature		(tank number)									
		SS	df	Test statistic	p	Test statistic	p	Test statistic	p	Test statistic	p	t, 380	t+2, 380	t, 750	t+2, 750	t, 1000	t+2, 1000
Total Protein																	
Spring	June 2012		(1,36)	F = 5.22	0.01	F = 0.41	0.58	F = 0.99	0.458	F = 0.70	0.51	a	a	b	a	a	a
Summer	July 2012	160206	2	H = 0.071	0.96	H = 0.008	0.99	H = 0.071	0.74	H = 0.069	0.65	nd					
Summer	August 2012		(1, 36)	F = 2.16	0.13	F = 2.70	0.24	F = 1.21	0.33	F = 1.60	0.21	nd					
Autumn	December 2012	160206	2	H = 2.012	0.63	H = 0.012	<0.01	H = 0.767	0.32	H = 0.433	0.12	a	a	a	a	a	b
Winter	February 2013	160206	2	H = 0.001	<0.01	H = 0.016	0.01	H = 1.382	0.49	H = 0.434	0.21	a	b	a	b	b	a
Spring	May 2013	160206	2	H = 0.450	0.20	H = 0.006	<0.01	H = 0.808	0.33	H = 2.456	0.78	ab	b	ab	a	a	a
Winter	February 2014	160206	2	H = 0.454	0.20	H = 0.522	0.23	H = 0.282	0.13	H = 0.065	0.95	nd					
Spring	May 2014	160206	2	H = 0.202	0.10	H = 0.036	0.02	H = 0.495	0.22	H = 0.989	0.43	a	ab	ab	ab	ab	b
Rubisco																	
Spring	June 2012		(1, 36)	F = 3.05	0.06	F = 12.22	0.07	F = 2.47	0.06	F = 0.46	0.63	nd					
Summer	July 2012		(1, 36)	F = 7.60	<0.01	F = 13.58	0.06	F = 4.28	0.06	F = 0.50	0.61	a	b	a	b	c	d
Summer	August 2012		(1, 36)	F = 0.70	0.51	F = 5.98	0.14	F = 2.94	0.06	F = 1.70	0.20	nd					
Autumn	December 2012	160206	2	H = 0.453	0.21	H = 0.048	0.02	H = 4.236	0.88	H = 0.543	0.32	a	c	c	b	ab	a
Winter	February 2013	160206	2	H = 1.985	0.63	H = 6.478	0.96	H < 0.01	<0.01	H = 0.345	0.21	a	a	b	c	c	a
Spring	May 2013	160206	2	H = 1.062	0.41	H = 0.012	0.01	H = 0.029	0.01	H = 0.567	0.23	a	b	a	b	b	c
Winter	February 2014	160206	2	H = 0.167	0.08	H = 0.238	0.11	H = 4.645	0.90	H = 0.202	0.10	nd					
Spring	May 2014	160206	2	H = 3.923	0.86	H = 0.456	0.20	H = 2.770	0.75	H = 0.283	0.14	nd					
Phycocerythrin																	
Spring	June 2012		(1, 36)	F = 1.53	0.23	F = 59.99	0.01	F = 1.32	0.08	F = 0.75	0.48	a	b	a	c	a	c
Summer	July 2012	160206	2	H = 2.526	0.28	H = 0.830	0.66	H = 4.525	0.10	H = 0.675	0.31	nd					
Summer	August 2012		(1, 36)	F = 0.41	0.66	F = 39.96	0.02	F = 0.74	0.07	F = 0.62	0.54	a	b	a	b	a	b
Autumn	December 2012	160206	2	H = 0.801	0.34	H = 0.193	0.09	H = 5.696	0.942	H = 0.234	0.46	nd					
Winter	February 2013		(1, 36)	F = 1.73	0.194	F = 0.001	0.95	F = 1.09	0.07	F = 1.29	0.29	nd					
Spring	May 2013	160206	2	H = 0.738	0.31	H = 0.001	<0.01	H = 0.053	<0.01	H = 0.435	0.23	a	a	b	a	a	c
Winter	February 2014		(1, 36)	F = 0.65	0.52	F = 0.32	0.63	F = 1.01	0.06	F = 1.32	0.28	nd					
Spring	May 2014	160206	2	H = 3.701	0.84	H = 0.888	0.36	H = 3.102	0.79	H = 0.765	0.39	nd					

t = ambient temperature; t+2 = ambient temperature + 2°C at 380, 750 or 1000 ppm pCO_2 . Different letters (a-d) indicate a significant difference between treatments. nd = no difference. The difference is considered significant when $p < 0.05$ (indicated by the red values).

3.9.4 Calcification

3.9.4.1 *Between months within treatments*

Rate of calcification (CaCO_3 (whole mass) $\mu\text{mol g}^{-1} \text{h}^{-1}$) in *L. glaciale* differed significantly between months in treatments: *t*, 380: $H_{6, 42} = 13.62$, $p = 0.048$; *t+2*, 380: $H_{6, 62} = 15.413$, $p = 0.017$; *t*, 750: $H_{6, 62} = 20.861$, $p = 0.02$; *t*, 1000: $H_{8, 42} = 18.747$, $p = 0.005$. However, there was no significant difference in calcification rate between months in algae exposed to elevated temperature and $p\text{CO}_2$ (*t+2*, 750: $H_{8, 42} = 11.953$, $p = 0.063$; *t+2*, 1000: $H_{8, 42} = 4.795$, $p = 0.570$). In general calcification increased during the months when temperature was greatest (Figure 3.16).

3.9.4.2 *Between treatments within months*

Within some months calcification differed in response to exposure to elevated temperature and $p\text{CO}_2$ (p values are summarised in Table 3.7). During summer (July 2012) rate of calcification in *L. glaciale* significantly increased in response to elevated temperature at ambient $p\text{CO}_2$, and increased in response to elevated $p\text{CO}_2$ (750 μatm) and ambient temperature (Figure 3.16). During spring (May 2013/14) calcification rate was significantly affected by the interaction between increased temperature and $p\text{CO}_2$ (Figure 3.16 and Table 3.7) with the greatest calcification rates observed in treatments *t+2* $^\circ\text{C}$, 750 and 1000 μatm . There was no significant effect of temperature or $p\text{CO}_2$ during autumn and winter months (Table 3.7).

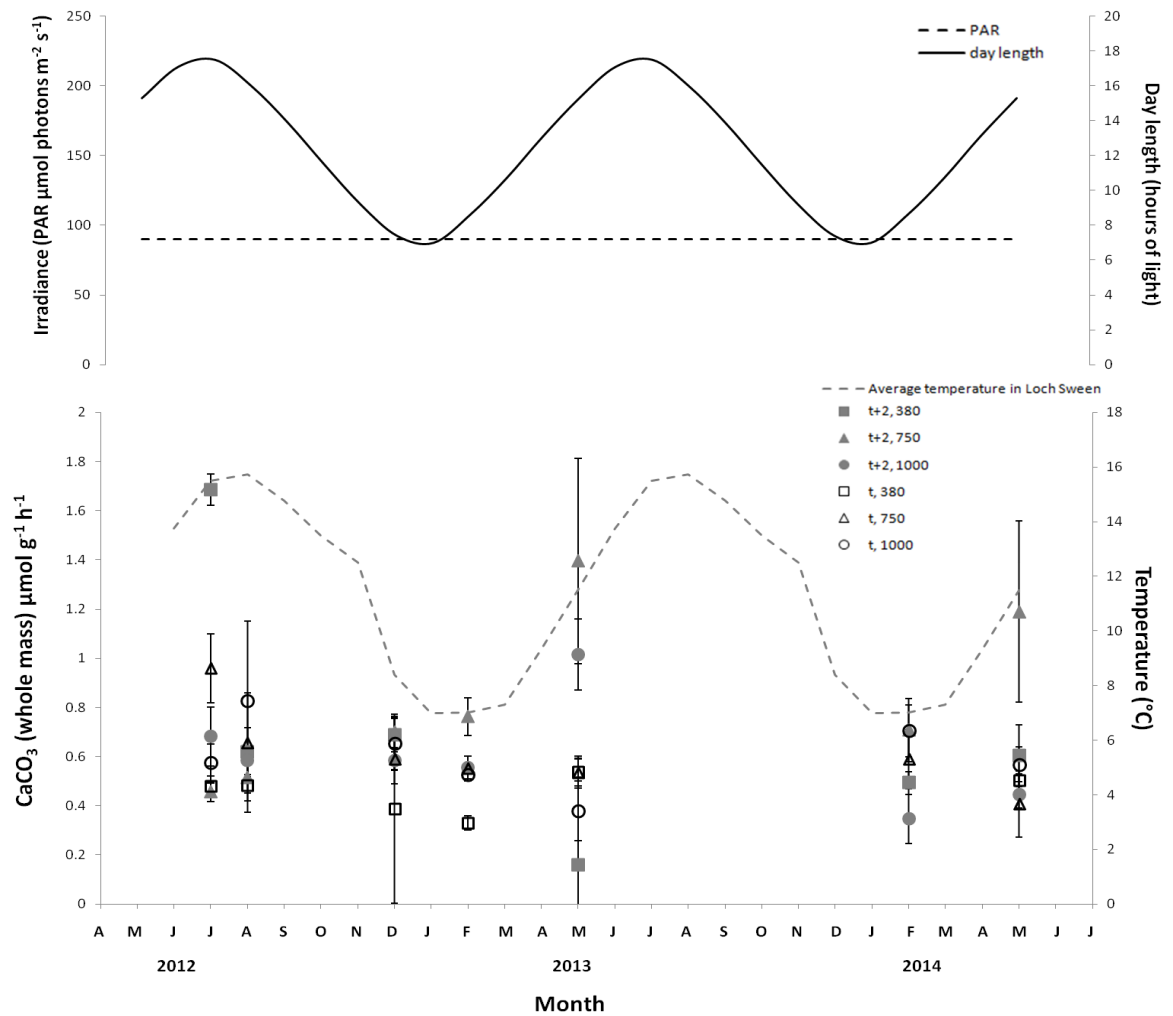


Figure 3.16 Effect of elevated temperature and $p\text{CO}_2$ on calcification rate (CaCO_3 (whole mass) $\mu\text{mol g}^{-1} \text{h}^{-1}$) in *Lithothamnion glaciale* over a two year experimental period. Mean \pm SE. t = ambient temperature (average temperature in Loch Sween); $t+2$ = ambient temperature + 2°C at 380, 750 or 100 $\mu\text{atm } p\text{CO}_2$.

Table 3.7 Summary Scheirer-ray-hare tests followed by Tukey HSD post hoc tests testing the effects of elevated temperature and $p\text{CO}_2$ on rate of calcification (CaCO_3 (whole mass) $\mu\text{mol g}^{-1} \text{h}^{-1}$) in *Lithothamnion glaciale* during each month of a two year experiment. The difference is considered significant when $p < 0.05$ (indicated by the red values). t = ambient temperature; t+2 = ambient temperature + 2°C at 380, 750 or 1000 ppm $p\text{CO}_2$. Different letters (a-d) indicate a significant difference between treatments. nd = no difference. SS = sum of squares.

		Statistical data										Tukey HSD Test							
		Source of variation								(tank number)				t, 380	t+2, 380	t, 750	t+2, 750	t, 1000	t+2, 1000
		$p\text{CO}_2$		Temperature		$p\text{CO}_2$ *temperature													
		SS	df	H	p	H	p	H	p	Test statistic	p								
Calcification																			
Summer	July 2012	13685	2	0.03	0.02	0.015	0.01	4.22	0.88	0.67	0.34	a	b	c	a	ad	d		
Summer	August 2012	11440	2	0.75	0.31	0.32	0.15	1.22	0.46	0.20	0.10	nd							
Autumn	December 2012	14910	2	0.52	0.23	0.28	0.13	0.92	0.37	0.36	0.22	nd							
Winter	February 2013	16206	2	0.43	0.20	3.61	0.84	2.42	0.70	0.54	0.35	nd							
Spring	May 2013	16206	2	0.73	0.31	2.32	0.69	0.03	0.04	1.21	0.63	a	a	a	b	a	b		
Winter	February 2014	10416	2	0.42	0.19	1.03	0.40	0.71	0.30	0.85	0.41	nd							
Spring	May 2014	14910	2	0.33	0.15	1.21	0.45	0.011	0.01	2.34	0.98	a	a	a	b	a	a		

3.9.5 Growth and repair

3.9.5.1 Growth

Growth of *L. glaciale* decreased significantly in response to the elevated temperature treatment ($F_{1,102} = 11.645$, $p < 0.001$), although elevated $p\text{CO}_2$ did significantly increase growth under the elevated temperature conditions ($F_{1,102} = 11.645$, $p = 0.004$, see Figure 3.17).

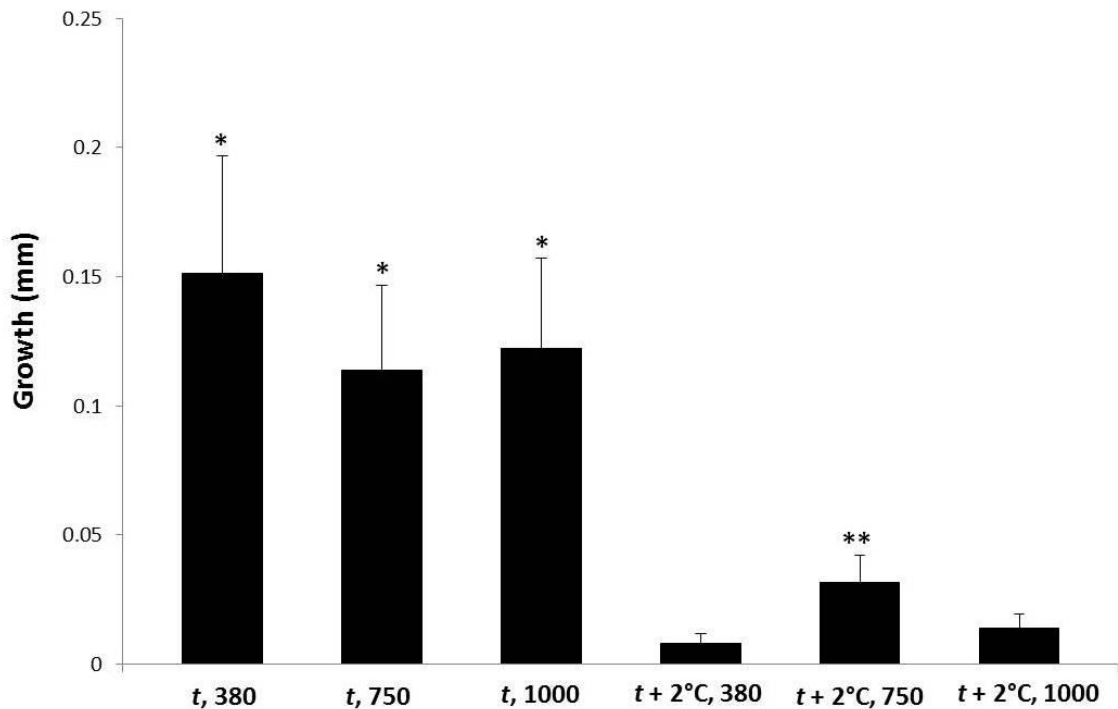


Figure 3.17 Mean \pm SE of growth (mm) of *Lithothamnion glaciale* after 24 months exposure to elevated $p\text{CO}_2$ and temperature. Asterisk (*) indicates a significant difference.

3.9.5.2 Re-growth and repair

The algae in the elevated temperature treatment significantly decreased the re-growth and repair of photosynthetic cells on *Lithothamnion glaciale* after a branch breakage at $p\text{CO}_2$ 380 ppm ($H_{1,36} = 5.452$, $p = 0.02$). However, under elevated temperature conditions, elevated $p\text{CO}_2$ (750 and 1000 ppm) significantly increased the re-growth of photosynthetic material ($H_{1,36} = 10.594$, $p = 0.005$, see Figure 3.18).

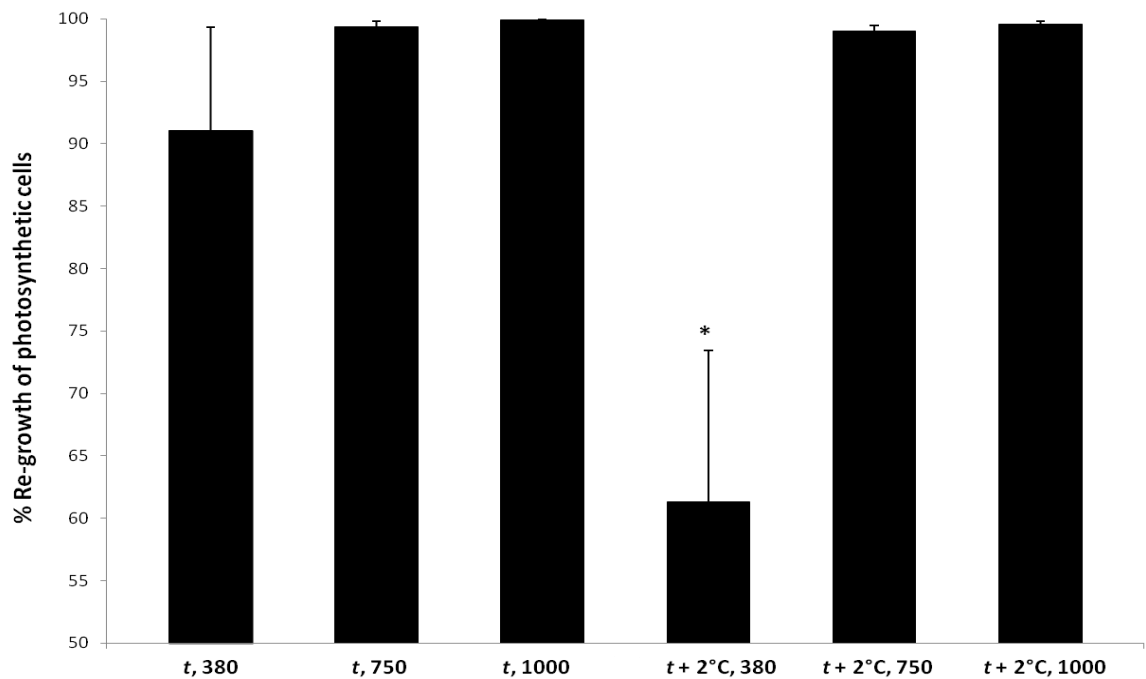


Figure 3.18 Mean \pm SE of re-growth of photosynthetic material on *Lithothamnion glaciale* after branch breakage after four months exposure to elevated $p\text{CO}_2$ and temperature. Asterisk (*) indicates a significant difference. Data represents the % coverage of new material on the total area of exposed calcium carbonate skeleton after breakage.

3.9.6 Scope for acclimatisation

To assess for evidence of acclimatisation to elevated temperature and $p\text{CO}_2$ treatments differences in physiological parameters between year one (May and February 2013) and the same months in year two (May and February 2014) were assessed, p values are summarised in Table 3.8.

3.9.6.1 Photosynthetic characteristics

Only comparisons between photosynthetic characteristics measured in May 2013 and May 2014 are made because rapid light curves were unable to be run in February 2014. E_k and $r\text{ETR}_{\text{max}}$ decreased in May 2014 compared to May 2013 in all treatments, although the control decreased the least relative to algae in the other treatments. $F_q'/F_{m' \text{max}}$ and α increased in algae in the control treatment and combined elevated $p\text{CO}_2$ (750 μatm) and temperature, and decreased in algae in the elevated temperature treatment, in May 2014 compared to May 2013 (refer to Figure 3.12 and Table 3.8).

3.9.6.2 Proteins

3.9.6.2.1 Total Protein

There was no significant difference in total protein concentration in algae in May 2013 compared to May 2014 in any treatment. In addition, total protein concentration did not change in algae in the control treatment in February 2013 compared to February 2014. However, total protein concentration did significantly decrease in algae exposed to elevated temperature ($t+2$, 380) and a combined treatment ($t+2$, 750) in February 2014 compared to February 2013 (Table 3.8 and Figure 3.15).

3.9.6.2.2 Rubisco

There was no significant difference in Rubisco concentration in algae in May 2013 compared to May 2014 in algae in the control treatment. Rubisco concentration significantly increased in May 2014 compared to May 2013 in algae exposed to elevated $p\text{CO}_2$ (1000 μatm) and the combined treatment ($t+2$, 750) to concentrations greater than those observed in the control. Rubisco concentration decreased in May 2014 compared to May 2013 in algae exposed to the combined treatment ($t+2$, 1000) to a concentration similar to that observed in the control (Table 3.8 and Figure 3.15).

Rubisco concentration in algae in the control treatment was significantly greater in February 2014 compared to 2013, and algae exposed to a combined treatment ($t+2$, 1000) followed a similar pattern. Rubisco concentration was lower in February 2014 compared to 2013 in algae exposed to elevated $p\text{CO}_2$ (t , 750 and 1000) (Table 3.8 and Figure 3.15).

3.9.6.2.3 Phycoerythrin

Phycoerythrin concentration was greater in algae in February 2014 compared to 2013 in algae under control conditions. In algae exposed to elevated $p\text{CO}_2$ (t , 750 and 1000) concentration was lower in February 2014 compared to 2013. Concentration was greater in February 2014 compared to 2013 in algae exposed to a combined treatment ($t+2$, 1000) (Table 3.8 and Figure 3.15).

Phycoerythrin concentration was lower in algae in May 2014 compared to 2013 in algae under control conditions. In algae exposed to a combined treatment ($t+2$, 750) and elevated $p\text{CO}_2$ (t , 1000) concentration was greater in May 2014 compared to 2013.

Phycoerythrin was lower in May 2014 compared 2013 in the other combined treatment (t+2, 1000) (Table 3.8 and Figure 3.15).

3.9.6.3 Calcification

In May 2014 compared to 2013 calcification rate in algae under control conditions did not change. Calcification rate of algae exposed to elevated $p\text{CO}_2$ (t, 1000) decreased to a rate similar to that of the control between May 2013 and 2014. There was no change in calcification rate between May 2013 and May 2014 in algae in the other treatments (Figure 3.16 and Table 3.8).

Calcification rate of algae under control conditions was greater in February 2014 compared to February 2013. Calcification rate was lower in February 2014 compare to 2013 in algae exposed to elevated temperature (t+2, 380). There was no change in calcification rate between May 2013 and May 2014 in algae in the other treatments (Figure 3.16 and Table 3.8).

3.10 Discussion

In the present study there is strong evidence to suggest that the physiological response of *L. glaciale* to elevated temperature and $p\text{CO}_2$ is linked to seasonal patterns in temperature, irradiance and day length. This link has been highlighted in previous studies (Martin et al., 2013b), and demonstrates that it is critical to consider the interaction of seasonal changes in environmental conditions when interpreting the response of marine organisms to global climate change. Furthermore, despite continuance and the maintenance of key physiological processes (calcification and photosynthesis) and evidence of acclimatisation, overall growth dramatically declined in response to elevated temperature. This suggests that the energetic cost of maintaining calcification and photosynthesis at elevated temperature and $p\text{CO}_2$ may be at the expense of growth. The following discussion will address the measured physiological factors and discuss them in the context of global climate and natural variability.

3.10.1 Environmental parameters

Temperature, irradiance and day length followed strong seasonal patterns in the field, and salinity was stable throughout the year with no discernible seasonal pattern (Figure 3.3). Temperature, day length and salinity in the laboratory followed the same seasonal pattern observed in the field. Carbonate chemistry parameters measured in both the field and the laboratory were similar across all seasons, although the actual values differed slightly. It is likely that the differences observed between carbonate chemistry observed in the laboratory compared to the field are due to biological activity in the experimental tanks.

3.10.2 Photosynthesis

Calculated photosynthetic characteristics, photochemical quenching and photo-protective parameters observed in *L. glaciale* in both the field and the laboratory followed strong seasonal patterns, and the response of photosynthetic efficiency in *L. glaciale* to elevated $p\text{CO}_2$ and temperature differed among seasons. Significant differences in photosynthetic characteristics in the laboratory were generally observed during year one of the study, and a significant response to elevated $p\text{CO}_2$ was generally only when combined with temperature.

3.10.2.1 Light

E_k is the optimal light for efficient photosynthesis and represents the balance between energy capture and the capacity for the system to process energy (i.e. electron transport rate). E_k observed in the field followed a seasonal pattern, with optimal light for efficient photosynthesis greatest during the spring (June) and lowest during the late autumn/ winter (December-February) (Figure 3.4). The differences in E_k throughout the year are most likely related to an interaction between seasonal changes in PAR, temperature and day length (hours of light). Comparison between *in situ* average (mean) PAR and E_k , suggests *L. glaciale* were photosynthesising under suboptimal light conditions for most of the year, with exception to August, December and February, where E_k values were close to the *in situ* average PAR (Figure 3.4). The suboptimal *in situ* average PAR may explain the decreased photochemical yield ($F_q'/F_m'_{max}$) during early summer and spring compared to late autumn and winter (Figure 3.4). Indeed, analysis of light curves suggests F_q'/F_m' (normalised to E/E_k Figure 3.5) is lower in algae during the summer, compared to other seasons, when light conditions are suboptimal ($E/E_k < 1$). It is likely therefore, that day length may be key for acquiring sufficient energy (light) for the maintenance of other physiological functions, such as calcification, at this time of year.

In the laboratory, under control conditions ($t, 380$), E_k was generally lower, and the range of values was smaller, compared to that observed in the field. This suggests some impact of laboratory conditions, although E_k still followed a seasonal pattern similar to that observed in the field. During June-August 2012 E_k was greater compared to PAR in most treatments (Figure 3.12), although E_k was only significantly affected by the experimental treatments in June. During June E_k was greater than PAR in all treatments with exception to the control ($t, 380$) and significantly increased in response to elevated pCO_2 ; during July E_k was greater compared to PAR in all treatments with exception to elevated temperature ($t+2, 380$); and during August E_k was greater than PAR in all elevated temperature treatments ($t+2, 380, 750, 1000$). This pattern suggests that elevated temperature and/ or pCO_2 may increase the light level required for efficient photosynthesis during these months. PAR in the laboratory was $90 \mu\text{mol m}^{-2} \text{s}^{-1}$ for the duration of the experimental period and *in situ* average PAR in July and August was $80\text{-}110 \mu\text{mol m}^{-2} \text{s}^{-1}$, suggesting light conditions in the laboratory were similar to those observed in the field for this time of year. As *L. glaciale* observed in the field are already operating under suboptimal or close to optimal light conditions during July and August, a

further increase in E_k in response to elevated temperature and/ or $p\text{CO}_2$ may have significant implications for the survival and/ or distribution of *L. glaciale* in the future. Under contemporary conditions a major constraint on the distribution of *L. glaciale* is their requirement for light, restricting them to depths shallower than 32m in northern Europe (Hall-Spencer, 1998). Therefore, a requirement for more light in response to climate change could result in a loss of habitats currently located on the edge of their photo limit, e.g. deep maerl beds or maerl beds in areas prone to turbid waters.

While, in general *L. glaciale* was photosynthesising at suboptimal light levels under laboratory conditions during June-August 2012, during the colder months (December 2012, February 2013/ 14 and May 2013/ 14) in general light conditions were above E_k . During these months there was no significant effect of elevated $p\text{CO}_2$ or temperature on any of the calculated photosynthetic characteristics of *L. glaciale*, with the exception of a significant increase in E_k and $F_q'/F_m'_{max}$ in response to elevated temperature during December. The increase in $F_q'/F_m'_{max}$ during December is likely because elevated temperature increased E_k close to the experimental PAR ($90 \mu\text{mol m}^{-2} \text{s}^{-1}$). Therefore, while algae in the elevated temperature treatment ($t+2$, 380) were operating under light conditions close to optimal, algae in the other treatments were operating under light conditions above optimal. Excess light can lead to increased production of damaging reactive oxygen species as byproducts of photosynthesis (Muller et al., 2001). Indeed, there is an increase in non-photochemical quenching (1-qN) with increasing light in all treatments (Figure 3.14).

3.10.2.2 Temperature and photosynthesis

The initial photochemical reactions are independent on temperature, however, several associated aspects of photosynthesis are temperature dependent (e.g. enzymatic activity and electron transport) (Davison, 1991). Light harvesting efficiency (α) can vary with changes in temperature. In the present study results observed in the field suggest α and $F_q'/F_m'_{max}$ increased with decreasing temperature, and E_k (optimal light level for efficient photosynthesis) decreased with decreasing temperature. This suggests a greater degree of acclimation to low-light during low temperatures compared high temperatures, and may in part be because the amount of light required to reach the compensation point (I_c ; rate of photosynthesis exactly matches respiration) can decrease as temperature decreases (Davison, 1991). Similar results have been observed in the crustose coralline

algae, *L. cabiochae* (Martin et al., 2013b) and other marine algal species (Davison, 1991, Palmisano et al., 1987). In general α followed the same general trend in the laboratory, to that observed in the field (Figure 3.12). During late autumn (December) E_k significantly increased in response to elevated temperature. This is likely to be attributable to enzymatic activity and electron transport working progressively faster as temperature increases, particularly at this time of year when temperature is close to the annual minimum. Concurrently, $rETR_{max}$ and $F_q'/F_m'_{max}$ also increased in response to elevated temperature. Indeed, analysis of $rETR$ light curves (normalised to E/E_k , Figure 3.13) suggests at optimal light levels ($E/E_k=1$) and above ($E/E_k>1$) algae exposed to elevated temperature may be more efficient. However, at suboptimal light levels ($E/E_k<1$) $rETR$ is more similar between treatments. Field observations suggest that current *in situ* PAR is close to E_k at this time of year, in the future under elevated temperature PAR is likely to be below E_k . This suggests algae have to operate under suboptimal light levels at this time of year in the future. However, when elevated temperature was combined with elevated pCO_2 , E_k values were similar to those observed in the control, as were $F_q'/F_m'_{max}$ and $rETR_{max}$.

3.10.2.3 Photoprotective mechanisms

At suboptimal light electron transport serves to optimise light use efficiency, while at above optimal light it operates to dissipate excess excitation *via* photoprotective mechanisms (e.g. heat dissipation, Foyer et al., 2012, Maxwell and Johnson, 2000). During late autumn (December), summer (August) and winter (January) PAR observed in the field was close to E_k (optimal light for efficient photosynthesis). Therefore, fluctuations above E_k (i.e. excess light) may occur more readily than in other months where observed PAR was well below E_k . Indeed, examination of $1-qN$ (normalised to E/E_k) *in situ*, suggest an increase in non-photochemical quenching during the summer and winter compared to autumn months (Figure 3.6). In general, the seasonal pattern in photoprotective mechanisms observed in the laboratory followed a similar pattern to that observed in the field. During the summer non-photochemical quenching ($1-qN$) was lowest at combined elevated pCO_2 (1000 μatm) and temperature ($t+2$, 1000), and during the autumn qN was lowest in the control treatment (t , 380). Concordantly, α , $F_q'/F_m'_{max}$ and F_q'/F_m' were highest in the combined treatment ($t+2$, 1000) during the summer, and highest in the control (t , 380) during the autumn (Figure 3.12 and Figure 3.13). Photo-protective mechanisms are essential to the survival of algae, providing protection against photo-

damage of the photosynthetic membrane (Pascal et al., 2005), however, these mechanisms can be energy expensive (Goss and Jakob, 2012). Therefore, in treatments where algae were more efficient at harvesting light (α), there was a decrease in non-photochemical quenching, which may account for the observed increase in $F_q'/F_m'_{max}$, and *vice versa*. During winter and spring there was less variability in qN between treatments compared to the other seasons, this is likely because there was no significant impact of elevated pCO_2 or temperature during these months, suggesting photo-protective mechanisms may also be similar across all treatments.

3.10.2.4 PAR

The average annual PAR reported here is representative of values measured at specific monthly time points. PAR was measured *in situ*, at each time point, between 1100 and 1400 to coincide with midday (i.e. direct, downward sunlight). Therefore, the average PAR across a whole day (i.e. including dawn and dusk) may actually be lower than the values reported here, although variability would increase. There may also be days when light availability is higher or lower depending of other environmental factors, e.g. cloud cover. Therefore, although representative of *in situ* PAR at the set time points, the time series presented here is only demonstrative of one year; more years should be assessed to confirm this point.

3.10.3 Protein

Total protein concentration did not differ significantly between months in *L. glaciale* in the field (Figure 3.7). However, there was a detectable seasonal pattern with maximum protein concentrations observed in December and the lowest during August. Similarly, although not always significant, protein concentration followed a seasonal pattern in all laboratory treatments. However, maximum protein concentration was generally observed during July-August, with a decrease in December and February (Figure 3.15). Total protein concentration in both the laboratory and the field followed a very similar pattern to the Rubisco and Phycoerythrin concentration.

3.10.3.1 Total protein

In the laboratory, the seasonal variability in total protein, and the variability in the response of protein concentration to elevated temperature and pCO_2 , may be indicative of physiological stress caused by elevated temperature and pCO_2 . *Corallina officinalis*

decreased total protein levels (and growth) in response to elevated $p\text{CO}_2$ after 35 days exposure, suggested to be a tradeoff to maintain calcification (Hofmann et al., 2013). Indeed, the present study observed a decrease in total protein in response to elevated temperature (during autumn, winter and spring), and growth in elevated temperature treatments was significantly reduced compared to algae grown under ambient temperature. Alternatively, the up-regulation of specific proteins (i.e. heat shock proteins) in response to stress has also been reported in the red algae, *Chondrus crispus* (Collen et al., 2006), although the role and production of these proteins in marine algae in response to climate change has received very limited, if any, study.

3.10.3.2 *Phycoerythrin*

Seasonal changes in phycoerythrin were observed in both the laboratory and the field, however, the seasonal pattern in phycoerythrin observed in the laboratory was the opposite of that observed in the field. Phycoerythrin is a red protein-pigment complex, found in red algae it is an accessory light-harvesting pigment to the main chlorophyll pigments. Phycoerythrin concentration can change dependent on irradiance; with greater concentrations observed under low irradiance compared to high light levels (Cole and Sheath, 1990). Presumably the increase in concentration is to increase light harvesting efficiency under decreased irradiance. This change in phycoerythrin concentration is in concordance with the pattern observed in the field; increased phycoerythrin in winter compared to summer, following seasonal changes in irradiance. However, the laboratory study was conducted at a single irradiance (PAR 90 $\mu\text{mol photons m}^{-2} \text{s}^{-1}$), and although the PAR used was average for the study site, it was higher than that usually experienced by the algae during the winter *in situ*. The increased irradiance during the winter under laboratory conditions most likely contributed to the observed decrease in phycoerythrin concentration during the winter months. Despite reduced concentrations of phycoerythrin during the winter algae still maintained light harvesting efficiency (α), which was greater during the winter compared to the summer in the laboratory across all treatments (Figure 3.12). In addition, the concentration of phycoerythrin in response to elevated temperature and $p\text{CO}_2$ differed between seasons (Table 3.6). During spring and summer phycoerythrin concentration increased in response to elevated temperature and $p\text{CO}_2$, this may be linked to the increase in E_k and decrease in α observed during this time (Figure 3.12). Phycoerythrin concentration did not respond significantly during the winter to elevated temperature or $p\text{CO}_2$, although

the general decrease observed may have led to the reallocation of resources (i.e. nitrogen) for the production of other proteins used in key physiological processes and/ or stress response. Reallocation of resources and changes in phycoerythrin concentration in response to elevated temperature and $p\text{CO}_2$ may also have contributed to the seasonal variability in total protein observed in the laboratory.

3.10.3.3 *Rubisco*

Rubisco concentration followed a similar seasonal pattern to phycoerythrin in both the field and laboratory study. Similarly to phycoerythrin, the seasonal pattern in Rubisco concentration observed in the laboratory was opposite to that observed in the field and it is likely the difference in seasonal patterns between the laboratory and field is also related to irradiance as discussed for phycoerythrin. Although, changes in Rubisco concentration may also be linked to a resource optimisation involving the reallocation of resources including nitrogen, a major component of Rubisco (Leahey et al., 2009).

The increase in $p\text{CO}_2$ has the potential to promote photosynthesis by increasing the amount of substrate available to Rubisco (Koch et al., 2013). Although, species-specific responses may be influenced by the presence of carbon concentrating mechanisms (CCMs), which can utilise bicarbonate (HCO_3^-) as a substrate if CO_2 is limited (Giordano et al., 2005), and whether the algae is carbon limited (Johnson et al., 2014). In the present study, the concentration of Rubisco increased in summer, spring and winter in response to an increase in $p\text{CO}_2$. Rubisco concentration also increased during the autumn but only in response to elevated temperature. The increase in Rubisco in response to elevated $p\text{CO}_2$ suggests algae may be carbon limited at ambient $p\text{CO}_2$ levels and/ or rely more on diffusion of CO_2 for photosynthesis under high- CO_2 conditions, as opposed to CCMs. CCMs are energy expensive, therefore under high- CO_2 conditions obtaining CO_2 via diffusion would allow for the reallocation of energy to other physiological process, if indeed the algae utilises CCMs when carbon is more limited. In the present study, $r\text{ETR}_{\text{max}}$, α , and $F_q'/F_{m' \text{max}}$ increased in response to elevated $p\text{CO}_2$, but only when combined with elevated temperature, during the spring and summer, suggesting there may be a link between increased Rubisco and photosynthetic efficiency.

3.10.4 Calcification, growth and repair

Temperature above the upper limits of the normal range experienced by *Lithothamnion glaciale* appears to have a significantly negative impact on growth and repair in *L. glaciale*. Although calcification rate either did not change, or indeed increased in response to environmental change, changes in respiration rate are likely to have impacted overall growth of the algae. Furthermore, it is likely warming amplified the effects of elevated $p\text{CO}_2$ on skeletal dissolution, negatively impacting growth. Repair efficiency of damaged thalli branches was also significantly negatively affected by elevated temperature, although elevated $p\text{CO}_2$ appeared to off-set the negative impact of elevated temperature on re-growth and repair of *L. glaciale* in the short term.

3.10.4.1 Calcification

Calcification rate in the field followed a strong seasonal pattern; this is likely to be due to the relationship between calcification and photosynthesis, the changes of which are related to seasonal differences in temperature and irradiance (Pentecost, 1978). Calcification is affected by photosynthesis due to changes in internal pH and the formation of the organic matrix in the cell walls required for calcite deposition (Martin et al., 2013b). Internal changes in pH are affected by photosynthesis and respiration, therefore calcification is mainly regulated by these processes (Gao et al., 1993, Martin et al., 2013b). In the field, maximal calcification rates were observed during the summer and minimal rates in the winter, as reported previously for red coralline algae (Martin et al., 2006), corresponding to seasonal changes in irradiance, day length and temperature. In the laboratory, calcification rate still followed a similar seasonal pattern to that observed in the field in all treatments, with the exception of algae exposed to combined elevated temperature and $p\text{CO}_2$ ($t+2$, 750 and 1000 μatm) which did not differ significantly between months. In the present study E_k (optimal light for efficient photosynthesis) increased in response to elevated $p\text{CO}_2$ and temperature during spring and autumn. The increased E_k in response to elevated temperature and $p\text{CO}_2$, compared to control conditions, is likely to have contributed to the loss of the seasonal pattern, if indeed photosynthesis stimulates calcification in *L. glaciale*. Conversely, if calcification stimulates photosynthesis, the decrease in calcification rate in response to elevated $p\text{CO}_2$ and temperature may have led to the increase in E_k , although published literature suggests that it is photosynthesis that stimulates calcification. In addition, the loss of seasonal patterns in calcification in algae exposed to elevated temperature and $p\text{CO}_2$ may

also be in part due to the use of a single irradiance during the experimental period. Although, it is important to note the average PAR experienced *in situ* during spring and autumn is below the annual average ($90 \mu\text{mol photons m}^{-2} \text{s}^{-1}$) at which the experiment was conducted (Figure 3.3). Other photochemical characteristics (α , $r\text{ETR}_{\text{max}}$ and F_q'/F_m' $_{\text{max}}$), which may indicate changes in photosynthetic efficiency which may subsequently impact calcification, were also affected by elevated temperature and $p\text{CO}_2$ depending on season (Figure 3.12).

The response of calcification rate in coralline algae to elevated $p\text{CO}_2$ and temperature has also been shown to differ within seasons, suggesting an interaction between environmental change and seasonal patterns in irradiance, day length and temperature (Martin et al., 2013b). The present study observed seasonal differences in the response of *L. glaciale* to elevated temperature and $p\text{CO}_2$. During the spring elevated temperature had a positive effect on calcification but only when combined with $p\text{CO}_2$, and the lowest calcification rate was observed under elevated temperature at ambient $p\text{CO}_2$. In contrast during summer the highest calcification rates were observed under elevated temperature and ambient $p\text{CO}_2$, and elevated $p\text{CO}_2$ (750 μatm) at ambient temperature, with calcification in combined treatments being no different from the control. During autumn and winter months, when ambient temperatures were lowest, there was no observed effect of elevated temperature or $p\text{CO}_2$ on calcification rate. Results of the present study suggest the effects of temperature and $p\text{CO}_2$ on calcification in *L. glaciale* are more significant during months when ambient temperatures are highest, demonstrating that it is critical to consider the interaction of environmental change with seasonal patterns of temperature.

3.10.4.2 Growth

Over the two year experimental period growth was maintained in all treatments, although growth of algae in all elevated temperature treatments was significantly decreased, compared to those algae at ambient temperature (Figure 3.17). Although increased temperature during the summer is known to have a positive effect on the growth (and repair) of calcified algae, suboptimal growth may occur at temperatures above (or below) the temperature range to which the algae are most adapted (Fortes and Lüning, 1980). Temperature can affect the rate of enzymatic reactions, electron transport rate, and can influence the properties of common cellular components such as lipids,

proteins and carbohydrates (Raven and Hurd, 2012b, Raven and Geider, 1988), which may impact growth. In red algae, high temperature inhibition of photosynthesis is associated with a disruption of energy transfer between phycobilisomes (phycoerythrin) and PSII (Kuebler et al., 1991), which in turn may decrease growth. Furthermore, warming can amplify the effects of elevated $p\text{CO}_2$ on calcification and skeletal dissolution (Diaz-Pulido et al., 2012). Although in the present study calcification increased in response to elevated temperature during spring when combined with $p\text{CO}_2$ and increased in response to temperature and $p\text{CO}_2$ during the summer, overall growth was negatively impacted by elevated temperature and $p\text{CO}_2$, suggesting it is unlikely changes in photosynthesis are the sole factors influencing the growth of calcified algae. Other features of metabolism such as the rate of dark respiration and efflux of organic carbon (e.g. dissolution) will also influence the amount of fixed carbon available for growth (Davison, 1991). Dark respiration is known to present a strong seasonal pattern following changes in temperature in the calcifying red alga *Lithophyllum cabiochae*, with the highest rates reported during summer and lowest during winter (Martin et al., 2013b). The general trend in dark respiration over all four seasons for *L. cabiochae* was an increase under elevated temperature (3°C rise above ambient), except in summer under 700 μatm , where dark respiration declined in response to elevated temperature (Martin et al., 2013b). Furthermore, it is suggested, the light level required to meet the compensation point (I_c , rate of photosynthesis exactly matches respiration) may increase with increasing temperature, as described for *Laminaria saccharina*, where light harvesting efficiency declined and dark respiration increased in response to elevated temperature (Davison, 1991). Therefore, although calcification rate may not change, or indeed increase in response to environmental change, changes in respiration rate are likely to impact overall growth.

3.10.4.3 Branch repair

The present study assessed repair of broken branches on *L. glaciale* thalli during the highest temperature months of the year, the optimal growth season, in year two of the study (June-October 2013). During July and August ambient temperature (t) was at the upper most temperature experienced by *L. glaciale* in the field (ambient for the time of year), with temperature in the elevated treatment ($t+2^\circ\text{C}$) 2°C above that usually experienced by the maerl. Calcification rate of algae in the month prior to the start of the breakage and repair experiment (May 2013) was lowest in algae exposed to elevated

temperature ($t+2$, 380), and greatest in those thalli exposed to elevated temperature combined with elevated $p\text{CO}_2$ ($t+2$, 750 1000, Figure 3.16). It is likely suboptimal calcification of *L. glaciale* at temperatures outwith the normal temperature range of the algae may also translate into the observed decrease in repair efficiency at elevated temperature ($t+2$, 380). Although, the observed decrease in repair efficiency of the broken algae branches at the elevated temperature appears to be improved by exposure to elevated $p\text{CO}_2$, with algae exposed to elevated temperature combined with elevated $p\text{CO}_2$ (750 and 1000 μatm) achieving % re-growth of photosynthetic cells similar to that of the control (t , 380). This response may be as a result of the increase in substrate (dissolved inorganic carbon, DIC) utilised in photosynthesis. Photosynthesis under ambient DIC conditions is often unsaturated, and several macroalgae species have shown increased photosynthesis and growth under elevated $p\text{CO}_2$ conditions (Zou, 2005, Gao et al., 1991, Gao et al., 1993, Kubler et al., 1999). However, more recently several studies suggest that although growth may be maintained under high $p\text{CO}_2$, the structural integrity of the algae may be compromised (Ragazzola et al., 2012, Burdett et al., 2012a). At high $p\text{CO}_2$, new *L. glaciale* cells were more elongated and wider, resulting in decreased cell density (Ragazzola et al., 2012). Therefore, although in the present study observed results suggest that branch repair in the elevated $p\text{CO}_2$ treatments was similar to that of the control thalli, this may come at a cost to the internal structure and/or cell density of the algae exposed to elevated $p\text{CO}_2$. Furthermore, a reduction in cell density may have implications for overall photosynthetic efficiency of the algae in the long term.

3.10.5 Scope for acclimatisation

Differences in the response of marine calcifiers to elevated temperature and $p\text{CO}_2$ has been link to acclimatisation in previous experiments. Form and Riebesell (2012) observed differences in cold water coral physiology between short (24h) and longer term (months) experiments; by which the response to acidified conditions after 24 h was different to that observed after several months. Johnson et al. (2014) also found evidence of acclimatisation of tropical crustose coralline algae to ocean acidification. Currently, little is known about species scope for acclimatisation to elevated temperature and $p\text{CO}_2$. Understanding acclimatisation potential in species can help improve our understanding of how marine ecosystems may change in the future.

3.10.5.1 Calcification

In May of year one calcification rate significantly increased in response to the combined treatments (t+2, 750 and 1000). In May of year two calcification rate in the combined treatment of elevated temperature and $p\text{CO}_2$ at 750 μatm decreased to a rate similar to that observed in the control, while calcification rate in the combined treatment of elevated temperature and $p\text{CO}_2$ at 1000 remained high. Therefore, there was still a significant effect of elevated temperature and $p\text{CO}_2$ on calcification rate in May of year two. However, there was evidence of acclimatisation of calcification rate in algae to elevated temperature and $p\text{CO}_2$ at 750 μatm (Table 3.8 and Figure 3.16). In February of year one and year two there was no significant effect of elevated temperature and $p\text{CO}_2$ on calcification rate. However, there were significant differences in rate between February of year one and year two in the elevated temperature treatment, which increased to a rate more similar to that of the control. Although, there was no significant difference between calcification rate in the control and elevated temperature treatment during February in year one, an increase in rate towards the rate observed in the control suggests there is a degree of acclimation by algae in this treatment. In the present study overall growth was significantly negatively impacted by elevated temperature. There is evidence of acclimation to elevated temperature in the present study, and an increase in calcification rate in algae in the elevated temperature treatment in year two suggests overall growth in this treatment may improve in the long term. However, when combined with elevated $p\text{CO}_2$, calcification rate increased in both year one and two compared to the control, but this did not translate into increased growth. This suggests skeletal dissolution and respiration may also increase under elevated $p\text{CO}_2$. Therefore, unless respiration (or other physiological parameters i.e. photosynthesis) also acclimates to elevated temperature and $p\text{CO}_2$, overall growth of coralline algae will be negatively impacted by climate change in the future regardless of whether calcification rate acclimates or not.

3.10.5.2 Proteins

During May 2013 total protein concentration increased in response to the elevated temperature treatment (t+2, 380). In May 2014 this pattern still remained, suggesting there was no acclimation, in terms of total protein concentration, to elevated temperature during May. In contrast, during February 2013 algae significantly increased total protein in response to elevated temperature and $p\text{CO}_2$, however in February 2014

there was no effect of elevated $p\text{CO}_2$ on protein concentration. Indeed, comparison between total protein concentration in February 2013 and 2014 suggests protein concentration in elevated temperature (t+2, 380) and a combined treatment (t+2, 750) significantly decreased to values similar to those observed in the control. This provides some evidence of acclimatisation, in terms of total protein, to elevated temperature and $p\text{CO}_2$ during February.

During May in year one there was a significant increase in Rubisco concentration in response to elevated temperature and $p\text{CO}_2$. However, in the same month in year two of the study, Rubisco concentration in the combined treatment (t+2, 1000) was lower and a concentration similar to the control was observed. This suggests some scope for acclimatisation, in terms of Rubisco concentration, to elevated temperature and $p\text{CO}_2$ in the long term. During February, Rubisco concentration in the control significantly increased in year two compared to year one. There were also differences in Rubisco concentration in algae in the other treatments between February year one and year two (Table 3.8). However, there were no significant differences between treatments in February 2013 or 2014. Suggesting the observed differences in Rubisco concentration between February year one and year two may be linked to the laboratory conditions, rather than acclimatisation. Similarly, this effect was also observed in Phycoerythrin concentration when comparing February year one with year two. In May of year one phycoerythrin concentration significantly increased in response to combined elevated temperature and $p\text{CO}_2$ at 1000 μatm , but significantly decreased when temperature was combined with $p\text{CO}_2$ at 750 μatm . Phycoerythrin concentration then decreased and increased, respectively, in May of year two, resulting in no significant difference between treatments in May 2014. However, phycoerythrin concentration also changed between years one and two in the control. Therefore, there may be some evidence of acclimatisation, however a change in the control also suggests that laboratory conditions may also be having an effect.

3.10.5.3 Photosynthesis

Evidence for acclimatisation of the photosynthetic characteristics ($F_q'/F_{m'_{max}}$, E_k , $r\text{ETR}_{max}$, α) to elevated $p\text{CO}_2$ and temperature was difficult to ascertain because in all cases the control differed significantly between year one and year two (Table 3.8). In all cases there was no significant difference between treatments in both May 2013 and May

2014. Suggesting the differences observed between year one and year two may be as result of laboratory conditions. Although in general $rETR_{max}$ and E_k decreased in May of year two compared to year one (Figure 3.12) resulting in a general increase in $F_q'/F_{m'}'_{max}$ and α in year two, compared to year one. It is likely this may be an acclimation response to the single irradiance used in the laboratory study.

3.10.6 Wider implications

Maerl are among the slowest growing algal species and are very long-lived and, with growth rates as low as 0.1 to 2 mm yr⁻¹ it can take thousands of years for maerl beds to accumulate (Blake and Maggs, 2003, Bosence and Wilson, 2003). In addition, maerl requires water motion (i.e. current or wave action) in order to prevent fouling, burial by sediment, overgrowth by other algae and invertebrates, and to maintain them in a free living, unattached state (Foster, 2001, Steller et al., 2003). Although maerl are not found in areas with extremely high wave action and/ or currents, water movement can still result in mechanical damage and breakage, and more so with the occurrence of storms. In addition, recruitment to free-living maerl populations and reproduction is predominantly from fragmentation of thalli and/ or branches shed from attached branched crusts, with vegetative propagation from unattached plants reportedly very rare (Freiwald, 1995, Cabioch, 1969). The fragility, relatively slow growth and recovery rate, and reliance on fragmentation for reproduction and recruitment of free-living corallines may make them particularly susceptible to anthropogenic impacts (Bosence and Wilson, 2003, Wilson et al., 2004), particularly if, as evidence of the present study suggests, environmental change further decreases growth rate. In addition, a decrease in growth in response to elevated temperature and pCO_2 may also affect the size, shape, and branching patterns of maerl thalli, decreasing the morphological diversity currently present between maerl beds. Impacts on morphology may have implications for the distribution of maerl beds, limiting the type of environments in which they may survive. In addition, the southern distribution limits of *L. glaciale* may shift north as temperature increases leading to a loss of biodiversity, habitat provision, and ecosystem services in Scottish waters. Ecosystem services include the long term storage of organic and inorganic carbon (Burrows et al., 2014). Aggregations of free-living corallines in Scotland, and indeed globally, are extensive and area and volume can be large (Burrows et al., 2014), and it suggested that maerl beds may significantly contribute to carbon storage in coastal waters (Burrows et al., 2014). Therefore, a decrease in growth rate would

dramatically impact the contribution of coralline algae to carbon storage with implications for the carbon budget in Scottish waters and globally.

3.10.7 Conclusions

Coralline algae are considered to be among the most vulnerable organisms to global climate change due to the high solubility of their high-Mg calcite skeleton under acidified and warming conditions. However, the present study provides evidence that suggests *L. glaciale* can maintain, and even increase, calcification and photosynthesis during long-term exposure to elevated temperature and $p\text{CO}_2$. However, despite maintenance of these key physiological processes and evidence of acclimatisation, overall growth was severely negatively impacted by elevated temperature. Coralline algae perform a critical role in coastal ecosystems, and future projections for elevated temperature and $p\text{CO}_2$ may have major implications for the continuance of free-living coralline algae habitats, with critical ecological implications for coastal marine systems. Furthermore, by understanding natural variability and the role it may play in influencing a species response to global climate change it may provide an insight into the potential for organisms to acclimatise and adapt to changing ocean conditions in the future.

4

Short-term experiment: Light availability mediates coralline algal responses to multiple stressors

Irradiance is key in coralline algal photosynthesis yet the role of light availability on mediating coralline algal responses to multiple stressors remains scant. The present study examines net photosynthesis and photosynthetic characteristics in the free-living coralline algae, *Lithothamnion glaciale* in response to sub-diel changes in irradiance in algae exposed to elevated temperature and $p\text{CO}_2$.

4.1 Light-saturated photosynthesis and temperature

Generally, photosynthesis in algae increase with increasing temperature under light saturated conditions until an optimum point, beyond which photosynthesis declines rapidly (Davison, 1991, Oates and Murray, 1983). The factors limiting light-saturated photosynthesis include electron transport rate (Voncaemmerer and Farquhar, 1981), rate of carbon fixation by Rubisco (Rivkin, 1990) and / or rate of ATP regeneration (Stitt et al., 1987). In red algae, inhibition of photosynthesis at high-temperature has been linked with a disruption of energy transfer between phycobilisomes and PSII (Kuebler et al., 1991). In general, the high-temperature thermostability of photosynthetic enzymes has

been shown to exceed that of whole plant photosynthesis in marine algae (Descolas-Gros and de Billy, 1987).

4.2 Light-limited photosynthesis and temperature

Under limited light the response of photosynthesis to temperature is very different. Although the initial photochemical reactions are independent of temperature, temperature can impact the rate of the other photosynthetic processes (e.g. enzymes, photophosphorylation, electron transport) (Davison, 1991, Raven and Geider, 1988, Raven and Hurd, 2012b). Because of the dependence of temperature on many associated aspects of photosynthesis, in the short-term (hours), the light harvesting efficiency (α ; the slope of the initial light-limited region of the photosynthesis-irradiance curve) is likely to decline with increasing temperature, while dark respiration increases (Davison, 1991). These changes mean that the amount of light required to reach the compensation point (I_c ; the amount of light where photosynthesis exactly matches respiration) increases as temperature increases. Additionally the rate of net photosynthesis (at sub-saturating light levels) decreases or increases at a reduced rate compared to light light-saturated photosynthesis (Davison, 1991).

4.3 $p\text{CO}_2$, temperature, photosynthesis and irradiance

The availability of dissolved inorganic carbon (DIC) may influence photosynthesis, particularly if ambient levels of DIC are sub-saturating. However, any benefit of elevated $p\text{CO}_2$ is likely to be more readily realised where photosynthesis is light-saturated and/ or temperature is close to optimum, because at low temperature electron transport and carbon fixation is limited reducing the ability of the algae to use light (Davison, 1991). The availability of DIC may also affect the response of photosynthesis to changes in temperature. Temperature-sensitive processes that may be influenced by the availability of DIC, and may influence the overall rate of photosynthesis, including; diffusion of CO_2 , carbonic anhydrase activity, active transport of CO_2 and/ or HCO_3^- across the plasmalemma and/ or chloroplast membranes (Davison, 1991). Photosynthesis in coralline algae grown under ambient conditions, as well as elevated $p\text{CO}_2$ and temperature, follow seasonal patterns, with increased photosynthesis occurring concurrent with seasonal increases in irradiance and temperature (Martin et al., 2013b),

although the algae did experience a significant decrease in net productivity in response to elevated $p\text{CO}_2$ during the summer, autumn and winter (Martin et al., 2013b). Thus there is evidence to suggest irradiance may play a role in mediating the photosynthetic response of coralline algae to global change; however this has not yet been specifically tested.

While we have insight into the influence that changes in day length may have on photosynthesis, growth, calcification, and other key physiological functions (Dring et al., 1996, Wilson et al., 2004), laboratory studies are often conducted using average ambient photosynthetically active radiation (PAR), based on average day-time irradiance experienced *in situ* for the time of year (e.g. Ries et al., 2009, Egilsdottir et al., 2013, Kamenos et al., 2013). However, habitat heterogeneity and the complex geometry of algae results in intra- and / or inter-structural (branch) thallus shading (Burdett et al., 2012b). Also, diurnal irradiance patterns mean reduced PAR at dawn and dusk (Burdett, 2014). Therefore, PAR changes at short temporal and spatial scales mean the response of algae to ocean acidification and warming is likely highly variable at diel time scales within a single individual due to mediation by light availability. Thus, this may determine the diel photo-physiological responses of coralline algae to multiple stressors in the natural habitat, producing divergent responses from those generated in laboratory experiments using averaged PAR levels.

4.4 Aims of this chapter

This chapter will investigate the response of coralline algae to elevated temperature and $p\text{CO}_2$ during sub-diel changes in light availability. Net photosynthesis and key photosynthetic characteristics were quantified in the free-living *Lithothamnion glaciale* in response to elevated temperature and $p\text{CO}_2$ under increasing PAR levels.

It is hypothesised that the response of coralline algae to elevated temperature and $p\text{CO}_2$ is mediated by irradiance; increased PAR will decrease the impact of multiple stressors on net productivity.

4.5 Methods

4.5.1 Experimental set-up

Lithothamnion glaciale specimens were hand collected from Loch Sween, Scotland (56°01.99' N, 05°36.13' W), using SCUBA from 7 m depth in February 2012. *In situ*, the algae experience an annual temperature range of 6-16 °C, light levels of 12-120 $\mu\text{mol m}^{-2} \text{s}^{-1}$ PAR; pH remains at ~ 8.1 throughout the year (Rix et al., 2012). After collection, thalli were transferred into seawater holding tanks (380 $\mu\text{atm } p\text{CO}_2$, ambient temperature). Individual *L. glaciale* thalli were placed into 24 one litre plastic aquaria and allocated randomly to 1 of 4 different treatments (n = 6 thalli per treatment): (1) ambient *in situ* temperature (7 °C) at 380 $\mu\text{atm } p\text{CO}_2$ (control, t, 380), (2) ambient temperature +3°C at 380 $\mu\text{atm } p\text{CO}_2$ (temperature treatment, t+3, 380), (3) ambient temperature at 1000 $\mu\text{atm } p\text{CO}_2$ ($p\text{CO}_2$ treatment, t, 1000), and (4) ambient temperature +3 °C at 1000 $\mu\text{atm } p\text{CO}_2$ (multiple stressor treatment, t+3, 1000). These $p\text{CO}_2$ and temperature levels were chosen to simulate contemporary environmental levels and those predicted for 2100 (IPCC, 2013). Seawater acidification was achieved by bubbling CO_2 gas and air mixture directly into each individual aquarium. Aquaria were placed into a water-bath to maintain the required temperature (Teco Seachill TR15 Aquarium Chiller) (see section 2.1.3, short-term set-up). In all treatments, algae were exposed to ambient light conditions present in the field at the time of collection (PAR: 12 $\mu\text{mol m}^{-2} \text{s}^{-1}$) supplied via LED tile lamps (48 LED clip light, 27.4 x 15.4 x 7 cm) suspended above the aquaria. Algae were exposed to the experimental treatments for 7 days before photosynthetic characteristics and net productivity were assessed.

4.5.2 Environmental parameters

4.5.2.1 Carbonate chemistry

Total alkalinity (A_T), $p\text{CO}_2$, salinity and temperature were determined for each treatment; $p\text{CO}_2$ was monitored continuously and recorded every 5 minutes throughout the experiment using a LI-COR CO_2 gas analyser (LI-820, LI-COR Environmental – GmbH, Bad Homburg, Germany). Temperature and salinity were recorded daily using a handheld conductivity meter (Pro 2030, YSI, Ohio, USA). A_T ($\mu\text{mol kg}^{-1}$) was determined from seawater samples taken at the beginning and end of the experiment using the open-cell titration method described by Yao and Byrne (1998b) and detailed in Chapter 2 (section 2.6). On collection, A_T seawater samples were poisoned with mercuric chloride (40 μl of a

50% saturated solution) (Riebesell et al., 2010), and stored in 12 ml screw top borosilicate glass vials (Exetainer, Labco Ltd., UK) until analysis (see Chapter 2, section 2.7). Additional carbonate system parameters (DIC, calcite and aragonite saturation, $[\text{HCO}_3^-]$ and $[\text{CO}_3^{2-}]$) were calculated from A_T , $p\text{CO}_2$, salinity and temperature using the software program CO2SYS as described in Chapter 2 (section 2.9).

4.5.2.2 Photosynthetically active radiation

PAR ($\mu\text{mol photons m}^{-2} \text{s}^{-1}$) was recorded using an underwater quantum sensor (Apogee QSO-E underwater quantum sensor connected to a Gemini voltage data logger).

4.5.3 Photosynthesis

4.5.3.1 Net photosynthesis (light response curves)

Photosynthetic light response curves were performed at the end of the experimental period to assess the light-mediated response of net photosynthesis in *L. glaciale* to elevated $p\text{CO}_2$ and temperature. *L. glaciale* thalli were placed in 220 ml incubation chambers fitted with a magnetic stirrer and oxygen optode connected to a temperature-compensated oxygen analyser (Oxy-4 Mini with Temp-4, Presens & Loligo systems). Chambers were filled with seawater from the experimental aquaria and algae were allowed to acclimate for 30 minutes. Chambers were maintained at the treatment levels throughout analysis. Oxygen production / respiration were recorded over six 30 minute periods for each thallus at six increasing levels of PAR (LED tile lamps; 48 LED clip light, 27.4 x 15.4 x 7 cm); (1) 12.03 ± 2.51 , (2) 36.53 ± 6.17 , (3) 62.90 ± 9.16 , (4) 85.15 ± 12.01 , (5) 105.36 ± 3.58 , and (6) $117.78 \pm 3.54 \mu\text{mol m}^{-2} \text{s}^{-1}$ (mean \pm SD). Light increments were chosen based on the range of PAR experienced by *L. glaciale* in the field at the collection site over a diel cycle (see Rix et al., 2012). Following the incubations, each algal thallus was weighed and rates of oxygen production / respiration were converted to $\mu\text{g C g}^{-1} \text{tissue h}^{-1}$ using a respiratory quotient of 0.8 (equal to CO_2 eliminated / O_2 consumed (Hatcher, 1988, Hatcher, 1989)).

4.5.3.2 Chlorophyll-*a* fluorescence (PAM fluorometry)

A Diving-PAM fluorometer was used at the end of the experimental period to assess the photosynthetic characteristics of *L. glaciale* using rapid light curves (RLCs). The PAM fluorometer measures chlorophyll-*a* fluorescence and provides quantitative information about the state of Photosystem II, which can be used to estimate key

characteristics of photosynthesis (Maxwell and Johnson, 2000). When combined with other techniques for assessing photosynthesis (i.e. O₂ production) it can provide a full picture of the photosynthetic response of algae to their environment (Maxwell and Johnson, 2000). See Chapter 2 (section 2.2) for a detailed description of using the Diving-PAM to perform RLCs. Photosynthetic characteristics (E_k (light saturation coefficient, $\mu\text{mol m}^{-2} \text{s}^{-1}$), $r\text{ETR}_{\text{max}}$ and $r\text{ETR}$ (calculated maximum and relative electron transport rate, $\mu\text{mol electrons m}^{-2} \text{s}^{-1}$), $F_q'/F_{m'_{\text{max}}}$ and $F_q'/F_{m'}$ (calculated maximum and effective photochemical efficiency of PSII under actinic light, dimensionless) (relative electron transport rate, $\mu\text{mol electrons m}^{-2} \text{s}^{-1}$)) were determined using methods as previously described (Suggett et al., 2007, Hennige et al., 2008, Burdett et al., 2012b) (see Chapter 2, section 2.2).

4.5.4 Statistical analysis

Two-way ANOVAs were used to investigate differences in photochemical characteristics, between algae exposed to a control treatment (t , 380 μatm), elevated temperature ($t + 3$, 380 μatm), elevated $p\text{CO}_2$ (t , 1000 μatm) and a multiple stressor treatment ($t + 3$, 1000 μatm). Each algal thallus used during the oxygen evolution light curves was repeatedly measured at each increasing light level. Therefore, a repeated measures ANOVA was used to assess differences in net productivity (oxygen evolution) between treatments at each increasing light level used in the light curves. Where assumptions of ANOVA were not met data were log transformed (net photosynthesis, $F_q'/F_{m'_{\text{max}}}$ and α). Differences between means / medians were considered to be significant when $p \leq 0.05$. All analyses were conducted with SPSS v18.0.

4.6 Results

4.6.1 Environmental parameters

4.6.1.1 Carbonate chemistry

The seawater physico-chemical parameters for the experimental period are summarised in Table 4.1.

Table 4.1 Mean±SD seawater physico-chemical parameters measured or calculated for the aquaria during the experimental period.

Treatment	t°C, 380 µatm (control)	t°C, 1000 µatm	t + 3°C, 380 µatm	t + 3°C, 1000 µatm
Salinity	36.33±0.5	34.6±1.1	34.6±0.5	35.3±0.5
Temperature (°C)	6.70±0.1	6.7±0.1	10.3±0.1	10.2±0.1
pH*	8.20±0.03	7.7±0.08	8.23±0.04	7.73±0.06
DIC (µmol kg ⁻¹)*	1858.1±1.7	1994.4±9.6	1841.9±2.6	1978.1±9.3
A _T (µmol kg ⁻¹)	2488.7±213.3	2206.8±284.9	2285.8±278.1	2078.5±435.8
pCO ₂ (µatm)	368.0±0.7	1120.3±81.4	368.1±0.7	1120.3±81.4
HCO ₃ ⁻ (µmol kg ⁻¹)*	2124.7±162.9	2092.4±250.3	1937.7±206.2	1961.2±401.5
CO ₃ ²⁻ (µmol kg ⁻¹)*	145.4±22.5	45.2±15.6	137.6±31.9	44.7±14.9
Ω _{cal} *	3.46±0.53	1.08±0.37	3.30±0.77	1.07±0.35
Ω _{ara} *	2.17±0.33	0.68±0.24	2.07±0.48	0.68±0.22

Temperature, salinity, total alkalinity (A_T) and dissolved inorganic carbon (DIC) were measured; pH, pCO₂, HCO₃⁻, CO₃²⁻, calcite saturation (Ω_{cal}), aragonite saturation (Ω_{ara}) (indicated by an *) were calculated using CO2SYS. Treatments: t = ~7°C, t + 3 = ~10°C; at 1000 µatm or 380 µatm pCO₂.

4.6.2 Photosynthetic characteristics

4.6.2.1 Net photosynthesis and photosynthetic light response curves

Net photosynthesis increased significantly with increasing irradiance in all treatments ($F_{1,74} = 63.10$, $p < 0.001$, Figure 4.1). Maximum net photosynthesis was observed in algae in the control treatment between 62 - 105 µmol m⁻² s⁻¹. Maximum net photosynthesis in all other treatments was observed at 105 µmol m⁻² s⁻¹, with a decrease in net photosynthesis in all treatments at 117 µmol m⁻² s⁻¹ (Figure 4.1). At 12-62 µmol m⁻² s⁻¹, net photosynthesis in *L. glaciale* decreased significantly in response to elevated pCO₂ compared to algae in the control treatment ($F_{1,74} = 26.994$, $p < 0.001$, Figure 4.1), with net respiration reported in the multiple stressor treatment at 12 µmol m⁻² s⁻¹ (-30.21 ± 13.82 O₂ µmol g⁻¹ h⁻¹, mean±SE). Temperature had no significant effect on net photosynthesis at any light level ($F_{1,74} = 1.34$, $p = 0.250$).

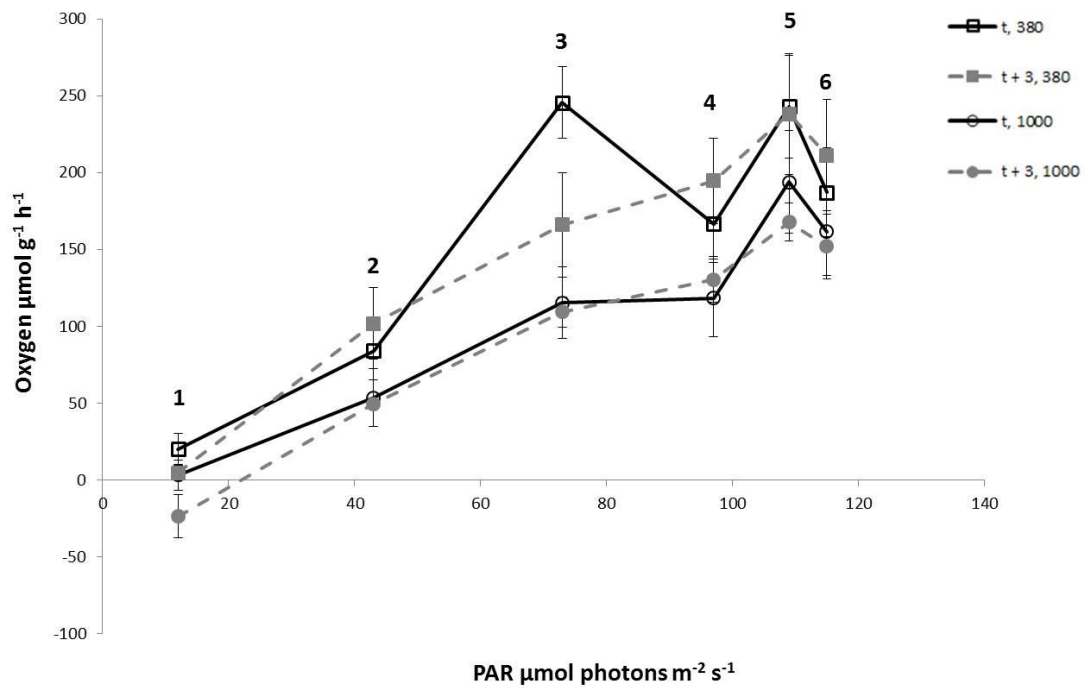


Figure 4.1 Net photosynthetic light response curves (oxygen $\mu\text{mol g}^{-1} \text{h}^{-1}$, MEAN \pm SD) of *Lithothamnion glaciale* exposed to elevated temperature and $p\text{CO}_2$ ($n = 6$). Experimental treatments: $t = \sim 7^\circ\text{C}$, $t + 3 = \sim 9^\circ\text{C}$, at $1000 \mu\text{atm}$ or $380 \mu\text{atm } p\text{CO}_2$. Numbers 1-6 correspond to each light level increment used to perform the light curve: (1) 12.03 ± 2.51 (experimental PAR level), (2) 36.53 ± 6.17 , (3) 62.90 ± 9.16 , (4) 85.15 ± 12.01 , (5) 105.36 ± 3.58 , and (6) $117.78 \pm 3.54 \mu\text{mol m}^{-2} \text{s}^{-1}$. Light increments were chosen based on the irradiance range experienced by *L. glaciale in situ*.

4.6.2.2 PAM fluorometry

Exposure to elevated $p\text{CO}_2$ significantly increased the optimum light level for efficient photosynthesis (E_k) and $r\text{ETR}_{\text{max}}$ in *L. glaciale* (E_k : $F_{1,19} = 0.027$, $p = 0.021$; $r\text{ETR}_{\text{max}}$: $F_{1,19} = 0.002$, $p = 0.008$, Figure 4.2a and b). Elevated temperature had no effect (E_k : $F_{1,19} = 0.667$, $p = 0.470$; $r\text{ETR}_{\text{max}}$: $F_{1,19} = 2.698$, $p = 0.270$, Figure 4.2a and b). Elevated $p\text{CO}_2$ and temperature had no significant effect on $F_q'/F_m'_{\text{max}}$ ($F_{1,19} = 0.188$, $p = 0.352$), with an average of 0.64 ± 0.03 (mean \pm SD) across all treatments. $F_q'/F_m'_{\text{max}}$ and F_q'/F_m' are similar (Figure 4.3).

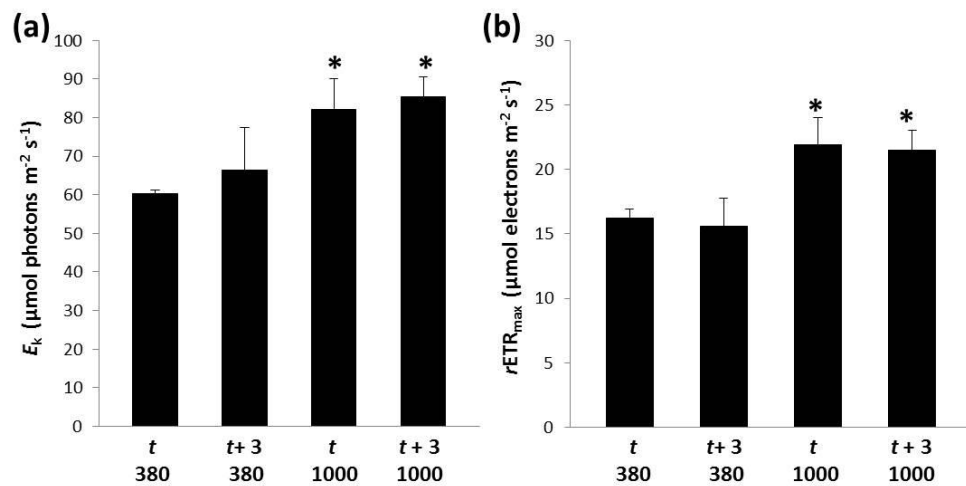


Figure 4.2 MEAN \pm SE effect of elevated temperature and $p\text{CO}_2$ on the photosynthetic yield parameters of *L. glaciale*. Results are expressed as mean \pm SE (n =6). (a) E_k ($\mu\text{mol photons m}^{-2} \text{s}^{-1}$), (b) $rETR_{\text{max}}$ ($\mu\text{mol electrons m}^{-2} \text{s}^{-1}$). Treatments: t = $\sim 7^\circ\text{C}$, t + 3 = $\sim 10^\circ\text{C}$; at 1000 ppm or 380 ppm $p\text{CO}_2$. Asterisk (*) indicates a significant difference.

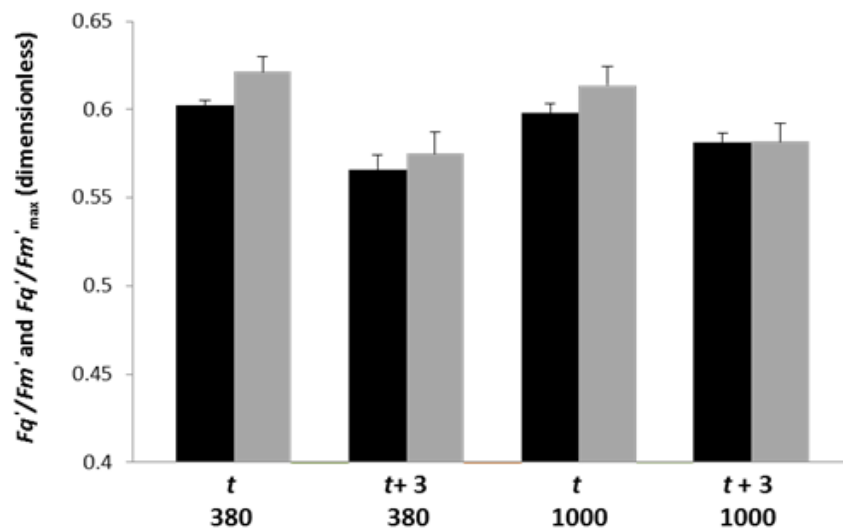


Figure 4.3 The effect of elevated temperature and $p\text{CO}_2$ on the relative and calculated maximum photochemical efficiency of PSII in *Lithothamnion glaciale*. Results are expressed as mean \pm SE (n =6). Black bars: F_q'/F_m' ; Grey bars: $F_q'/F_{m'_{\text{max}}}$. Treatments: t = $\sim 7^\circ\text{C}$, t + 3 = $\sim 10^\circ\text{C}$; at 1000 ppm or 380 ppm $p\text{CO}_2$. Asterisk (*) indicates a significant difference.

4.7 Discussion

Light availability mediates the response of coralline algae to elevated temperature and $p\text{CO}_2$. At low PAR in ambient conditions photosynthesis occurs in *Lithothamnion glaciale*. However, low PAR combined with elevated temperature and $p\text{CO}_2$ leads to net respiration. Under increased PAR, elevated temperature and $p\text{CO}_2$ have less impact on photosynthesis suggesting that irradiance may play an integral part in the response of coralline algae to multiple stressors.

4.7.1 Photosynthesis

Under low light conditions, coralline algal photosynthetic systems operate at maximal efficiency, utilising the majority of light harvested to drive photosynthesis. In *Lithothamnion glaciale* acclimated to low light ($12 \mu\text{mol m}^{-2} \text{s}^{-1}$), comparison of $F_q'/F_{m'}'_{max}$ with F_q'/F_{m}' , suggests that effective photochemical efficiency of algae is operating close to the calculated maximal photosynthesis (Figure 4.3). However despite operating close to maximal efficiency, under low light conditions photosynthetic rate may only slightly exceed respiration, meaning net photosynthetic production by the algal cells is relatively poor (Whitmarsh and Govindjee, 1999). The addition of other stressors (elevated temperature and $p\text{CO}_2$) may therefore increase the energetic requirements of coralline algae, forcing them into net respiration during the day (Figure 4.1). Both temperature regimes used in the present study ($t = \sim 7^\circ\text{C}$ and $t + 3 = \sim 10^\circ\text{C}$), were within the ecological range of *Lithothamnion glaciale*, which may explain why no significant effect of solely temperature was observed in the photosynthetic response of the algae. Although, when elevated temperature was combined with elevated $p\text{CO}_2$, $r\text{ETR}_{max}$ (calculated from RLC measurements) increased significantly in algae at $12 \mu\text{mol photons m}^{-2} \text{s}^{-1}$ (Figure 4.2b). Most likely because temperature can impact the rate electron transport within algal cells (Raven and Hurd, 2012b, Raven and Geider, 1988), coupled with an increased availability of substrate for photosynthesis. However, this is only a calculated potential maximum rate, realisation of which will depend on other environmental factors. Net photosynthesis in algae from all treatments did increase with increasing irradiance. However, under irradiances below $62 \mu\text{mol m}^{-2} \text{s}^{-1}$ there was a significant reduction in net photosynthesis in algae exposed to elevated $p\text{CO}_2$ (Figure 4.1). While under higher PAR ($85 - 117 \mu\text{mol photons m}^{-2} \text{s}^{-1}$) elevated $p\text{CO}_2$ had no effect. This suggests that there may be a tipping point (compensation point) between $62 - 85 \mu\text{mol photons m}^{-2} \text{s}^{-1}$ PAR, at which irradiance becomes sufficient enough to fulfill the energetic requirements of algae exposed to multiple stressors. This response is concordant with the observed increase in the optimal light level (E_k) for efficient photosynthesis in *L. glaciale*, in response to elevated temperature and $p\text{CO}_2$ (Figure 4.2a), and presumably due to the additional energetic requirements by calcifying organisms under acidified conditions (Nelson, 2009).

4.7.2 Wider implications

An irradiance-mediated response of coralline algae to multiple stressors may have considerable implications for the future of *L. glaciale* inhabiting naturally low light

environments. Changing environmental conditions will mean the addition of multiple stressors (elevated temperature and $p\text{CO}_2$) that may increase the energetic requirements of the coralline algae. This increase in energetic requirements may result in a necessity for more light by the algae in the future. Under contemporary conditions a major constraint on the distribution of *L. glaciale* is their requirement for light, restricting them to depths shallower than 32m in northern Europe (Hall-Spencer, 1998). Photosynthesis and respiration occur simultaneously in the algae. When exposed to enough light respiration rate is relatively low compared to photosynthesis, resulting in a net consumption of CO_2 and production of oxygen. However, in the absence of light or under low light respiration occurs and photosynthesis stops or is significantly reduced, resulting in a net consumption of oxygen and production of CO_2 (i.e. release of previously fixed carbon). In addition, photosynthesis and respiration influence the pH of the cell and therefore can influence calcification rates (Martin et al., 2013b). Photosynthesis increases pH in the cell and thereby promotes calcification (Gao et al., 1993), while respiration decreases pH and may therefore hinder calcification (De Beer and Larkum, 2001). Therefore, in the future if optimal light level for photosynthesis increases (due to environmental changes), this may mean that the light available in some coralline algal habitats will become insufficient (i.e. respiration rate is greater than photosynthetic rate more regularly than under contemporary conditions). Therefore, it is likely coralline algal habitats currently located on, or close to, their photo limit may be lost or reduced in the future. Furthermore, the habitat heterogeneity and the complex geometry of the algae that results in intra- and inter-structural thallus (branch) shading (Burdett et al., 2012b) and diurnal irradiance patterns, will also have implications for the continuance of coralline regardless of its depth. For algae inhabiting optimal light conditions under climate change, the effects of thallus shading and diurnal irradiance patterns are likely to be apparent at the ecosystem level; whereby although net productivity for each thallus may only be slightly reduced, net productivity of the whole ecosystem may decrease significantly. In addition, increasing optimal light under acidified conditions may mean algae growing at high latitudes may be amongst the most impacted by changing environmental conditions. Likely because of the dramatic seasonal differences in light availability (i.e. much reduced day length and light availability during the winter months) and lower temperatures experienced at high latitudes. In addition, the reduced light availability is overlain by projected earlier shoaling of the carbonate saturation depth (i.e.

impacting calcification) (Brodie et al., 2014) that may mean the loss of high latitude habitats far sooner than habitats more southerly distributed. Future climate change experiments should consider seasonal and diurnal patterns in irradiance and day length, and spatial differences associated with *in situ* natural variability.

4.7.3 Conclusions

Light availability mediates the response of coralline algae to multiple stressors. The present study suggests that coralline algae experiencing low light intensities, combined with elevated temperature and $p\text{CO}_2$ will resort to net respiration during the day to survive while the optimal light for efficient photosynthesis increases when algae are exposed to multiple stressors (elevated temperature and $p\text{CO}_2$). This will be a particular problem in future for algae inhabiting low irradiance habitats mediating their sensitivity to the progression of a multiple stressor environmental scenario. Irradiance must therefore be carefully considered in both future empirical studies and survival projections that evaluate the response of coralline algae to multiple stressors.

5

Short term experiment: Seasonal differences in the effects of climate change on light limited photosynthesis and calcification in red coralline algae

While low-light is often associated with seasonal changes, it is not just confined to the winter months. Time of day, cloud cover, water clarity and habitat heterogeneity can all generate sub-saturating light levels for photosynthesis throughout the whole year. In addition, seasonal differences in temperature cause *in situ* free-living coralline algae to experience a difference in temperature of $\sim 10^{\circ}\text{C}$ throughout the course of a year. The short-term experiment described in part a (Chapter 4) identified that light availability mediates the net photosynthetic response of low-light acclimated coralline algae to elevated temperature and $p\text{CO}_2$. This chapter compares the response of coralline algae to elevated temperature and $p\text{CO}_2$ under sub-saturating light at both winter and summer temperatures³.

³ The equipment used to run the net photosynthesis light curves detailed in Chapter 4 was borrowed, and was unavailable for use to repeat the same measurements during the summer. Therefore this experiment was designed solely to assess the physiological parameters described.

5.1 Global climate change and coralline algae

Projected changes in seawater carbonate chemistry (ocean acidification; ocean acidification, decreasing ocean pH and carbonate saturation state, as a result of increasing seawater $p\text{CO}_2$) may have a significant impact on algal physiological processes, particularly those which utilise dissolved inorganic carbon (DIC; HCO_3^- , CO_3^{2-} , CO_2) as a substrate; photosynthesis and calcification. In calcifying photosynthesisers, any benefit of increased availability of DIC (i.e. increase in substrate for photosynthesis) for photosynthesis may be negated by the increased metabolic cost of calcification, and dissolution of calcified skeletons as carbonate becomes undersaturated in seawater (Nelson, 2009, Brodie et al., 2014). Although empirical evidence is conflicting (Noisette et al., 2013b, Kamenos et al., 2013, McCoy and Ragazzola, 2014), it appears that in coralline algae calcification may increase or be maintained under exposure to elevated $p\text{CO}_2$ (Ries et al., 2009, Kamenos et al., 2013, Martin et al., 2013a) while photosynthesis may reduce by 28% on average in response to exposure to high- CO_2 (Kroeker et al., 2013b). Increasing temperature may also induce physiological changes (e.g. increase / decrease growth rate) in coralline algae (e.g. Kamenos and Law, 2010), as temperature can impact the rate of enzymatic reactions, electron transport rate and solute movement within algal cells, and influences the properties of common cellular components such as lipids, proteins and carbohydrates (Raven and Hurd, 2012b, Raven and Geider, 1988). Therefore, it is possible that the short-term physiological response of coralline algae to elevated temperature and $p\text{CO}_2$ may be very different under winter temperatures compared to the summer.

5.2 *In situ* irradiance

The study discussed in Chapter 4 assesses the effect of sub-diel changes in irradiance (photosynthetically active radiation; PAR $\mu\text{mol m}^{-2} \text{s}^{-1}$) on net photosynthesis in algae exposed to elevated $p\text{CO}_2$ and temperature. The algae assessed in the study were acclimated to PAR of $12 \mu\text{mol m}^{-2} \text{s}^{-1}$, which although ambient for the time of collection, is lower than the annual average PAR recorded in Loch Sween ($90 \mu\text{mol m}^{-2} \text{s}^{-1}$) (Rix et al., 2012). Light availability experienced by the *L. glaciale in situ* is affected by both seasonal changes in irradiance and day length, and diel and sub-diel changes in irradiance related to other factors including time of day, cloud cover, water clarity (i.e. algal blooms) and habitat heterogeneity. This means algae *in situ* experience rapid diel and sub-diel

reductions in irradiance, as well as prolonged periods of reduced light availability during both the summer and winter (Figure 5.1).

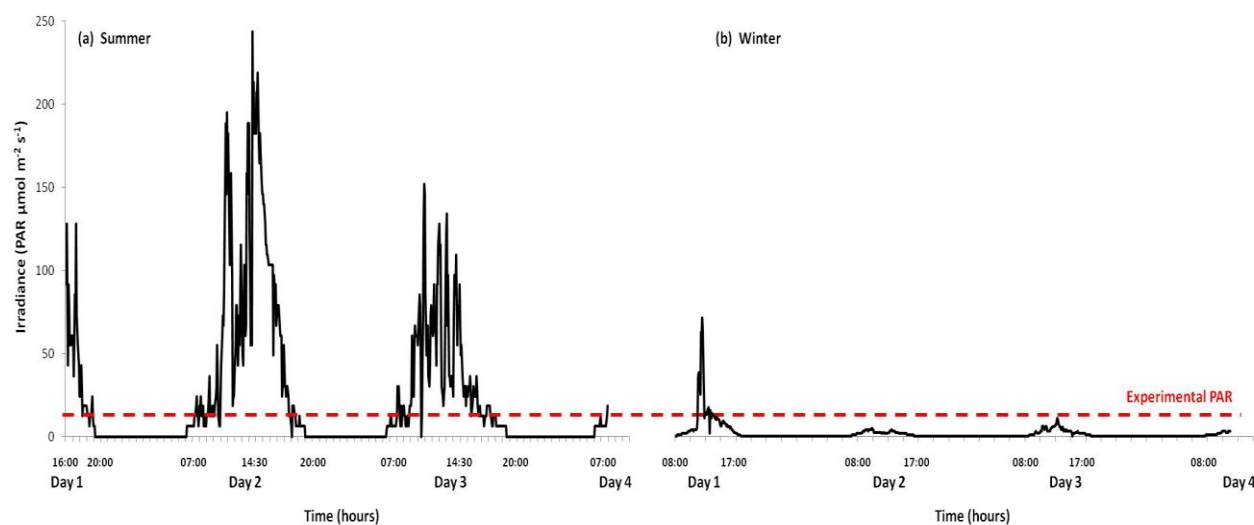


Figure 5.1 Irradiance recorded in Loch Sween, Scotland (collection site of *L. glaciale*) Irradiance (PAR $\mu\text{mol m}^{-2} \text{s}^{-1}$) was recorded at a depth of 6 m on the mearl bed using a PAR meter (Apogee QSO-E underwater quantum sensor connected to a Gemini voltage data logger). . (a) Irradiance recorded during August 2012 (b) Irradiance recorded during February 2012. The dotted represents the light level at which the experiments were run during the summer and the winter.

5.3 Aims of the chapter

Chapter 4 indicates that the response of photosynthesis to temperature and $p\text{CO}_2$ may be mediated by light availability. The study in chapter 4 was conducted during the winter, where both temperature treatments (i.e. ambient (t) and projected increased temperature ($t+3^\circ\text{C}$)) were within the physiological range of the algae, *Lithothamnion glaciale*. However, during the summer, ambient temperature is at the upper limit of the temperature range experienced by the algae, therefore the projected increased temperature is 3°C outwith this range. Furthermore, there are periods of low PAR ($\leq 12 \mu\text{mol photons m}^{-2} \text{s}^{-1}$) during these high temperature months (Figure 5.1). With this in mind, the following study was conducted to compare differences in photosynthetic characteristics, Rubisco, phycoerythrin and chlorophyll-*a* concentration, and calcification in *Lithothamnion glaciale* in response to elevated temperature and $p\text{CO}_2$ during the summer and the winter after a seven days growing under sub-saturating irradiance ($12 \mu\text{mol m}^{-2} \text{s}^{-1}$ PAR).

5.4 Methods

5.4.1 Experimental set-up

The experimental set-up was repeated twice; summer (August) and winter (February). *Lithothamnion glaciale* were hand collected from Loch Sween, Scotland (56°01.99' N, 05°36.13' W), using SCUBA from 7 m depth. *In situ*, the algae experience an annual temperature range of 6-16 °C, light levels of 12-120 $\mu\text{mol m}^{-2} \text{s}^{-1}$ PAR and pH 8.1 (Rix et al., 2012). After collection, thalli were transferred into seawater holding tanks ($p\text{CO}_2$ 380 μatm , ambient temperature). Individual *L. glaciale* thalli were placed into 24 one L plastic aquaria and allocated randomly to 1 of 4 different treatments (n = 6 thalli per treatment): (1) ambient *in situ* temperature (7 or 15 °C, winter and summer, respectively) at 380 $\mu\text{atm } p\text{CO}_2$ (control, (t, 380)), (2) ambient +3 °C at 380 $\mu\text{atm } p\text{CO}_2$ (temperature treatment, (t+3, 380)), (3) ambient °C at 1000 $\mu\text{atm } p\text{CO}_2$ ($p\text{CO}_2$ treatment, (t, 1000)), and (4) ambient +3 °C at 1000 $\mu\text{atm } p\text{CO}_2$ (multiple stressor treatment (t+3, 1000)). These $p\text{CO}_2$ and temperature levels were chosen to simulate contemporary environmental levels and those predicted for 2100 (IPCC, 2013). Environmental conditions were maintained as detailed in chapter 2, section 2.1.3 (short-term mesocosm set-up). In all treatments during both the summer and winter PAR was 12 $\mu\text{mol m}^{-2} \text{s}^{-1}$. PAR during the summer can reach in excess of 200 $\mu\text{mol m}^{-2} \text{s}^{-1}$, however, time of day, cloud cover, water clarity and habitat heterogeneity can all generate extended periods of sub-saturating light levels for photosynthesis (i.e. PAR of $\sim 12 \mu\text{mol m}^{-2} \text{s}^{-1}$) at this time of year at sub diel time scales (Figure 5.1). Similarly, during the winter abiotic environmental factors can result in sub diel fluctuations in light availability, although PAR is also generally low at this time of year (Figure 5.1). Therefore, PAR 12 $\mu\text{mol m}^{-2} \text{s}^{-1}$ was used because it is ecologically relevant and sub saturating in both the winter and the summer. Light was supplied via LED tile lamps (48 LED clip light, 27.4 x 15.4 x 7 cm) suspended above the aquaria to provide even lighting. Algae were exposed to the experimental treatments for 7 days before photosynthetic characteristics and net productivity were assessed.

5.4.2 Environmental parameters

5.4.2.1 Carbonate chemistry

Partial pressure of carbon dioxide ($p\text{CO}_2$), total alkalinity (A_T), salinity and temperature were determined for each treatment; $p\text{CO}_2$ was monitored continuously and

recorded every 5 minutes throughout the experiment using a LI-COR gas analyser and computer software (LI-820 CO₂ Analyzer, LI-COR Environmental – GmbH, Bad Homburg, Germany). Temperature and salinity were recorded daily using a handheld conductivity meter (Pro 2030, YSI, Ohio, USA). A_T ($\mu\text{mol kg}^{-1}$) was determined from seawater samples taken at the beginning and end of the experiment using the open-cell titration method described by Yao and Byrne (1998b) and detailed in Chapter 2. On collection, A_T seawater samples were poisoned with mercuric chloride (40 μl of a 50% saturated solution) (Riebesell et al., 2010), and stored in 12 ml screw top borosilicate glass vials (Exetainer, Labco Ltd., UK) until analysis (see Chapter 2). Additional carbonate system parameters (DIC, calcite and aragonite saturation, $[\text{HCO}_3^-]$ and $[\text{CO}_3^{2-}]$) were calculated from A_T , $p\text{CO}_2$, salinity and temperature using the software program CO2SYS as described in Chapter 2.

5.4.2.2 Photosynthetically active radiation

PAR ($\mu\text{mol m}^{-2} \text{s}^{-1}$) was recorded using a PAR meter (Apogee QSO-E underwater quantum sensor connected to a Gemini voltage data logger).

5.4.3 Photosynthesis

5.4.3.1 Chlorophyll- α fluorescence (PAM fluorometry)

A Diving-PAM fluorometer was used at the end of each experimental period to assess the photosynthetic characteristics of *L. glaciale* using rapid light curves (RLCs). See Chapter 2, section 2.2, for a detailed description of using the Diving-PAM to perform RLCs.

Photosynthetic characteristics (E_k ($\mu\text{mol photons m}^{-2} \text{s}^{-1}$), $r\text{ETR}_{\text{max}}$ ($\mu\text{mol electrons m}^{-2} \text{s}^{-1}$), F_q'/F_m' (dimensionless), α (dimensionless)), were determined using methods as previously described (Suggett et al., 2007, Hennige et al., 2008, Burdett et al., 2012b) (see also Chapter 2, section 2.2).

5.4.3.2 Chlorophyll- a concentration

To determine the concentration of chlorophyll- a in the algae a few branches of the *L. glaciale* thallus were removed (1 g) and were ground directly in cold methanol using a shaker mill with agate grinding jars and balls at 30 s/seconds (Retsch MM400, Haan, Germany). The slurry was then centrifuged (5 mins at 4000 x g) to separate the ground *L. glaciale* from the chlorophylls in solution. Chlorophyll- a concentration was then determined spectrophotometrically, as previously described (Porra et al., 1989).

5.4.3.3 Total protein, Rubisco and phycoerythrin concentration

To extract proteins, 1-2 branches of *L. glaciale* (~0.5g) was ground directly in sodium dodecyl sulphate (SDS) buffer (Invitrogen, UK, 0.5 ml) using an automated sample grinder (Retsch MM400, Haan, Germany) as detailed in Chapter 2, section 2.3.1.3 (extraction: method 3). An aliquot of the protein extract was reserved and frozen for total protein analysis. Total protein concentration was then determined spectrophotometrically, as previously described (Bradford, 1976). Rubisco and phycoerythrin concentrations were determined from the protein extract using 1D-gel electrophoresis and image J analysis as described in Chapter 2. Protein bands were excised from the gel and subjected to in-gel trypsin digest and identified using the Mass Spectrometry method described in Chapter 2, identifying Rubisco and Phycoerythrin.

5.4.4 Calcification

Calcification rate of *L. glaciale* was determined using the alkalinity anomaly technique (Smith and Key, 1975, Ohde and Hossain, 2004), in which algal thalli were incubated in stirred 220 ml chambers for a 2 h period. Samples of incubation water were taken at the beginning and end of the experimental period, and A_T determined using the method described by Yao and Byrne (1998b). Calcification ($\mu\text{mol CaCO}_3 \text{ g h}^{-1}$) was estimated using the equation:

$$\text{Calcification} = 0.5(\Delta A_T) \cdot V / \Delta T / \text{TDW}$$

where ΔA_T is the change of total alkalinity (mol/kg), W is the weight of experimental seawater (kg) and ΔT is the experimental period (h), as described in chapter 2.

5.4.5 Statistical analysis

Two-way ANOVAs (factors; temperature and $p\text{CO}_2$) were used to investigate differences in (1) calcification, (2) photochemical characteristics, (3) and protein concentrations, between algae exposed to a control treatment (t , 380), elevated temperature ($t+3$, 380), elevated $p\text{CO}_2$ (t , 1000) and a combined treatment ($t+3$, 1000) during both the summer and the winter under PAR $12 \mu\text{mol m}^{-2} \text{ s}^{-1}$. Where assumptions of ANOVA were not met ($F_q'/F_{m'}'_{\text{max}}$ and a in algae during the winter), a non-parametric

Mann Whitney U test was used. Differences between means / medians were considered to be significant when $p \leq 0.05$. All analyses were conducted with SPSS v18.0.

5.5 Results

Some of the results published in this section are repeated from Chapter 4 to allow for a comparison between summer and winter.

5.5.1 Environmental parameters

The seawater physico-chemical parameters are summarised below in Table 5.1. Data from the winter experiment is repeated from Chapter 4.

Table 5.1 Mean \pm SD of seawater physico-chemical parameters measured or calculated for the aquaria during the experimental periods in summer and winter.

Temperature, salinity, total alkalinity (A_T) and dissolved inorganic carbon (DIC) were measured; pH, pCO_2 , HCO_3^- , CO_3^{2-} , calcite saturation (Ω_{cal}), aragonite saturation (Ω_{ara}) (indicated by an *) were calculated using CO2SYS. Summer: $t = \sim 15^\circ C$, $t + 3 = \sim 18^\circ C$; Winter: $t = \sim 7^\circ C$, $t + 3 = \sim 10^\circ C$; at 1000 ppm or 380 ppm pCO_2

Treatment	Summer				Winter			
	$t^\circ C$, 380 μatm (control)	$t^\circ C$, 1000 μatm	$t + 3^\circ C$, 380 μatm	$t + 3^\circ C$, 1000 μatm	$t^\circ C$, 380 μatm (control)	$t^\circ C$, 1000 μatm	$t + 3^\circ C$, 380 μatm	$t + 3^\circ C$, 1000 μatm
Salinity	34.33 \pm 0.58	34.33 \pm 1.52	32.67 \pm 1.15	32.67 \pm 0.58	36.33 \pm 0.57	34.66 \pm 1.15	34.66 \pm 0.56	35.33 \pm 0.57
Temperature ($^\circ C$)	14.47 \pm 0.29	14.50 \pm 0.26	18.50 \pm 0.17	18.53 \pm 0.05	6.70 \pm 0.10	6.77 \pm 0.15	10.30 \pm 0.10	10.23 \pm 0.05
pH*	8.29 \pm 0.01	7.81 \pm 0.01	8.36 \pm 0.01	7.89 \pm 0.01	8.20 \pm 0.03	7.70 \pm 0.08	8.23 \pm 0.04	7.73 \pm 0.06
DIC ($\mu mol kg^{-1}$)*	1815.4 \pm 7.0	1966.8 \pm 2.6	1795.8 \pm 3.1	1953.3 \pm 1.9	1858.1 \pm 1.7	1994.4 \pm 9.6	1841.9 \pm 2.6	1978.1 \pm 9.3
A_T ($\mu mol kg^{-1}$)	2206.09 \pm 10.44	2200.68 \pm 90.28	2222.22 \pm 38.12	2217.17 \pm 23.14	2488.76 \pm 213.34	2206.83 \pm 284.99	2285.88 \pm 278.18	2078.56 \pm 435.83
pCO_2 (μatm)	366.22 \pm 5.19	1168.87 \pm 0.49	366.22 \pm 5.19	1168.87 \pm 0.49	368.05 \pm 0.77	1120.352 \pm 81.48	368.05 \pm 0.77	1120.352 \pm 81.48
HCO_3^- ($\mu mol kg^{-1}$)*	1833.75 \pm 18.42	2059.63 \pm 81.37	1809.52 \pm 23.10	2058.16 \pm 17.33	2124.72 \pm 162.91	2092.42 \pm 250.35	1937.72 \pm 206.26	1961.23 \pm 401.56
CO_3^{2-} ($\mu mol kg^{-1}$)*	146.07 \pm 2.14	55.11 \pm 4.18	163.50 \pm 6.41	62.66 \pm 2.17	145.42 \pm 22.52	45.25 \pm 15.61	137.63 \pm 31.95	44.79 \pm 14.92
Ω_{cal} *	3.51 \pm 0.02	1.32 \pm 0.11	3.96 \pm 0.14	1.51 \pm 0.04	3.46 \pm 0.53	1.08 \pm 0.37	3.30 \pm 0.77	1.07 \pm 0.35
Ω_{ara} *	2.21 \pm 0.02	0.83 \pm 0.06	2.48 \pm 0.09	0.95 \pm 0.03	2.17 \pm 0.33	0.68 \pm 0.24	2.07 \pm 0.48	0.68 \pm 0.22

5.5.2 Photosynthetic characteristics

5.5.2.1 Chlorophyll- α fluorescence (PAM fluorometry)

Elevated temperature significantly reduced both $F_q'/F_m'_{max}$ and a in algae during summer ($F_{1,19} = 0.481$, $p = 0.002$ and $F_{1,19} = 0.537$, $p = 0.003$, respectively, see Figure 5.2a, d). There was no significant effect of increased temperature or pCO_2 on $F_q'/F_m'_{max}$ and a in algae during the winter ($F_{1,19} = 0.188$, $p = 0.352$ and $F_{1,19} = 0.667$, $p = 0.479$, respectively, see Figure 5.2e, h). Exposure to high- CO_2 significantly increased the optimum light level for efficient photosynthesis, E_k in algae in both summer and winter ($F_{1,19} = 5.524$, $p = 0.005$ and $F_{1,19} = 0.027$, $p = 0.021$, respectively, see Figure 5.2c, g). Elevated pCO_2 and temperature had no significant effect on $rETR_{max}$ in the summer ($F_{1,19} =$

3.178, $p = 0.071$, Figure 5.2b), but elevated $p\text{CO}_2$ significantly increased $r\text{ETR}_{\text{max}}$ during the winter ($F_{1,19} = 0.002$, $p = 0.008$, see Figure 5.2f). $r\text{ETR}$ increases as irradiance increases in algae exposed to elevated $p\text{CO}_2$ during both the summer and the winter (Figure 5.3).

During the summer and winter, under optimal light ($E/E_k = 1$) and suboptimal light ($E/E_k < 1$) $r\text{ETR}$ is similar across treatments. During the summer at above optimal light ($E/E_k > 1$) $r\text{ETR}$ increases in all treatments with exception to control treatment. Similarly, during the winter at above optimal light levels ($E/E_k > 1$) $r\text{ETR}$ increases in all treatments, although the control is lower compared to other treatments (Figure 5.3). Comparison of $F_q'/F_{m'_{\text{max}}}$ with $F_q'/F_{m'}$, suggests effective photochemical efficiency of algae at PAR $12 \mu\text{mol m}^{-2} \text{s}^{-1}$ is operating close to the calculated potential maximal efficiency during both the summer and the winter (Figure 5.4).

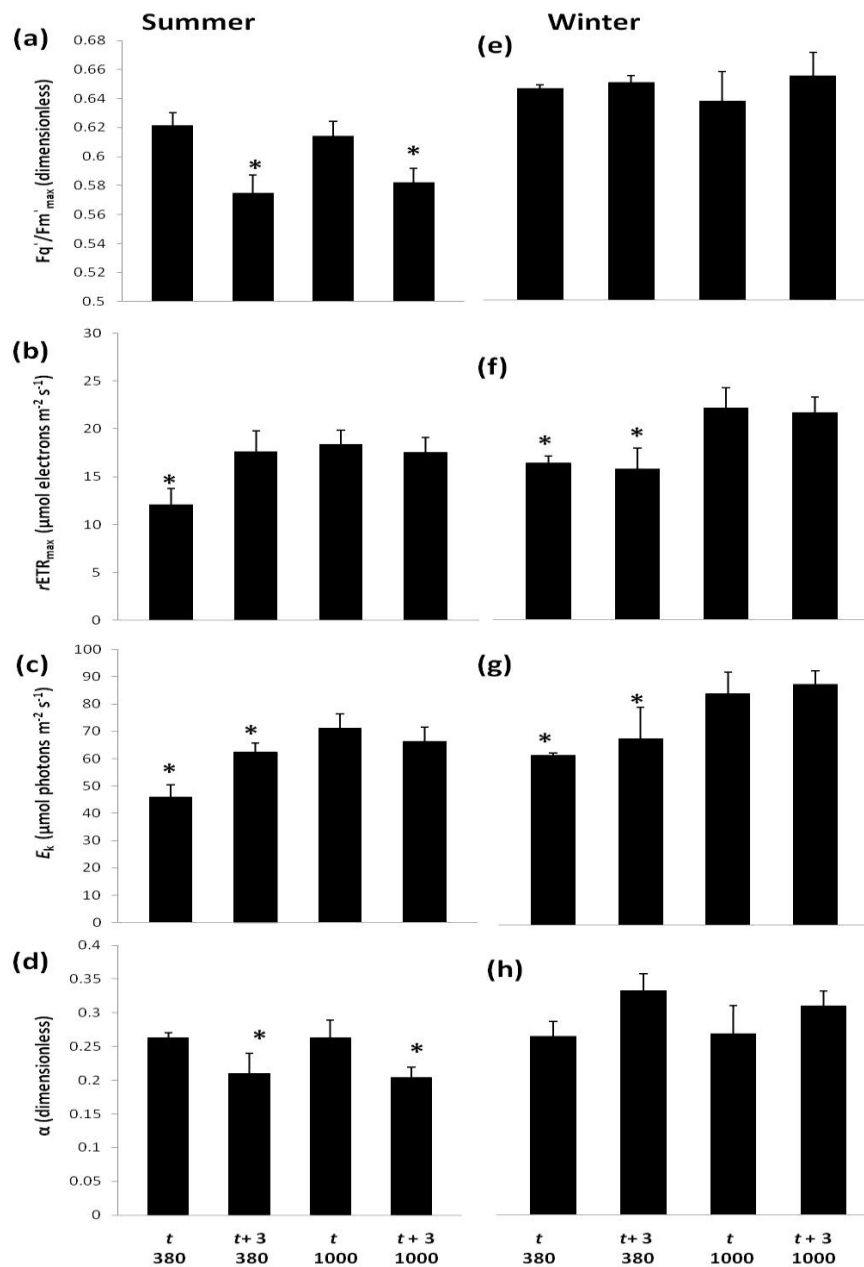


Figure 5.2 Short-term effect of elevated temperature and $p\text{CO}_2$ on the photosynthetic yield parameters of *L. glaciale* calculated from RLCs during the summer and winter. Results are expressed as mean \pm SE (n =6). (a,e) $rETR_{\max}$ ($\mu\text{mol electrons m}^{-2} \text{s}^{-1}$), (b,f) E_k ($\mu\text{mol m}^{-2} \text{s}^{-1}$), (c,g) $F_q'/F_{m'} \max$ (dimensionless), and (d,h) α (dimensionless). Treatments: t = ambient; $\sim 7^\circ\text{C}$ (winter) or 15°C (summer), t + 3 = ambient+ 3°C ; at 1000 μatm or 380 μatm $p\text{CO}_2$. PAR: $12.03 \pm 2.51 \mu\text{mol m}^{-2} \text{s}^{-1}$, mean \pm SE. Asterisk (*) indicates a significant difference.

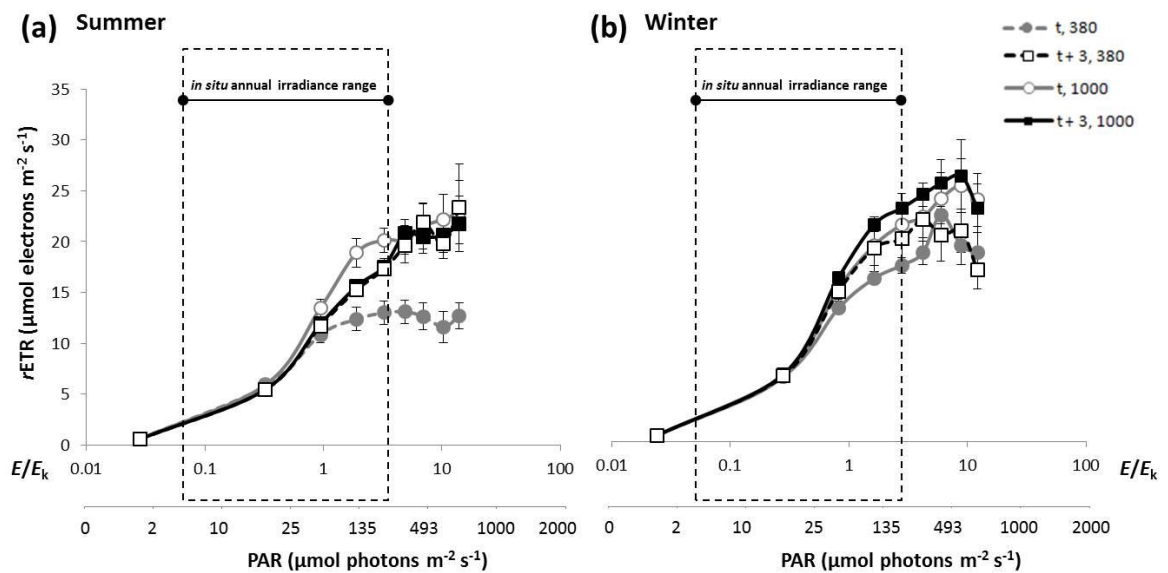


Figure 5.3 $rETR$ ($\mu\text{mol electrons m}^{-2} \text{s}^{-1}$) curve responses of *Lithothamnion glaciale* in response to elevated temperature and $p\text{CO}_2$ during the summer and the winter. Results are expressed as mean \pm SE ($n = 6$). t = ambient; $\sim 7^\circ\text{C}$ (winter) or 15°C (summer), $t + 3$ = ambient $+3^\circ\text{C}$; at $1000 \mu\text{atm}$ or $380 \mu\text{atm}$ $p\text{CO}_2$. Data normalised to E/E_k . Experimental PAR: $12.03 \pm 2.51 \mu\text{mol m}^{-2} \text{s}^{-1}$. *In situ* irradiance range in Loch Sween (the collection site of algae): $12\text{--}120 \mu\text{mol m}^{-2} \text{s}^{-1}$ (see Rix et al., 2012).

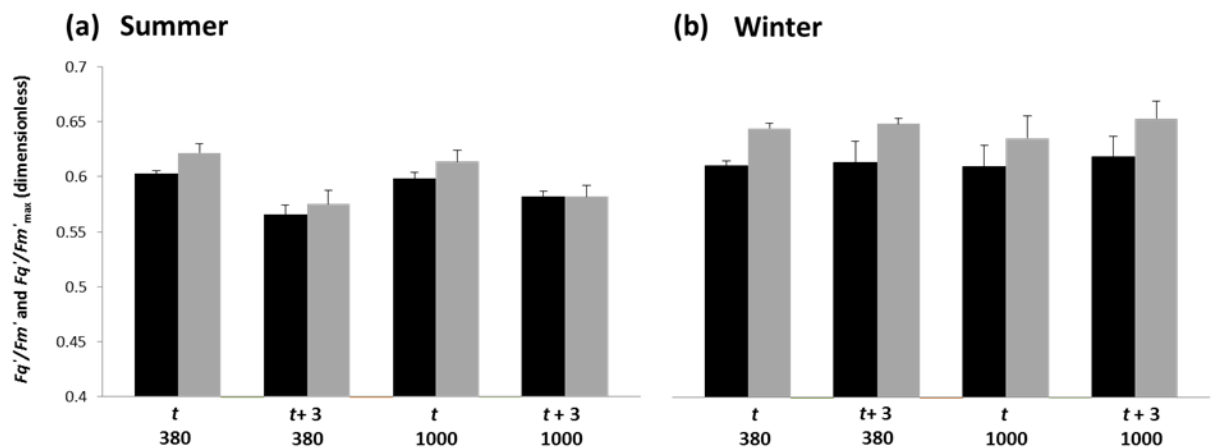


Figure 5.4 The effect of elevated temperature and $p\text{CO}_2$ on the relative and calculated maximum photochemical efficiency of PSII in *Lithothamnion glaciale* during the summer and the winter. Results are expressed as mean \pm SE ($n = 6$). Black bars: F_q'/F_m' ; Grey bars: $F_q'/F_m'_{max}$. Treatments: t = ambient; $\sim 7^\circ\text{C}$ (winter) or 15°C (summer), $t + 3$ = ambient $+3^\circ\text{C}$; at $1000 \mu\text{atm}$ or $380 \mu\text{atm}$ $p\text{CO}_2$. Asterisk (*) indicates a significant difference.

5.5.2.2 Chlorophyll concentration

There was no significant effect of elevated temperature or $p\text{CO}_2$ on chlorophyll- a concentration in algae during either summer or winter ($F_{1,20} = 1.162$, $p = 0.123$, and $F_{1,20} = 2.339$, $p = 0.645$, respectively).

5.5.2.3 Total protein

Elevated temperature significantly decreased total protein concentration in algae during the winter ($F_{1,16} = 1.171$, $p = 0.048$, see Figure 5.5b), although there was no significant effect of increased $p\text{CO}_2$ ($F_{1,16} = 2.071$, $p = 0.063$, see Figure 5.5b). There was no significant effect of increased temperature or $p\text{CO}_2$ on total protein concentration in the summer ($F_{1,16} = 1.568$, $p = 0.555$, see Figure 5.5a).

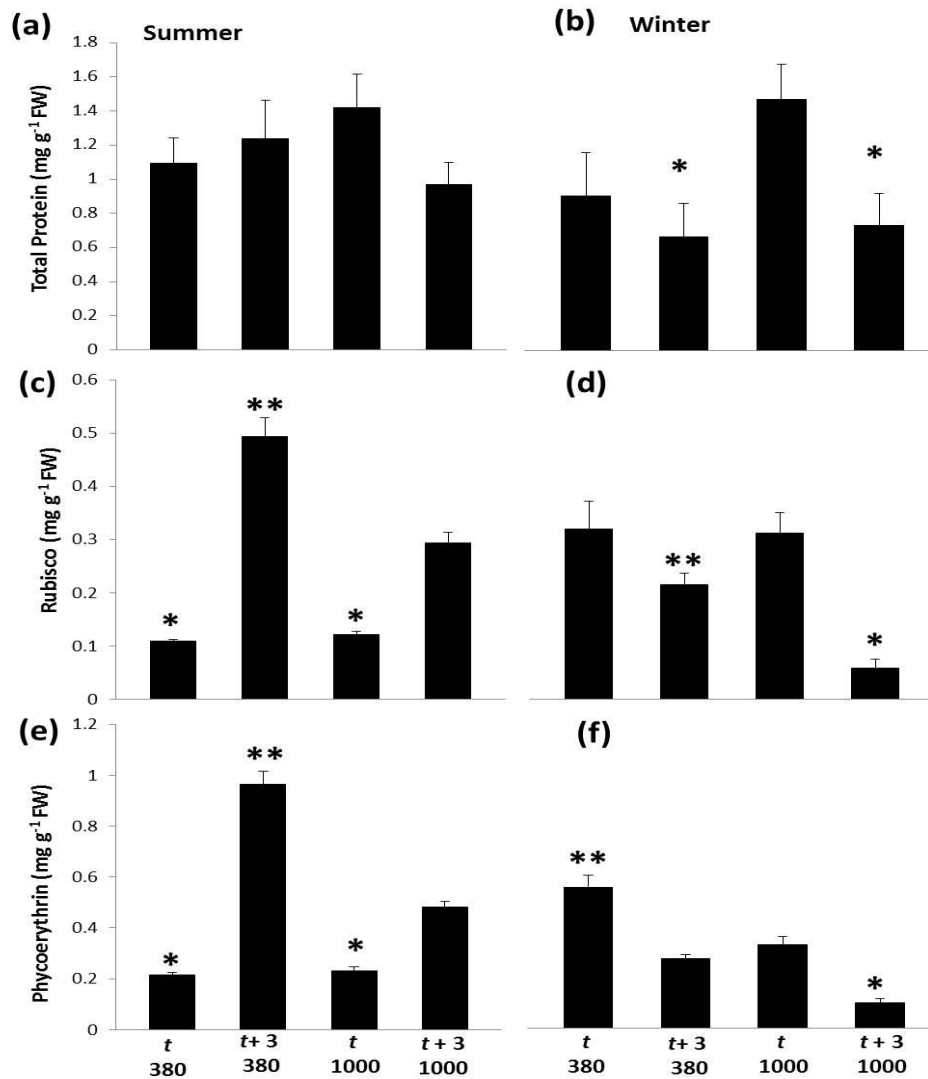


Figure 5.5 Short-term effect of elevated temperature and $p\text{CO}_2$ on total protein, Rubisco and phycoerythrin concentration in *L. glaciale* during the summer and winter. Results are expressed as mean \pm SE ($n = 6$). (a) Total protein ($\mu\text{g ml}^{-1}$), (b) Rubisco concentration (c) Phycoerythrin concentration (band intensity from 1D SDS gel). Treatments: t = ambient; $\sim 7^\circ\text{C}$ (winter) or 15°C (summer), $t + 3$ = ambient+ 3°C ; at $1000 \mu\text{atm}$ or $380 \mu\text{atm}$ $p\text{CO}_2$. PAR: $12.03 \pm 2.51 \mu\text{mol photons m}^{-2} \text{s}^{-1}$, Asterisk (*) indicates a significant difference.

5.5.2.4 Rubisco concentration

During the winter, Rubisco concentration in algae significantly reduced in response to elevated $p\text{CO}_2$ and temperature (temperature: $F_{1,20} = 2.479$, $p < 0.001$; $p\text{CO}_2$: $F_{1,20} = 2.479$, $p = 0.022$, see Figure 5.5d). Exposure to both elevated temperature and high- CO_2 increased Rubisco concentration in algae during the summer (temperature: $F_{1,20} = 36.868$, $p < 0.001$; $p\text{CO}_2$: $F_{1,20} = 36.868$, $p = 0.002$, see Figure 5.5c). During the summer, the highest concentration of Rubisco was recorded in algae the elevated temperature treatment ($t+3^\circ\text{C}$, $380 \mu\text{atm}$), with a significant reduction in concentration in algae in response to the combined treatment ($F_{1,20} = 36.868$, $p < 0.001$).

5.5.2.5 Phycoerythrin

During the winter, phycoerythrin concentration in algae significantly reduced in response to elevated $p\text{CO}_2$ and temperature (temperature: $F_{1,20} = 1.316$, $p < 0.001$; $p\text{CO}_2$: $F_{1,20} = 1.316$, $p < 0.001$, see Figure 5.5f). Exposure to both elevated temperature and $p\text{CO}_2$ increased phycoerythrin concentration in algae during the summer (temperature: $F_{1,20} = 54.513$, $p < 0.001$; $p\text{CO}_2$: $F_{1,20} = 54.513$, $p < 0.001$, see Figure 5.5e). During the summer, the highest concentration of phycoerythrin was recorded in algae under ambient $p\text{CO}_2$ ($380 \mu\text{atm}$) and elevated temperature (ambient + 2°C), with a significant reduction in concentration in algae in response to the combined treatment ($F_{1,20} = 54.513$, $p < 0.001$).

5.5.3 Calcification

During the winter calcification rate ($\text{CaCO}_3 \mu\text{mol g}^{-1}$ (live tissue) h^{-1}) significantly increased in response to elevated temperature ($F_{1,20} = 0.297$, $p = 0.044$, see Figure 5.6), although elevated $p\text{CO}_2$ had no significant effect ($F_{1,20} = 0.297$, $p = 0.549$). During the summer, calcification increased significantly in response to elevated temperature ($F_{1,20} = 5.208$, $p = 0.034$), although decreased significantly in response to elevated $p\text{CO}_2$ ($F_{1,20} = 5.208$, $p = 0.004$, see Figure 5.6).

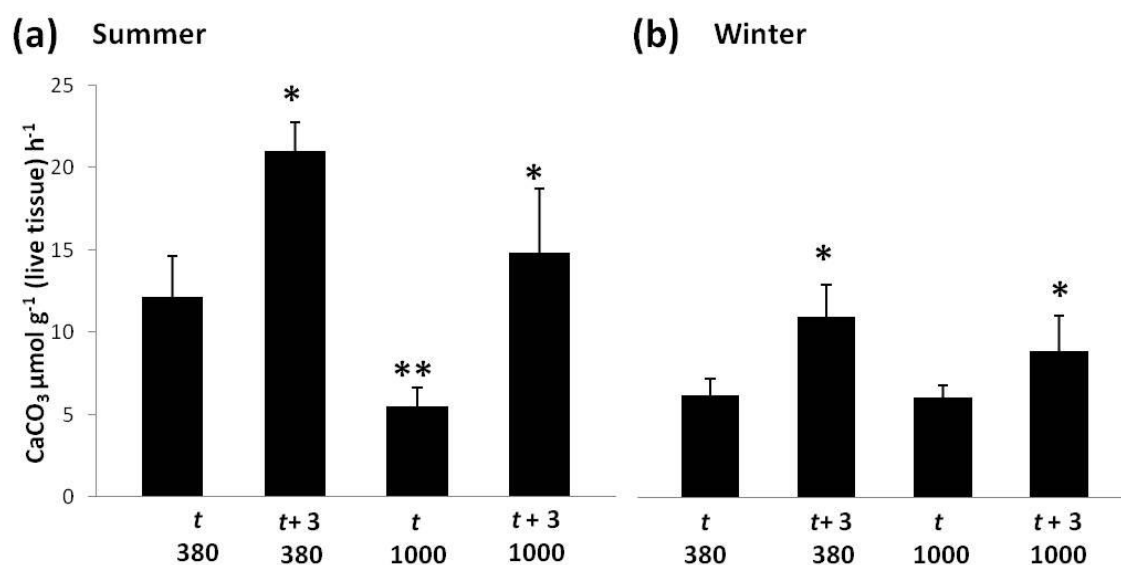


Figure 5.6 Short-term effect of elevated temperature and $p\text{CO}_2$ on calcification rate ($\mu\text{mol g}^{-1}$ (live tissue) h^{-1}) in *Lithothamnion glaciale* during summer and winter. Results are expressed as mean \pm SE (n = 6 Treatments: t = ambient; $\sim 7^\circ\text{C}$ (winter) or 15°C (summer), t + 3 = ambient + 3°C ; at 1000 μatm or 380 μatm $p\text{CO}_2$. PAR: $12.03 \pm 2.51 \mu\text{mol m}^{-2} \text{s}^{-1}$, Asterisk (*) indicates a significant difference.

5.6 Discussion

At sub saturating light levels the short term physiological response of *Lithothamnion glaciale* to elevated temperature and $p\text{CO}_2$ differs in algae exposed to summer temperatures compared to those exposed to winter temperatures. Results suggest that under environmental conditions analogous to projected climate change scenarios the light harvesting efficiency and maximum photochemical efficiency of PSII may decrease during the summer. The optimal light level for efficient photosynthesis increases during both summer and winter in response to elevated $p\text{CO}_2$, presumably due to the additional energetic requirements of calcifying algae under acidified conditions. In addition, calcification increases in response to elevated temperature during both the summer and winter, and decreases in response to elevated $p\text{CO}_2$ during the summer.

5.6.1 Photosynthetic characteristics

In the present study, light harvesting efficiency (α) was lower in *L. glaciale* during the summer, compared to algae during the winter. In addition α in response to elevated temperature (t + 3°C) during the summer (Figure 5.2d). Similarly, a decline in α with increasing temperatures has been reported in other marine algal species (Davison, 1991, Palmisano et al., 1987). This is likely because the amount of light level required to reach

the compensation point (I_c ; the amount of light where photosynthesis exactly matches respiration) increases as temperature increases (Davison, 1991). Consequently, there was also a significant decrease in $F_q'/F_{m'_{max}}$ in *L. glaciale* during the summer under elevated temperature (i.e. $t + 3^\circ\text{C}$) (Figure 5.2a). This significant decrease in $F_q'/F_{m'_{max}}$ and α in response to elevated temperature during the summer, compared to algae in the winter study, is likely because the elevated experimental temperature during the summer study was above the normal thermal range experienced by this species. Suggesting that under projected increases in temperature, light harvesting efficiency (α) and maximum photochemical efficiency of PSII ($F_q'/F_{m'_{max}}$) may decrease.

Concordant with the decrease in α and $F_q'/F_{m'}$, during both the summer and winter E_k increased in *L. glaciale* in response to elevated temperature and elevated $p\text{CO}_2$ (i.e. $t+3$, 1000 and t , 1000) (Figure 5.2). This increase in E_k suggests under global climate change scenarios the optimal light level for efficient photosynthesis is greater, presumably due to the additional energetic requirements by calcifying algae under acidified conditions.

In the present study, $r\text{ETR}_{\text{max}}$ increased under elevated temperature and $p\text{CO}_2$ during both summer and winter, although examination of $r\text{ETR}$ light response curves suggests PAR at $12 \mu\text{mol m}^{-2} \text{s}^{-1}$ may not be great enough to realise this maximum potential (Figure 5.3c, d). Critically, these results suggest that although PAR at $12 \mu\text{mol m}^{-2} \text{s}^{-1}$ is enough to realise the $r\text{ETR}_{\text{max}}$ calculated for contemporary conditions (i.e. t , 380), the irradiance range experienced by the algae *in situ* may not reach PAR levels high enough to realise $r\text{ETR}_{\text{max}}$ calculated for algae under projected climate change scenarios (Figure 5.3c, d). In the future, under acidified conditions, this may mean more light energy is required to drive photosynthesis in coralline algae or efficiency (and productivity) will reduce. A reduction in productivity has significant negative implications for coralline algae based ecosystems and an increase in the amount of light required may have implications for coralline algae distribution, particularly those inhabiting already low light environments (i.e. deep habitats and high latitude).

5.6.2 Proteins

Elevated temperature ($t+3$, 380) was associated with a decrease in intracellular Rubisco concentration in *L. glaciale* during the winter, with a further decrease in response to elevated $p\text{CO}_2$ ($t+3$, 1000), this may be a resource optimisation process involving the reallocation of resources including nitrogen, a major component of Rubisco (Leakey et al., 2009). In contrast, during the summer Rubisco concentration in *L. glaciale* increased in response to elevated $p\text{CO}_2$ and temperature, compared to the control, although, Rubisco concentration in algae exposed to the combined treatment declined compared to algae exposed to solely elevated temperature (Figure 5.5). The activation state of Rubisco can also be reduced under elevated temperatures (Crafts-Brandner and Salvucci, 2000), and the CO_2 compensation point is raised (Bowes, 1991) which can result in a decreased specificity for CO_2 at elevated temperatures (Bowes, 1991). This may have contributed to the decrease in $F_q'/F_{m'_{\max}}$, $F_q'/F_{m'}$ in algae exposed to elevated temperatures (i.e. $t+3$) during the summer study.

The observed changes in total protein concentration were likely to be, in part due to changes in Rubisco concentration (i.e. Rubisco may be up to 30% of the soluble leaf protein, Jensen, 2000). However, changes in total protein can also be indicative of physiological stress caused by environmental factors. *Corallina officinalis* decreased total protein levels (and growth) in response to elevated $p\text{CO}_2$ after 35 days exposure, suggested to be a trade-off to maintain calcification (Hofmann et al., 2012a).

5.6.3 Pigments

Phycoerythrin is an accessory photoreceptor pigment to the main chlorophyll pigments responsible for photosynthesis in the Rhodophyta (Glazer et al., 1976). This pigment reflects red light and absorbs blue light, allowing red algae to thrive in contemporary environments where light is more limited (i.e. deep water) (MacColl et al., 1996). Often, photosynthetic performance and pigment content are closely associated with annually repeating patterns in abiotic environmental factors, particularly irradiance levels (Aguilera et al., 2002). The greater concentration of phycoerythrin reported under ambient conditions (i.e. t , 380) during the winter, compared to the summer, may be due to the natural increase in pigment during the winter to cope with decreased irradiance *in situ*. The elevated levels of phycoerythrin in response to elevated temperature and $p\text{CO}_2$ during the summer may be an attempt to acclimatise to the low light conditions during

the experiment, and may be an indication that more light energy is required to sufficiently drive photosynthetic rates under elevated temperature and $p\text{CO}_2$. Interestingly, there was no change in chlorophyll- α concentration across all treatments. This is likely because either there is a heavy reliance of *L. glaciale* on phycoerythrin for light harvesting under low-irradiance or chlorophyll- a is more robust to climate change than other photosynthetic pigments.

5.6.4 Calcification

During both summer and winter elevated temperature was associated with an increase in calcification in *L. glaciale*. Although during the summer calcification decreased in response to elevated $p\text{CO}_2$ (Figure 5.6). Similar results were reported in the encrusting polymorph of *L. glaciale* in the Arctic at summer temperatures (Büdenbender et al., 2011). The authors attributed this response, in part, to carbon fertilisation of photosynthesis at elevated $p\text{CO}_2$ (i.e. elevated substrate ($p\text{CO}_2$) resulting in greater photosynthetic rates, thus providing more energy), however Hofmann et al. (2012a) suggest evidence for this in calcifying macroalgae is weak. Several studies (Gao and Zheng, 2010, Hofmann et al., 2012a, Hofmann et al., 2012b, Cornwall et al., 2012), including this one, reported a decrease in photosynthetic rates of calcifying macroalgae in response to elevated $p\text{CO}_2$. It is more likely the increased rate in calcification is related to resource reallocation within the algae (i.e. the decrease in intracellular Rubisco concentration and the reallocation of nitrogen). Merrett et al. (1993) demonstrated a requirement of NO_3 for calcification in microalgae, although this is likely to reflect the link between calcification and growth (Sciandra et al., 2003). Nitrogen is also required to build amino acids, proteins, chlorophyll and nucleic acids (Postgate, 1982). However, an increase in calcification rate does not necessarily result in a higher net deposition of CaCO_3 (Hofmann et al., 2012a, Hofmann et al., 2012b). The inconsistency between calcification rates and skeletal inorganic carbon may be attributable to greater dissolution rates in the dark (Martin and Gattuso, 2009, Hofmann et al., 2012a, Kamenos et al., 2013). Under low irradiance it is likely dissolution may play a significant role with respect to the energetic requirements and response of calcification and growth under global climate change scenarios.

5.6.5 Wider implications

While the incidences of sub-saturating light as a result of cloud cover and day length may be decreased during the summer compared to the winter months, limited light as a result of habitat heterogeneity and the complex geometry of the algae is not seasonally dependant. Therefore the changes to the photosynthetic characteristics of *L. glaciale* (i.e. α) as a result of elevated temperatures may have significant negative implications during periods of limiting light in both the summer and the winter. In the future this may lead to a substantially reduced and/ or loss of habitat of algae living in conditions where irradiance is already limited (i.e. deep water habitats), as discussed in chapter 4 (i.e. respiration vs. Photosynthesis). Although, during the summer day length is longer and generally PAR is greater than $12 \mu\text{mol photons m}^2 \text{s}^{-1}$ (Figure 5.1). Therefore, the increased light (longer day length and periods of higher PAR) experienced during the summer may be enough to offset the negative effects of elevated temperature and $p\text{CO}_2$. During the summer at above optimal light ($E/E_k > 1$) $r\text{ETR}$ continued to increase in algae exposed to elevated temperature and $p\text{CO}_2$ (Figure 5.3). The same pattern was observed during the winter, however shorter day length and generally low irradiance means that algae may not have the same advantage during winter months. Seasonal differences in calcification will also have implications for algae survival in the future. Although an increase in calcification was reported in response to elevated temperature in the present study, as discussed this may not translate into increased growth (see also chapter 3). Particularly if there is a decrease in photosynthetic rate relative to respiration as discussed in chapter 4. Free-living red calcifying algae provides an integral contribution to the local biogenic habitat, maintaining biodiversity and ecosystem provision linked to commercial fish and shellfish species, habitat loss and/ or reduction would result in considerable negative ecological implications for marine habitats and provision in the future.

5.6.6 Conclusions

At sub-saturating light levels seasonal differences in temperature impact the physiological response of free-living coralline algae to climate change. Calcification may increase in response to elevated temperature during both the summer and winter, and decrease in response to elevated $p\text{CO}_2$ during the summer. During the summer the light harvesting efficiency and maximum photochemical efficiency of PSII in *L. glaciale* may decrease under acidified conditions, while the optimal light level for efficient

photosynthesis increases during both summer and winter. This is concurrent with results from chapter 4, which suggests that coralline algae experiencing low-light intensities ($12 \mu\text{mol photons m}^{-2} \text{s}^{-1}$) during the winter, combined with elevated $p\text{CO}_2$ will resort to net respiration during the day, although this response can be mitigated by increasing irradiance. It is unlikely light availability will increase in the future, therefore if the light available in the future is not sufficient to maintain key physiological functions in coralline it is likely there will be loss of habitats and a change in the distribution of *L. glaciale*.

6

Coral reef calcifying algae persist in naturally variable environments, but at what cost?

The natural spatial and temporal physico-chemical variability of coastal environments is likely to increase with global change. To understand the impact of projected increases in environmental variability on marine organisms in coastal habitats we must understand their responses to contemporary natural variability.

6.1 Natural variability, climate change and coral reefs

Anthropogenically accelerated global climate change represents a major threat to marine organisms (IPCC, 2013), of which ocean acidification (OA, decreasing ocean pH and carbonate saturation state, as a result of increasing seawater $p\text{CO}_2$) and rising seawater temperatures (Meehl et al., 2007, Gattuso and Hansson, 2011) have been highlighted as the areas of most concern for coastal marine systems. Critically, coastal ecosystems can also be highly dynamic environments compared to their open ocean counterpart (Duarte et al., 2013) and are projected to become increasingly variable over the next century due to the complex interaction between anthropogenic climate change and the dynamic regional / local drivers of coastal ecosystem environments (Duarte et al., 2013).

Coastal seawater biogeochemical dynamics are controlled largely by the interaction between terrestrial (i.e. watershed processes and nutrient input), open ocean, and atmospheric (i.e. global climate change) processes (Aufdenkampe et al., 2011). Furthermore, in contrast to the open ocean, coastal environments are often subjugated by benthic communities which often include ecosystem engineering species (e.g. corals, macroalgae, seagrass, mangroves, burrowed mud, mangroves, salt marshes). These species have the capability to impact and transform the local environmental conditions (Gutiérrez et al., 2011). All these factors combined mean that both spatially and temporally the coastal zone carbon system can be considerably more dynamic than its open ocean counterpart (Borges and Gypens, 2010). On fringing coral reefs, spatial environmental differences occur because the reef crest, with near continuous contact with the open ocean, is generally more environmentally stable than the reef flat, which can be extremely variable due to isolation of the water mass from the open ocean during low tide (Kayanne et al., 1995, Bates et al., 2001, Anthony et al., 2008, Burdett et al., 2013, Shaw et al., 2012). Some of this spatial variability is likely to be driven by biological processes often associated with the benthic community (i.e. photosynthesis/ respiration/ calcification, Price et al., 2012) which can differ between locations. Furthermore, biological activity follows temporal patterns in abiotic environmental factors (i.e. temperature and irradiance). Therefore, within these naturally variable coastal ecosystems the same sessile species occupying adjacent locales may experience differing environmental conditions during their continuance, while also contending with local biotic pressures (e.g. grazing pressure; Lewis and Wainwright, 1985). Marine organisms inhabiting these naturally variable contemporary marine environments may be more resilient to future global climate change scenarios due to their pre-exposure to environmental extremes (Egilsdottir et al., 2013) and therefore may provide information on the processes species employ to survive highly variable and extreme conditions. Ecosystems and habitats with naturally variable environmental conditions provide *in situ* test beds ideal for such investigations (Johnson et al., 2012, Kroeker et al., 2013a, Porzio et al., 2011, Burdett et al., 2013, Egilsdottir et al., 2013).

6.2 Global climate change and marine calcifying algae

Projected changes in seawater carbonate chemistry mean marine organisms that utilise dissolved inorganic carbon species (DIC; HCO_3^- , CO_3^{2-} , CO_2) as a substrate for physiological processes (i.e. photosynthesis and calcification) are likely to be amongst those most impacted by greater environmental variability and OA (Kroeker et al., 2013b). In contrast to photosynthesis, which may benefit from the increased availability of dissolved inorganic carbon (DIC) (Koch et al., 2013), calcification may decrease in seawater with a reduced carbonate saturation state (Orr et al., 2005). Calcifying algae perform both photosynthesis and calcification, thus may exhibit a complex response to the projected changes in seawater DIC. However, any benefit of increased DIC for photosynthesis will depend on (1) whether or not algal photosynthesis is saturated by present day levels of DIC, and which species of DIC is / are employed as the substrate, (2) the intracellular activity and concentration of key proteins (Short and Neckles, 1999, Koch et al., 2013), and (3) the extent to which any benefit gained may be negated by the increased metabolic cost of calcification (and dissolution of calcified skeletons) as carbonate becomes undersaturated in seawater. Therefore, successful recruitment and growth of calcifying algae in variable environments now and in the future (e.g. tropical reef flats) may require a trade-off between sufficient intraspecific phenotypic plasticity (e.g. variable morphology and physiology), and optimisation of available resources (Ragazzola et al., 2013, Wood et al., 2008, Hennige et al., 2008). For example, *in situ* temperate and tropical species of the partially calcifying macroalgal genus *Padina* (Dictyoaceae, Phaeophyta) thrive under highly acidified conditions associated with CO_2 vent systems in the Mediterranean, albeit with reduced CaCO_3 (aragonite) content within their whorls (Johnson et al., 2012). In contrast, tropical reef-flat seawater exhibiting a highly variable carbonate saturation state had no significant effect on the calcification of *Padina gymnospora* (Burdett et al., 2013), but this was accompanied by an elevated intracellular concentration of the secondary metabolite dimethylsulphoniopropionate during periods of minimum carbonate saturation state, perhaps to maintain metabolic function (Burdett et al., 2013).

The response of calcifying algae to changes in the magnitude and variability of seawater carbonate saturation state is likely to be highly dependent on their carbonate

structure, calcification method (Ries et al., 2009, Price et al., 2012), and ability to utilise and acquire increasing CO₂ (e.g. photosynthesis *via* diffusive CO₂ and / or the use of HCO₃⁻ *via* carbon concentrating mechanisms) (Hepburn et al., 2011, Giordano et al., 2005). For example, coralline red algae (composed of high-Mg calcite the most thermodynamically unstable calcite polymorph) show a reduction in photosynthesis by an average of 28% in response to exposure to high-CO₂ conditions (Kroeker et al., 2013b). In naturally acidified conditions (CO₂ vents), calcareous red algae reduce in abundance with decreasing pH (Hall-Spencer et al., 2008), and may eventually be out-competed by fleshy macroalgae in low pH conditions, probably because of a decrease in the growth rate of calcareous algae and an increase in the growth rate of fleshy species (Kroeker et al., 2013c). A comprehensive meta-analysis by Kroeker et al. (2013b) suggests that calcifying algae may be amongst the most negatively impacted marine organisms with respect to ocean acidification and global warming, but empirical evidence is conflicting (Noisette et al., 2013b) and more investigations into the physiological impact of low and variable carbonate saturation state of calcifying marine algae are required (Burdett et al., 2013).

6.3 Tropical calcifying algae

Calcifying algae play an integral role within coral reef communities and have been shown to be a major contributor to reef formation and protection (Hillis-Colinvaux, 1986, Adey, 1978, Chisholm, 2000), carbonate sand production (Drew, 1983, Multer, 1988), primary productivity (Wanders, 1976, Hawkins and Lewis, 1982, Crossland et al., 1991) and nitrogen fixation (Wiebe et al., 1975). In addition, they provide a food source to grazers and substrata for the settlement of invertebrate larvae and increase biodiversity by offering habitat heterogeneity (Adey, 1998). Among the different groups of calcified algae the mode and extent of calcification varies widely. *Padina gymnasopra* is partially calcifying brown macroalgae that develops thin white calcified bands across fan shaped blades (whorls) and is an abundant component of coral reef communities across the tropics (Figure 6.1).

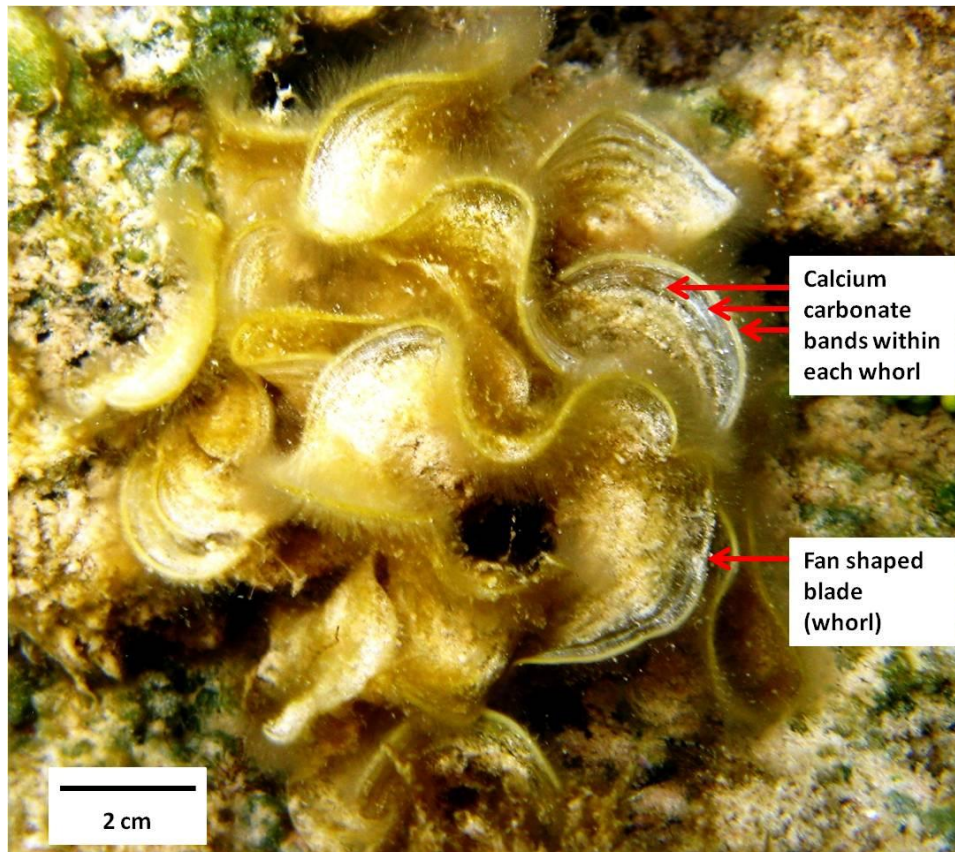


Figure 6.1 *Padina gymnospora*.
Photographed on the Suleman Coral Reef, Dahad, Egypt. Photo: P. Donohue

6.4 Aims of this chapter

This chapter aims to investigate the differences in (1) size and (2) photophysiological characteristics of *P. gymnospora* growing in locations characterised by low (reef crest) and high (reef flat) environmental variability across a fringing coral reef. This will improve our understanding of how environmentally-dependent phenotypes and *in situ* studies may provide insight into the response of marine organisms to projected changes in coastal environmental variability.

It was hypothesised that there would be a physiological trade-off required by *P. gymnospora* to cope with the more variable environmental conditions associated with the reef flat on the Suleman Reef. This re-allocation of energy was likely to be at the expense of photochemical efficiency and growth.

6.5 Methods

6.5.1 Sample site

The study was conducted on the Suleman Reef, Dahab, Egypt (28°28'47"N, 34°30'49"E) during August 2010, using snorkelling. Suleman Reef is a fringing reef with a ~90-100 m wide reef flat, followed by a ~10-20 m wide reef crest and a reef slope to a depth of >8 m (Figure 6.2). *Padina gymnospora* was present on both the reef crest and reef flat.

6.5.2 Sampling points

To determine temporal (diel periodicity) and spatial (reef flat vs reef crest) variation in seawater chemistry, and photosynthetic characteristics of *P. gymnospora*, two time series studies were conducted over 45 and 36 hour periods, respectively. Seawater and *P. gymnospora* samples were collected from both the reef crest (100-120 m from the shore) and reef flat (40-90 m from the shore) at T13, T21, T29, T36 and T45 hours (where T0 was 00:00 on day one). Time points were selected to coincide with different levels of irradiance: low light intensity (T29), high light intensity (T13 and T36) and dark (T21 and T45).

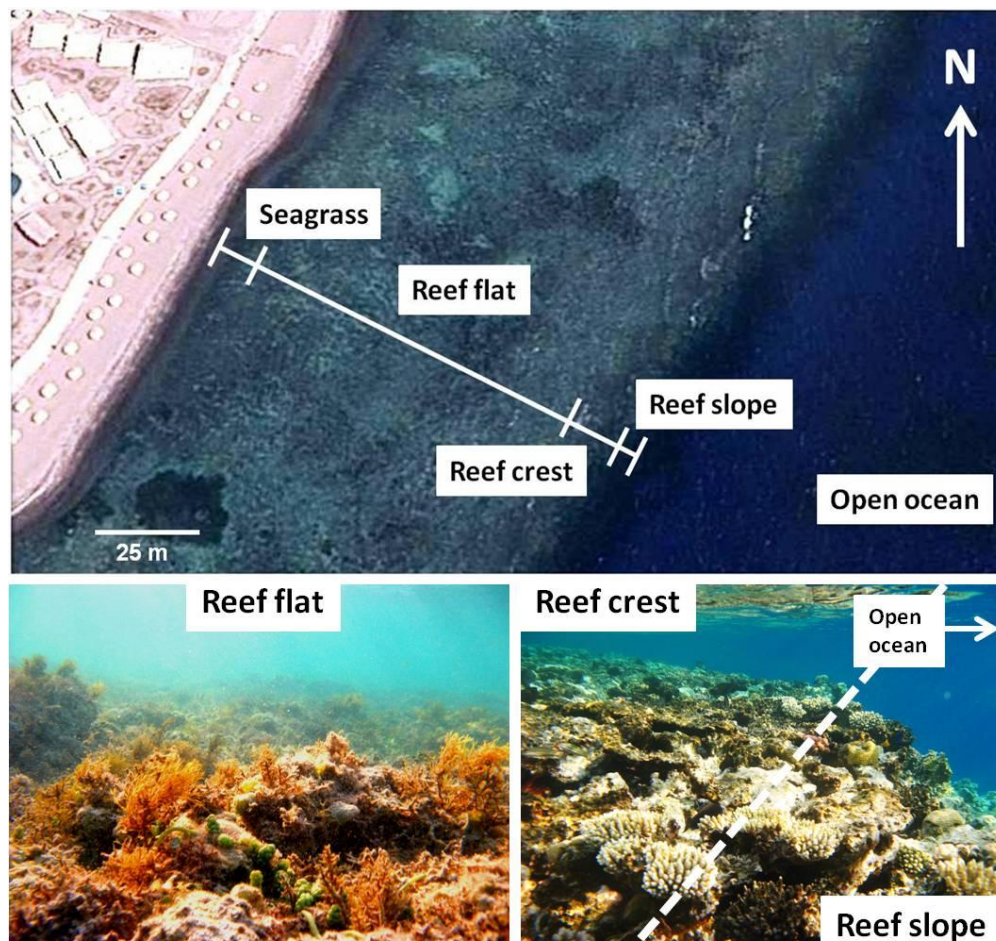


Figure 6.2 Suleman reef transect location and examples of the benthic community within each sample zone.

Water and macroalgae samples were taken from the reef flat and crest. Distance from the top of the reef crest and the shore is ~120 m. The reef flat is dominated by fleshy and coralline macroalgae and the reef crest is dominated by branching corals and encrusting coralline algae. Aerial image: Google Earth, photos: P. Donohue.

6.5.3 Environmental parameters

6.5.3.1 Physico-chemical seawater parameters and depth

Dissolved inorganic carbon (DIC) and total alkalinity (A_T) were determined from seawater samples collected at each sampling time point on both the reef flat and crest. On collection, seawater samples were poisoned with mercuric chloride (40 μ l of a 50% saturated solution) (Riebesell et al., 2010), stored in 12 ml screw top borosilicate glass vials (Exetainer, Labco Ltd., UK) and transported back to the UK for analysis. Seawater samples were analysed for A_T and DIC using the methodology described in Chapter 2. Salinity and water temperature were measured *in situ* using a handheld meter (Pro 2030, YSI, Ohio, USA). Additional carbonate system parameters ($p\text{CO}_2$, calcite and aragonite saturation, $[\text{HCO}_3^-]$ and $[\text{CO}_3^{2-}]$ and pH) were calculated from A_T , DIC, salinity and temperature using the software program CO2SYS (Pierrot et al., 2006), method described in Chapter 2.

6.5.3.2 Net community photosynthesis (dissolved oxygen)

Dissolved oxygen (% DO) was measured *in situ* using a temperature and salinity corrected handheld meter (Pro 2030, YSI, Ohio, USA) on both the reef flat and crest at each time point. The relationship between DO and carbonate chemistry seawater parameters (DIC; HCO_3^- , CO_3^{2-} , $p\text{CO}_2$) was used to infer the extent to which net community photosynthesis / respiration contributed to the variability in physico-chemical seawater parameters on the reef flat and crest.

6.5.3.3 Photosynthetically active radiation

Photosynthetically active radiation (PAR, $\mu\text{mol photons m}^{-2} \text{ s}^{-1}$) on the reef flat and crest was determined *in situ* for the duration of the sampling period using PAR meters located on the reef flat and crest (Apogee QSO-E underwater quantum sensor connected to a Gemini voltage data logger).

6.5.4 Determination of thallus size and abundance

The size of individuals were measured from both the reef crest and the flat ($n = 34$ per site) for comparison. The height of the tallest whorl on each thallus was measured and the total number of blades associated with each thallus was determined. Abundance of *P. gymnospora* was determined using point-intercept transects. Three transects were carried out across the reef platform from the shore to the reef slope; the presence or absence of *P. gymnospora* was recorded every 0.5 m.

6.5.5 Photosynthetic characteristics

At each time point *P. gymnospora* from both the reef flat and crest ($n = 5$ individuals per site) were collected for quantification of Rubisco concentration and assessment of photosynthetic characteristics.

6.5.5.1 Rubisco concentration

To extract proteins, one whorl of *P. gymnospora* (~0.5g) was ground directly in sodium dodecyl sulphate (SDS) buffer (Invitrogen, UK, 0.5 ml) using a mortar and pestle to produce a paste. The paste was then transferred to a microcentrifuge tube (Eppendorf, 1.5 ml), boiled for 5 min, and centrifuged at 14 000 r.p.m. for 1 – 2 min to yield a cell-free protein extract. Protein extracts were analysed by 1D-gel electrophoresis as described in Chapter 2. Gels were Coomassie stained (0.1% Coomassie Brilliant Blue R250, 40% MeOH, 10% Acetic Acid). A protein of molecular weight ~55 kDa (the known molecular

weight of Rubisco) was excised from the gel and subjected to in-gel trypsin digest and identified using the Mass Spectrometry method described in Chapter 2.

6.5.5.2 Photosynthetic characteristics

A Diving-PAM fluorometer was used to perform rapid light curves (RLCs; 0 – 1455 $\mu\text{mol photons m}^{-2} \text{s}^{-1}$) to assess the photosynthetic characteristics of *P. gymnospora* as previously described in Chapter 2. Quasi dark-acclimation was achieved by the use of a surface holder (Walz GmbH, Germany), as described in Chapter 2, achieving $88 \pm 4.7\%$ (mean \pm SE, $n = 6$) of the maximum photochemical yield, determined from 60-min dark-acclimated algae (see Figure 6.3).

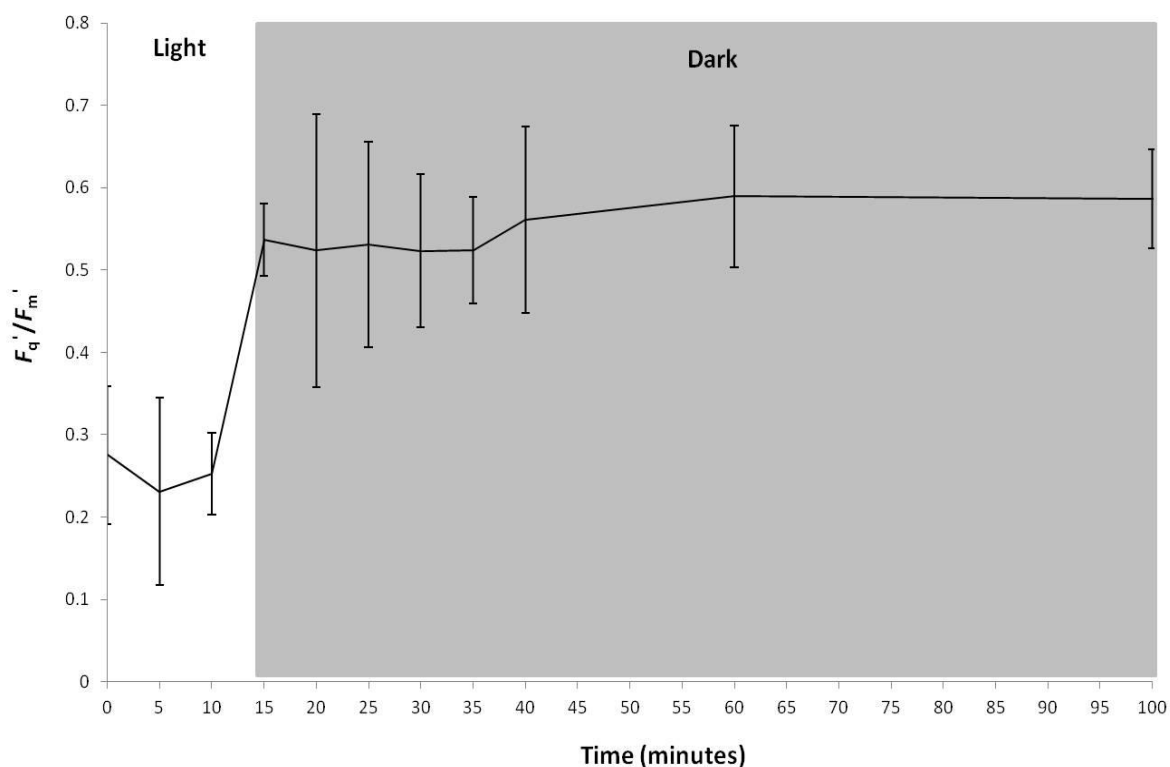


Figure 6.3 Yield measurements of *Padina gymnospora* in the light (0-10 mins) and in dark (15-100 mins).

Lights were turned off after 14 mins 50 s, therefore the first dark-acclimated yield value represents the quasi dark-acclimated value (10 s of darkness). Data presented as mean \pm SD, $n = 6$.

6.5.5.3 Night time samples

It is difficult to measure chlorophyll fluorescence yield in the absence of non-photochemical quenching (Maxwell and Johnson, 2000). Therefore, any estimations of non-photochemical quenching are relative to a dark acclimated point, hence there is a requirement for a dark-acclimated, non-stressed (in terms of irradiance exposure) reference point to be estimated. In the present study, the reference point consisted of

RLCs conducted on dark-acclimated thalli during the night, where the algae had been in darkness for ~ 3 hours before measurements were obtained. Measurements obtained differ from measurements taken under actinic light because in dark acclimated samples all reaction centres in PSII are open.

6.5.6 Statistical analysis

One-way ANOVAs were used to investigate differences in (1) thallus size, (2) the number of whorls associated with each thallus, (3) abundance, and (4) photochemical characteristics between algae located on the reef crest and the reef flat. Photochemical data from each time series were pooled to investigate the effect of location on mean photochemical efficiency (described by F_q'/F_m' , E_k , α , $rETR_{max}$). A two-way ANOVA was used to investigate the effect of location and time of day (index for irradiance) on Rubisco concentration in the algae. Some data were transformed using $\log_{10}(x)$ ($rETR_{max}$ at T29) to meet test assumptions of normality and homogeneity of variance. Where assumptions of ANOVA were not met (F_q'/F_m' and E_k at T29), a non-parametric Kruskal-Wallis test was used. Differences between means / medians were considered to be significant when $p \leq 0.05$. If a significant difference between locations was found, a Tukey-Kramer post hoc test was used post-ANOVA. Pearson product-moment correlation analysis was used to quantify the relationship between dissolved oxygen (a proxy for net community photosynthesis) and environmental parameters (DIC, HCO_3^- , CO_3^{2-} , CO_2 , pH and temperature). All analyses were conducted with SPSS v18.0.

6.6 Results

6.6.1 Environmental parameters

6.6.1.1 Physico-chemical seawater parameters and depth

The physico-chemical seawater parameters of the reef platform are summarised in Figure 6.4. The range of all parameters was greatest on the reef crest compared to the reef flat, with the exception of A_T (Figure 6.4h). Seawater depth averaged 0.63 ± 0.27 m (mean \pm SD) on the reef flat and 0.82 ± 0.29 m (mean \pm SD) on the reef crest.

6.6.1.2 Net community photosynthesis and physico-chemical seawater parameters

The relationship between DO (a proxy for net community photosynthesis / respiration) (Hatcher, 1988) and carbonate chemistry seawater parameters (DIC, HCO_3^- , CO_3^{2-} , pCO_2) is described in Figure 6.5. DIC, pCO_2 and HCO_3^- concentration decreased

with increased net community photosynthesis (i.e. increased DO; $r = -0.904$, $p < 0.001$, $r = -0.753$, $p < 0.001$, $r = -0.850$, $p < 0.001$, respectively, Figure 6.5a, b, d). In contrast, CO_3^{2-} and pH increased with increasing net community photosynthesis (i.e. increasing DO; $r = 0.716$, $p < 0.001$ and $r = 0.564$, $p = 0.001$, respectively, Figure 6.5c, e). Net community photosynthesis also increased with increasing temperature ($r = 0.945$, $p < 0.001$, Figure 6.5f).

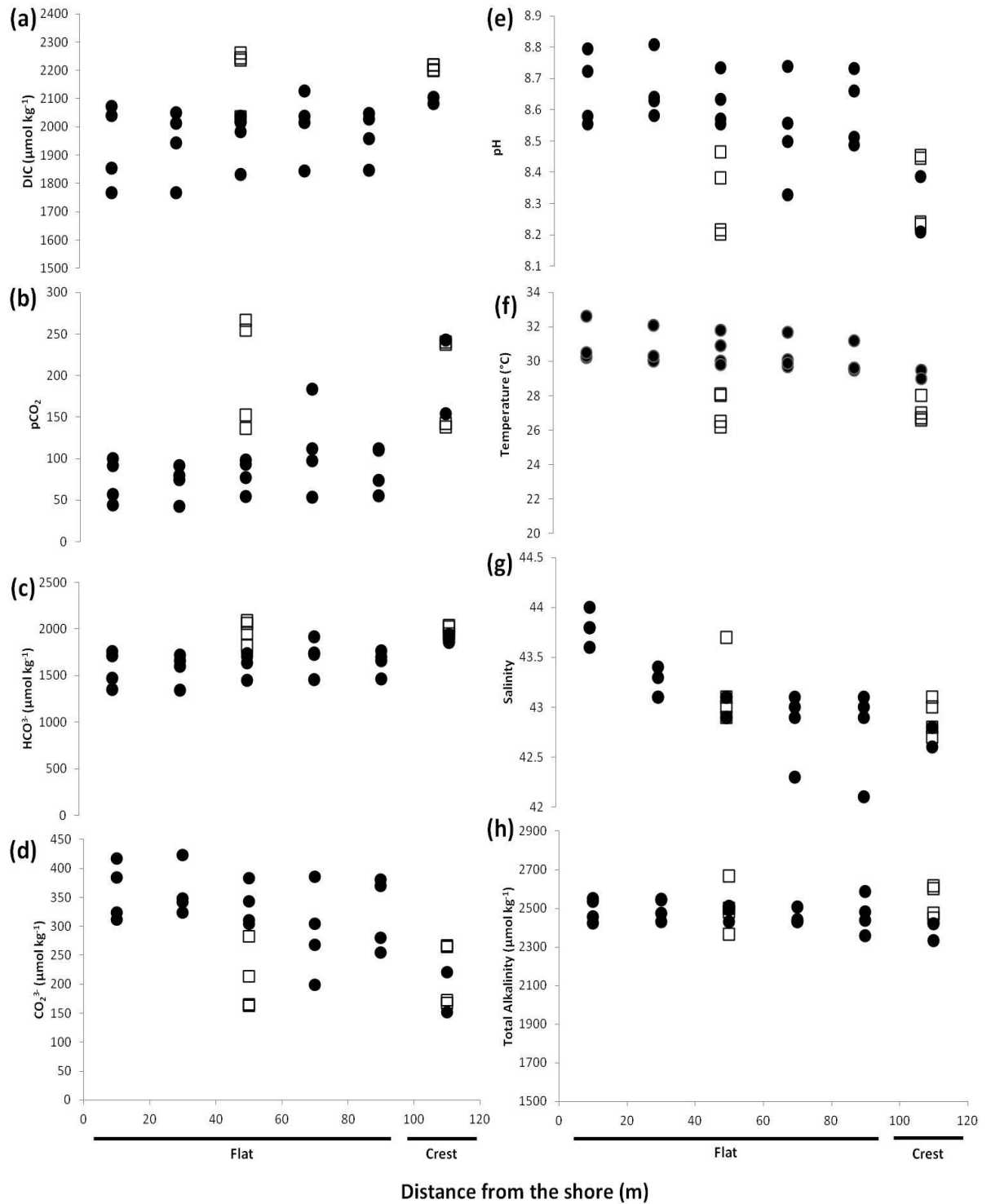


Figure 6.4 Physico-chemical parameters on the Suleman reef.

Abiotic parameters measured on the reef crest and reef flat throughout the diel cycle on the Suleman Reef, Dahab, Egypt. (a) Dissolved inorganic carbon (DIC), (b) pCO_2 , (c) HCO_3^- (d) CO_3^{2-} (e) pH, (f) water temperature, (g) salinity, (h) total alkalinity (A_T). (a) - (d) were measured. (e) - (h) were calculated using CO2SYS. Solid black circles: values collected during high irradiance (T13 and T36), open black squares: values collected during low irradiance (T29) and dark (T21 and T45).

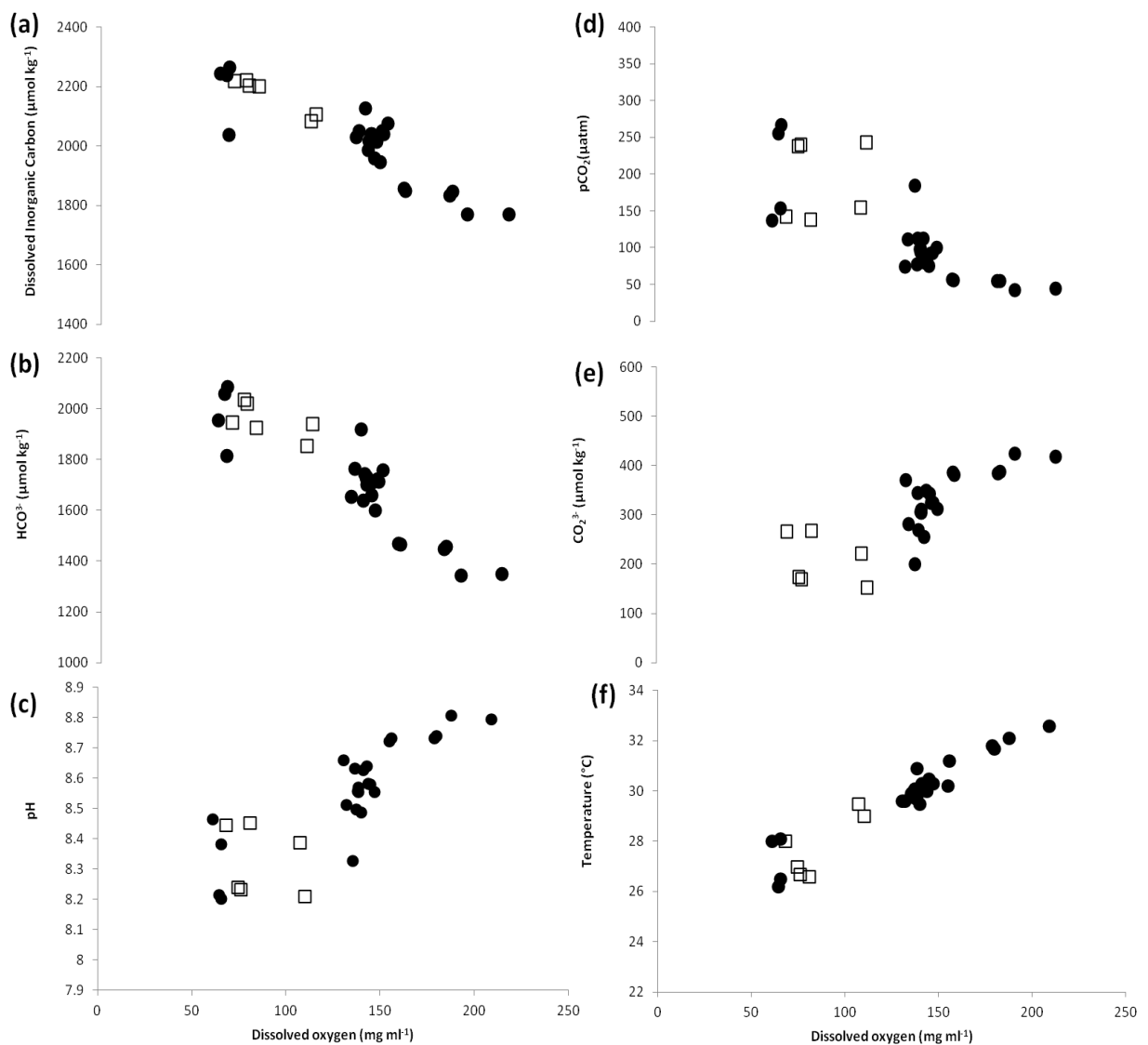


Figure 6.5 Net community photosynthesis on the Suleman reef flat and crest. The relationship between dissolved oxygen (= net community photosynthesis / respiration) and (a) DIC, (b) HCO_3^- , (c) pH, (d) pCO_2 , (e) CO_3^{2-} and (f) water temperature on the Suleman reef platform. Solid black circles: reef flat, open black squares: reef crest.

6.6.1.3 Photosynthetically active radiation during the day

PAR on the reef crest at T29 (0500; low irradiance) was $392.39 \pm 169.85 \mu\text{mol photons m}^{-2} \text{s}^{-1}$ (mean \pm SD) and $320.15 \pm 116.18 \mu\text{mol photons m}^{-2} \text{s}^{-1}$ (mean \pm SD) on the reef flat. PAR on the reef crest at T13 and T36 (1300; high irradiance) was $1701.06 \pm 420.03 \mu\text{mol photons m}^{-2} \text{s}^{-1}$ (mean \pm SD) and $1967.56 \pm 314.20 \mu\text{mol photons m}^{-2} \text{s}^{-1}$ (mean \pm SD).

6.6.2 Thallus size and abundance

Padina gymnospora thalli on the reef flat and crest were the same height (3.26 ± 0.16 and 3.07 ± 0.19 cm, respectively (mean \pm SE), $F_{1,66} = 0.540$, $p = 0.465$). However, thalli located on the crest had significantly more whorls (~44% more) than those on the reef flat (6.94 ± 0.77 and 3.94 ± 0.57 , respectively, $F_{1,66} = 9.883$, $p = 0.002$). There was no

significant effect of location on the abundance of *P. gymnospora* between the reef crest and reef flat (16.7 ± 8.6 and 13.57 ± 1.1 % of total number of point counts, respectively, $F_{1,4} = 0.138$, $p = 0.729$).

6.6.3 Photosynthetic characteristics

6.6.3.1 Intracellular Rubisco concentration

Using gel band intensity, both time (equivalent to irradiance level, $F_{2,17} = 12.887$, $p = 0.001$) and location ($F_{1,17} = 16.510$, $p = 0.002$) had a significant effect on Rubisco intracellular concentration in *P. gymnospora* (Figure 6.6). Under high (T13 and T36) and low irradiance (T29), thalli located on the reef crest had significantly higher intracellular Rubisco concentrations compared to thalli located on the reef flat. As irradiance increased, intracellular Rubisco concentrations significantly increased in thalli located on the reef crest compared to the reef flat (Figure 6.6b).

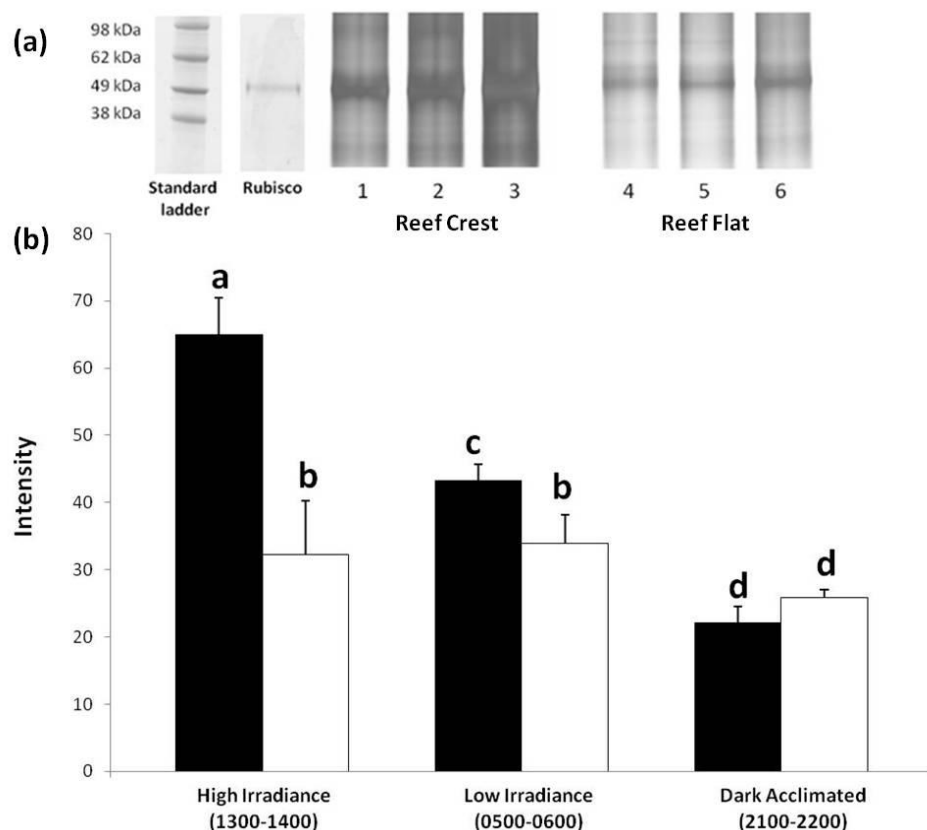


Figure 6.6 Rubisco concentration in *Padina gymnospora*.

(a) Bis-Tris 4 12% Gel of stained with Coomassie staining. Left to right: Pre-stained standard of known molecular weights indicated by values (kDa), Rubisco standard at 55 kDa, Lanes 1-3: Reef crest, Lanes 4-6: Reef flat; (b) Effect (mean \pm SD) of time and location on Rubisco concentration in *P. gymnospora*. Black bars: reef crest, white bars: reef flat. Letters indicate significantly different groups between time and location ($P < 0.05$).

6.6.3.2 Photochemical parameters

6.6.3.2.1 Calculated photosynthetic characteristics ($F_q'/F_m'_{max}$, E_k , α , $rETR_{max}$): temporal changes

Algae in both locations followed a similar diel pattern (Figure 6.7), although algae located on the reef flat consistently exhibited decreased photosynthetic efficiency (described by $F_q'/F_m'_{max}$, E_k , α , $rETR_{max}$). In general, $F_q'/F_m'_{max}$ and α were highest under low irradiance (T29, Figure 6.7a, c), whilst E_k and $rETR_{max}$ were highest under high irradiance (T13 and T36; Figure 6.7b, d). With the exception of $F_q'/F_m'_{max}$, all calculations of photosynthetic efficiency (E_k , α , $rETR_{max}$) were lowest in dark-acclimated samples (T21 and T45) from both the reef flat and crest (Figure 6.7b, c, d). $F_q'/F_m'_{max}$ was lowest on the reef crest under high irradiance, whilst $F_q'/F_m'_{max}$ was lowest on the reef flat in dark-acclimated samples (Figure 6.7a).

6.6.3.2.2 Calculated photosynthetic characteristics ($F_q'/F_m'_{max}$, E_k , α , $rETR_{max}$): spatial differences

Photochemical data from both time series were pooled for statistical analysis to investigate the effect of location on mean photochemical efficiency (described by $F_q'/F_m'_{max}$, E_k , α , $rETR_{max}$). Under low irradiance (T29) mean $F_q'/F_m'_{max}$ and α were both significantly higher in algae located on the reef crest compared to the flat ($H_{1,18} = 17.396$, $p < 0.001$ and $F_{1,18} = 8.913$, $p = 0.008$, respectively). However, there was no significant difference in $rETR_{max}$ and E_k between algae located on the reef crest and flat ($F_{1,18} = 3.991$, $p = 0.061$ and $H_{1,18} = 0.359$, $p = 0.549$, respectively). Under high irradiance (T13 and T36) mean α was significantly higher in algae located on the reef crest compared to the flat ($F_{1,38} = 7.140$, $p = 0.011$). However, there was no significant effect of location on F_q'/F_m' , $rETR_{max}$ or E_k ($F_{1,38} = 0.707$, $p = 0.406$; $F_{1,38} = 0.022$, $p = 0.881$; $F_{1,38} = 0.832$, $p = 0.367$, respectively) under high light intensities. In dark acclimated samples (T21 and T45) mean $F_q'/F_m'_{max}$, $rETR_{max}$ and α parameters were significantly greater in algae located on the reef crest compared to the flat ($F_{1,28} = 18.683$, $p < 0.001$, $F_{1,28} = 5.780$, $p = 0.023$ and $F_{1,28} = 16.225$, $p < 0.001$, respectively). However there was no significant effect of location on E_k ($F_{1,28} = 2.776$, $p = 0.107$).

6.6.3.2.3 Measured photochemical (photochemical quenching) parameters (F_q'/F_m' (and F_v/F_m), qP and rETR): spatial and temporal differences

Photochemical data from both time series were pooled to produce light-response curves of photochemical quenching parameters (described by F_q'/F_m' , qP, rETR) in algae from each location and under each irradiance level. Under low irradiance (T29) light-response curves suggest greater F_q'/F_m' and rETR was observed in algae on the reef crest compared to the reef flat (Figure 6.8a and g), although qP did not differ between algae from each location (Figure 6.8d). Under high irradiance (T13 and T36) rETR in algae located on the reef flat increased, compared to rETR recorded in these algae at low irradiance, however, rETR in algae from the reef crest did not change under different irradiances (Figure 6.8). Under high irradiance F_q'/F_m' and qP was greater in algae located on the reef crest compared to thalli located on the flat (Figure 6.8b). Dark acclimated light-response curves indicate greater potential rETR in algae on the reef crest and concurrent increased potential photochemical yield (termed F_v/F_m in dark-acclimated samples). In contrast, no noticeable difference in qP potential between algae from the two locations was observed (Figure 6.8c, f, i).

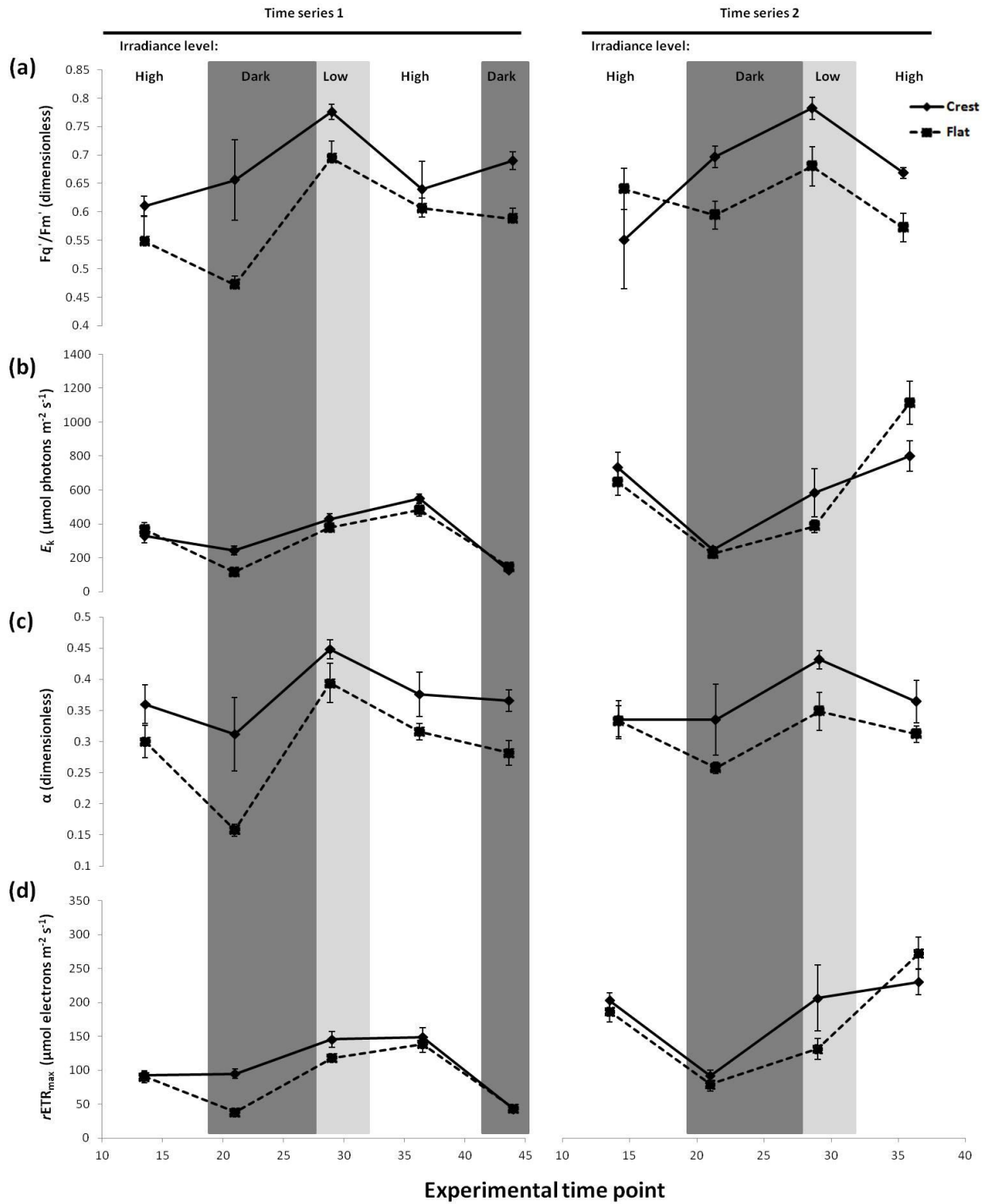


Figure 6.7 Diel pattern of calculated photosynthetic yield parameters of *P. gymnospora* located on the reef crest and flat.

(a) F_q/F_m' (dimensionless), (b) E_k ($\mu\text{mol photons m}^{-2} \text{s}^{-1}$), (c) α (dimensionless), (d) $rETR_{max}$ ($\mu\text{mol electrons m}^{-2} \text{s}^{-1}$). Black diamonds / solid line: reef crest, black squares / dotted line: reef flat. Values mean \pm SE.

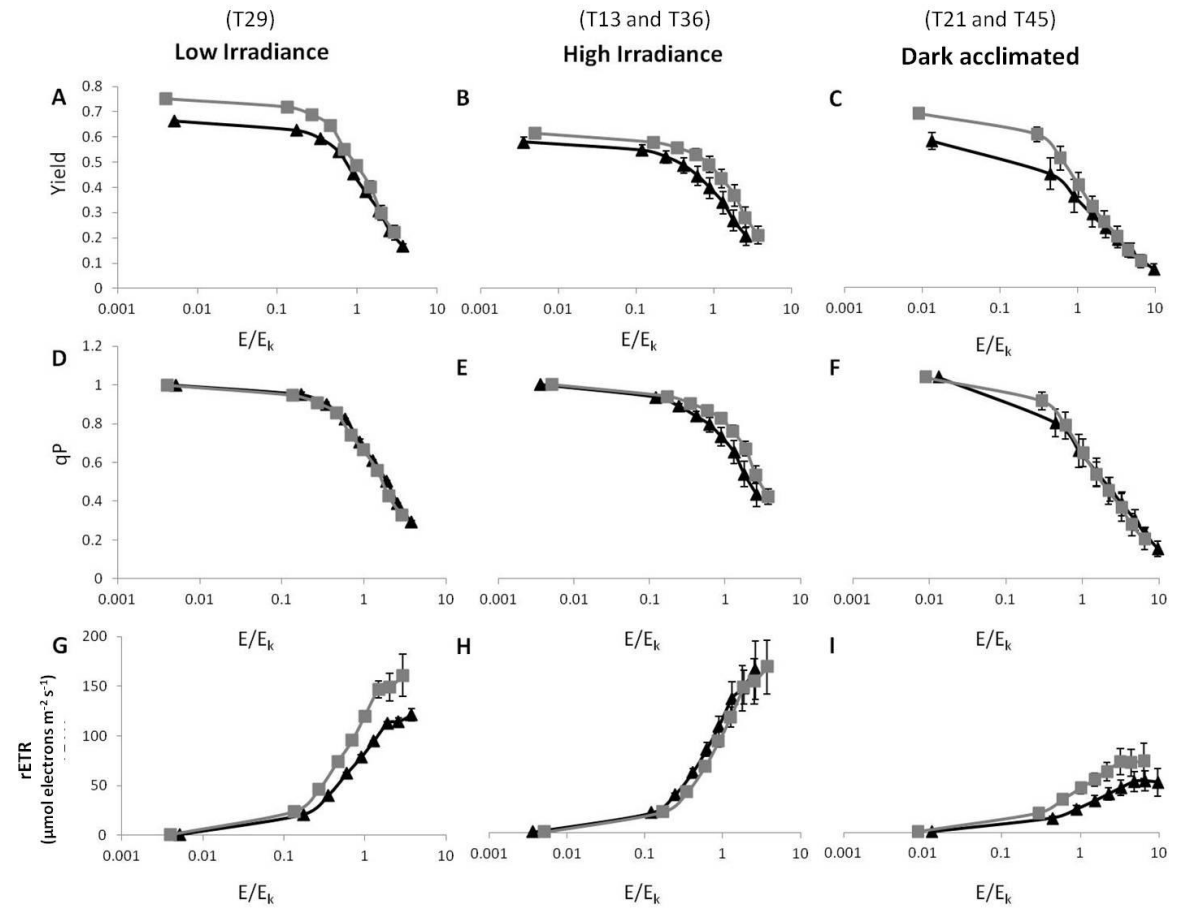


Figure 6.8 Photochemical response of *Padina gymnospora* located on the Suleman reef. Reef crest (grey squares) and the reef flat (black triangles) under high and low irradiance and dark acclimated; (a, b, c) yield (termed F_q'/F_m' or F_v/F_m in dark adapted samples), (d, e, f) qP and (g, h, i) rETR ($\mu\text{mol electrons m}^{-2} \text{s}^{-1}$). Data normalised to E/E_k ; values are mean \pm SE.

6.6.3.3 Photo-protection (qN)

qN (plotted as $1 - qN$, Figure 6.9) was greater in algae located on the reef flat at both high and low irradiance. Furthermore, qN was highest in algae from both the reef flat and crest under high, compared to low, irradiance.

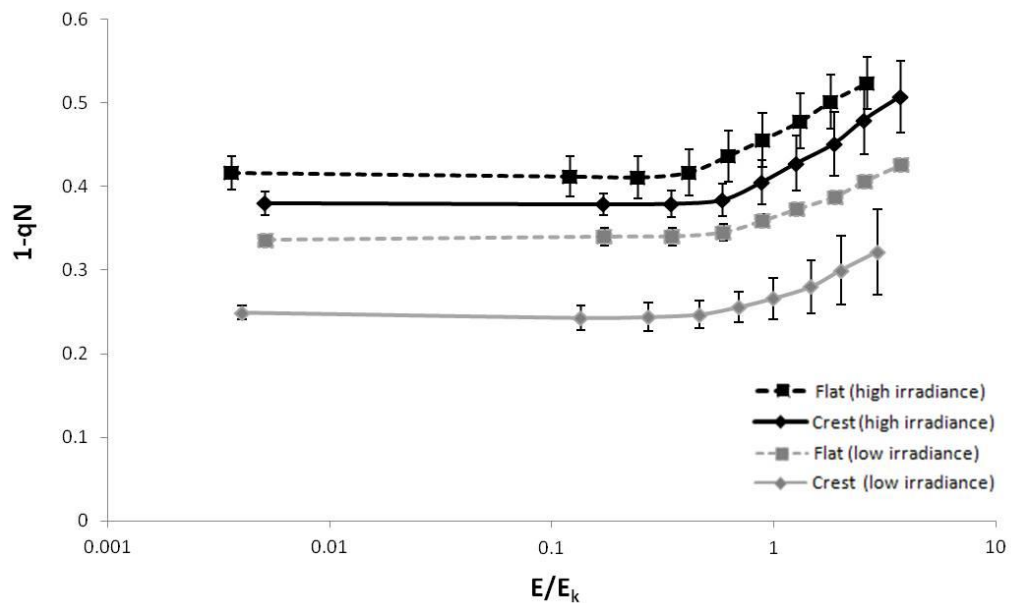


Figure 6.9 *Padina gymnospora* photo-protective response ($1-qN$) in different locations. Photo-protective response of *P. gymnospora* located on the reef crest and the reef flat under high and low irradiance. Data normalised to E/E_k , values are mean \pm SE.

6.7 Discussion

Padina gymnospora growing under different ranges of environmental variability on a tropical coral reef appear to exhibit different biochemical and morphological phenotypes, suggesting intraspecific phenotypic variation dependant on local conditions. As marine organisms inhabiting naturally variable contemporary marine environments may be more resilient to future global climate change scenarios (Egilsdottir et al., 2013), this response may indicate a potential for acclimatisation of partially calcifying marine macroalgae under projected climate change scenarios of decreasing saturation state, increasing temperature and increasing variability for coastal habitats.

6.7.1 Biological and Physical Control of physico-chemical seawater parameters

Cyclical physical processes (e.g. tidal excursions and incursions), the depth profile of the Suleman Reef (average depth: 0.8 m) and the benthic community cause local diel patterns in the physico-chemical parameters of the water mass across the reef platform. The Suleman Reef flat is dominated by macroalgae whose diel pattern in community photosynthesis and respiration follow diel variations in irradiance and temperature (Figure 6.4). CO_2 and HCO_3^- are key DIC species employed as substrates for photosynthesis in brown algae (Raven and Hurd, 2012a) (e.g. photosynthesis *via* diffusive CO_2 and / or the use of HCO_3^- *via* carbon concentrating mechanisms). Decreasing seawater CO_2 and

HCO_3^- concentrations (and DIC) with increasing DO (Figure 6.5a, b, d) suggests uptake of CO_2 and HCO_3^- by macroalgae for photosynthesis; a relationship concordant with macroalgae dominated habitats. Concurrently pH increases in accordance with decreasing DIC and increasing DO (Figure 6.5c). The strong *in situ* relationship detected in the present study between net community photosynthesis and physico-chemical seawater parameters highlights the impact the benthic community has on local environmental variability on the Suleman Reef, particularly on the reef flat (Figure 6.5). Similar relationships between biological processes and seawater physico-chemical parameters occur in other macroalgal-dominated tropical reef systems (Albright et al., 2013, Anthony et al., 2011, Kleypas et al., 2011). On the Suleman Reef, the relationship between net community photosynthesis and environmental variability is reduced on the reef crest (Figure 6.5), most likely because of the crest's near-continuous contact with the open ocean and decreased macroalgal abundance. Furthermore, the strong relationship between community photosynthesis and the physico-chemical seawater parameters on the reef flat suggests limited exchange / mixing between water on the reef flat and the open ocean during this study.

6.7.2 Phenotypic variation in algal photo-physiology

Reef flat physico-chemical variability was associated with reduced intracellular Rubisco concentrations in *P. gymnospora*. Rubisco is the major enzyme responsible for incorporating CO_2 into plants and algae during photosynthesis and is a major rate-limiting step in carbon fixation (Jensen, 2000). It is likely that the decrease in calculated photochemical yield parameters ($F_q'/F_{m'_{\max}}$, E_k , α , $r\text{ETR}_{\max}$) and measured photochemical (photochemical quenching) parameters ($F_q'/F_{m'}$, qP , $r\text{ETR}_{\max}$) in thalli on the reef flat compared to those on the crest is related to the reduced intracellular Rubisco concentration. Decreased Rubisco concentration and acclimation of photosynthesis under high- CO_2 is likely to be a resource optimisation process involving the reallocation of resources including nitrogen, a major component of Rubisco (Leakey et al., 2009). Thus decreased Rubisco concentrations may allow the reallocation of nitrogen to other physiological processes essential for optimal growth and development (e.g. light harvesting, electron transport, carbohydrate synthesis, and non-photosynthetic processes) (Drake et al., 1997, Bowes, 1991). While similar processes occur in seagrasses (Koch et al., 2013), no change in Rubisco activity and concentration in a range of

Mediterranean macroalgae species (including *Padina pavonia*) under high-CO₂ conditions have been observed in short-term laboratory experiments (Israel and Hophy, 2002).

Diel patterns in calculated photochemical yield parameters (F_q'/F_m' , E_k , α , $rETR_{max}$) occurred, and were all consistently higher on the reef flat (Figure 6.7). Similarly, measured photochemical (photochemical quenching) parameters (F_q'/F_m' , qP , $rETR_{max}$) were consistently higher in algae on the reef crest (Figure 6.8). Increased F_q'/F_m' (Figure 6.7a) and F_q'/F_m' light-response curves (Figure 6.8a, b) in algae located on the reef crest suggests that these algae were able to use a greater proportion of absorbed light energy to drive photosynthesis compared to algae on the flat, although there was little difference in qP in algae between the reef crest and reef flat (Figure 6.8d, e, f), which suggests the proportion of closed reaction centres in PSII is similar in algae from both locations, despite the difference in efficiency between locations. F_q'/F_m' and F_q'/F_m' is greatest in algae from both locations under low irradiance, most likely due to increased α , a measure of efficiency at which the algae harvests light under light-limited conditions (Figure 6.7c). Under high irradiance, F_q'/F_m' and α decreased in algae on both the reef flat and crest, probably in part due to stress caused by excess light (Demmig-adams and Adams, 1992, Franklin and Forster, 1997). Concurrently, the use of photo-protective mechanisms (i.e. non-photochemical quenching (qN), Figure 6.9) increased under high irradiance in algae on both the reef flat and crest. Photo-protective mechanisms are essential to the survival of algae, providing protection against photo-damage of the photosynthetic membrane (Pascal et al., 2005). These mechanisms can, however, be energy expensive (Goss and Jakob, 2012). qN was highest in algae located on the reef flat, concurrent with the decreased α present in algae from the same location. If algae on the reef flat are less efficient at harvesting light (α) due the variable environmental conditions, the likelihood of photo-damage and photo-inhibition as a result of excess light energy may be increased, necessitating a requirement for efficient photo-protection mechanisms. Furthermore, the difference in F_v/F_m ($(F_q'/F_m')/qP$) between the reef crest and flat, which reflects a difference in the potential photochemical efficiency (dark acclimated) of PSII, also suggests a difference in the efficiency of non-photochemical quenching between locations (Figure 6.8c) (Maxwell and Johnson, 2000).

In addition to catalysing carbon fixation, Rubisco also catalyses the oxygenation of ribulose 1,5-biphosphate during photorespiration. This dual role of Rubisco means

carboxylation and oxygenation are competitive reactions; CO₂ and O₂ compete for the same active sites on the Rubisco molecule (Lorimer, 1981). The elevated levels of DO (and concurrent decrease in DIC) reported in this study under high irradiance may have intensified O₂ inhibition (i.e. increased photorespiration) in *P. gymnospora*, contributing to the observed reduction in $F_q'/F_{m'_{max}}$ (Figure 6.7a) and $F_q'/F_{m'}$ (Figure 6.8b).

Furthermore, the highest temperatures coincided with high irradiance; the activation state of Rubisco can be reduced under elevated temperature (Kobza and Edwards, 1987, Holaday, 1992) and the CO₂ compensation point is raised (Bowes, 1991). The latter is likely attributable to decreased specificity for CO₂ at increased temperatures (Bowes, 1991, Brookes and Farquhar, 1985), which may have also resulted in greater losses of CO₂ to photorespiration, and consequential reductions in $F_q'/F_{m'_{max}}$ and $F_q'/F_{m'}$ as the temperature increased (Vu et al., 1997).

Across the reef platform, *P. gymnospora* $rETR_{max}$ and $rETR$ was highest under high irradiance (Figure 6.7d and Figure 6.8g, respectively), most likely as a result of the increased light energy available for the production of adenosine triphosphate (ATP) to drive the light reactions (Holm-Hansen, 1970). $rETR_{max}$ and $rETR$ decreased during dark and low irradiance conditions (Figure 6.7d and Figure 6.8i, respectively), concurrent with the absent / decreased PAR. However, within aquatic systems, decreased pH (caused by elevated CO₂), may also restrict photochemical efficiency by disrupting the CO₂ accumulation pathway at the site of Rubisco, and / or interference with electron transport (Anthony et al., 2008, Sinutok et al., 2011, Price et al., 2011). It is likely, therefore, that the reduction in $rETR_{max}$ and $F_q'/F_{m'_{max}}$ observed in *P. gymnospora* on the reef flat, compared to those algae on the reef crest, may be due to the lower pH observed during the dark and low irradiance periods. These findings are similar to laboratory studies on other tropical calcified algae species (e.g. *Halimeda spp.*), which reported decreases in photochemical efficiency under high-CO₂ conditions (Gao and Zheng, 2010, Price et al., 2011, Sinutok et al., 2011).

6.7.3 Growth and abundance

Although there was no significant effect of location on the abundance of *P. gymnospora*, the decreased thallus size (and thus biomass) suggests a reduced growth of *P. gymnospora* on the more environmentally variable reef flat. The observed decrease in thallus size (and inferred reduced growth) may be as a result of cycles between

dissolution and calcification linked to the more variable environment associated with the reef flat. Thus, calcification may be more energetically costly on the reef flat, combined with exposure to conditions that may frequently promote dissolution of calcium carbonate (see also chapter 3). A decrease in biomass may restrict the ability of *P. gymnospora* to compete for space and light on the reef (McCook et al., 2001). Furthermore, calcifying macroalgae are some of the most significant reefal producers of biogenic calcium carbonate (Milliman and Muller, 1974) and organic matter, and are major contributors to primary productivity (Gattuso et al., 1997, Martin et al., 2006). Although *Padina sp.* can grow with no calcification under naturally acidified conditions (Johnson et al., 2012), calcifying macroalgae such as *P. gymnospora* contribute to reefal sediment formation (Whalan et al., 2012); a decrease in the growth of this significant contributor to both calcium carbonate and organic matter may thus alter sediment production and ecosystem dynamics on the reef platform.

6.7.4 Conclusions

This investigation shows that exposure to environmentally variable conditions analogous to those projected to occur under global climate change may result in altered energy allocation in *P. gymnospora* and highlights the important role phenotypic variation may play in the response of marine organisms to environmental conditions in the future. Algae on the reef flat may re-allocate energy to expensive mechanisms such as photo-protection, at the expense of photochemical efficiency and growth, suggesting that, while *P. gymnospora* may be able to survive under projected climate change, the physiological trade-off required to cope with the environmental conditions in the future may have significant negative ecological implications for tropical reef habitats. Furthermore, this study also highlights the advantages (albeit with some limitations previously highlighted in similar studies; Cigliano et al., 2010, Hall-Spencer, 2011, Johnson et al., 2012) of using an *in situ* ecosystem-based approach to understand the impact of global climate change on marine organisms with consideration of a natural ecosystem, and refine projections of biotic responses based on short-term laboratory and modelling experiments (Johnson et al., 2012, Wernberg et al., 2012).

7

Intraspecific differences in the response of cold water corals to climate change

Cold-water corals make up some of the most heterogeneous, biologically diverse, three-dimensional ecosystems known in the deep sea. However, due to the difficulty in accessing these habitats, to date there is little information about how these organisms may respond to global climate change. This study was carried out as part of the *Changing Oceans Expedition 2012* (James Cook cruise 073). I investigated protein composition in *Lophelia pertusa* from two environmentally different locations to determine whether their response to elevated temperature and $p\text{CO}_2$ would differ depending on their prior environmental experience.

7.1 Global climate change and cold-water corals

Cold-water coral growth is controlled by an interplay between specific physical dynamics including temperature, salinity, oxygen availability and local hydrodynamics (Dullo et al., 2008, Dorschel et al., 2007), coupled with biogeochemical dynamics including carbonate ion concentration and nutrients (Findlay et al., 2013, Findlay et al., 2014). Overall reef development is controlled by an interaction between local hydrography and sedimentary dynamics (Roberts et al., 2006). *Lophelia pertusa* requires temperatures between 4 - 13°C and salinities 35 - 38, with oxygen concentrations greater than 3 ml l⁻¹ in waters saturated with calcium carbonate (CaCO₃) (Dodds et al., 2007, Davies et al., 2008, Freiwald et al., 2004, Taviani et al., 2005).

7.1.1 Calcification and carbonate chemistry

The form of CaCO_3 used by corals is aragonite, the saturation state (Ω) of which is a key factor in coral calcification. As Ca^{2+} concentrations are generally 20-30 times that of CO_3^{2-} , and do not vary considerably, the saturation state of CaCO_3 is largely determined by changes in CO_3^{2-} (Wicks and Roberts, 2012). Therefore, the forecast changes in ocean carbonate chemistry as a result of ocean acidification (OA, decreasing ocean pH and CO_3^{2-} , as a result of increasing seawater $p\text{CO}_2$) may have significant implications for the survival of cold-water corals in the future. OA will affect the availability of CO_3^{2-} , and consequently aragonite availability used in the calcification process. In addition, many cold-water corals are found at high latitudes and deeper depths, areas that already exhibit a lower $\Omega_{\text{aragonite}}$ (Vierod et al., 2014, Guinotte et al., 2006, Steinacher et al., 2009). Models predict that the aragonite saturation horizon will become shallower with increasing OA, and it is anticipated that the majority of the cold-water coral reef habitats known today will be exposed to waters under saturated with respect to aragonite ($\Omega < 1$) by the end of the century (Guinotte et al., 2006). Thus, not only may the calcification process of cold water corals be hampered by the rapidly changing environmental conditions, but in addition, the crucial balance between processes that promote reef framework growth and processes that degrade the structure (bioerosion and dissolution) may be altered.

7.1.2 Calcification response to climate change

Calcification may be one of the most important physiological functions of corals, without which recruitment, growth and survival of coral reefs and associated community would be in jeopardy. As such, the response of calcification in cold-water corals to projected environmental change scenarios has been a priority for investigation. In general, cold-water coral calcification has shown resistance or a decrease in response to OA (McCulloch et al., 2012a, Maier et al., 2013a, Maier et al., 2013b, Hennige et al., 2014, Maier et al., 2009, Form and Riebesell, 2012). However, calcification rate is the result of the balance between energetic requirement and available resources; therefore maintenance of calcification under acidified conditions is likely to mean a deficiency in energy used to maintain other physiological functions. Hennige et al. (2014) found evidence of an energetic imbalance in *L. pertusa*, reporting a decrease in respiration rate but maintenance of calcification rate in response to ocean acidification, suggested to be facilitated by the utilisation of lipid reserves. However, Movilla et al. (2014b) found no

difference in organic matter, lipid content, skeletal microdensity or porosity in both *Desmophyllum dianthus* or *Dendrophyllia cornigera* in response to acidified conditions, despite a decrease, and no change, in growth rate (Movilla et al., 2014a, Movilla et al., 2014b). The high level of variability in the response of calcification in cold water coral in ocean acidification experiments suggests there may be other factors to consider in order to understand the effect of OA on cold-water corals (e.g. *in situ* natural environment and prior experience of experimental polyps). Despite resistance of coral calcification to acidified conditions in empirical studies, the low abundance of cold-water corals distributed below the aragonite saturation horizon (ASH) suggests the increased energetic demands of maintaining calcification under low $\Omega_{\text{aragonite}}$ (and elevated $p\text{CO}_2$) are not readily met under contemporary conditions (Hennige et al., 2014). Identification of key proteins that change in response to climate change may provide more information about the energetic requirements of cold water corals, and how corals may reallocate resources to prioritise particular physiological functions under acidified conditions.

7.2 Cold-water coral reefs and contemporary environmental conditions

It has been suggested that the prior environmental experience of an organism may influence its response to global climate change (e.g. coralline algae, Egilsdottir et al., 2013). Carilli et al. (2012) demonstrated that tropical corals subjected to larger year-to-year fluctuations in maximum ocean temperature were more resistant to warming events. In addition, Hennige et al. (2014) noted that respiration rates of freshly collected coral were higher than coral collected and acclimated to laboratory conditions for several months prior to experimentation. Therefore, it is likely that the same species of coral freshly collected from two environmentally different reefs may respond differently to elevated $p\text{CO}_2$ and temperature. In a recent study carried out at the same time as the present study (*Changing Oceans Expedition 2012 - RRS James Cook cruise 073*), Findlay et al. (2014) assessed the variability of nutrient and carbonate system dynamics across a range of temporal and spatial scales at the Mingulay Reef Complex and the Logachev carbonate mounds.

7.2.1 Mingulay Reef Complex

The Mingulay complex consists of a number of individual reefs and is the only known inshore *Lophelia* reef complex in UK waters. Located on the European continental

shelf, east of the outer Hebrides, Scotland (Figure 7.1), the reefs are a relatively shallow (120-190 m) complex that developed during the Holocene with the oldest coral from within the reef mounds dated at 7.68 ka (Douarin et al., 2014).

7.2.2 Logachev coral carbonate mounds

The flanks of the Rockall Bank, situated in the northeast Atlantic, approximately 400 km west of the Outer Hebrides, contain extensive cold-water coral reefs (Findlay et al., 2014, Roberts et al., 2003, van Weering et al., 2003). One such site is the Logachev coral carbonate mounds on the southwest flank of the Rockall bank (Figure 7.1). The reefs are deeper than those found at the Mingulay Reef Complex, ranging from 400-800 m. Major oceanic banks such as Rockall are distinctive in channeling major ocean currents along their flanks (Findlay et al., 2014, McGrath et al., 2012), and it is these hydrodynamic systems that enable the colonisation of cold-water coral reefs and development of carbonate mounds (Wilson, 1979, Roberts et al., 2003). Coral carbonate mounds, such as those at Logachev, are the result of successive periods of interglacial coral growth (Findlay et al., 2014), compared to the Mingulay Reef Complex which is formed from a 'single generation' Holocene accumulation (Roberts et al., 2006).

7.2.3 Environmental conditions

The key carbonate chemistry parameters for each site are summarised in Table 7.1. The seawater properties on the Mingulay Reef Complex were likely influenced by its close proximity to the coast and addition of freshwater run-off, and the Wyville-Thomson Overflow Water was identified below 700 m at Logachev (Findlay et al., 2014). Oxygen concentration decreases with depth; dissolved oxygen was 250.3-286.9 $\mu\text{mol L}^{-1}$ on the Mingulay Reef Complex compared to 206.1-268.2 $\mu\text{mol L}^{-1}$ on the Logachev coral carbonate mounds (Findlay et al., 2014). pH and $\Omega_{\text{aragonite}}$ were lower at Logachev than at Mingulay, and $p\text{CO}_2$ was greater at Logachev compared to Mingulay (Table 7.2) (Findlay et al., 2014). Findlay et al. (2014) also highlighted the variability in environmental conditions at each site; localised downwelling at Mingulay and upwelling at Logachev caused large fluctuations in dissolved inorganic carbon, pH and $\Omega_{\text{aragonite}}$. Findlay et al. (2014) suggest that cold-water corals are thriving in variable conditions at both Mingulay and Logachev that are traditionally considered unsuitable for marine calcifiers (i.e. low $\Omega_{\text{aragonite}}$).

Table 7.1 Environmental conditions in the surface water and reef-top water above the Mingulay Reef Complex and the Logachev coral carbonate mounds in May 2012.

	Mingulay (Surface 0-20 m)	Mingulay (Reef top 100–120 m)	Logachev (Surface 0-25 m)	Logachev (Reef top 795-845m)
Salinity	34.99±0.003	35.27±0.005	35.42±0.004	35.22±0.0004
Temperature (°C)	9.6±0.020	9.3±0.003	11.3±0.004	7.6±0.024
A_T ($\mu\text{mol kg}^{-1}$)	2303.4±0.8	2312.5±0.8	2313.1±1.1	2319.6±1.4
DIC ($\mu\text{mol kg}^{-1}$)	2079.0±1.0	2117.4±1.6	2119.1±1.7	2170.1±3.5
pH	8.140±0.0027	8.074±0.0036	8.041±0.004	7.988±0.007
$p\text{CO}_2$ (μatm)	309.0±2.2	365.5±3.4	405.7±4.7	405.8±6.4
$\Omega_{\text{aragonite}}$	2.40±0.01	2.09±0.01	2.13±0.01	1.53±0.02

Mean±SE measured values include salinity, temperature, total alkalinity (A_T) and dissolved inorganic carbon (DIC); and calculated values using CO2SYS for *in situ* pH, $p\text{CO}_2$ and aragonite saturation state ($\Omega_{\text{aragonite}}$). All values were obtained from the British Oceanographic Data Centre (BODC); (Findlay, 2013, Findlay and Woodward, 2013) published in (Findlay et al., 2014, Hennige et al., 2014).

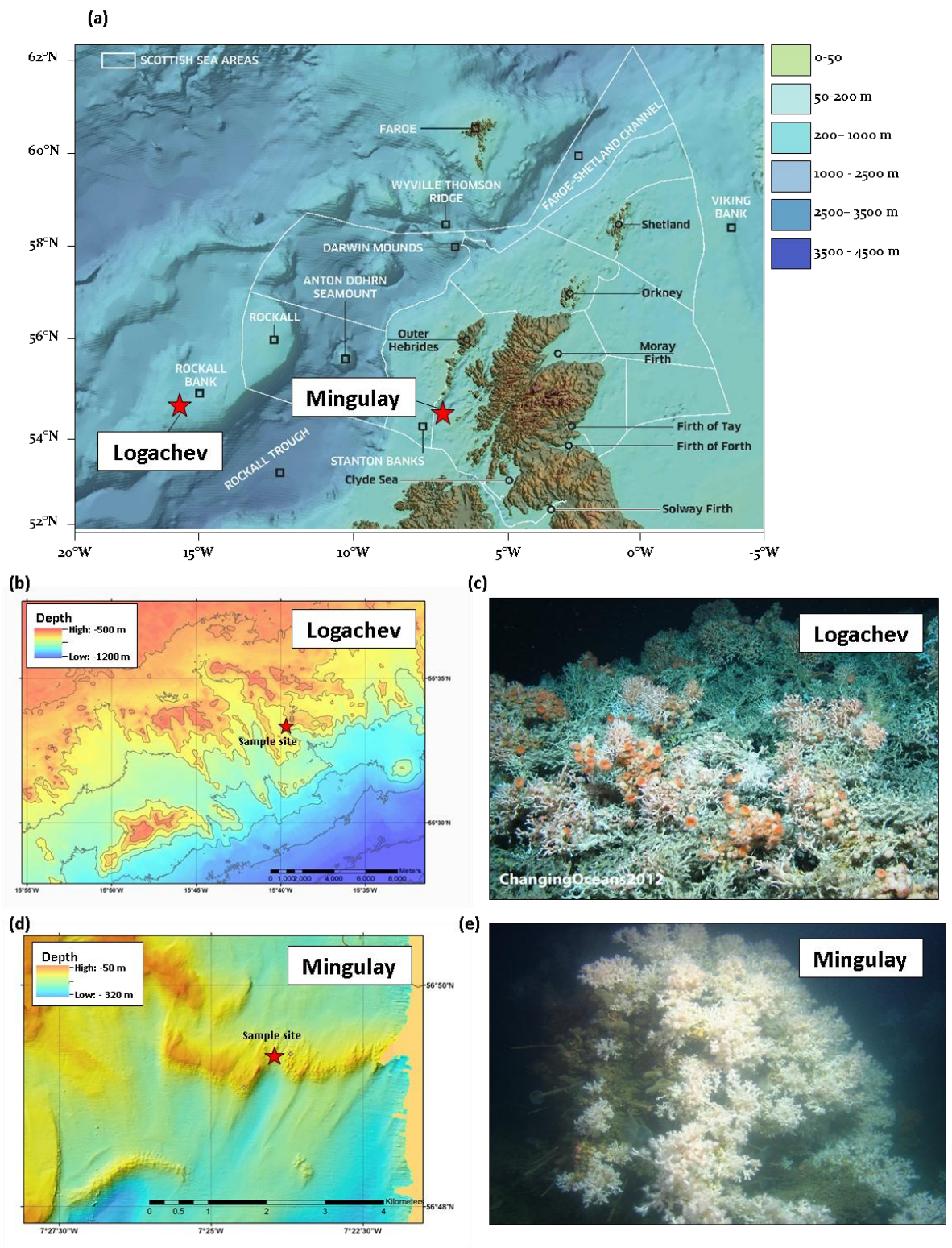


Figure 7.1 Map and example habitats of the sites from which *Lophelia pertusa* was sampled in the northeast Atlantic during the 'changing oceans' expedition 2012 (a) map (adapted from Scotland's Marine Atlas (Baxter et al., 2011)), showing the location of the sample sites: Mingulay Reef Complex and Logachev; (b) bathymetric map of the Logachev area (produced using ArcGIS 9, ESRI), highlighting the location of the fine scale sample sites; (c) example of the large coral carbonate mounds topped with large *Lophelia pertusa* structures at Logachev; (d) bathymetric map of the Mingulay Reef Complex (produced using ArcGIS 9, ESRI), highlighting the location of the fine scale sample sites; (e) example of a shallower *L. pertusa* reef at the Mingulay Reef Complex. Photographic images were taken during the Changing Oceans Expedition 2012 (RRS James Cook cruise 073). Images b and d courtesy of Herriot-Watt University.

7.3 Aims of this chapter

This chapter aims to investigate intraspecific differences in *Lophelia pertusa* collected from two environmentally different sites in response to short term exposure to elevated temperature and $p\text{CO}_2$. The study aims to improve our understanding of the high level of variability between cold water coral climate change experiments and suggest how prior experience may influence the response of marine organisms to elevated temperature and $p\text{CO}_2$.

It was hypothesised that there would be a difference in total protein concentration and protein profile in response to elevated temperature and $p\text{CO}_2$, and a difference in response of coral from each location. The coral collected from Logachev is hypothesised to cope better under elevated $p\text{CO}_2$ due to pre-exposure *in situ* to higher $p\text{CO}_2$ and lower pH compared to coral collected from Mingulay.

7.4 Methods

7.4.1 Sample collection

Lophelia pertusa colonies were collected from the Logachev reef complex (55° 29.64 N, 15° 49.59 W) from depths ranging between 800-844 m, and Area 1 within the Mingulay reef complex (56° 49.38 N, 7° 22.56 W) from depths between 135-140 m (Roberts et al., 2005, Roberts et al., 2009), during the 'Changing Oceans Expedition' on the *RRS James Cook* cruise 073 (May-June 2012). Key carbonate chemistry parameters from both the Mingulay Reef Complex and Logachev coral carbonate mounds are described in Table 7.1 (Findlay and Woodward, 2013, Findlay, 2013). Coral samples were obtained using the *Holland-1* remotely operated vehicle (ROV) using a grab and live video feed (Figure 7.2). Coral samples were acclimated to laboratory conditions for 2 days prior to starting the experiments in a holding tank maintained at ambient seabed temperature (9°C), which was sufficient for physiological stability in the control treatment, as demonstrated by Hennige et al. (2014). During collection, coral samples were consistently taken from the top of the sampled colonies to ensure that relatively young polyps were used during the experiment, as polyp age impacts physiology (Maier et al., 2009). After the acclimatisation period, corals were carefully fragmented into smaller pieces for the experiment. The fragments consisted of 3-5 polyps. The fragments were attached to pre-labeled bases made of PVC pipe with Grotech Korafix epoxy (Figure 7.3b).

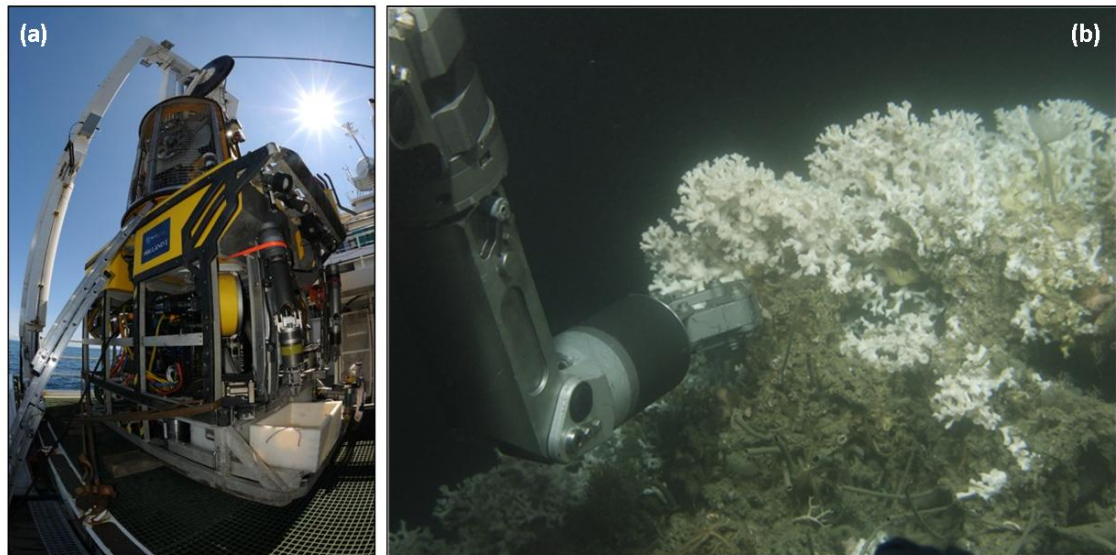


Figure 7.2 The *Holland-1* remote operated vehicle (ROV)
 (a) The ROV onboard the *RRS James Cook* (cruise 073) during the *Changing Oceans Expedition 2012* (b) The grab attached to the ROV collecting samples of *L. pertusa*, and photograph is a screen shot from the live feed HD video camera used to locate the coral colonies. Photographic images were taken during the *Changing Oceans Expedition 2012* (*RRS James Cook* cruise 073).

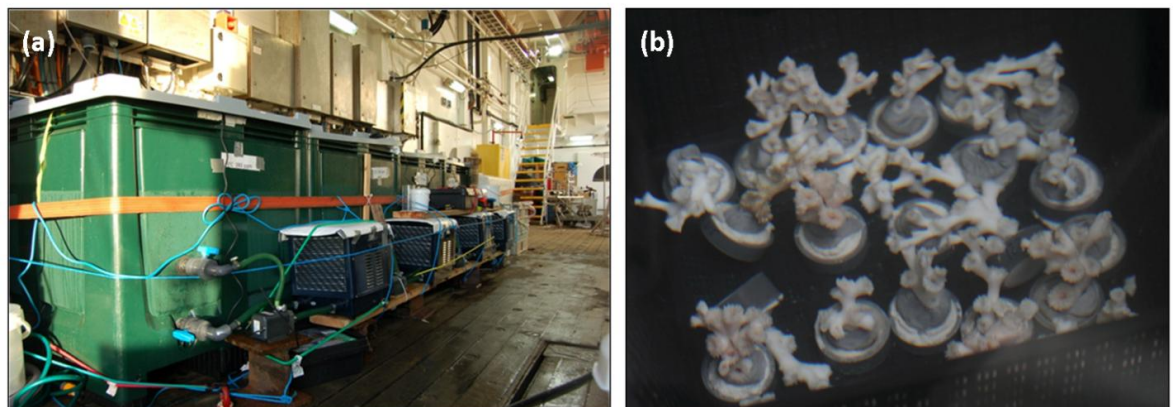


Figure 7.3 Experimental tanks and potted coral fragments on board the *RRS James Cook* (cruise 073) during the *Changing Oceans Expedition 2012*.
 (a) The experimental tanks on the deck of the *RRS James Cook* (b) *L. pertusa* coral fragments potted in labelled bases made of PVC pipe with Grotech Korafix epoxy. Photographic images were taken during the *Changing Oceans Expedition 2012* (*RRS James Cook* cruise 073).

7.4.2 Experimental set-up

Five colonies of *L. pertusa* were identified from each population (Mingulay and Logachev) and fragments from individual colonies were split between one of four treatments to prevent colony pseudo-replication within treatments. The experimental period was 21 days (Mingulay) and 14 days (Logachev), with samples collected at T7, T9, T14 and T21 (where T \emptyset was day zero). The four treatments were nominally; (1) ambient *in situ* temperature (9 °C) at 380 μ atm $p\text{CO}_2$ (control, *t*, 380), (2) ambient temperature +3°C at

380 $\mu\text{atm } p\text{CO}_2$ (temperature treatment, $t+3$, 380), (3) ambient temperature at 750 $\mu\text{atm } p\text{CO}_2$ ($p\text{CO}_2$ treatment, $t,750$), and (4) ambient temperature +3 °C at 750 $\mu\text{atm } p\text{CO}_2$ (multiple stressor treatment, $t+3$, 750). These $p\text{CO}_2$ and temperature conditions were chosen to simulate contemporary environmental conditions and those predicted for 2100 (IPCC, 2013). Prior to the start of the experiment one polyp from each fragment, used in the experiment, was removed and immediately frozen in liquid nitrogen to obtain $T\emptyset$ total protein information. Four 600 l incubation tanks were fitted with external power-head pumps (EHEIM Universal 1260) and chillers (Aqua-Medic Titan 500) to maintain water temperature at ambient reef temperature and + 3 °C (Figure 7.3a). Once corals had been added to experimental tanks, the temperature elevated treatment tanks was ramped by 1°C every other day until 12 °C was reached. Water was circulated in each tank using submerged power-head pumps (EHEIM Universal 1260). Air enriched with CO_2 was bubbled into the elevated CO_2 treatments, controlled using gas mixing pumps (H. Wösthoff Messtechnik GmbH, Bochum, Germany) and monitored by a LiCor 820 gas analyser (see chapter 2). Ambient salinity was maintained (~35) throughout the experimental period. Every other day, a ~50% water change was conducted on each of the treatment tanks. Natural seawater for water exchanges in the experimental tanks was pumped from deep water (40 – 50 m depth) by means of a deep sea water pump (KPZ GmbH), which was attached to a CTD (conductivity, temperature, depth gauge) frame.

7.4.3 Experimental carbonate chemistry

The pH was recorded four times daily, measured using a pH meter (Sevengo, Mettler Toledo). These data were checked independently by calculated carbonate chemistry data from total alkalinity (A_T) at set time points, and from measured CO_2 gas inputs (LiCor-820, see chapter 2). Collection of samples for A_T were collected and analysed as detailed in chapter 2. Salinity and temperature were also measured four times daily using a hand-held conductivity meter (Pro 2030, YSI, Ohio, USA). Carbonate parameters were calculated from A_T , $p\text{CO}_2$ salinity and temperature using CO2SYS as detailed in chapter 2.

7.4.4 Protein extraction and solubilisation

Samples of *L. pertusa* were frozen immediately in liquid N_2 upon collection and kept frozen at -20°C until analysis. *L. pertusa* samples were processed in accordance with

methods described in Chapter 2 (section 2.3.1.3 (extraction method 3) in preparation for the 1D gels used to fractionate the proteins. However, due to the developmental nature of the present study with regards to the protein extraction solubilisation an earlier method was used to solubilise the proteins prior to mass spectrometry analysis (chapter 2).

7.4.4.1 Protein identification and visualisation

1D polyacrylamide gels were used for analytical separation of the proteins (see Chapter 2, section 2.3.2); gels were stained using Coomassie Brilliant Blue (see section 2.3.2.1.). Proteins were excised from the gel and subjected to in-gel trypsin digestion and mass spectrometry analysis for protein identification (see section 2.3.2.3).

7.4.5 Total protein

To extract proteins, 1-2 polyps of *L. pertusa* (~0.5g) was ground directly in sodium dodecyl sulphate (SDS) (Invitrogen, UK, 0.5 ml) using an automated sample grinder (Retsch MM400, Haan, Germany) as detailed in Chapter 2, section 2.3.1.3 (extraction: method 3). Total protein concentration was then determined spectrophotometrically, as previously described by Bradford (1976) and detailed in chapter 2.

7.4.6 Statistical analysis

Two-way repeated measure ANOVAs were used to investigate differences in total protein concentration, between coral exposed to a control treatment (*t*, 380), elevated temperature (*t*+3, 380), elevated *p*CO₂ (*t*, 800) and a combined treatment (*t*+3, 800) in fragments from both Logachev and Mingulay reef complexes. Differences between means / medians were considered to be significant when $p \leq 0.05$. All analyses were conducted with SPSS v18.0.

7.5 Results

7.5.1 Environmental parameters

The experimental conditions for each treatment are summarised in Table 7.2.

Table 7.2 Environmental conditions in experimental tanks on board the *RRS James Cook* (cruise 073) during the *Changing Oceans Expedition 2012*.

Parameter	Treatment			
	<i>t</i> , 380 (control)	<i>t</i> +3, 380 (high temperature)	<i>t</i> , 800 (high CO ₂)	<i>t</i> +3, 800 (combined)
Temperature (°C)	9.06±0.02	12.30±0.10	8.90±0.11	12.30±0.02
Salinity	35.3±0.02	35.4±0.03	35.2±0.08	35.4±0.05
A _T (μmol kg ⁻¹)	2197±34.9	2170±57.3	2299±8.52	2277±27.0
DIC (μmol kg ⁻¹)	2031±30.5	1986±49.5	2227±7.86	2189±24.8
pH	8.03±0.01	8.02±0.01	7.76±0.00	7.76±0.00
pCO ₂ (μatm)	396±2.08	396±2.08	817±2.49	817±2.49
Ω _{aragonite}	1.82±0.05	2.01±0.10	1.09±0.01	1.30±0.04

Mean±SE values of measured temperature, salinity, total alkalinity (A_T) and pCO₂, and derived dissolved inorganic carbon (DIC), pH, and aragonite saturation (Ω_{aragonite}) for treatments; *t*, 380 (control), *t*+3, 380 (high temperature), *t*, 800 (high CO₂), *t*+3, 800 (high temperature combined with high CO₂), whereby, *t*= ~9°C, *t* + 3 = ~12°C, at 800 or 380 μatm pCO₂

7.5.2 Total protein

7.5.2.1 Mingulay Reef Complex

Total protein in *Lophelia pertusa* significantly increased in response to elevated pCO₂ (F_{1,4} = 11.647, p = 0.027, Figure 7.4), although there was no effect of time or elevated temperature on total protein concentration (F_{3,12} = 0.422, p = 0.740, F_{1,4} = 0.653, p = 0.464, respectively). TØ measurements of total protein concentration in *L. pertusa* were similar across all colonies (F_{1,19} = 0.041, p = 0.842). All colonies responded to the experimental conditions by increasing total protein concentration in the first 7 days, after which the total protein in coral fragments in the control (*t*, 380) and elevated temperature treatment (*t*+3, 380) were similar for the duration of the experiment. Fragments in the elevated pCO₂ treatment (*t*, 800) increased total protein until day 9, after which total protein decreased. Coral in the combined treatment increased total protein concentration until day 14, after which total protein decreased, although it was still at higher concentration than that observed in the control (Figure 7.4).

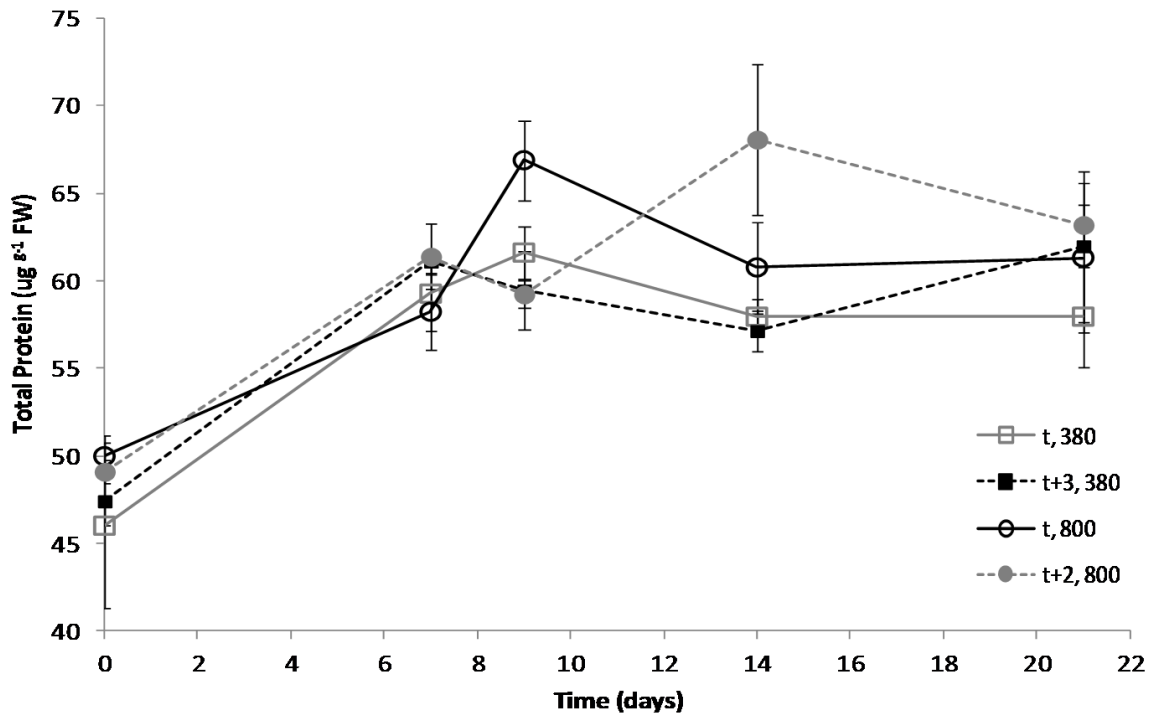


Figure 7.4 The effect of elevated temperature and $p\text{CO}_2$ on total protein ($\mu\text{g g}^{-1}$ (fresh weight) FW^{-1}) in *Lophelia pertusa* collected from the Mingulay Reef Complex over 21 days. $\text{mean} \pm \text{SE}$; where t = ambient temperature at time of collection (9°C), $t+3$ = ambient temperature + 3°C , at either $p\text{CO}_2$ 380 or 800 μatm .

7.5.2.2 Logachev coral carbonate mounds

$T\emptyset$ measurements of total protein concentration in *Lophelia pertusa* were similar across all colonies ($F_{1,19} = 1.235$, $p = 0.283$), after which total protein in *L. pertusa* significantly decreased over time in coral fragments in all treatments ($F_{1,4} = 11.534$, $p = 0.027$, with exception to the control (t , 380). After an initial increase observed on day 9, total protein decreased to values similar to $T\emptyset$ concentrations. Total protein in the fragments exposed to the control treatment was similar at each sample point throughout the 14 day experimental period. There was no change in total protein in response to elevated temperature or $p\text{CO}_2$ ($F_{3,12} = 4.474$, $p = 0.102$, $F_{1,4} = 0.548$, $p = 0.500$, respectively).

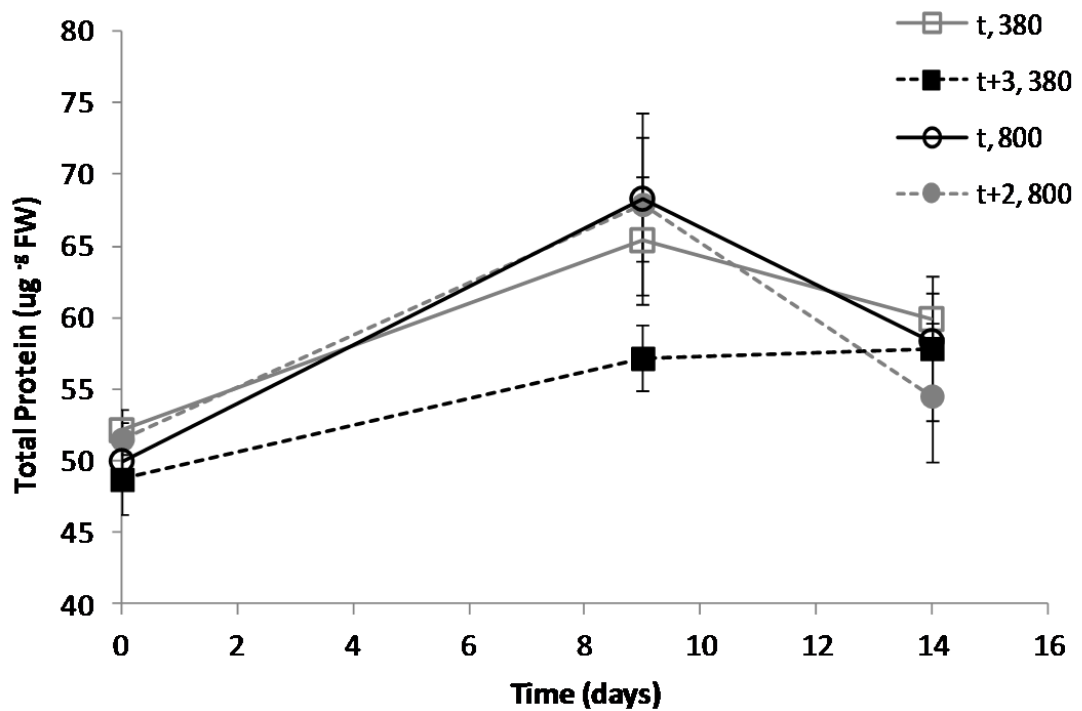


Figure 7.5 The effect of elevated temperature and $p\text{CO}_2$ on total protein ($\mu\text{g g}^{-1}$ (fresh weight) FW^{-1}) in *Lophelia pertusa* collected from the Logachev coral carbonate mounds over 14 days. $\text{mean} \pm \text{SE}$; where t = ambient temperature at time of collection (9°C), $t+3$ = ambient temperature + 3°C , at either $p\text{CO}_2$ 380 or 800 μatm .

7.5.3 Protein identification and visualisation

Proteins were identified by mass spectrometry. However, there was an inconsistency between the actual molecular weight of the identified protein and the location from which the protein was excised from the gel (i.e. molecular weight of the identified protein based on its location on the gel). This can occur for a variety of reasons; (1) coincidental peptide matches occur, due to randomly similar peptide (2) peptide fragment masses (3) proteins bound to other protein complexes (4) many proteins have very similar sequences. Therefore, due to uncertainty in protein identifications the gels were qualitatively examined to assess differences in the protein profile of each colony in response to elevated $p\text{CO}_2$ and temperature (Figure 7.6), although no specific protein species could be assigned to the bands.

7.5.3.1 Protein profile

The protein profile of polyps from each colony from both Mingulay and Logachev changed over time and in response to elevated temperature and $p\text{CO}_2$. Proteins in the molecular mass range 3-198 kDa were visualised (Figure 7.6).

7.5.3.1.1 Mingulay Reef Complex

The protein profile of polyps from Mingulay in the control treatment remained very similar over the 21 day exposure period. There were differences in proteins in the low molecular weight (<14 kDa) area of the gel at each time point (Figure 7.6). A 28 kDa protein was more defined under the combined treatment after 14 days, although after 21 days this protein was barely visible in any treatment. Differences in protein intensity were also observed in the proteins with molecular weights ranging 60-80 kDa; band intensity increased, compared to the control, after 9 days. In addition, the protein at 140 kDa appeared more defined in response to elevated $p\text{CO}_2$ and temperature compared to the control after 7 days, it then appeared in response to the combined treatment after 9 and 14 days, although was barely visible after 21 days in the combined treatment. After 21 days protein production decreased across all the treatments in coral, although there appeared to be more differences between the protein profiles across the treatments compared to the other time points (Figure 7.6a).

7.5.3.1.2 Logachev coral carbonate mounds

The protein profile of polyps from Logachev in the control treatment remained very similar over the 14 day exposure period, although there were more bands in the profile after 14 days compared to the profile after 9 days (Figure 7.6b). After 9 days the protein profile of coral in the elevated $p\text{CO}_2$ treatment (t, 800) showed fewer (or very diffuse bands) compared to the other treatments, however more distinct proteins were observed after 14 days exposure (Figure 7.6b). There was more variability in the protein profile in polyps from Logachev compared to those from Mingulay, and more variability over time (Figure 7.6b). Intensity of the protein at ~28 kDa increased under elevated $p\text{CO}_2$ after 9 days and 14 days, although this protein was barely visible in coral under elevated temperature and the combined treatment. Changes to proteins in the molecular weight range 60-80 kDa were also observed, and the intensity of the proteins was less compared to Mingulay after 14 days. Also, the protein at 140 kDa in coral from Logachev was more defined in response to elevated temperature.

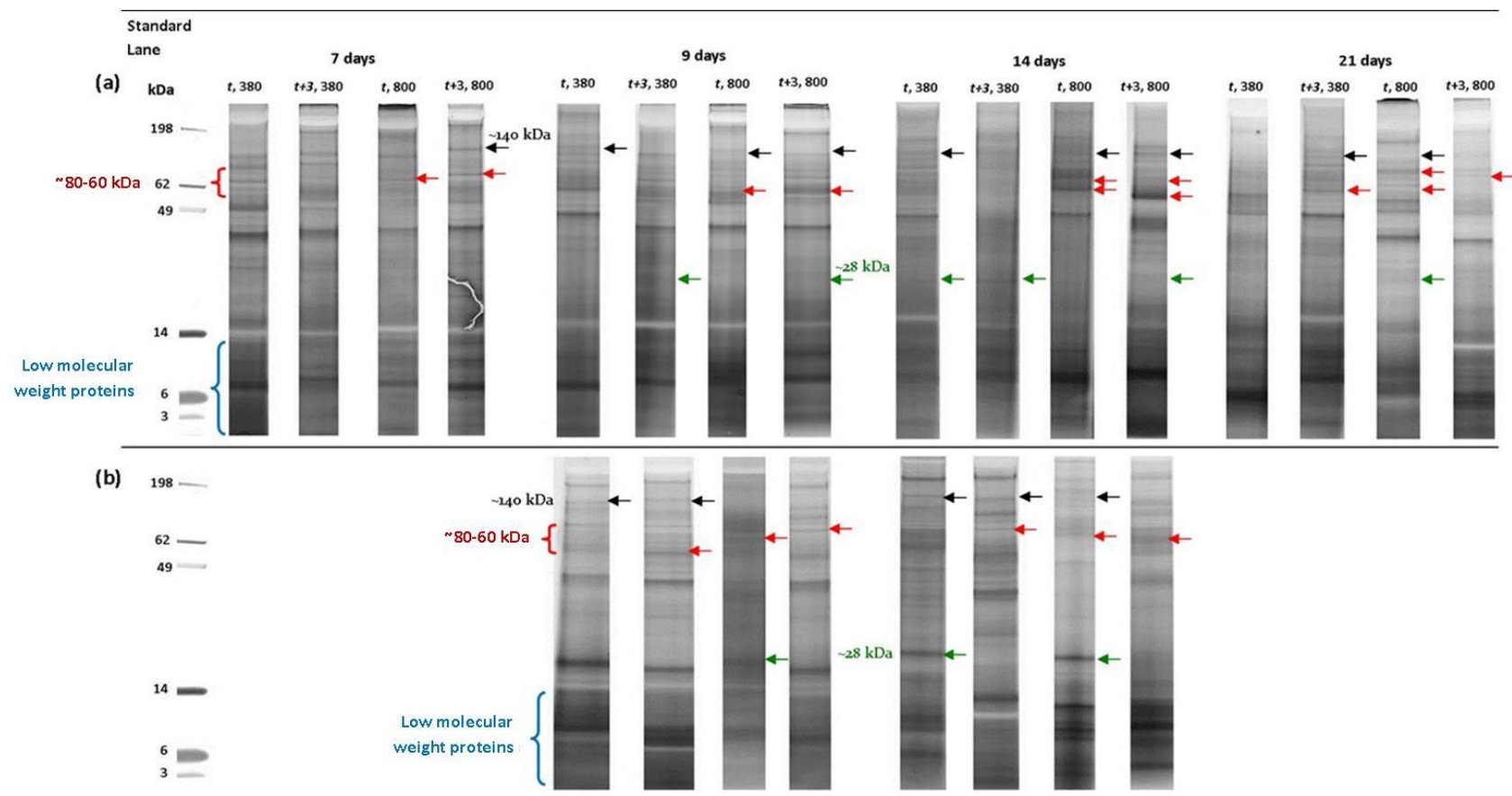


Figure 7.6 The effect of elevated pCO_2 and temperature on the protein profile of one colony from the Mingulay Reef Complex and one colony from the Logachev coral carbonate mounds over 21 days and 14 days, respectively.

Bis-Tris 4 12% Gel of stained with Coomassie staining. Left to right: Pre-stained standard of known molecular weights indicated by values (kDa), thereafter, the protein profiles displayed are from polyps from the same colony and each lane represents a polyp exposed to each of the four different treatments at each of the sampled time points. (a) A colony from the Mingulay Reef Complex (b) A colony from the Logachev carbonate mounds. t = ambient temperature at time of collection (9°C), $t+3$ = ambient temperature + 3°C , at either pCO_2 380 or 800 μatm . Specific differences are indicated by a triangle or asterisk, see 'results' (section 7.6.3) for details.

7.6 Discussion

Driven by large hydrodynamics, it has been suggested that the natural fluctuations in the physicochemical conditions (including oxygen, carbon, nutrients and food supply) found at the Mingulay Reef Complex and the Logachev coral carbonate mounds, may provide flexibility for these cold-water corals, increasing their potential for adaptation to survive changing environmental conditions (Findlay et al., 2014). This link between prior environmental experience and response to surviving changing conditions has previously been described in tropical corals (Carilli et al., 2012) and marine calcifying algae (Raven, 2011, Egilisdottir et al., 2013), although there is also evidence to suggest that this may not always be the case (Noisette et al., 2013b). The present study provides evidence to suggest that the response of cold-water corals to elevated temperature and $p\text{CO}_2$ may differ in polyps from two environmentally distinct locations. Intraspecific differences in the response of corals from different locations may also explain the high levels of variability found in cold-water coral ocean acidification experiments and suggests natural environmental conditions should be considered for control conditions during empirical studies and interpretation of results. Particularly, as several recent studies have reported cold-water corals are able to continue calcifying under elevated $p\text{CO}_2$ and low $\Omega_{\text{aragonite}}$ (Maier et al., 2013a, Maier et al., 2013b, McCulloch et al., 2012a).

7.6.1 Protein concentration

Results of the present study suggest a 'shock reaction' in polyps from both Mingulay and Logachev, with an increase in protein concentration across all treatments between T_0 and 7 days or 9 days, respectively (Figure 7.4 Figure 7.5). This response is likely to be due to the collection process; interestingly the response was similar in corals from both locations, as was T_0 total protein concentration, despite the difference in depth and environmental conditions between Logachev and Mingulay. Elevated temperature and $p\text{CO}_2$ did not have a significant effect on total protein concentration in coral from the Logachev carbonate mounds, although total protein did differ significantly between time points, with a decrease after 14 days to levels similar to those measured at T_0 (Figure 7.5). In contrast, *L. pertusa* from the Mingulay Reef Complex significantly increased total protein in response to elevated $p\text{CO}_2$, although the response of coral in each treatment differed slightly at each time point (Figure 7.4). Differences in *L. pertusa* physiology between short (24 h) and longer-term (months) experiments has also been

noted by Form and Riebesell (2012); by which the response to acidified conditions observed after 24 h was different to that observed after several months. It is likely that the differences in response of total protein over time is linked to the process of acclimatisation of the coral to the experimental conditions (e.g. adjustment of metabolic pathways). Hennige et al. (2014) reported a two-week period was observed before any noticeable differences in respiration were observed between *L. pertusa* in control and acidified conditions. Likewise, the present study observed no difference in response to elevated temperature or $p\text{CO}_2$ in *L. pertusa* from Logachev over 14 days. Continued exposure to elevated $p\text{CO}_2$ and temperature may have yielded a different response, although, interestingly, coral from Mingulay did exhibit a significant response (in terms of total protein concentration) to elevated $p\text{CO}_2$ after only 9 days exposure. Although no effect of elevated temperature or $p\text{CO}_2$ was observed in coral from Logachev, the present study suggests that there may have been a change in the protein profile (Figure 7.6), suggesting different proteins may have been up and/ or down regulated in response to acidified conditions and elevated temperature, while overall protein concentration was not affected. This may be due to a change in energetic requirements of different physiological functions, reallocation of resources or changing metabolic pathways (e.g. Hennige et al., 2014).

7.6.2 Proteins and physiological functions

The present study demonstrated changes in total protein concentration and the protein profile of *Lophelia pertusa* in response to elevated temperature and $p\text{CO}_2$. This suggests that the coral is making molecular level changes to cope with the experimental environment. Scleractinian corals can up-regulate pH at the site of calcification enabling corals to raise the saturation state of their calcifying medium, thus increasing or maintaining calcification even in seawater that may be undersaturated with regards to aragonite (McCulloch et al., 2012a). This process is driven by the enzyme Ca^{2+} ATPase, which pumps Ca^+ ions from the calciblastic cells into the calcifying space in exchange for H^+ ions (Allemand et al., 2004, Cohen and McConnaughey, 2003). Therefore, if cold-water corals employ this mechanism, an increase in concentration and/ or activity of this enzyme may occur under increasingly acidified conditions. In the present study a ~140 kDa protein (molecular weight of Ca^{2+} ATPase) generally appeared more defined (i.e. increased concentration) in polyps from Mingulay under the elevated $p\text{CO}_2$ treatments (Figure 7.6a). In contrast, the polyps from Logachev only exhibited a protein at ~140 kDa

under elevated $p\text{CO}_2$ (t , 800) after 14 days, although the protein was present in both the control and elevated temperature treatments after both 9 and 14 days. However, protein presence and absence or relative intensity only gives an indication of the relative concentration of a protein and not activity; further work is required to identify Ca^{2+} ATPase in *Lophelia pertusa*, and the assessment of its activity in response to acidified conditions would provide more detail on the mechanisms employed by the cold-water coral to maintain calcification under elevated $p\text{CO}_2$.

Biominerals contain both organic and inorganic components. Collectively termed the organic matrix, the organic components are reported to play a crucial role in biomineralisation (Tambutte et al., 2007). Puvarel et al. (2007) were able to detect the presence of low molecular mass matrix components (<5 kDa) in azooxanthellate corals and suggested that these low molecular weight components were likely peptides involved in the regulation of coral skeleton mineralisation. In the present study, the protein profiles of coral from both Mingulay and Logachev suggest several changes in concentration and presence/ absence of low molecular weight proteins in response to elevated temperature and $p\text{CO}_2$, which may suggest the involvement of these low molecular weight components in key physiological functions (i.e. organic matrix and calcification). However, further work would be required to confirm this, particularly as peptide fragments masses are also likely to occur in the low molecular weight area of the gel. In addition, invertebrate organic matrix proteins have biochemical features (i.e. acidic proteins) which can make their characterisation more difficult (Gotliv et al., 2003). Tambutté et al. (2007) were able to demonstrate the presence of carbonic anhydrase in the organic matrix as well as the tissue of the azooxanthellate coral, *Tubastrea aurea*. Carbonic anhydrase catalyses the interconversion of CO_2 and bicarbonate (Fabry et al., 2008), and can play an important role when carbon is limited. The role of carbonic anhydrase in the interconversion of CO_2 means that this enzyme is crucial to coral calcification, and activity and expression are likely to change in response to elevated temperature and $p\text{CO}_2$. Indeed, Moya et al. (2013) demonstrated a decrease in the expression of a large number of genes encoding carbonic anhydrases in nonsymbiotic coral juveniles in response to elevated $p\text{CO}_2$. Moya et al. (2013) suggests that there may be a reduced requirement for carbonic anhydrase activity in extracellular calcifying medium and in the calciblastic cell under acidification to maintain appropriate pH at the

calcification site. In contrast, carbonic anhydrase was up-regulated in adult coral, *P. damicornis*, exposed to acidified conditions for three weeks. In the present study, a ~28 kDa protein (molecular weight of carbonic anhydrase) appears more defined (increased concentration) in response to elevated temperature and $p\text{CO}_2$ compared to the control, in coral from Mingulay. In contrast, the protein at 28 kDa appears less defined (decreased concentration) in response to elevated $p\text{CO}_2$ and temperature compared to the control in coral from Logachev. Carbonic anhydrase is a key enzyme during biomineralisation in cold water corals (Figure 7.7). An increase in concentration may suggest an increase in calcification rate. Indeed, calcification has been shown to increase in response to acidified conditions (and low $\Omega_{\text{aragonite}}$) in *L. pertusa* (Maier et al., 2009, Form and Riebesell, 2012). This response is most likely attributed to the corals ability to control pH at the site of calcification, increasing the carbonate saturation state of the calcifying fluid, thus promoting calcification despite the external environmental conditions (McCulloch et al., 2012a, McCulloch et al., 2012b).

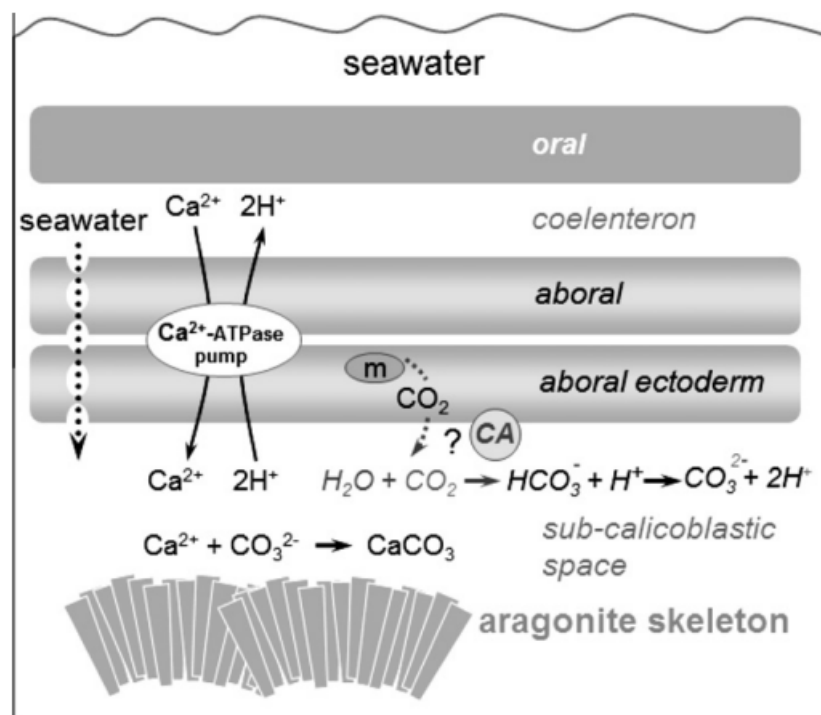


Figure 7.7 Schematic of the calcification process in azooxanthellate cold-water corals Taken from (McCulloch et al., 2012b). Removal of protons from the calcification site occurs primarily via Ca^{2+} -ATPase exchangers that pump 2H^+ ions from the calcifying medium into the coelenterons in exchange for each Ca^{2+} ions. The carbonic anhydrases (CA) catalyse the forward reactions converting seawater derived HCO_3^- into CO_3^{2-} ions (Moya et al., 2008), the latter being essential for calcification. Due to the greater pH_{cf} in azooxanthellate corals (see discussion), it is likely that diffusion of CO_2 into the sub-calicoblastic space is minimal and thus the DIC of the calcifying fluid is similar to that in seawater (Erez, 2003).

Corals are known to induce heat shock proteins in response to environmental stressors (Chow et al., 2009). Heat shock protein expression is increased when cells are exposed to environmental stressors and they play an important role in cellular repair and protective mechanisms; key in enabling proper protein folding and complex assembly; prevent protein aggregation and regulate stress-induced cell apoptosis (Chow et al., 2009, Bukau and Horwich, 1998). Heat shock proteins can help corals survive conditions that may otherwise be lethal (Kregel, 2002). Indeed, Cummings et al. (2011) determined an increase in heat shock protein HSP70 gene expression in response to changes in seawater $p\text{CO}_2$ in the Antarctic bivalve, *Laternula elliptica*, and it has been suggested that heat shock proteins may increase thermal robustness of fertilization in marine invertebrates (Parker et al., 2009). In addition, sublethal responses to stress, such as the expression of heat shock proteins, can be used as biomarkers for an early indication of physiological stress caused by environmental change (Byrne, 2011). In the present study there are various proteins on the profile of the coral from both Logachev and Mingulay between ~80-60 kDa (the molecular weight of HSP80, 70 and 60) that appear up-regulated in response to elevated $p\text{CO}_2$ and temperature. Although additional work is required to confirm the expression of heat shock proteins in *Lophelia pertusa* in response to climate change, this may provide evidence of the reallocation of energy in the coral from both sites in response to stressful conditions (i.e. elevated temperature and $p\text{CO}_2$). Heat shock proteins may facilitate the continuation of physiological functions in the short term, however, prolonged exposure and continued requirement for expression of these proteins may impact coral physiology in the long term.

7.6.3 *In situ* environment and response of coral to elevated temperature and $p\text{CO}_2$

Differences in the fine-scale nutrient and carbonate system dynamics between the Mingulay Reef Complex and the Logachev carbonate mounds (as reported by Findlay et al., 2014) may offer an explanation as to the intraspecific differences in the short term response of the cold water coral, *Lophelia pertusa*, to elevated temperature and $p\text{CO}_2$. Indeed, there is evidence to suggest prior exposure can influence the ability of tropical coral to withstand heat stress (Carilli et al., 2012), although survival in tropical coral is tightly linked to the coral symbiont. Thermal acclimation capacity has also been suggested to underlie the susceptibility of other marine invertebrates to increasing global temperature (Stillman, 2003). In the present study coral collected from the Mingulay

Reef complex responded differently to elevated temperature and $p\text{CO}_2$, compared to coral collected from the Logachev carbonate mounds. There is environmental variability at both sites, however, it is suggested that the prior experience of corals from Logachev to lower fluctuations in pH and $\Omega_{\text{aragonite}}$ and increased $p\text{CO}_2$ may mean that corals are better able to cope with the projected climate change scenarios. Egilsdottir et al. (2013) demonstrate calcareous alga from tidal pools, where $p\text{CO}_2$ fluctuates over diel and seasonal cycles, is relatively robust to acidified conditions compared to other subtidal calcareous algae. Similarly, species from hydrothermal vents, where organisms can experience high fluctuations in $p\text{CO}_2$, can have high activities of carbonic anhydrase relative to species from shallower more stable environments (Fabry et al., 2008). The intraspecific variability observed in corals from different reefs in response to climate change may also help explain the high variability found in cold water coral ocean acidification experiments, suggesting *in situ* conditions should be considered during empirical studies in the future. Indeed, Hennige et al. (2010) demonstrated substantial intraspecific variability in tropical coral physiology between corals under different environmental conditions. In addition to the environment, the genetic diversity within the reef may also influence the coral's ability to adapt to changing conditions. The coral carbonate mounds at Logachev are a result of successive periods of interglacial coral growth (Findlay et al., 2014), compared to the Mingulay Reef Complex which was formed from a single generation Holocene accumulation (Roberts et al., 2006). Therefore, depending on recruitment, there may be differences in the genetic diversity of coral reefs (i.e. one huge colony vs. many different colonies), which may influence the ability of coral to adapt to the changing conditions.

7.6.4 Conclusions

Cold water coral reefs make significant contributions to biodiversity in the deep sea, benefit commercial fisheries and have significant value as paleoclimatic resources. These benefits mean that the response of these coral reefs to global climate change has implications for the local and global economic, political and social development and sustainability. Thus far the response of cold water corals in ocean acidification experiments has been highly variable. The present study provides evidence of intraspecific variability in the response of cold water corals to global climate change that may be dependent upon their prior environmental experience. Although more work is required to specifically identify how the corals may reallocate resources and prioritise

particular physiological functions under elevated temperature and $p\text{CO}_2$, the present study provides evidence of molecular level changes that may be early indicators of physiological stress compared to whole organism measurements.

8

Discussion and conclusion

The oceans are one of the world's most valuable assets. In addition to providing habitats for a vast range of organisms, and food and income for millions of people worldwide, the oceans are also a major carbon sink and have regulated the Earth's climate for thousands of years. Now the Earth's climate is changing at an unparalleled rate due to the increasing anthropogenic use of fossil fuels and widespread deforestation. This means that the oceans are absorbing more carbon dioxide than they have in the last 650, 000 years causing ocean acidification; decreasing ocean pH as a result of increasing seawater $p\text{CO}_2$ (IPCC, 2013). At the beginning of this study the guidelines stated that the control $p\text{CO}_2$ concentration for laboratory studies should be $380 \mu\text{atm}$ (Meehl et al., 2007), concordant with the then current atmospheric $p\text{CO}_2$. Four years later, the most recent literature reports that current concentrations of atmospheric $p\text{CO}_2$ have now risen to $400 \mu\text{atm}$ (IPCC, 2013). This demonstrates the unprecedented speed at which our climate is changing and highlights the urgency for research into the potential implications this change may have on marine systems. In addition, increasing atmospheric CO_2 is causing mean global temperature to rise, and consequently sea surface temperature is also increasing. If seawater temperature and pH continue to change as projected they are likely to have profound biological consequences for marine systems worldwide. Global climate change is also overlain by the natural variability, and it is likely that this variability will influence the response of marine organisms to global climate change. Climate change and ocean acidification have been the most-studied topics in marine science in recent times; however our knowledge of how marine organisms may respond in the future is still ambiguous. There is an urgent need for robust experimentation to assess the response of keystone species to changing climatic conditions.

In many marine coastal ecosystems marine calcifiers form an integral part of the community; responsible for the construction of biogenic structures that underpin the ecosystem and create habitat for many associated species. Red coralline algae are one such species and form a major component of many coastal marine ecosystems worldwide. Recently there has been increasing interest in the response of red coralline algae to global climate change. Previous studies on climate change and coralline algae have focused primarily on decreased pH, with some including elevated temperature, and the response of photosynthesis (e.g. Martin et al., 2013b, Semesi et al., 2009, Martin and Gattuso, 2009), metabolism (e.g. Noisette et al., 2013a), calcification (e.g. Büdenbender et al., 2011, Burdett et al., 2012a), dissolution (e.g. Diaz-Pulido et al., 2012) and structure (e.g. Kamenos et al., 2013, Egilsdottir et al., 2013, McCoy and Ragazzola, 2014, Ragazzola et al., 2012). Previous work has also investigated acclimatisation to variable *in situ* pH and the influence that this may have on the response of tropical crustose coralline algae to elevated temperature and $p\text{CO}_2$ (Johnson et al., 2014). In addition, Martin et al. (2013b) conducted a one year experiment on the response of red coralline algae to elevated temperature and $p\text{CO}_2$, which also considered seasonal variability in environmental conditions. Of the studies on *Lithothamnion glaciale*, previous work has focused solely on ocean acidification and none have considered their response in the context of natural variability. Furthermore, despite its importance for the growth, and its seasonal and sub diel variability, no studies have assessed the importance of light availability for coralline algae survival in the context of global climate change.

Cold-water corals are key contributors to biodiversity and habitat provision in the deep sea. However, only recently have they been the subject of ecological research, and we have very little understanding of their potential response to global climate change. Previous work has focused on calcification and results have been variable (McCulloch et al., 2012a, Maier et al., 2013a, Maier et al., 2013b, Hennige et al., 2014, Maier et al., 2009, Form and Riebesell, 2012). Recent studies suggest that there are environmental differences between cold water coral reef habitats (Findlay et al., 2014), however our knowledge of how their prior environmental experience may influence their response to climate change is limited.

Understanding the consequences of climate change for keystone species should be a priority for research. Using a variety of techniques in the laboratory and field this

research aimed to provide a better understanding of the impact global climate change may have on key marine calcifiers in the context of:

1. Natural variability and the role it may play in influencing a species response to global climate change: Temporal differences in environmental conditions (i.e. seasonal and sub diel changes) and the impact that these have on the response of marine organisms to global climate change (chapter 3, 4 and 5); the influence of *in situ* environmental variability on the response of marine organisms to elevated temperature and $p\text{CO}_2$ (chapter 7), and expressed phenotypes (chapter 6).
2. Acclimatisation: provide an insight into the scope for acclimatisation to elevated temperature and $p\text{CO}_2$ (chapter 3), and the role acclimatisation to *in situ* variables (e.g. low or variable pH) may play in influencing a species response to global climate change (Chapter 7).

8.1 Natural variability and global climate change

Global climate change is overlain by the natural variability of a system. Natural variability has a significant effect on the physiology of marine organisms under contemporary conditions, particularly light availability (inc. day length) and temperature. However, natural variability and the prior environmental experience of organisms are rarely considered in the context of climate change. If we are to make accurate projections about the future of marine organisms we must first understand present-day natural variability, and the role it might play in influencing the response of marine organisms to global climate change.

8.1.1 Seasonal environmental variability

The field study and the length of the long term laboratory experiment in chapter 3 are unique. The laboratory experiment is the longest study to date on the effects of elevated temperature and $p\text{CO}_2$ on a marine organism. The inclusion of the time series field study has allowed for results obtained in the laboratory experiment to be analysed in the context of natural variability. This approach also means that the study has been able to differentiate between the effects of the treatments (i.e. elevated temperature and $p\text{CO}_2$) and any effect due to laboratory conditions. Thus, the inclusion of the field study in

conjunction with the laboratory study has provided a more realistic outline of the response of red coralline algae to global climate change compared to previous studies.

Results suggest that seasonal differences in environmental conditions will greatly influence the response of coralline algae to global climate change; whereby coralline algae will respond differently to elevated temperature and $p\text{CO}_2$ depending on the season (chapter 3 and 5). While it is difficult to specify a particular season where the impact of climate change may be greater compared to others, there are some identifiable patterns:

- There were more significant responses to elevated temperature and $p\text{CO}_2$ during summer and spring compared to autumn and winter during both the short (chapter 5) and long term (chapter 3) experiments.
- Calcification was only affected by treatments (e.g. elevated temperature and $p\text{CO}_2$) during the summer and spring (chapter 3), and during winter but only in algae acclimatised to low light (chapter 5).
- In general optimal light level for efficient photosynthesis (E_k) either didn't change or increased in response to elevated temperature and / or $p\text{CO}_2$ in all seasons (chapter 3, 4 and 5).
- During the long term experiment (chapter 3), where elevated temperature and $p\text{CO}_2$ were significant, the affected parameter responded positively in all seasons, with the exception of growth and repair.
- During the short term experiment (chapter 5) more negative responses were observed during the winter compared to summer.

These results suggest that different physiological parameters are affected during different seasons. Suggesting that in the future there will be periods when the environmental conditions are more stressful for each physiological parameter, and periods where seasonal changes in environmental conditions may provide a respite from the most stressful conditions for each parameter. However, the periods of more (and less) stressful conditions are not the same for each physiological parameter, resulting in

year round stress for the algae as a whole. The net result of this is a negative impact of climate change on marine calcifying algae in the form of significantly reduced growth (chapter 3).

8.1.2 Calcification and dissolution

Calcification in coralline algae and the cold water coral was either maintained or increased in response to elevated $p\text{CO}_2$ and / or temperature in both the short and long term studies. Recently, several studies have described how some marine calcifiers (i.e. cold water corals) are able to modify the seawater chemistry close to the site of calcification (McCulloch et al., 2012a). Bicarbonate may be used as a substrate for calcification (as opposed to carbonate ions) and can be derived either directly from seawater or mitochondrial CO_2 (and converted by carbonic anhydrase) (Roleda et al., 2012). This suggests that the primary threat to marine calcifiers may in fact be dissolution rather than impaired calcification (Roleda et al., 2012). Indeed, the present study provides evidence to support this theory. Calcification rate was either maintained or increased during both short and long term exposure to elevated $p\text{CO}_2$ and / or temperature; however this did not translate into growth, which significantly decreased in rate in response to elevated temperature. Furthermore, the present research suggests that light availability mediates the photosynthetic response of coralline algae to elevated temperature and $p\text{CO}_2$, and the optimum light level required for photosynthesis will increase in the future. The tight link between photosynthesis, respiration and calcification, means that any change in photosynthetic rate (i.e. a decrease) relative to respiration rate will also hamper calcification in coralline algae the future.

8.1.3 The importance of light

In situ PAM fluorometry research suggested *L. glaciale* are acclimated to an optimum light level (E_k) that is either above or similar to ambient PAR (photosynthetically active radiation; chapter 3). This suggests that coralline algae in Loch Sween are regularly exposed to suboptimal light conditions. Thus, it is probable that sub diel changes (i.e. changes in cloud cover) and seasonal differences in PAR provide periodic light conditions above and / or equal to E_k that may explain how coralline algae can successfully grow in Loch Sween. Under laboratory conditions, results in chapters 3, 4 and 5 suggest that E_k either didn't change or increased in response to elevated temperature and / or $p\text{CO}_2$ in all seasons. The present study also found evidence to suggest that light availability may

mitigate the response of coralline algae to elevated temperature and $p\text{CO}_2$ (chapter 4). These results suggest that light availability will be a key factor influencing the survival of coralline algae in the future; whereby more light will be required to mitigate the negative physiological consequences of global climate change. This is likely to influence the distribution of algae in the future. Under contemporary conditions light availability is a major constraint on the distribution of coralline algae (Hall-Spencer, 1998). Light availability is unlikely to change (i.e. increase) in the future (Saikkonen et al., 2012), therefore, a requirement for more light will result in a loss of habitats currently located on the edge of their photo limits. The requirement for more light will also have implications as species distributions shift in response to global climate change (e.g. the poleward shift of organisms to follow thermoclines) by further limiting the number of suitable locations for coralline algae habitats.

8.1.4 Prior environmental experience

Natural variability in marine systems means that the same species inhabiting different locations will experience different environmental regimes. The present study provides evidence that prior environmental experience can influence the response of marine organisms to elevated temperature and $p\text{CO}_2$ (chapter 7), and expressed phenotypes (chapter 6). The results suggest that there are likely to be intraspecific differences in the response of marine organisms to global climate change. Comparison of the same species from different environmental regimes has improved our understanding of the role that natural variability may play in influencing the response of marine organisms to global climate change and provided an insight into the potential for organisms to acclimatise and adapt in the future. It is likely that exposure to low or variable *in situ* pH will facilitate an organism's physiological plasticity in their response to environmental change, providing them with increased adaptation potential for surviving conditions in the future.

8.2 Acclimatisation

The present study provides the longest experiment to date assessing the response of a marine organism to global climate change (chapter 3). The length of the study means that it is the first to be able to compare repeated months (i.e. February and May in year one and two), thus evaluate the scope for acclimatisation of coralline algae to elevated temperature and $p\text{CO}_2$ in the context of natural (seasonal) variation. Results suggest that

there is some scope for acclimatisation of *Lithothamnion glaciale* to elevated $p\text{CO}_2$ and temperature in both February and May, although the same physiological parameter did not always acclimatise in both months and acclimatisation was also dependent on $p\text{CO}_2$ level (i.e. $p\text{CO}_2$ 750 or 1000 μatm) in some cases. Calcification acclimatised to elevated temperature and $p\text{CO}_2$ at 750 μatm , but not at $p\text{CO}_2$ 1000 μatm , suggesting that coralline algal calcification may be able to acclimatise to $p\text{CO}_2$ projected for the mid century but not for the end of century projections. Differences over time in the response of marine calcifiers to global climate change have been linked to acclimatisation (e.g. Form and Riebesell, 2012). There is also increasing evidence that organisms exposed to high and / or variable *in situ* $p\text{CO}_2$ may be acclimatised to ocean acidification at least within the scope of the *in situ* variability (e.g. chapter 7 and Johnson et al., 2014). Although acclimatisation potential to climate change will not be solely dependent on prior environmental experience, the low variability of carbonate chemistry parameters *in situ* in Loch Sween (chapter 3) means that coralline algae may have less plasticity in their physiology to cope with elevated temperature and / or $p\text{CO}_2$. Thus, it is highly probable that, although there was evidence of scope for acclimatisation, prior experience of low *in situ* variability may, in part, be the reason that the net result of exposure to elevated temperature and $p\text{CO}_2$ was negative in the form of significantly reduced growth (chapter 3). Nevertheless, *Lithothamnion glaciale* did show some acclimatisation potential, therefore in the long term (> 2 years) the algae may be able to recover from the short term (< 2 years) negative impacts of increased temperature and $p\text{CO}_2$. This is particularly important because *in situ* environmental changes due to climate change will be slower than those manipulated in the laboratory. If marine organisms are able to acclimatise to elevated temperature and $p\text{CO}_2$ this will have dramatic implications for their survival in the future, because acclimatisation is the first step towards adaptation.

8.3 Future work and research direction

8.3.1 Natural variability

8.3.1.1 Implications for empirical studies

Natural variability in environmental conditions will greatly influence the response of marine organisms to global climate change (chapter 3, 4 and 5). This has implications for predicting the response of marine organisms to global climate change. If natural variability is not taken into account during empirical studies, and an organism responds

differently depending on the season and / or time of day, we cannot directly; (1) compare studies to identify patterns in the response of different organisms and / or phyla to global climate change and (2) make the most informed predictions about their future. Thus far there has been considerable variability in the response of coralline algae (and other organisms e.g. cold water coral) to global climate change. Although some of the variability is likely to be due to interspecific differences in response, studies are often compared without consideration of any temporal / spatial differences in environmental conditions that there may be between the studies. For example, a study examining elevated temperature during the summer is likely to set the 'elevated temperature' treatment outside the normal temperature range of the species. However, for a study conducted during the winter the 'elevated temperature' treatment is likely to be within the normal temperature range of the species. In this scenario the two studies may report different results. However, the variability may be due to seasonal differences in their response to climate change, as opposed to fundamental differences between the species; whereby if the two studies had been conducted during the same season, or compared with consideration of seasonal variability, results may have been more similar and/ or different conclusions drawn. Similarly, the same species inhabiting different locations (i.e. locations at the extremes of their range limit) may also respond differently to global climate change. Projecting the response of marine organisms to global climate change is a primary objective of the research. However, patterns in the response of marine organisms to global climate change are difficult to identify amongst the variability in organismal responses. Therefore, identification of the sources of variation is fundamental if we are to make informed decisions about the future of marine organisms.

8.3.1.2 *In situ* studies

While laboratory based studies are important in advancing our knowledge of climate change's impact on marine organisms, *in situ* locations with naturally variable or high $p\text{CO}_2$ could become a test bed for climate change studies. The use of such sites could enhance our understanding of the impact that global climate change may have on marine organisms with consideration of other ecosystem processes (i.e. natural variability / grazing / hydrography). This will allow us to explore the effects of elevated $p\text{CO}_2$ (and / or temperature) on marine organism's already acclimatised low or variable $p\text{CO}_2$ *in situ* (e.g. chapter 7) and allow us to assess the physiological plasticity of species in the context of climate change. Chapter 6 explored the difference in biochemical and morphological

phenotypes between *Padina gymnospora* growing on the environmentally stable reef crest and the more variable (in terms of carbonate chemistry) reef flat. Findings suggest that observed differences may be an indication that individuals existing in more variable (in terms of carbonate chemistry) habitats may have acclimatisation potential (i.e. phenotypic differences) against climate change, at least within the scope of the *in situ* variability. Chapter 6 provided an indication of physiological plasticity within the species; the next stage would to (1) perform manipulative transplant experiments whereby individuals from the environmentally stable reef crest are transplanted to the more variable flat, and (2) a laboratory study to identify intraspecific differences in the response of individuals from the environmentally different locations. A move towards combining *in situ* studies with laboratory based experiments would enable us to refine projections about the response of marine organisms to global climate change that are currently based solely on relatively short-term laboratory and / or modeling experiments.

8.3.1.3 The importance of light

Chapter 4 provides evidence that light availability mediates the response of red coralline algae to global climate change. However, more work is required to understand the specific implications that this may have in terms of habitat depth, latitudinal distribution, diurnal irradiance patterns (i.e. day length), habitat heterogeneity and the complex geometry of the algae that results in intra and inter-structural thallus (branch) shading.

8.3.1.4 Multiple stressors

In general, $p\text{CO}_2$ only had a significant effect when elevated temperature was also significant, either individually and/ or in combined treatments during all seasons (chapter 3 and 5). This highlights the significance of multiple stressor experiments. Such experiments are particularly important because, in the future, marine organisms will be exposed to multiple simultaneously changing environmental factors associated with global climate change, and it is unlikely that single factors will change one at a time (i.e. just ocean acidification). Ideally, future empirical studies should consider multiple stressors associated with change in the context of natural variability.

8.3.2 Acclimatisation

8.3.2.1 Rate of change

The present study provided evidence of the maintenance of key physiological functions (albeit different from the control) and acclimatisation potential of coralline algae (chapter 3) exposed to elevated temperature and $p\text{CO}_2$. This suggests that, if acclimatisation occurs, in the long term (greater than 2 years) the algae may be able to recover from the short term (less than 2 years) negative impacts (i.e. decreased growth) of increased temperature and $p\text{CO}_2$ experienced in the laboratory. Previous laboratory studies suggest that the structural integrity of *L. glaciale* may be compromised under exposure to acidified conditions (e.g. Ragazzola et al., 2012). However, there is also evidence to suggest that coralline algae structure may be more sensitive to the rate of environmental change rather than the magnitude of the change (Kamenos et al., 2013), and there may be more resistance to *in situ* changes compared to the laboratory (Burdett et al., 2013). Currently there is very little understanding about how the rate of environmental change may influence the impact on algae physiology and the implications that this may have for acclimatisation and recovery potential.

8.3.2.2 Mechanisms that promote acclimatisation

Chapter 7 demonstrated intraspecific differences in changes to the protein profile of the cold water coral, *Lophelia pertusa* collected from two different environments, in response to elevated temperature and $p\text{CO}_2$. Coral collected from Logachev, a deeper site with lower fluctuations in pH and $\Omega_{\text{aragonite}}$ may be acclimatised to acidified conditions. This means that they may be better able to cope with ocean acidification (compared to corals from less variable or lower $p\text{CO}_2$ environments), at least within the scope of the *in situ* variability. Although there were some conclusions drawn about the changes in the protein profile, the specific mechanisms for acclimatisation were beyond the scope of this study. Changes in the protein profiles were also observed in coralline algae in response to elevated temperature and $p\text{CO}_2$ (chapter 3 and 5). Currently there is little known about the mechanisms for acclimatisation to global climate change by marine organisms. Examination of molecular level responses, and the identification and assessment of key proteins, would increase our understanding of processes that may underlie acclimatisation potential and adaptation.

8.3.3 Growth, breakage and repair

Climate change is projected to significantly impact marine calcifying organisms because of the increased potential for carbonate dissolution under acidified conditions (Caldeira and Wickett, 2005). The present study provided evidence that calcification was unaffected or increased in response to elevated temperature and $p\text{CO}_2$, and demonstrated its scope for acclimatisation (chapter 3). However, overall growth and repair efficiency was significantly negatively affected. Structural analysis of the new growth on the algae thalli would provide important information about the nature of the impact on the growth. Such analysis would provide important information to support the findings of the present study.

8.4 Wider implications of this research

8.4.1 Impact of global climate change on marine systems

Thus far, most organismal climate change research has reported negative consequences for marine organisms under projected scenarios, although there is considerable variability within and between phyla. The speed at which our climate is changing suggests that keystone species, particularly those that contribute significantly in terms of ecosystem services, should be the priority for research. Negative consequences of climate change on these key organisms will have considerable implications for local and global economic, political and social development, and sustainability in the future. This research has added to our knowledge of the impact that global change may have on key marine calcifiers, namely free-living red coralline algae (maerl) and cold water corals. The present study also provides evidence for sources of variation between studies, and makes suggestions about factors that should be considered (i.e. natural variability) in future empirical studies that may reduce this variability. This knowledge improves our ability to predict the consequences of climate change on marine organisms.

8.4.2 Biodiversity and ecosystem services

Free-living red coralline algae and cold water corals are among some of the slowest growing marine species and it can take thousands to millions of years for these habitats to accumulate. The age of these habitats coupled with their slow-growth rates, means that these biogenic reefs contain high-resolution palaeoclimatic information. The cold water coral reefs are likely to be key speciation centres in the deep sea (Roberts et al., 2005). In addition, both maerl beds and cold water coral reefs are key contributors to

biodiversity and habitat provision. Due to their longevity and high biodiversity, maerl beds and cold water coral reefs have long been recognised for their conservation importance. However, more recently their benefits to commercial fisheries (Hall-Spencer and Stehfest, 2009, Husebo et al., 2002, Costello et al., 2005), recreational activities (Henry et al., 2013) and long term storage of organic and inorganic carbon (Burrows et al., 2014), has been acknowledged. Thus, it is in the economic and political interests of society to understand the potential impacts that global climate change may have on these keystone species in order to develop provisions and management strategies for the future.

8.4.3 Policy and management strategies

The Marine (Scotland) Act 2010 incorporates marine spatial planning approaches and creates a new legislative and ecosystem-based management framework to manage competing demands on Scotland's marine environment. The Act places a duty on Scottish Ministers to prepare and adopt a National Marine Plan that sets out specific policies for the sustainable development and conservation of Scotland's seas in addition to achieving economic, social and marine ecosystem objectives. The Marine (Scotland) Act contains new powers to enable the government to designate a network of marine protected areas (MPAs), which include maerl beds and cold water coral reefs in Scottish waters. Each MPA will include a management plan. This research provides information on factors that may impact the distribution and survival of coralline algae habitats and cold water coral reefs in the future and could contribute to the long term planning of the MPA network and management strategies for the marine environment.

8.5 Conclusions

Climate change and ocean acidification are one of the most-studied topics in marine science in recent times; however our knowledge of how marine organisms may respond in the future is still ambiguous. The unprecedented rate of change means that there is an urgent need for robust experimentation to assess the response of keystone species to changing climatic conditions. This research focused on improving our understanding of the impact of warming and acidification on key marine calcifiers in the context of (1) natural variability and the role that it may play in influencing a species response to global climate change (2) acclimatisation, including; the potential scope for acclimatisation to elevated temperature and $p\text{CO}_2$; and the role acclimatisation to *in situ*

variable and low pH may play in influencing a species response to global climate change. This research has shown that natural variability will dramatically influence the response of marine organisms to global climate change. The results suggest that different physiological parameters are affected during different seasons, and the net result of this is a negative impact of climate change on marine calcifying algae in the form of significantly reduced growth. The study provides evidence to suggest that light availability will significantly influence the survival of coralline algae in the future. Results suggest that optimal light level for efficient photosynthesis (E_k) will increase in response to elevated temperature and/ or $p\text{CO}_2$ in all seasons. The present study also found evidence to suggest that light availability may mitigate the response of coralline algae to elevated temperature and $p\text{CO}_2$. In addition, the study provides evidence of acclimatisation potential to elevated temperature and $p\text{CO}_2$ in coralline algae, and suggests that prior environmental experience will also influence the response of marine organisms to global climate change. This research contributes to our knowledge about the potential effects of climate change on key marine calcifiers. It also provides an insight into the role overlaying natural variability will play in the response of marine organisms to global climate change. Information may be used to direct future climate change research and management strategies for the protection of the marine environment.

References

- ADEY, W. H. 1970. EFFECTS OF LIGHT AND TEMPERATURE ON GROWTH RATES IN BOREAL-SUBARCTIC CRUSTOSE CORALLINES. *Journal of Phycology*, 6, 269-&
- ADEY, W. H. 1978. Algal ridges of the Caribbean sea and West Indies*. *Phycologia*, 17, 361-367.
- ADEY, W. H. 1998. Coral reefs: Algal structured and mediated ecosystems in shallow, turbulent, alkaline waters. *Journal of Phycology*, 34, 393-406.
- ADEY, W. H. & MC KIBBIN, D. L. 1970. Studies on the Maerl Species *Phymatolithon calcareum* (Pallas) nov. comb. and *Lithothamnium coralloides* Crouan in the Ria de Vigo. *Botanica Marina*.
- ADKINS, J. F., HENDERSON, G. M., WANG, S. L., O'SHEA, S. & MOKADEM, F. 2004. Growth rates of the deep-sea scleractinia *Desmophyllum cristagalli* and *Enallopsammia rostrata*. *Earth and Planetary Science Letters*, 227, 481-490.
- AGUILERA, J., BISCHOF, K., KARSTEN, U., HANELT, D. & WIENCKE, C. 2002. Seasonal variation in ecophysiological patterns in macroalgae from an Arctic fjord. II. Pigment accumulation and biochemical defence systems against high light stress. *Marine Biology*, 140, 1087-1095.
- AITKEN, A. & LEARMONTH, M. P. 2009. Protein Determination by UV Absorption. In: WALKER, J. M. (ed.) *Protein Protocols Handbook, Third Edition*.
- AKINS, R. E. & TUAN, R. S. 1992. MEASUREMENT OF PROTEIN IN 20 SECONDS USING A MICROWAVE BCA ASSAY. *Biotechniques*, 12, 496-499.
- ALBRIGHT, R., LANGDON, C. & ANTHONY, K. R. N. 2013. Dynamics of seawater carbonate chemistry, production, and calcification of a coral reef flat, central Great Barrier Reef. *Biogeosciences*, 10, 6747-6758.
- ALLEMAND, D., FERRIER-PAGES, C., FURLA, P., HOULBREQUE, F., PUVEREL, S., REYNAUD, S., TAMBUTTE, E., TAMBUTTE, S. & ZOCCOLA, D. 2004. Biomineralisation in reef-building corals: from molecular mechanisms to environmental control. *Comptes Rendus Palevol*, 3, 453-467.
- ALMGREN, T. & FONSELIUS, S. H. 1976. Determination of alkalinity and total carbonate. In: *Methods of seawater analysis*. (eds) K. Grasshoff, Chapter 8, Verlag Chemie., 97-115.
- ANDERSON, D. H. & ROBINSON, R. J. 1946. RAPID ELECTROMETRIC DETERMINATION OF THE ALKALINITY OF SEA WATER USING A GLASS ELECTRODE. *Industrial and Engineering Chemistry-Analytical Edition*, 18, 767-769.
- ANDERSSON, I. & BACKLUND, A. 2008. Structure and function of Rubisco. *Plant Physiology and Biochemistry*, 46, 275-291.
- ANTHONY, K. R. N., DIAZ-PULIDO, G., VERLINDEN, N., TILBROOK, B. & ANDERSSON, A. J. 2013. Benthic buffers and boosters of ocean acidification on coral reefs. *Biogeosciences*, 10, 4897-4909.
- ANTHONY, K. R. N., KLEYPAS, J. A. & GATTUSO, J. P. 2011. Coral reefs modify their seawater carbon chemistry - implications for impacts of ocean acidification. *Global Change Biology*, 17, 3655-3666.
- ANTHONY, K. R. N., KLINE, D. I., DIAZ-PULIDO, G., DOVE, S. & HOEGH-GULDBERG, O. 2008. Ocean acidification causes bleaching and productivity loss in coral reef builders. *Proceedings of the National Academy of Sciences*, 105, 17442-17446.
- AUFDENKAMPE, A. K., MAYORGA, E., RAYMOND, P. A., MELACK, J. M., DONEY, S. C., ALIN, S. R., AALTO, R. E. & YOO, K. 2011. Riverine coupling of biogeochemical

- cycles between land, oceans, and atmosphere. *Frontiers in Ecology and the Environment*, 9, 53-60.
- BANKS, I. R., SPECHT, C. A., DONLIN, M. J., GERIK, K. J., LEVITZ, S. M. & LODGE, J. K. 2005. A chitin synthase and its regulator protein are critical for chitosan production and growth of the fungal pathogen *Cryptococcus neoformans*. *Eukaryotic Cell*, 4, 1902-1912.
- BATES, N. R. 2007. Interannual variability of the oceanic CO₂ sink in the subtropical gyre of the North Atlantic Ocean over the last 2 decades. *Journal of Geophysical Research-Oceans*, 112.
- BATES, N. R., AMAT, A. & ANDERSSON, A. J. 2010. Feedbacks and responses of coral calcification on the Bermuda reef system to seasonal changes in biological processes and ocean acidification. *Biogeosciences*, 7, 2509-2530.
- BATES, N. R., SAMUELS, L. & MERLIVAT, L. 2001. Biogeochemical and physical factors influencing seawater fCO₂, and air-sea CO₂ exchange on the Bermuda coral reef. *Limnology and Oceanography*, 46, 833-846.
- BAXTER, J. M., BOYD, I. L., COX, M., DONALD, A. E., MALCOLM, S. J., MILES, H., MILLER, B., MOFFAT, C. F. & (EDITORS) 2011. Scotland's Marine Atlas: Information for the national marine plan. *Marine Scotland, Edinburgh*.
- BENSOUSSAN, N. & GATTUSO, J.-P. 2007. Community primary production and calcification in a NW Mediterranean ecosystem dominated by calcareous macroalgae. *Marine Ecology Progress Series*, 334, 37-45.
- BIOMAERL, BARBERA, C., BORDEHORE, C., BORG, J. A., GLÉMAREC, M., GRALL, J., HALL-SPENCER, J. M., DE LA HUZ, C. H., LANFRANCO, E., LASTRA, M., MOORE, P. G., MORA, J., PITA, M. E., RAMOS-ESPLA, A. A., RIZZO, M., SANCHEZ-MATA, A., SEVA, A., SCHEMBRI, P. J. & VALLE, C. 2003. Conservation and management of northeast Atlantic and Mediterranean maerl beds. *Aquatic Conservation: Marine and Freshwater Ecosystems*, 13, S65-S76.
- BISCHOFF, W. D., MACKENZIE, F. T. & BISHOP, F. C. 1987. Stabilities of synthetic magnesian calcites in aqueous solution: Comparison with biogenic materials. *Geochimica et Cosmochimica Acta*, 51, 1413-1423.
- BLAKE, C. & MAGGS, C. A. 2003. Comparative growth rates and internal banding periodicity of maerl species (Corallinales, Rhodophyta) from northern Europe. *Phycologia*, 42, 606-612.
- BOERNER, S. A., ISHAM, C. R., LEE, Y. K., TIBODEAU, J. D., KAUFMANN, S. H. & BIBLE, K. C. 2009. The Nitric Acid Method for Protein Estimation in Biological Samples. In: WALKER, J. M. (ed.) *Protein Protocols Handbook, Third Edition*.
- BORGES, A. V. & GYPENS, N. 2010. Carbonate chemistry in the coastal zone responds more strongly to eutrophication than to ocean acidification. *Limnology and Oceanography*, 55, 346-353.
- BOSENCE, D. & WILSON, J. 2003. Maerl growth, carbonate production rates and accumulation rates in the northeast Atlantic. *Aquatic Conservation-Marine and Freshwater Ecosystems*, 13, S21-S31.
- BOWES, G. 1991. GROWTH AT ELEVATED CO₂ - PHOTOSYNTHETIC RESPONSES MEDIATED THROUGH RUBISCO. *Plant Cell and Environment*, 14, 795-806.
- BRADFORD, M. M. 1976. A rapid and sensitive method for the quantitation of microgram quantities of protein utilizing the principle of protein-dye binding. *Analytical Biochemistry*, 72, 248-254.
- BRAHMI, C., MEIBOM, A., SMITH, D., STOLARSKI, J., AUZOUX-BORDENAVE, S., NOUET, J., DOUMENC, D., DJEDIAT, C. & DOMART-COULON, I. 2010. Skeletal growth, ultrastructure and composition of the azooxanthellate scleractinian coral <i>Balanophyllia regia</i>. *Coral Reefs*, 29, 175-189.

- BRELAND, J. A. & BYRNE, R. H. 1993. SPECTROPHOTOMETRIC PROCEDURES FOR DETERMINATION OF SEA-WATER ALKALINITY USING BROMOCRESOL GREEN. *Deep-Sea Research Part I-Oceanographic Research Papers*, 40, 629-641.
- BRODIE, J., WILLIAMSON, C. J., SMALE, D. A., KAMENOS, N. A., MIESZKOWSKA, N., SANTOS, R., CUNLIFFE, M., STEINKE, M., YESSON, C., ANDERSON, K. M., ASNAGHI, V., BROWNLEE, C., BURDETT, H. L., BURROWS, M. T., COLLINS, S., DONOHUE, P. J. C., HARVEY, B., FOGGO, A., NOISETTE, F., NUNES, J., RAGAZZOLA, F., RAVEN, J. A., SCHMIDT, D. N., SUGGETT, D., TEICHBERG, M. & HALL-SPENCER, J. M. 2014. The future of the northeast Atlantic benthic flora in a high CO₂ world. *Ecology and Evolution*, 4, 2787-2798.
- BROECKER, W. & CLARK, E. 2001. A dramatic Atlantic dissolution event at the onset of the last glaciation. *Geochemistry Geophysics Geosystems*, 2, art. no.-2001GC000185.
- BROOKES, A. & FARQUHAR, G. D. 1985. Effect of temperature on the CO₂/O₂ specificity of ribulose-1, 5-biphosphate carboxylase/ oxygenase and the rate of respiration in the light. *Planta*, 165, 397-406.
- BROOKS, M. D. & NIYOGI, K. K. 2011. Use of a Pulse-Amplitude Modulated Chlorophyll Fluorometer to Study the Efficiency of Photosynthesis in Arabidopsis Plants. In: JARVIS, R. P. (ed.) *Chloroplast Research in Arabidopsis: Methods and Protocols, Vol II*.
- BUDDEMEIER, R. W., KLEYPAS, J. A. & ARONSON, R. B. 2004. Coral reefs Potential Contributions of Climate Change to Stresses on Coral Reef Ecosystems Prepared for the & Global climate change. *Prepared for the Pew Center on Global Climate Change*.
- BÜDENBENDER, J., RIEBESELL, U. & FORM, A. 2011. Calcification and carbonate dissolution of an Arctic coralline red algae exposed to ocean acidification. *EGU General Assembly 2011*. Vienna, Austria.
- BUKAU, B. & HORWICH, A. L. 1998. The Hsp70 and Hsp60 chaperone machines. *Cell*, 92, 351-366.
- BURDETT, H. 2014. Climate change ecology: Older and wiser. *Nature Clim. Change*, 4, 668-669.
- BURDETT, H., ALOISIO, E., CALOSI, P., FINDLAY, H., WIDDICOMBE, S., HATTON, A. & KAMENOS, N. 2012a. The effect of chronic and acute low pH on the intracellular DMSP production and epithelial cell morphology of red coralline algae. *Mar Biol Res*, 8, 756 - 763.
- BURDETT, H., DONOHUE, P., HATTON, A., ALWANY, M. & KAMENOS, N. 2013. Spatiotemporal Variability of Dimethylsulphoniopropionate on a Fringing Coral Reef: The Role of Reefal Carbonate Chemistry and Environmental Variability. *PLoS ONE*, 8, e64651.
- BURDETT, H., HENNIGE, S., FRANCIS, F. & KAMENOS, N. 2012b. The photosynthetic characteristics of red coralline algae, determined using pulse amplitude modulation (PAM) fluorometry. *Bot Mar*, 55, 499 - 509.
- BURDETT, H., KAMENOS, N. & LAW, A. 2011. Using coralline algae to understand historic marine cloud cover. *Palaeogr Palaeoclim Palaeoecol*, 302, 65 - 70.
- BURDETT, H., KEDDIE, V., MACARTHUR, N., MCDOWALL, L., MCLEISH, J., SPIELVOGEL, E., HATTON, A. & KAMENOS, N. 2014. Dynamic photoinhibition exhibited by red coralline algae in the red sea. *BMC Plant Biology*, 14, 139.
- BURDETT, H. L. 2013. PhD Thesis: DMSP Dynamics in Marine Coralline Algal Habitats. *University of Glasgow*.
- BURDETT, H. L., HENNIGE, S. J., FRANCIS, F. T. Y. & KAMENOS, N. A. 2012c. The photosynthetic characteristics of red coralline algae, determined using pulse amplitude modulation (PAM) fluorometry. *Botanica Marina*, 55, 499-509.

- BURROWS, M. T., KAMENOS, N. A., HUGHES, D. J., STAHL, H., HOWE, J. A. & TETT, P. 2014. Assessment of carbon budgets and potential blue carbon stores in Scotland's coastal and marine environment. *Scottish Natural Heritage Commissioned Report No. 761*.
- BYRNE, M. 2011. IMPACT OF OCEAN WARMING AND OCEAN ACIDIFICATION ON MARINE INVERTEBRATE LIFE HISTORY STAGES: VULNERABILITIES AND POTENTIAL FOR PERSISTENCE IN A CHANGING OCEAN. In: GIBSON, R. N., ATKINSON, R. J. A. & GORDON, J. D. M. (eds.) *Oceanography and Marine Biology: An Annual Review, Vol 49*.
- BYRNE, R. H., MECKING, S., FEELY, R. A. & LIU, X. 2010. Direct observations of basin-wide acidification of the North Pacific Ocean. *Geophysical Research Letters*, 37.
- CABIOCH, J. 1969. PERSISTENCE OF JUVENILE STAGES AND POSSIBILITY OF A NEOTENY IN LITHOPHYLLUM INCRUSTANS PHILIPPI. *Comptes Rendus Hebdomadaires Des Seances De L Academie Des Sciences Serie D*, 268, 497-&.
- CAIRNS, S. D. 1994. Scleractinia of the temperate North Pacific. *Smithsonian Contributions to Zoology*, 0, III-VII, 1-150.
- CALDEIRA, K. & WICKETT, M. 2005. Ocean model predictions of chemistry changes from carbon dioxide emissions to the atmosphere and ocean. *J Geophys Res*, 110, C09S04.
- CALDEIRA, K. & WICKETT, M. E. 2003. Oceanography: Anthropogenic carbon and ocean pH. *Nature*, 425, 365-365.
- CARILLI, J., DONNER, S. D. & HARTMANN, A. C. 2012. Historical Temperature Variability Affects Coral Response to Heat Stress. *Plos One*, 7.
- CHIAL, H. J. & SPLITTGERBER, A. G. 1993. A COMPARISON OF THE BINDING OF COOMASSIE BRILLIANT BLUE TO PROTEINS AT LOW AND NEUTRAL PH. *Analytical Biochemistry*, 213, 362-369.
- CHISHOLM, J. R. M. 2000. Calcification by crustose coralline algae on the northern Great Barrier Reef, Australia. *Limnology and Oceanography*, 45, 1476-1484.
- CHOW, A. M., FERRIER-PAGES, C., KHALOUEI, S., REYNAUD, S. & BROWN, I. R. 2009. Increased light intensity induces heat shock protein Hsp60 in coral species. *Cell Stress & Chaperones*, 14, 469-476.
- CIGLIANO, M., GAMBI, M. C., RODOLFO-METALPA, R., PATTI, F. P. & HALL-SPENCER, J. M. 2010. Effects of ocean acidification on invertebrate settlement at volcanic CO₂ vents. *Marine Biology*, 157, 2489-2502.
- COHEN, A. L. & MCCONNAUGHEY, T. A. 2003. Geochemical perspectives on coral mineralization. In: DOVE, P. M., DEYOREO, J. J. & WEINER, S. (eds.) *Biom mineralization*.
- COLE, M. K. & SHEATH, R. G. 1990. (eds.) *Biology of red algae. Cambridge University Press, Cambridge*.
- COLLEN, J., HERVE, C., GUISE-MARSOLLIER, I., LEGER, J. J. & BOYEN, C. 2006. Expression profiling of *Chondrus crispus* (Rhodophyta) after exposure to methyl jasmonate. *Journal of Experimental Botany*, 57, 3869-3881.
- COMPTON, S. J. & JONES, C. G. 1985. MECHANISM OF DYE RESPONSE AND INTERFERENCE IN THE BRADFORD PROTEIN ASSAY. *Analytical Biochemistry*, 151, 369-374.
- CONGDON, R. W., MUTH, G. W. & SPLITTGERBER, A. G. 1993. THE BINDING INTERACTION OF COOMASSIE BLUE WITH PROTEINS. *Analytical Biochemistry*, 213, 407-413.
- CONNELL, S. D., KROEKER, K. J., FABRICIUS, K. E., KLINE, D. I. & RUSSELL, B. D. 2013. The other ocean acidification problem: CO₂ as a resource among competitors for ecosystem dominance. *Royal Society Philosophical Transactions Biological Sciences*, 368, 20120442-20120442.

- CORNWALL, C. E., HEPBURN, C. D., PRITCHARD, D., CURRIE, K. I., MCGRAW, C. M., HUNTER, K. A. & HURD, C. L. 2012. CARBON-USE STRATEGIES IN MACROALGAE: DIFFERENTIAL RESPONSES TO LOWERED PH AND IMPLICATIONS FOR OCEAN ACIDIFICATION. *Journal of Phycology*, 48, 137-144.
- COSTANZA, R., DARGE, R., DEGROOT, R., FARBER, S., GRASSO, M., HANNON, B., LIMBURG, K., NAEEM, S., ONEILL, R. V., PARUELO, J., RASKIN, R. G., SUTTON, P. & VANDENBELT, M. 1997. The value of the world's ecosystem services and natural capital. *Nature*, 387, 253-260.
- COSTELLO, M. J., MCCREA, M., FREIWALD, A., LUNDALV, T., JONSSON, L., BETT, B. J., VAN WEERING, T. C. E., DE HAAS, H., ROBERTS, J. M. & ALLEN, D. 2005. *Role of cold-water Lophelia pertusa coral reefs as fish habitat in the NE Atlantic*.
- CRAFTS-BRANDNER, S. J. & SALVUCCI, M. E. 2000. Rubisco activase constrains the photosynthetic potential of leaves at high temperature and CO₂. *Proceedings of the National Academy of Sciences*, 97, 13430-13435.
- CROSSLAND, C. J., HATCHER, B. G. & SMITH, S. V. 1991. ROLE OF CORAL REEFS IN GLOBAL OCEAN PRODUCTION. *Coral Reefs*, 10, 55-64.
- CULBERSON, C., PYTKOWIC, R. M. & HAWLEY, J. E. 1970. SEAWATER ALKALINITY DETERMINATION BY PH METHOD. *Journal of Marine Research*, 28, 15-&.
- CUMMINGS, V., HEWITT, J., VAN ROOYEN, A., CURRIE, K., BEARD, S., THRUSH, S., NORKKO, J., BARR, N., HEATH, P., HALLIDAY, N. J., SEDCOLE, R., GOMEZ, A., MCGRAW, C. & METCALF, V. 2011. Ocean Acidification at High Latitudes: Potential Effects on Functioning of the Antarctic Bivalve *Laternula elliptica*. *Plos One*, 6.
- DAINTITH, J. 2004. *Oxford Dictionary of Chemistry*
- DAVIES, A. J., WISSHAK, M., ORR, J. C. & ROBERTS, J. M. 2008. Predicting suitable habitat for the cold-water coral *Lophelia pertusa* (Scleractinia). *Deep-Sea Research Part I-Oceanographic Research Papers*, 55, 1048-1062.
- DAVISON, I. R. 1991. ENVIRONMENTAL EFFECTS ON ALGAL PHOTOSYNTHESIS: TEMPERATURE. *Journal of Phycology*, 27, 2-8.
- DE BEER, D. & LARKUM, A. W. D. 2001. Photosynthesis and calcification in the calcifying algae *Halimeda discoidea* studied with microsensors. *Plant Cell and Environment*, 24, 1209-1217.
- DE GROOT, T. A. M. & ORFORD, J. D. 1999. Climate change and coastal evolution in Europe. *Geologie En Mijnbouw-Netherlands Journal of Geosciences*, 77, 207-208.
- DEMMIG-ADAMS, B. & ADAMS, W. W. 1992. PHOTOPROTECTION AND OTHER RESPONSES OF PLANTS TO HIGH LIGHT STRESS. *Annual Review of Plant Physiology and Plant Molecular Biology*, 43, 599-626.
- DENNY, M., MACH, K., TEPLER, S. & MARTONE, P. 2013. Indefatigable: an erect coralline alga is highly resistant to fatigue. *Journal of Experimental Biology*, 216, 3772-3780.
- DESCOLAS-GROS, C. & DE BILLY, G. 1987. TEMPERATURE ADAPTATION OF RUBP CARBOXYLASE - KINETIC-PROPERTIES IN MARINE ANTARCTIC DIATOMS. *Journal of Experimental Marine Biology and Ecology*, 108, 147-158.
- DIAZ-PULIDO, G., ANTHONY, K. R. N., KLINE, D. I., DOVE, S. & HOEGH-GULDBERG, O. 2012. INTERACTIONS BETWEEN OCEAN ACIDIFICATION AND WARMING ON THE MORTALITY AND DISSOLUTION OF CORALLINE ALGAE1. *Journal of Phycology*, 48, 32-39.
- DICKSON, A. G. 1981. AN EXACT DEFINITION OF TOTAL ALKALINITY AND A PROCEDURE FOR THE ESTIMATION OF ALKALINITY AND TOTAL INORGANIC CARBON FROM TITRATION DATA. *Deep-Sea Research Part a-Oceanographic Research Papers*, 28, 609-623.

- DICKSON, A. G. 1990. THERMODYNAMICS OF THE DISSOCIATION OF BORIC-ACID IN SYNTHETIC SEAWATER FROM 273.15-K TO 318.15-K. *Deep-Sea Research Part a-Oceanographic Research Papers*, 37, 755-766.
- DICKSON, A. G. 2010. STANDARDS FOR OCEAN MEASUREMENTS. *Oceanography*, 23, 34-47.
- DICKSON, A. G. & MILLERO, F. J. 1987. A COMPARISON OF THE EQUILIBRIUM-CONSTANTS FOR THE DISSOCIATION OF CARBONIC-ACID IN SEAWATER MEDIA. *Deep-Sea Research Part a-Oceanographic Research Papers*, 34, 1733-1743.
- DICKSON, A. G., SABINE, C. L. & CHRISTIAN, J. R. 2007. Guide to best practices for ocean CO₂ measurements. *PICES Special publication*, 3, 1-191.
- DODDS, L. A., ROBERTS, J. M., TAYLOR, A. C. & MARUBINI, F. 2007. Metabolic tolerance of the cold-water coral *Lophelia pertusa* (Scleractinia) to temperature and dissolved oxygen change. *Journal of Experimental Marine Biology and Ecology*, 349, 205-214.
- DOE 1994. Handbook of methods for the analysis of the various parameters of the carbon dioxide system in sea water; version 2. A.G. Dickson & C. Goyet, eds., *ORNL/CDIAC-74*.
- DONEY, S. C., BALCH, W. M., FABRY, V. J. & FEELY, R. A. 2009. OCEAN ACIDIFICATION: A CRITICAL EMERGING PROBLEM FOR THE OCEAN SCIENCES. *Oceanography*, 22, 16-+.
- DONEY, S. C., RUCKELSHAUS, M., DUFFY, J. E., BARRY, J. P., CHAN, F., ENGLISH, C. A., GALINDO, H. M., GREBMEIER, J. M., HOLLOWED, A. B., KNOWLTON, N., POLOVINA, J., RABALAIS, N. N., SYDEMAN, W. J. & TALLEY, L. D. 2012. Climate Change Impacts on Marine Ecosystems. *Annual Review of Marine Science*, Vol 4, 4, 11-37.
- DORE, J. E., LUKAS, R., SADLER, D. W., CHURCH, M. J. & KARL, D. M. 2009. Physical and biogeochemical modulation of ocean acidification in the central North Pacific. *Proceedings of the National Academy of Sciences of the United States of America*, 106, 12235-12240.
- DORSCHER, B., HEBBELN, D., FOUBERT, A., WHITE, M. & WHEELER, A. J. 2007. Hydrodynamics and cold-water coral facies distribution related to recent sedimentary processes at Galway Mound west of Ireland. *Marine Geology*, 244, 184-195.
- DOUARIN, M., SINCLAIR, D. J., ELLIOT, M., HENRY, L.-A., LONG, D., MITCHISON, F. & ROBERTS, J. M. 2014. Changes in fossil assemblage in sediment cores from Mingulay Reef Complex (NE Atlantic): Implications for coral reef build-up. *Deep-Sea Research Part II-Topical Studies in Oceanography*, 99, 286-296.
- DRAKE, B. G., GONZALEZMELER, M. A. & LONG, S. P. 1997. More efficient plants: A consequence of rising atmospheric CO₂? *Annual Review of Plant Physiology and Plant Molecular Biology*, 48, 609-639.
- DREW, E. 1983. Halimeda biomass, growth rates and sediment generation on reefs in the central great barrier reef province. *Coral Reefs*, 2, 101-110.
- DRING, M. J., WAGNER, A., BOESKOV, J. & LUNING, K. 1996. Sensitivity of intertidal and subtidal red algae to UVA and UVB radiation, as monitored by chlorophyll fluorescence measurements: Influence of collection depth and season, and length of irradiation. *European Journal of Phycology*, 31, 293-302.
- DUARTE, C. M., HENDRIKS, I. E., MOORE, T. S., OLSEN, Y. S., STECKBAUER, A., RAMAJO, L., CARSTENSEN, J., TROTTER, J. A. & MCCULLOCH, M. 2013. Is Ocean Acidification an Open-Ocean Syndrome? Understanding Anthropogenic Impacts on Seawater pH. *Estuaries and Coasts*, 36, 221-236.

- DULLO, W.-C., FLOEGEL, S. & RUEGGEBERG, A. 2008. Cold-water coral growth in relation to the hydrography of the Celtic and Nordic European continental margin. *Marine Ecology Progress Series*, 371, 165-176.
- DYRSSEN, D. & SILLEN, L. G. 1967. Alkalinity and total carbonate determination in seawater: a plea for P-T- independent data. *Tellus*, 19, 113-121.
- EDMOND, J. M. 1970. HIGH PRECISION DETERMINATION OF TITRATION ALKALINITY AND TOTAL CARBON DIOXIDE CONTENT OF SEA WATER BY POTENTIOMETRIC TITRATION. *Deep-Sea Research*, 17, 737-&.
- EGILSDOTTIR, H., NOISETTE, F., NOEL, L., OLAFSSON, J. & MARTIN, S. 2013. Effects of pCO₂ on physiology and skeletal mineralogy in a tidal pool coralline alga *Corallina elongata*. *Marine Biology*, 160, 2103-2112.
- ELLIOT, W. H. & ELLIOT, D. C. 2005. Biochemistry and molecular biology, Third Edition. *Oxford University Press, Oxford, United Kingdom*.
- EMERSON, R. & ARNOLD, W. 1932. The photochemical reaction in photosynthesis. *Journal of General Physiology*, 16, 191-205.
- EREZ, J. 2003. The source of ions for biomineralization in foraminifera and their implications for paleoceanographic proxies. In: DOVE, P. M., DEYOREO, J. J. & WEINER, S. (eds.) *Biomineralization*.
- FABRY, V. J., SEIBEL, B. A., FEELY, R. A. & ORR, J. C. 2008. Impacts of ocean acidification on marine fauna and ecosystem processes. *Ices Journal of Marine Science*, 65, 414-432.
- FALINI, G., ALBECK, S., WEINER, S. & ADDADI, L. 1996. Control of Aragonite or Calcite Polymorphism by Mollusk Shell Macromolecules. *Science*, 271, 67-69.
- FALKOWSKI, P. G. & RAVEN, J. A. 1997. Aquatic Photosynthesis. *Blackwell, Oxford*.
- FALKOWSKI, P. G. & RAVEN, J. A. 2013. *Aquatic photosynthesis*, Princeton University Press.
- FALTER, J. L., LOWE, R. J., ZHANG, Z. & MCCULLOCH, M. 2013. Physical and Biological Controls on the Carbonate Chemistry of Coral Reef Waters: Effects of Metabolism, Wave Forcing, Sea Level, and Geomorphology. *Plos One*, 8.
- FEELY, R. A., DONEY, S. C. & COOLEY, S. R. 2009. Ocean Acidification: Present Conditions and Future Changes in a High-CO₂ World. *Oceanography*, 22, 36-47.
- FENG, W., ZHAO, T., ZHOU, Y., LI, F., ZOU, Y., BAI, S., WANG, W., YANG, L. & WU, X. 2013. Optimization of enzyme-assisted extraction and characterization of collagen from Chinese sturgeon (*Acipenser sturio* Linnaeus) skin. *Pharmacognosy magazine*, 9, S32-7.
- FINDLAY, H. 2013. CTD data from James Cook Research Cruise JC073. British Oceanographic Data Centre, Natural Environment Research Council.
- FINDLAY, H. & WOODWARD, E. 2013. Carbon and nutrients concentrations associated with RRS James Cook cruise JC073. British Oceanographic Data Centre, Natural Environment Research Council.
- FINDLAY, H. S., ARTIOLI, Y., NAVAS, J. M., HENNIGE, S. J., WICKS, L. C., HUVENNE, V. A. I., WOODWARD, E. M. S. & ROBERTS, J. M. 2013. Tidal downwelling and implications for the carbon biogeochemistry of cold-water corals in relation to future ocean acidification and warming. *Global Change Biology*, 19, 2708-2719.
- FINDLAY, H. S., HENNIGE, S. J., WICKS, L. C., NAVAS, J. M., WOODWARD, E. M. S. & ROBERTS, J. M. 2014. Fine-scale nutrient and carbonate system dynamics around cold-water coral reefs in the northeast Atlantic. *Scientific Reports*, 4.
- FORM, A. U. & RIEBESELL, U. 2012. Acclimation to ocean acidification during long-term CO₂ exposure in the cold-water coral *Lophelia pertusa*. *Global Change Biology*, 18, 843-853.
- FORSTER, P., RAMASWAMY, V., ARTAXO, P., BERNTSEN, T., BETTS, R., FAHEY, D. W., HAYWOOD, J., LEAN, J., LOWE, D. C., MYHRE, G., NGANGA, J., PRINN, R., RAGA,

- G. & VAN DORLAND, M. R. S. 2007. Changes in Atmospheric Constituents and in Radiative Forcing. In: *Climate Change 2007: The Physical Science Basis. Contribution of Working Group I to the Fourth Assessment Report of the Intergovernmental Panel on Climate Change Cambridge, United Kingdom and New York, NY, USA., Cambridge University Press.*
- FORTES, M. D. & LÜNING, K. 1980. Growth rates of North Sea macroalgae in relation to temperature, irradiance and photoperiod. *Helgoländer Meeresuntersuchungen*, 34, 15-29.
- FOSSA, J. H., MORTENSEN, P. B. & FUREVIK, D. M. 2002. The deep-water coral *Lophelia pertusa* in Norwegian waters: Distribution and fishery impacts. *Hydrobiologia*, 471, 1-12.
- FOSTER, M. 2001. Rhodoliths: Between rocks and soft places. *J Phycol*, 37, 659 - 667.
- FOSTER, M. S., AMADO FILHO, G. M., KAMENOS, N. A., RIOSMENA-RODRIGUEZ, R. & STELLER, D. L. 2013. Rhodoliths and Rhodolith Beds. *Smithsonian Contributions to the Marine Sciences*, 143-155.
- FOYER, C. H., NEUKERMANS, J., QUEVAL, G., NOCTOR, G. & HARBINSON, J. 2012. Photosynthetic control of electron transport and the regulation of gene expression. *Journal of Experimental Botany*, 63, 1637-1661.
- FRANKIGNOULLE, M. & BOUQUEGNEAU, J. M. 1990. DAILY AND YEARLY VARIATIONS OF TOTAL INORGANIC CARBON IN A PRODUCTIVE COASTAL AREA. *Estuarine Coastal and Shelf Science*, 30, 79-89.
- FRANKLIN, L. A. & FORSTER, R. M. 1997. The changing irradiance environment: consequences for marine macrophyte physiology, productivity and ecology. *European Journal of Phycology*, 32, 207-232.
- FRANTZ, B. R., FOSTER, M. S. & RIOSMENA-RODRIGUEZ, R. 2005. *Clathromorphum nereostratum* (Corallinales, Rhodophyta): The oldest alga? *Journal of Phycology*, 41, 770-773.
- FREIWALD, A. 1995. Sedimentological and biological aspects in the formation of branched rhodoliths in northern Norway. *Beitraege zur Palaeontologie*, 0, 7-19.
- FREIWALD, A., FOSSA, J. H., GREHAN, A., KOSLOW, J. A. & ROBERTS, J. M. 2004. Cold-water coral reefs: out of sight no longer out of mind. *UNEP-WCC, Cambridge. pp. 84.*
- FREIWALD, A. & HENRICH, R. 1994. REEFAL CORALLINE ALGAL BUILD-UPS WITHIN THE ARCTIC-CIRCLE - MORPHOLOGY AND SEDIMENTARY DYNAMICS UNDER EXTREME ENVIRONMENTAL SEASONALITY. *Sedimentology*, 41, 963-984.
- FRIEDRICH, T. D., RAY, F. A., SMITH, R. L. & LEHMAN, J. M. 2009a. Quantitation of Cellular Proteins by Flow Cytometry. In: WALKER, J. M. (ed.) *Protein Protocols Handbook, Third Edition.*
- FRIEDRICH, T. D., SMITH, R. L. & LEHMAN, J. M. 2009b. Quantitation of Cellular Proteins by Laser Scanning Cytometry. In: WALKER, J. M. (ed.) *Protein Protocols Handbook, Third Edition.*
- GANTT, E., SCOTT, J. & LIPSCHULTZ, C. 1986. PHYCOBILIPROTEIN COMPOSITION AND CHLOROPLAST STRUCTURE IN THE FRESH-WATER RED ALGA COMPSOPOGON-COERULEUS (RHODOPHYTA). *Journal of Phycology*, 22, 480-484.
- GAO, K., ARUGA, Y., ASADA, K., ISHIHARA, T., AKANO, T. & KIYOHARA, M. 1991. ENHANCED GROWTH OF THE RED ALGA PORPHYRA-YEZOENSIS UEDA IN HIGH CO₂ CONCENTRATIONS. *Journal of Applied Phycology*, 3, 355-362.
- GAO, K., ARUGA, Y., ASADA, K. & KIYOHARA, M. 1993. INFLUENCE OF ENHANCED CO₂ ON GROWTH AND PHOTOSYNTHESIS OF THE RED ALGAE GRACILARIA SP AND G-CHILENSIS. *Journal of Applied Phycology*, 5, 563-571.

- GAO, K. S. & ZHENG, Y. Q. 2010. Combined effects of ocean acidification and solar UV radiation on photosynthesis, growth, pigmentation and calcification of the coralline alga *Corallina sessilis* (Rhodophyta). *Global Change Biology*, 16, 2388-2398.
- GARCIA, H. E., LOCARNINI, R. A., BOYER, T. P. & ANTONOV, J. I. 2006. World oceans atlas 2005. Volume 4: Nutrients (phosphate, silicate, nitrate) In: Levitus (ed.) NOAA atlas NESDIS 64, pp1-396. *US Government Printing Office, Washington, DC*.
- GATTUSO, J.-P., ALLEMAND, D. & FRANKIGNOULLE, M. 1999. Photosynthesis and Calcification at Cellular, Organismal and Community Levels in Coral Reefs: A Review on Interactions and Control by Carbonate Chemistry. *American Zoologist*, 39, 160-183.
- GATTUSO, J.-P., PAYRI, C. E., PICHON, M., DELESALLE, B. & FRANKIGNOULLE, M. 1997. PRIMARY PRODUCTION, CALCIFICATION, AND AIR-SEA CO₂ FLUXES OF A MACROALGAL-DOMINATED CORAL REEF COMMUNITY (MOOREA, FRENCH POLYNESIA)1. *Journal of Phycology*, 33, 729-738.
- GATTUSO, J. P., FRANKIGNOULLE, M., BOURGE, I., ROMAINE, S. & BUDDEMEIER, R. W. 1998. Effect of calcium carbonate saturation of seawater on coral calcification. *Global and Planetary Change*, 18, 37-46.
- GATTUSO, J. P. & HANSSON, L. (eds.) 2011. *Ocean Acidification*: Oxford University Press, Oxford.
- GATTUSO, J. P. & LAVIGNE, H. 2009. Technical Note: Approaches and software tools to investigate the impact of ocean acidification. *Biogeosciences*, 6, 2121-2133.
- GIORDANO, M., BEARDALL, J. & RAVEN, J. A. 2005. CO₂ concentrating mechanisms in algae: Mechanisms, environmental modulation, and evolution. *Annual Review of Plant Biology*.
- GLAZER, A. 1985. Light harvesting by phycobilisomes. *Annual review of biophysics and biophysical chemistry*, 14, 47-77.
- GLAZER, A. N., APELL, G. S., HIXSON, C. S., BRYANT, D. A., RIMON, S. & BROWN, D. M. 1976. BILIPROTEINS OF CYANOBACTERIA AND RHODOPHYTA - HOMOLOGOUS FAMILY OF PHOTOSYNTHETIC ACCESSORY PIGMENTS. *Proceedings of the National Academy of Sciences of the United States of America*, 73, 428-431.
- GLAZER, A. N. & MELIS, A. 1987. Photochemical reaction centers: structure, organization, and function. *Annual review of plant physiology*, 38, 11-45.
- GONZALEZ-DAVILA, M., SANTANA-CASIANO, J. M., RUEDA, M. J. & LLINAS, O. 2010. The water column distribution of carbonate system variables at the ESTOC site from 1995 to 2004. *Biogeosciences*, 7, 3067-3081.
- GOSS, R. & JAKOB, T. 2012. Regulation and function of xanthophyll cycle-dependent photoprotection in algae. *Photosynthesis Research*, 106, 103-122.
- GOTLIV, B. A., ADDADI, L. & WEINER, S. 2003. Mollusk shell acidic proteins: In search of individual functions. *Chembiochem*, 4, 522-529.
- GOURETSKI, V., KENNEDY, J., BOYER, T. & KOEHL, A. 2012. Consistent near-surface ocean warming since 1900 in two largely independent observing networks. *Geophysical Research Letters*, 39.
- GOYET, C. & SNOVER, A. K. 1993. HIGH-ACCURACY MEASUREMENTS OF TOTAL DISSOLVED INORGANIC CARBON IN THE OCEAN - COMPARISON OF ALTERNATE DETECTION METHODS. *Marine Chemistry*, 44, 235-242.
- GRAY, S. E. C., DEGRANDPRE, M. D., LANGDON, C. & CORREDOR, J. E. 2012. Short-term and seasonal pH, pCO₂ and saturation state variability in a coral-reef ecosystem. *Global Biogeochemical Cycles*, 26.

- GRIPENBERG, S. 1936. Communication 10B. Vth Hydrological Conference of the Baltic States, Helsingfors, 15 pp. (cited in Almgren and Fonselius, 1976).
- GUINOTTE, J. M., ORR, J., CAIRNS, S., FREIWALD, A., MORGAN, L. & GEORGE, R. 2006. Will human-induced changes in seawater chemistry alter the distribution of deep-sea scleractinian corals? *Frontiers in Ecology and the Environment*, 4, 141-146.
- GUTIÉRREZ, J. L., JONES, C. G., BYERS, J. E., ARKEMA, K. K., BERKENBUSCH, K., COMMITO, J. A., DUARTE, C. M., HACKER, S. D., LAMBRINOS, J. G., HENDRIKS, I. E., HOGARTH, P. J., PALOMO, M. G. & WILD, C. 2011. *Physical ecosystem engineers and the functioning of estuaries and coasts*. In: E. Wolanski, D.S. McLusky (eds). *Treatise on estuarine and coastal science*, Waltham: Academic.
- HALFAR, J., HETZINGER, S., ZACK, T., SIMON, K., KRONZ, A., STENECK, R. S., ADEY, W., LEBEDNIK, P. A., SCHOENE, B. R. & FIETZKE, J. 2009. High-resolution analysis of trace elements in encrusting coralline red algae by laser ablation ICP-MS. *Geochimica Et Cosmochimica Acta*, 73, A487-A487.
- HALFAR, J., STENECK, R. S., JOACHIMSKI, M., KRONZ, A. & WANAMAKER, A. D., JR. 2008. Coralline red algae as high-resolution climate recorders. *Geology*, 36, 463-466.
- HALL-SPENCER, J. 1998. Conservation issues relating to maerl beds as habitats for molluscs. *Journal of Conchology*, SPECIAL PUBL., 271-286.
- HALL-SPENCER, J. 2011. No reason for complacency. *Nature Climate Change*, 1, 174-174.
- HALL-SPENCER, J. & STEHFEST, K. M. 2009. OSPAR Commission: Background document for *Lophelia pertusa* reefs. *UK Joint Nature Conservation Committee (JNCC)*.
- HALL-SPENCER, J. M., RODOLFO-METALPA, R., MARTIN, S., RANSOME, E., FINE, M., TURNER, S. M., ROWLEY, S. J., TEDESCO, D. & BUIA, M.-C. 2008. Volcanic carbon dioxide vents show ecosystem effects of ocean acidification. *Nature*, 454, 96-99.
- HALL, S. R., TAYLOR, P. D., DAVIS, S. A. & MANN, S. 2002. Electron diffraction studies of the calcareous skeletons of bryozoans. *Journal of Inorganic Biochemistry*, 88, 410-419.
- HAMA, T., MIYAZAKI, T., OGAWA, Y., IWAKUMA, T., TAKAHASHI, M., OTSUKI, A. & ICHIMURA, S. 1983. MEASUREMENT OF PHOTOSYNTHETIC PRODUCTION OF A MARINE-PHYTOPLANKTON POPULATION USING A STABLE C-13 ISOTOPE. *Marine Biology*, 73, 31-36.
- HANSSON, I. & JAGNER, D. 1973. EVALUATION OF ACCURACY OF GRAN PLOTS BY MEANS OF COMPUTER CALCULATIONS - APPLICATION TO POTENTIOMETRIC TITRATION OF TOTAL ALKALINITY AND CARBONATE CONTENT IN SEAWATER. *Analytica Chimica Acta*, 65, 363-373.
- HARLEY, C. D. G., ANDERSON, K. M., DEMES, K. W., JORVE, J. P., KORDAS, R. L., COYLE, T. A. & GRAHAM, M. H. 2012. EFFECTS OF CLIMATE CHANGE ON GLOBAL SEAWEED COMMUNITIES. *Journal of Phycology*, 48, 1064-1078.
- HARLEY, C. D. G., HUGHES, A. R., HULTGREN, K. M., MINER, B. G., SORTE, C. J. B., THORNER, C. S., RODRIGUEZ, L. F., TOMANEK, L. & WILLIAMS, S. L. 2006. The impacts of climate change in coastal marine systems. *Ecology Letters*, 9, 228-241.
- HATCHER, A. 1989. RQ OF BENTHIC MARINE-INVERTEBRATES. *Marine Biology*, 102, 445-452.
- HATCHER, B. G. 1988. CORAL-REEF PRIMARY PRODUCTIVITY - A BEGGARS BANQUET. *Trends in Ecology & Evolution*, 3, 106-111.

- HAWKINS, C. M. & LEWIS, J. B. 1982. Benthic primary production on a fringing coral reef in barbados, West Indies. *Aquatic Botany*, 12, 355-363.
- HAWKINS, S. J., SOUTHWARD, A. J. & GENNER, M. J. 2003. Detection of environmental change in a marine ecosystem - evidence from the western English Channel. *Science of the Total Environment*, 310, 245-256.
- HEDLEY, J. & MUMBY, P. 2002. Biological and remote sensing perspectives of pigmentation in coral reef organisms. *Adv Mar Biol*, 43, 277 - 317.
- HENDRICK, V. J., FOSTER-SMITH, R. L. & DAVIES, A. J. 2011. Biogenic Reefs and the Marine Aggregate Industry. *Marine ALSF Science Monograph Series No. 3. MEPPF 10/P149. (Edited by R.C. Newell & J. Measures). 60pp. ISBN: 978 0 907545 46 0.*
- HENDRIKS, I. E., OLSEN, Y. S., RAMAJO, L., BASSO, L., STECKBAUER, A., MOORE, T. S., HOWARD, J. & DUARTE, C. M. 2014. Photosynthetic activity buffers ocean acidification in seagrass meadows. *Biogeosciences*, 11, 333-346.
- HENNIGE, S., SMITH, D., PERKINS, R., CONSALVEY, M., PATERSON, D. & SUGGETT, D. 2008. Photoacclimation, growth and distribution of massive coral species in clear and turbid waters. *Mar Ecol Prog Ser*, 369, 77 - 88.
- HENNIGE, S. J., SMITH, D. J., WALSH, S.-J., MCGINLEY, M. P., WARNER, M. E. & SUGGETT, D. J. 2010. Acclimation and adaptation of scleractinian coral communities along environmental gradients within an Indonesian reef system. *Journal of Experimental Marine Biology and Ecology*, 391, 143-152.
- HENNIGE, S. J., WICKS, L. C., KAMENOS, N. A., BAKKER, D. C. E., FINDLAY, H. S., DUMOUSSEAUD, C. & ROBERTS, J. M. 2014. Short-term metabolic and growth responses of the cold-water coral *Lophelia pertusa* to ocean acidification. *Deep-Sea Research Part II-Topical Studies in Oceanography*, 99, 27-35.
- HENRY, L.-A., NAVAS, J. M., HENNIGE, S. J., WICKS, L. C., VAD, J. & MURRAY ROBERTS, J. 2013. Cold-water coral reef habitats benefit recreationally valuable sharks. *Biological Conservation*, 161, 67-70.
- HENRY, L.-A. & ROBERTS, J. M. 2007. Biodiversity and ecological composition of macrobenthos on cold-water coral mounds and adjacent off-mound habitat in the bathyal Porcupine Seabight, NE Atlantic. *Deep-Sea Research Part I-Oceanographic Research Papers*, 54, 654-672.
- HEPBURN, C. D., PRITCHARD, D. W., CORNWALL, C. E., MCLEOD, R. J., BEARDALL, J., RAVEN, J. A. & HURD, C. L. 2011. Diversity of carbon use strategies in a kelp forest community: implications for a high CO₂ ocean. *Global Change Biology*, 17, 2488-2497.
- HETZINGER, S., HALFAR, J., KRONZ, A., STENECK, R. S., ADEY, W., LEBEDNIK, P. A. & SCHOENE, B. R. 2009. HIGH-RESOLUTION MG/CA RATIOS IN A CORALLINE RED ALGA AS A PROXY FOR BERING SEA TEMPERATURE VARIATIONS FROM 1902 TO 1967. *Palaios*, 24, 406-412.
- HILLIS-COLINVAUX, L. 1986. Historical perspectives on algae and reefs: have reefs been misnamed? *Oceanus*, 29, 43-49.
- HOFMANN, L. C., STRAUB, S. & BISCHOF, K. 2012a. Competition between calcifying and noncalcifying temperate marine macroalgae under elevated CO₂ levels. *Marine Ecology Progress Series*, 464, 89-105.
- HOFMANN, L. C., STRAUB, S. & BISCHOF, K. 2013. Elevated CO₂ levels affect the activity of nitrate reductase and carbonic anhydrase in the calcifying rhodophyte *Corallina officinalis*. *Journal of Experimental Botany*, 64, 899-908.
- HOFMANN, L. C., YILDIZ, G., HANELT, D. & BISCHOF, K. 2012b. Physiological responses of the calcifying rhodophyte, *Corallina officinalis* (L.), to future CO₂ levels. *Marine Biology*, 159, 783-792.

- HOLADAY, A. S. 1992. Changes in the activities of enzymes of carbin metabolism in leaves during exposure of plants to low temperature. *Plant Physiology*, 98, 1105-1114.
- HOLM-HANSEN, O. 1970. ATP levels in algal cells as influenced by environmental conditions. *Plant and Cell Physiology*, 11, 689-700.
- HOLT, T. J., REES, E. I., HAWKINS, S. J. & SEED, R. 1998. Biogenic Reefs (volume IX). An overview of dynamic and sensitivity characteristics for conservation management of marine SACs. Scottish Association for Marine Science (UK Marine SACs Project).
- HUSEBO, A., NOTTESTAD, L., FOSSA, J. H., FUREVIK, D. M. & JORGENSEN, S. B. 2002. Distribution and abundance of fish in deep-sea coral habitats. *Hydrobiologia*, 471, 91-99.
- IPCC 2013. Climate Change 2013: The Physical Science Basis, Contribution of Working Group I to the Fifth Assessment Report of the Intergovernmental Panel on Climate Change [Stocker, T.F., D. Qin, G-K. Plattner, M. Tignor, S.K. Allen, J. Boschung, A. Nauels, Y. Xia, V. Bex and P.M. Midgley (eds.)]. *Cambridge University Press, Cambridge, United Kingdom and New York, NY, USA, 1535 pp.*
- ISRAEL, A. & HOPHY, M. 2002. Growth, photosynthetic properties and Rubisco activities and amounts of marine macroalgae grown under current and elevated seawater CO₂ concentrations. *Global Change Biology*, 8, 831-840.
- JASSBY, A. D. & PLATT, T. 1976. MATHEMATICAL FORMULATION OF RELATIONSHIP BETWEEN PHOTOSYNTHESIS AND LIGHT FOR PHYTOPLANKTON. *Limnology and Oceanography*, 21, 540-547.
- JENSEN, R. G. 2000. Activation of Rubisco regulates photosynthesis at high temperature and CO₂. *Proceedings of the National Academy of Sciences*, 97, 12937-12938.
- JOHNSON, J. E. & HOLBROOK, N. J. 2014. Adaptation of Australia's Marine Ecosystems to Climate Change: Using Science to Inform Conservation Management. *International Journal of Ecology*, 1-12.
- JOHNSON, K. M., KING, A. E. & SIEBURTH, J. M. 1985. Coulometric TCO₂ analyses for marine studies; an introduction. *Marine Chemistry*, 16, 61-82.
- JOHNSON, M. D., MORIARTY, V. W. & CARPENTER, R. C. 2014. Acclimatization of the Crustose Coralline Alga *Porolithon onkodes* to Variable pCO₂. *Plos One*, 9.
- JOHNSON, V. R., RUSSELL, B. D., FABRICIUS, K. E., BROWNLEE, C. & HALL-SPENCER, J. M. 2012. Temperate and tropical brown macroalgae thrive, despite decalcification, along natural CO₂ gradients. *Global Change Biology*, 18, 2792-2803.
- JOKIEL, P. L. 2011. OCEAN ACIDIFICATION AND CONTROL OF REEF CORAL CALCIFICATION BY BOUNDARY LAYER LIMITATION OF PROTON FLUX. *Bulletin of Marine Science*, 87, 639-657.
- JONSSON, L. G., NILSSON, P. G., FLORUTA, F. & LUNDALV, T. 2004. Distributional patterns of macro- and megafauna associated with a reef of the cold-water coral *Lophelia pertusa* on the Swedish west coast. *Marine Ecology Progress Series*, 284, 163-171.
- KAMENOS, N., STRONG, S., SHENOY, D., WILSON, S., HATTON, A. & MOORE, P. 2008a. Red coralline algae as a source of marine biogenic dimethylsulphoniopropionate. *Mar Ecol Prog Ser*, 372, 61 - 66.
- KAMENOS, N. A., BURDETT, H. L., ALOISIO, E., FINDLAY, H. S., MARTIN, S., LONGBONE, C., DUNN, J., WIDDICOMBE, S. & CALOSI, P. 2013. Coralline algal structure is more sensitive to rate, rather than the magnitude, of ocean acidification. *Global Change Biology*, 19, 3621-3628.

- KAMENOS, N. A., CUSACK, M. & MOORE, P. G. 2008b. Coralline algae are global palaeothermometers with bi-weekly resolution. *Geochimica Et Cosmochimica Acta*, 72, 771-779.
- KAMENOS, N. A., HOEY, T. B., NIENOW, P., FALLICK, A. E. & CLAVERIE, T. 2012. Reconstructing Greenland ice sheet runoff using coralline algae. *Geology*, 40, 1095-1098.
- KAMENOS, N. A. & LAW, A. 2010. TEMPERATURE CONTROLS ON CORALLINE ALGAL SKELETAL GROWTH1. *Journal of Phycology*, 46, 331-335.
- KAMENOS, N. A., MOORE, P. G. & HALL-SPENCER, J. M. 2004a. Maerl grounds provide both refuge and high growth potential for juvenile queen scallops (*Aequipecten opercularis* L.). *Journal of Experimental Marine Biology and Ecology*, 313, 241-254.
- KAMENOS, N. A., MOORE, P. G. & HALL-SPENCER, J. M. 2004b. Nursery-area function of maerl grounds for juvenile queen scallops *Aequipecten opercularis* and other invertebrates. *Marine Ecology Progress Series*, 274, 183-189.
- KAYANNE, H., SUZUKI, A. & SAITO, H. 1995. DIURNAL CHANGES IN THE PARTIAL-PRESSURE OF CARBON-DIOXIDE IN CORAL-REEF WATER. *Science*, 269, 214-216.
- KEELING, R. F., PIPER, S. C., BOLLENBACHER, A. F. & WALKER, J. M. 2008. *Atmospheric CO2 records from sites in the SIO air sampling network.*, Carbon Dioxide Information Analysis Center, Oak Ridge National Laboratory, US Department of Energy, Oak Ridge, TN, USA.
- KEY, R. M., KOZYZR, A., SABINE, C. L., LEE, K., WANNINKHOF, R., BULLISTER, J. L., FEELY, R. A., MILLERO, F. J., MORDY, C. & PENG, T. H. 2004. A global ocean carbon climatology: Results from Global Data Analysis Project (GLODAP). *Global Biogeochemical Cycles*, 18.
- KHATIWALA, S., TANHUA, T., FLETCHER, S. M., GERBER, M., DONEY, S. C., GRAVEN, H. D., GRUBER, N., MCKINLEY, G. A., MURATA, A., RIOS, A. F. & SABINE, C. L. 2013. Global ocean storage of anthropogenic carbon. *Biogeosciences*, 10, 2169-2191.
- KIRK, J. T. O. 2011. *Light and photosynthesis in aquatic ecosystems; Third edition.*, Cambridge university press.
- KIRSCHENBAUM, D. M. 1975. MOLAR ABSORPTIVITY AND A-1CM (1 PERCENT) VALUES FOR PROTEINS AT SELECTED WAVELENGTHS OF ULTRAVIOLET AND VISIBLE REGIONS .11. *Analytical Biochemistry*, 68, 465-484.
- KLEYPAS, J. A., ANTHONY, K. R. N. & GATTUSO, J. P. 2011. Coral reefs modify their seawater carbon chemistry - case study from a barrier reef (Moorea, French Polynesia). *Global Change Biology*, 17, 3667-3678.
- KNOLL, A. H., BARNBACH, R. K., PAYNE, J. L., PRUSS, S. & FISCHER, W. W. 2007. Paleophysiology and end-Permian mass extinction. *Earth and Planetary Science Letters*, 256, 295-313.
- KOBZA, J. & EDWARDS, G. E. 1987. Influences of leaf temperature on photosynthetic carbon metabolism in wheat. *Plant Physiology*, 83, 69-74.
- KOCH, M., BOWES, G., ROSS, C. & ZHANG, X.-H. 2013. Climate change and ocean acidification effects on seagrasses and marine macroalgae. *Global Change Biology*, 19, 103-132.
- KREGEL, K. C. 2002. Heat shock proteins: modifying factors in physiological stress responses and acquired thermotolerance. *Journal of Applied Physiology*, 92, 2177-2186.
- KROEKER, K. J., GAMBI, M. C. & MICHELI, F. 2013a. Community dynamics and ecosystem simplification in a high-CO2 ocean. *Proceedings of the National Academy of Sciences of the United States of America*, 110, 12721-12726.

- KROEKER, K. J., KORDAS, R. L., CRIM, R., HENDRIKS, I. E., RAMAJO, L., SINGH, G. S., DUARTE, C. M. & GATTUSO, J.-P. 2013b. Impacts of ocean acidification on marine organisms: quantifying sensitivities and interaction with warming. *Global Change Biology*, 19, 1884-1896.
- KROEKER, K. J., MICHELI, F. & GAMBI, M. C. 2013c. Ocean acidification causes ecosystem shifts via altered competitive interactions. *Nature Clim. Change*, 3, 156-159.
- KROMKAMP, J. C. & FORSTER, R. M. 2003. The use of variable fluorescence measurements in aquatic ecosystems: differences between multiple and single turnover measuring protocols and suggested terminology. *European Journal of Phycology*, 38, 103-112.
- KRUGER, N. J. 2009. The Bradford Method For Protein Quantitation. In: WALKER, J. M. (ed.) *Protein Protocols Handbook, Third Edition*.
- KRUMHANS, K. A. & SCHEIBLING, R. E. 2012. Production and fate of kelp detritus. *Marine Ecology Progress Series*, 467, 281-302.
- KUBLER, J. E., JOHNSTON, A. M. & RAVEN, J. A. 1999. The effects of reduced and elevated CO₂ and O₂ on the seaweed *Lomentaria articulata*. *Plant Cell and Environment*, 22, 1303-1310.
- KUEBLER, J. E., DAVISON, I. R. & YARISH, C. 1991. PHOTOSYNTHETIC ADAPTATION TO TEMPERATURE IN THE RED ALGAE LOMENTARIA-BAILEYANA AND LOMENTARIA-ORCADENSIS. *British Phycological Journal*, 26, 9-19.
- KUFFNER, I. B., ANDERSSON, A. J., JOKIEL, P. L., RODGERS, K. S. & MACKENZIE, F. T. 2008. Decreased abundance of crustose coralline algae due to ocean acidification. *Nature Geoscience*, 1, 114-117.
- KURSAR, T. A. & ALBERTE, R. S. 1983. Photosynthetic Unit Organization in a Red Alga Relationships between Light-Harvesting Pigments and Reaction Centers. *Plant physiology*, 72, 409-414.
- LANE, T. W., SAITO, M. A., GEORGE, G. N., PICKERING, I. J., PRINCE, R. C. & MOREL, F. M. M. 2005. Biochemistry A cadmium enzyme from a marine diatom. *Nature*, 435, 42-42.
- LAVIGNE, M., FIELD, M. P., ANAGNOSTOU, E., GROTTOLI, A. G., WELLINGTON, G. M. & SHERRELL, R. M. 2008. Skeletal P/Ca tracks upwelling in Gulf of Panama coral: Evidence for a new seawater phosphate proxy. *Geophysical Research Letters*, 35.
- LE QUERE, C. 2010. Trends in the land and ocean carbon uptake. *Current Opinion in Environmental Sustainability*, 2, 219-224.
- LE QUERE, C., RAUPACH, M. R., CANADELL, J. G., MARLAND, G. & ET AL. 2009. Trends in the sources and sinks of carbon dioxide. *Nature Geosci*, 2, 831-836.
- LE QUERE, C., TAKAHASHI, T., BUITENHUIS, E. T., ROEDENBECK, C. & SUTHERLAND, S. C. 2010. Impact of climate change and variability on the global oceanic sink of CO₂. *Global Biogeochemical Cycles*, 24.
- LEAKEY, A. D. B., AINSWORTH, E. A., BERNACCHI, C. J., ROGERS, A., LONG, S. P. & ORT, D. R. 2009. Elevated CO₂ effects on plant carbon, nitrogen, and water relations: six important lessons from FACE. *Journal of Experimental Botany*, 60, 2859-2876.
- LEVITUS, S., ANTONOV, J. I., BOYER, T. P., BARANOVA, O. K., GARCIA, H. E., LOCARNINI, R. A., MISHONOV, A. V., REAGAN, J. R., SEIDOV, D., YAROSH, E. S. & ZWENG, M. M. 2012. World ocean heat content and thermosteric sea level change (0-2000 m), 1955-2010. *Geophysical Research Letters*, 39.
- LEVITUS, S., ANTONOV, J. I., BOYER, T. P., LOCARNINI, R. A., GARCIA, H. E. & MISHONOV, A. V. 2009. Global ocean heat content 1955-2008 in light of recently revealed instrumentation problems. *Geophysical Research Letters*, 36.

- LEWIS, S. M. & WAINWRIGHT, P. C. 1985. HERBIVORE ABUNDANCE AND GRAZING INTENSITY ON A CARIBBEAN CORAL-REEF. *Journal of Experimental Marine Biology and Ecology*, 87, 215-228.
- LIN, M. T., OCCHIALINI, A., ANDRALOJC, P. J., PARRY, M. A. & HANSON, M. R. 2014. A faster Rubisco with potential to increase photosynthesis in crops. *Nature*, 513, 547-550.
- LORIMER, G. H. 1981. THE CARBOXYLATION AND OXYGENATION OF RIBULOSE 1,5-BISPHOSPHATE - THE PRIMARY EVENTS IN PHOTOSYNTHESIS AND PHOTO-RESPIRATION. *Annual Review of Plant Physiology and Plant Molecular Biology*, 32, 349-383.
- LOWRY, O. H., ROSEBROUGH, N. J., FARR, A. L. & RANDALL, R. J. 1951. PROTEIN MEASUREMENT WITH THE FOLIN PHENOL REAGENT. *Journal of Biological Chemistry*, 193, 265-275.
- LUEKER, T. J., DICKSON, A. G. & KEELING, C. D. 2000. Ocean pCO₂ calculated from dissolved inorganic carbon, alkalinity, and equations for K-1 and K-2: validation based on laboratory measurements of CO₂ in gas and seawater at equilibrium. *Marine Chemistry*, 70, 105-119.
- LUTHI, D., LE FLOCH, M., BEREITER, B., BLUNIER, T., BARNOLA, J.-M., SIEGENTHALER, U., RAYNAUD, D., JOUZEL, J., FISCHER, H., KAWAMURA, K. & STOCKER, T. F. 2008. High-resolution carbon dioxide concentration record 650,000-800,000[thinsp]years before present. *Nature*, 453, 379-382.
- MACCOLL, R., EISELE, L. E., WILLIAMS, E. C. & BOWSER, S. S. 1996. The Discovery of a Novel R-phycoerythrin from an Antarctic Red Alga. *Journal of Biological Chemistry*, 271, 17157-17160.
- MADSHUS, I. H. 1988. Regulation of intracellular pH in eukaryotic celss. *Biochemistry Journal*, 250, 1-8.
- MAIER, C., BILS, F., WEINBAUER, M. G., WATREMEZ, P., PECK, M. A. & GATTUSO, J. P. 2013a. Respiration of Mediterranean cold-water corals is not affected by ocean acidification as projected for the end of the century. *Biogeosciences*, 10, 5671-5680.
- MAIER, C., HEGEMAN, J., WEINBAUER, M. G. & GATTUSO, J.-P. 2009. Seawater carbonate chemistry and calcification of *Lophelia pertusa* during experiments, 2009. *Pangaea*.
- MAIER, C., SCHUBERT, A., SANCHEZ, M. M. B., WEINBAUER, M. G., WATREMEZ, P. & GATTUSO, J.-P. 2013b. End of the Century pCO₂ Levels Do Not Impact Calcification in Mediterranean Cold-Water Corals. *Plos One*, 8.
- MAIER, C., WATREMEZ, P., TAVIANI, M., WEINBAUER, M. G. & GATTUSO, J. P. 2012. Calcification rates and the effect of ocean acidification on Mediterranean cold-water corals. *Proceedings of the Royal Society B-Biological Sciences*, 279, 1716-1723.
- MANN, S. 1988. MOLECULAR RECOGNITION IN BIOMINERALIZATION. *Nature*, 332, 119-124.
- MANZELLO, D. P. 2010. Ocean acidification hot spots: Spatiotemporal dynamics of the seawater CO₂ system of eastern Pacific coral reefs. *Limnology and Oceanography*, 55, 239-248.
- MARTIN, S., CASTETS, M.-D. & CLAVIER, J. 2006. Primary production, respiration and calcification of the temperate free-living coralline alga *Lithothamnion corallioides*. *Aquatic Botany*, 85, 121-128.
- MARTIN, S., CHARNOZ, A. & GATTUSO, J.-P. 2013a. Photosynthesis, respiration and calcification in the Mediterranean crustose coralline alga *Lithophyllum cabiochae* (Corallinales, Rhodophyta). *European Journal of Phycology*, 48, 163-172.

- MARTIN, S., COHU, S., VIGNOT, C., ZIMMERMAN, G. & GATTUSO, J. P. 2013b. One-year experiment on the physiological response of the Mediterranean crustose coralline alga, *Lithophyllum cabiochae*, to elevated pCO₂ and temperature. *Ecology and Evolution*, 3, 676-693.
- MARTIN, S. & GATTUSO, J.-P. 2009. Response of Mediterranean coralline algae to ocean acidification and elevated temperature. *Global Change Biology*, 15, 2089-2100.
- MAXWELL, K. & JOHNSON, G. N. 2000. Chlorophyll fluorescence - a practical guide. *Journal of Experimental Botany*, 51, 659-668.
- MCCOOK, L., JOMPA, J. & DIAZ-PULIDO, G. 2001. Competition between corals and algae on coral reefs: a review of evidence and mechanisms. *Coral Reefs*, 19, 400-417.
- MCCOY, S. J. & RAGAZZOLA, F. 2014. Skeletal trade-offs in coralline algae in response to ocean acidification. *Nature Clim. Change*, 4, 719-723.
- MCCULLOCH, M., FALTER, J., TROTTER, J. & MONTAGNA, P. 2012a. Coral resilience to ocean acidification and global warming through pH up-regulation. *Nature Climate Change*, 2, 623-633.
- MCCULLOCH, M., TROTTER, J., MONTAGNA, P., FALTER, J., DUNBAR, R., FREIWALD, A., FÖRSTERRA, G., LÓPEZ CORREA, M., MAIER, C., RÜGGERBERG, A. & TAVIANI, M. 2012b. Resilience of cold-water scleractinian corals to ocean acidification: Boron isotopic systematics of pH and saturation state up-regulation. *Geochimica et Cosmochimica Acta*, 87, 21-34.
- MCGRATH, T., KIVIMAE, C., TANHUA, T., CAVE, R. R. & MCGOVERN, E. 2012. Inorganic carbon and pH levels in the Rockall Trough 1991-2010. *Deep-Sea Research Part I-Oceanographic Research Papers*, 68, 79-91.
- MEEHL, G. A., STOCKER T F, COLLINS W D, FRIEDLINGSTEIN P, GAYE A, GREGORY J, KITO A, KNUTTI R, MURPHY J, NODA A, RAPER S, WATTERSON I, WEAVER A & ZHAO Z 2007. Global Climate Projections. In: *Climate Change 2007: The Physical Science Basis. Contribution of Working Group I to the Fourth Assessment Report of the Intergovernmental Panel on Climate Change* [Solomon, S., D. Qin, M. Manning, Z. Chen, M. Marquis, K.B. Averyt, M. Tignor and H.L. Miller (eds.)]. *Cambridge University Press, Cambridge, United Kingdom and New York, USA*.
- MEHRBACH, C., CULBERSO, CH, HAWLEY, J. E. & PYTKOWIC, RM 1973. MEASUREMENT OF APPARENT DISSOCIATION-CONSTANTS OF CARBONIC-ACID IN SEAWATER AT ATMOSPHERIC-PRESSURE. *Limnology and Oceanography*, 18, 897-907.
- MERRETT, M. J., DONG, L. F. & NIMER, N. A. 1993. NITRATE AVAILABILITY AND CALCITE PRODUCTION IN EMILIANA-HUXLEYI LOHMANN. *European Journal of Phycology*, 28, 243-246.
- MIKKELSEN, A., ENGELSEN, S. B., HANSEN, H. C. B., LARSEN, O. & SKIBSTED, L. H. 1997. Calcium carbonate crystallization in the alpha-chitin matrix of the shell of pink shrimp, *Pandalus borealis*, during frozen storage. *Journal of Crystal Growth*, 177, 125-134.
- MILLIMAN, J. D. & MULLER, J. 1974. RELICT CARBONATE-RICH SEDIMENTS ON SOUTHWESTERN GRAND BANK, NEWFOUNDLAND - REPLY. *Canadian Journal of Earth Sciences*, 11, 1506-1506.
- MIMURO, M. & KIKUCHI, H. 2003. Antenna systems and energy transfer in cyanophyta and rhodophyta. *Light-Harvesting Antennas in Photosynthesis*. Springer.
- MORELL, M. K., PAUL, K., KANE, H. J. & ANDREWS, T. J. 1992. RUBISCO - MALADAPTED OR MISUNDERSTOOD. *Australian Journal of Botany*, 40, 431-441.

- MOVILLA, J., GORI, A., CALVO, E., OREJAS, C., LOPEZ-SANZ, A., DOMINGUEZ-CARRIO, C., GRINYO, J. & PELEJERO, C. 2014a. Resistance of Two Mediterranean Cold-Water Coral Species to Low-pH Conditions. *Water*, 6, 59-67.
- MOVILLA, J., OREJAS, C., CALVO, E., GORI, A., LOPEZ-SANZ, A., GRINYO, J., DOMINGUEZ-CARRIO, C. & PELEJERO, C. 2014b. Differential response of two Mediterranean cold-water coral species to ocean acidification. *Coral Reefs*, 33, 675-686.
- MOYA, A., HUISMAN, L., BALL, E. E., HAYWARD, D. C., GRASSO, L. C., CHUA, C. M., WOO, H. N., GATTUSO, J. P., FORET, S. & MILLER, D. J. 2013. Whole Transcriptome Analysis of the Coral *Acropora millepora* Reveals Complex Responses to CO₂-driven Acidification during the Initiation of Calcification. *Molecular Ecology*, 21, 2440-2454.
- MOYA, A., TAMBUTTE, S., BERTUCCI, A., TAMBUTTE, E., LOTTO, S., VULLO, D., SUPURAN, C. T., ALLEMAND, D. & ZOCCOLA, D. 2008. Carbonic anhydrase in the scleractinian coral *Stylophora pistillata* - Characterization, localization, and role in biomineralization. *Journal of Biological Chemistry*, 283, 25475-25484.
- MULLER, F. L. L. & BLEIE, B. 2008. Estimating the organic acid contribution to coastal seawater alkalinity by potentiometric titrations in a closed cell. *Analytica Chimica Acta*, 619, 183-191.
- MULLER, P., LI, X. P. & NIYOGI, K. K. 2001. Non-photochemical quenching. A response to excess light energy. *Plant Physiology*, 125, 1558-1566.
- MULTER, H. G. 1988. Growth rate, ultrastructure and sediment contribution of *Halimeda incrassata* and *Halimeda monile*, Nonsuch and Falmouth Bays, Antigua, W.I. *Coral Reefs*, 6, 179-186.
- MURPHY, D. M., SOLOMON, S., PORTMANN, R. W., ROSENLOF, K. H., FORSTER, P. M. & WONG, T. 2009. An observationally based energy balance for the Earth since 1950. *Journal of Geophysical Research-Atmospheres*, 114.
- MYERS, A. A. & HALL-SPENCER, J. M. 2004. A new species of amphipod crustacean, *Pleusymtes comitari* sp nov, associated with gorgonians on deep-water coral reefs off Ireland. *Journal of the Marine Biological Association of the United Kingdom*, 84, 1029-1032.
- NAKICENOVIC, N. 2000. Greenhouse gas emissions scenarios. *Technological Forecasting and Social Change*, 65, 149-166.
- NELSON, W. A. 2009. Calcified macroalgae – critical to coastal ecosystems and vulnerable to change: a review. *Marine and Freshwater Research*, 60, 787-801.
- NICHOLLS, R. J., WONG, P. P., BURKETT, V. R., CODIGNOTTO, J. O., HAY, J. E., MCLEAN, R. F., RAGOONADEN, S. & WOODROFFE, C. D. 2007. Coastal systems and low-lying areas. *Climate Change 2007: Impacts, Adaptation and Vulnerability. Contribution of Working Group II to the Fourth Assessment Report of the Intergovernmental Panel on Climate Change*, M.L. Parry, O.F. Canziani, J.P. Palutikof, P.J. van der Linden and C.E. Hanson, Eds., *Cambridge University Press, Cambridge, UK*, 315-356.
- NOISETTE, F., DUONG, G., SIX, C., DAVOULT, D. & MARTIN, S. 2013a. EFFECTS OF ELEVATED pCO₂ ON THE METABOLISM OF A TEMPERATE RHODOLITH LITHOTHAMNION CORALLIODES GROWN UNDER DIFFERENT TEMPERATURES. *Journal of Phycology*, 49, 746-757.
- NOISETTE, F., EGILSDOTTIR, H., DAVOULT, D. & MARTIN, S. 2013b. Physiological responses of three temperate coralline algae from contrasting habitats to near-future ocean acidification. *Journal of Experimental Marine Biology and Ecology*, 448, 179-187.

- OATES, B. R. & MURRAY, S. N. 1983. PHOTOSYNTHESIS, DARK RESPIRATION AND DESICCATION RESISTANCE OF THE INTERTIDAL SEaweEDS HESPEROPHYCUS-HARVEYANUS AND PELVETIA-FASTIGIATA F GRACILIS. *Journal of Phycology*, 19, 371-380.
- OHDE, S. & HOSSAIN, M. M. 2004. Seawater carbonate chemistry and calcification during an experiment with a coral *Porites lutea*, 2004. *Pangaea*.
- OHSAWA, N., OGATA, Y., OKADA, N. & ITOH, N. 2001. Physiological function of bromoperoxidase in the red marine alga, *Corallina pilulifera*: production of bromoform as an allelochemical and the simultaneous elimination of hydrogen peroxide. *Phytochemistry*, 58, 683-692.
- OLAFSSON, J., OLAFSDOTTIR, S. R., BENOIT-CATTIN, A., DANIELSEN, M., ARNARSON, T. S. & TAKAHASHI, T. 2009. Rate of Iceland Sea acidification from time series measurements. *Biogeosciences*, 6, 2661-2668.
- ORR, J. C., FABRY, V. J., AUMONT, O., BOPP, L., DONEY, S. C., FEELY, R. A., GNANADESIKAN, A., GRUBER, N., ISHIDA, A., JOOS, F., KEY, R. M., LINDSAY, K., MAIER-REIMER, E., MATEAR, R., MONFRAY, P., MOUCHET, A., NAJJAR, R. G., PLATTNER, G.-K., RODGERS, K. B., SABINE, C. L., SARMIENTO, J. L., SCHLITZER, R., SLATER, R. D., TOTTERDELL, I. J., WEIRIG, M.-F., YAMANAKA, Y. & YOOL, A. 2005. Anthropogenic ocean acidification over the twenty-first century and its impact on calcifying organisms. *Nature*, 437, 681-686.
- PALMISANO, A. C., SOOHOO, J. B. & SULLIVAN, C. W. 1987. EFFECTS OF 4 ENVIRONMENTAL VARIABLES ON PHOTOSYNTHESIS-IRRADIANCE RELATIONSHIPS IN ANTARCTIC SEA-ICE MICROALGAE. *Marine Biology*, 94, 299-306.
- PARKER, L. M., ROSS, P. M. & O'CONNOR, W. A. 2009. The effect of ocean acidification and temperature on the fertilization and embryonic development of the Sydney rock oyster *Saccostrea glomerata* (Gould 1850). *Global Change Biology*, 15, 2123-2136.
- PARMESAN, C. & YOHE, G. 2003. A globally coherent fingerprint of climate change impacts across natural systems. *Nature*, 421, 37-42.
- PASCAL, A. A., LIU, Z., BROESS, K., VAN OORT, B., VAN AMERONGEN, H., WANG, C., HORTON, P., ROBERT, B., CHANG, W. & RUBAN, A. 2005. Molecular basis of photoprotection and control of photosynthetic light-harvesting. *Nature*, 436, 134-137.
- PAUL, A. & SCHAFER-NETH, C. 2003. Modeling the water masses of the Atlantic Ocean at the Last Glacial Maximum. *Paleoceanography*, 18.
- PAYRI, C. E. 2000. Primary production and calcification of coral reef benthic algae. *Oceanis*, 26, 427-463.
- PENA, V. & BARBARA, I. 2008. Biological importance of an Atlantic European maerl bed off Benencia Island (northwest Iberian Peninsula). *Botanica Marina*, 51, 493-505.
- PENTECOST, A. 1978. CALCIFICATION AND PHOTOSYNTHESIS IN CORALLINA-OFFICINALIS L USING (CO₂)-C-14 METHOD. *British Phycological Journal*, 13, 383-390.
- PETIT, M. 2001. Mankind facing the additional anthropogenic greenhouse warming. *Comptes Rendus De L Academie Des Sciences Serie Ii Fascicule a-Sciences De La Terre Et Des Planetes*, 333, 775-786.
- PIERROT, D., LEWIS, E. & WALLACE, D. 2006. DOS Program developed for CO₂ system calculations. ORNL/CDIAC-105. Carbon Dioxide Information Center, Oak Ridge National Laboratory, US Department of Energy, Oak Ridge, TN.

- PLATTNER, G. K., JOOS, F., STOCKER, T. F. & MARCHAL, O. 2001. Feedback mechanisms and sensitivities of ocean carbon uptake under global warming. *Tellus Series B-Chemical and Physical Meteorology*, 53, 564-592.
- PORRA, R. J., THOMPSON, W. A. & KRIEDEMANN, P. E. 1989. DETERMINATION OF ACCURATE EXTINCTION COEFFICIENTS AND SIMULTANEOUS-EQUATIONS FOR ASSAYING CHLOROPHYLL-A AND CHLOROPHYLL-B EXTRACTED WITH 4 DIFFERENT SOLVENTS - VERIFICATION OF THE CONCENTRATION OF CHLOROPHYLL STANDARDS BY ATOMIC-ABSORPTION SPECTROSCOPY. *Biochimica Et Biophysica Acta*, 975, 384-394.
- PORTNER, H. O., LANGENBUCH, M. & REIPSCHLAGER, A. 2004. Biological impact of elevated ocean CO₂ concentrations: Lessons from animal physiology and earth history. *Journal of Oceanography*, 60, 705-718.
- PORZIO, L., BUIA, M. C. & HALL-SPENCER, J. 2011. Macroalgal communities of gas vents near Ischia island in the Mediterranean sea. *Pangaea*.
- POSTGATE, J. R. 1982. The fundamentals of Nitrogen Fixation. *Cambridge University Press, Cambridge*.
- POTIN, P., FLOCH, J. Y., AUGRIS, C. & CABIOCH, J. 1990. Annual growth rate of the calcareous red alga *Lithothamnion corallioides* (Corallinales, Rhodophyta) in the Bay of Brest, France. In: LINDSTROM, S. & GABRIELSON, P. (eds.) *Thirteenth International Seaweed Symposium*. Springer Netherlands.
- PRICE, N. N., HAMILTON, S. L., TOOTELL, J. S. & SMITH, J. E. 2011. Species-specific consequences of ocean acidification for the calcareous tropical green algae *Halimeda*. *Marine Ecology Progress Series*, 440, 67-78.
- PRICE, N. N., MARTZ, T. R., BRAINARD, R. E. & SMITH, J. E. 2012. Diel Variability in Seawater pH Relates to Calcification and Benthic Community Structure on Coral Reefs. *PLoS ONE*, 7, e43843.
- PUVEREL, S., HOULBRÄQUE, F., TAMBUTTÀ, E., ZOCCOLA, D., PAYAN, P., CAMINITI, N., TAMBUTTÀ, S. & ALLEMAND, D. 2007. Evidence of low molecular weight components in the organic matrix of the reef building coral, *Stylophora pistillata*. *Comparative Biochemistry and Physiology Part A: Molecular & Integrative Physiology*, 147, 850-856.
- QUICK, W. P. & HORTON, P. 1984. STUDIES ON THE INDUCTION OF CHLOROPHYLL FLUORESCENCE IN BARLEY PROTOPLASTS .1. FACTORS AFFECTING THE OBSERVATION OF OSCILLATIONS IN THE YIELD OF CHLOROPHYLL FLUORESCENCE AND THE RATE OF OXYGEN EVOLUTION. *Proceedings of the Royal Society Series B-Biological Sciences*, 220, 361-370.
- RAGAZZOLA, F., FOSTER, L. C., FORM, A., ANDERSON, P. S. L., HANSTEEN, T. H. & FIETZKE, J. 2012. Ocean acidification weakens the structural integrity of coralline algae. *Global Change Biology*, 18, 2804-2812.
- RAGAZZOLA, F., FOSTER, L. C., FORM, A. U., BUESCHER, J., HANSTEEN, T. H. & FIETZKE, J. 2013. Phenotypic plasticity of coralline algae in a High CO₂ world. *Ecology and Evolution*, 3, 3436-3446.
- RAHMAN, M. A. & HALFAR, J. 2014. First evidence of chitin in calcified coralline algae: new insights into the calcification process of *Clathromorphum compactum*. *Scientific reports*, 4.
- RAHMAN, M. A., OOMORI, T. & UEHARA, T. 2008. Carbonic anhydrase in calcified endoskeleton: novel activity in biocalcification in alcyonarian. *Marine Biotechnology*, 10, 31-38.
- RAHMAN, M. A., OOMORI, T. & WOERHEIDE, G. 2011. Calcite Formation in Soft Coral Sclerites Is Determined by a Single Reactive Extracellular Protein. *Journal of Biological Chemistry*, 286, 31638-31649.

- RALPH, P. J. & GADEMANN, R. 2005. Rapid light curves: A powerful tool to assess photosynthetic activity. *Aquatic Botany*, 82, 222-237.
- RASCHER, U., LIEBIG, M. & LUTTGE, U. 2000. Evaluation of instant light-response curves of chlorophyll fluorescence parameters obtained with a portable chlorophyll fluorometer on site in the field. *Plant Cell and Environment*, 23, 1397-1405.
- RAVEN, J., CALDEIRA, K., ELDERFIELD, H., HOEGH-GULDBERG, O., LISS, P., RIEBESELL, U., SHEPHERD, J., TURLEY, C. & WATSON, A. 2005. *Ocean acidification due to increasing atmospheric carbon dioxide*, Royal Society Policy Document, Clyvedon Press, Cardiff, UK.
- RAVEN, J. & HURD, C. 2012a. Ecophysiology of photosynthesis in macroalgae. *Photosynthesis Research*, 113, 105-125.
- RAVEN, J. A. 2011. EFFECTS ON MARINE ALGAE OF CHANGED SEAWATER CHEMISTRY WITH INCREASING ATMOSPHERIC CO₂. *Biology and Environment-Proceedings of the Royal Irish Academy*, 111B, 1-17.
- RAVEN, J. A. & GEIDER, R. J. 1988. TEMPERATURE AND ALGAL GROWTH. *New Phytologist*, 110, 441-461.
- RAVEN, J. A., GIORDANO, M., BEARDALL, J. & MABERLY, S. C. 2011. Algal and aquatic plant carbon concentrating mechanisms in relation to environmental change. *Photosynthesis Research*, 109, 281-296.
- RAVEN, J. A. & HURD, C. L. 2012b. Ecophysiology of photosynthesis in macroalgae. *Photosynthesis Research*, 113, 105-125.
- REUM, J. C., ALIN, S. R., FEELY, R. A., NEWTON, J., WARNER, M. & MCELHANY, P. 2014. Seasonal carbonate chemistry covariation with temperature, oxygen, and salinity in a fjord estuary: implications for the design of ocean acidification experiments. *PLoS One*, 9, e89619.
- RIEBESELL, U., FABRY, V. J., HANSSON, L., GATTUSO, J.-P. & (EDS.) 2010. Guide to best practices for ocean acidification research and data reporting, 260 p. Luxembourg: . *Publications Office of the European Union*.
- RIES, J. B. 2011. Skeletal mineralogy in a high-CO₂ world. *Journal of Experimental Marine Biology and Ecology*, 403, 54-64.
- RIES, J. B., COHEN, A. L. & MCCORKLE, D. C. 2009. Marine calcifiers exhibit mixed responses to CO₂-induced ocean acidification. *Geology*, 37, 1131-1134.
- RIVKIN, R. B. 1990. PHOTOADAPTATION IN MARINE-PHYTOPLANKTON - VARIATIONS IN RIBULOSE 1,5-BISPHOSPHATE ACTIVITY. *Marine Ecology Progress Series*, 62, 61-72.
- RIX, L. N., BURDETT, H. L. & KAMENOS, N. A. 2012. Irradiance-mediated dimethylsulphoniopropionate (DMSP) responses of red coralline algae. *Estuarine, Coastal and Shelf Science*, 96, 268-272.
- ROBERTS, J. M., BROWN, C. J., LONG, D. & BATES, C. R. 2005. Acoustic mapping using a multibeam echosounder reveals cold-water coral reefs and surrounding habitats. *Coral Reefs*, 24, 654-669.
- ROBERTS, J. M., DAVIES, A. J., HENRY, L. A., DODDS, L. A., DUINEVELD, G. C. A., LAVALEYE, M. S. S., MAIER, C., VAN SOEST, R. W. M., BERGMAN, M. J. N., HUEHNERBACH, V., HUVENNE, V. A. I., SINCLAIR, D. J., WATMOUGH, T., LONG, D., GREEN, S. L. & VAN HAREN, H. 2009. Mingulay reef complex: an interdisciplinary study of cold-water coral habitat, hydrography and biodiversity. *Marine Ecology Progress Series*, 397, 139-151.
- ROBERTS, J. M., LONG, D., WILSON, J. B., MORTENSEN, P. B. & GAGE, J. D. 2003. The cold-water coral *Lophelia pertusa* (Scleractinia) and enigmatic seabed mounds along the north-east Atlantic margin: are they related? *Marine Pollution Bulletin*, 46, 7-20.

- ROBERTS, J. M., WHEELER, A. J. & FREIWALD, A. 2006. Reefs of the Deep: The Biology and Geology of Cold-Water Coral Ecosystems. *Science*, 312, 543-547.
- ROLEDA, M. Y., BOYD, P. W. & HURD, C. L. 2012. BEFORE OCEAN ACIDIFICATION: CALCIFIER CHEMISTRY LESSONS1. *Journal of Phycology*, 48, 840-843.
- ROOT, D. D. & WANG, K. 2009. Kinetic Silver Staining of Proteins. In: WALKER, J. M. (ed.) *Protein Protocols Handbook, Third Edition*.
- ROWAN, K. S. 1989. *PHOTOSYNTHETIC PIGMENTS OF ALGAE*, Cambridge University Press, Cambridge, New York.
- SABINE, C. L., FEELY, R. A., GRUBER, N., KEY, R. M., LEE, K., BULLISTER, J. L., WANNINKHOF, R., WONG, C. S., WALLACE, D. W. R., TILBROOK, B., MILLERO, F. J., PENG, T.-H., KOZYR, A., ONO, T. & RIOS, A. F. 2004. The Oceanic Sink for Anthropogenic CO₂. *Science*, 305, 367-371.
- SAIKKONEN, K., TAULAVUORI, K., HYVONEN, T., GUNDEL, P. E., HAMILTON, C. E., VANNINEN, I., NISSINEN, A. & HELANDER, M. 2012. Climate change-driven species' range shifts filtered by photoperiodism. *Nature Climate Change*, 2, 239-242.
- SANTANA-CASIANO, J. M., GONZALEZ-DAVILA, M., RUEDA, M.-J., LLINAS, O. & GONZALEZ-DAVILA, E.-F. 2007. The interannual variability of oceanic CO₂ parameters in the northeast Atlantic subtropical gyre at the ESTOC site. *Global Biogeochemical Cycles*, 21.
- SCAVIA, D., FIELD, J. C., BOESCH, D. F., BUDDEMEIER, R. W., BURKETT, V., CAYAN, D. R., FOGARTY, M., HARWELL, M. A., HOWARTH, R. W., MASON, C., REED, D. J., ROYER, T. C., SALLENGER, A. H. & TITUS, J. G. 2002. Climate change impacts on US coastal and marine ecosystems. *Estuaries*, 25, 149-164.
- SCHREIBER, U. 2004. Pulse-amplitude-modulation (PAM) fluorometry and saturation pulse method: An overview. *Chlorophyll a Fluorescence: Signature of Photosynthesis*, 19, 279-+.
- SCIANDRA, A., HARLAY, J., LEFEVRE, D., LEMEE, R., RIMMELIN, P., DENIS, M. & GATTUSO, J. P. 2003. Response of coccolithophorid *Emiliania huxleyi* to elevated partial pressure of CO₂ under nitrogen limitation. *Marine Ecology Progress Series*, 261, 111-122.
- SEMESI, I. S., KANGWE, J. & BJORK, M. 2009. Alterations in seawater pH and CO₂ affect calcification and photosynthesis in the tropical coralline alga, *Hydrolithon* sp (Rhodophyta). *Estuarine Coastal and Shelf Science*, 84, 337-341.
- SHAW, E. C., MCNEIL, B. I. & TILBROOK, B. 2012. Impacts of ocean acidification in naturally variable coral reef flat ecosystems. *Journal of Geophysical Research: Oceans*, 117, C03038.
- SHERWOOD, O. A., HEIKOOP, J. M., SINCLAIR, D. J., SCOTT, D. B., RISK, M. J., SHEARER, C. & AZETSU-SCOTT, K. 2005a. *Skeletal Mg/Ca in *Primnoa resedaeformis*: relationship to temperature?*
- SHERWOOD, O. A., SCOTT, D. B., RISK, M. J. & GUILDERSON, T. P. 2005b. Radiocarbon evidence for annual growth rings in the deep-sea octocoral *Primnoa resedaeformis*. *Marine Ecology Progress Series*, 301, 129-134.
- SHORT, F. T. & NECKLES, H. A. 1999. The effects of global climate change on seagrasses. *Aquatic Botany*, 63, 169-196.
- SILVERMAN, J., LAZAR, B. & EREZ, J. 2007a. Community metabolism of a coral reef exposed to naturally varying dissolved inorganic nutrient loads. *Biogeochemistry*, 84, 67-82.
- SILVERMAN, J., LAZAR, B. & EREZ, J. 2007b. Effect of aragonite saturation, temperature, and nutrients on the community calcification rate of a coral reef. *Journal of Geophysical Research-Oceans*, 112.

- SINUTOK, S., HILL, R., DOBLIN, M. A., WUHRER, R. & RALPH, P. J. 2011. Warmer more acidic conditions cause decreased productivity and calcification in subtropical coral reef sediment-dwelling calcifiers. *Limnology and Oceanography*, 56, 1200-1212.
- SMITH, J. E., SCHWARCZ, H. P., RISK, M. J., MCCONNAUGHEY, T. A. & KELLER, N. 2000. Paleotemperatures from deep-sea corals: Overcoming 'vital effects'. *Palaios*, 15, 25-32.
- SMITH, P. K., KROHN, R. I., HERMANSON, G. T., MALLIA, A. K., GARTNER, F. H., PROVENZANO, M. D., FUJIMOTO, E. K., GOEKE, N. M., OLSON, B. J. & KLENK, D. C. 1985. MEASUREMENT OF PROTEIN USING BICINCHONINIC ACID. *Analytical Biochemistry*, 150, 76-85.
- SMITH, S. V. & KEY, G. S. 1975. CARBON-DIOXIDE AND METABOLISM IN MARINE ENVIRONMENTS. *Limnology and Oceanography*, 20, 493-495.
- SOLOMON, S., QIN, D., MANNING, M., CHEN, Z., MARQUIS, M., AVERYT, K. B., TIGNOR, M. & MILLER, H. L. 2007. *Contribution of Working Group I to the Fourth Assessment Report of the Intergovernmental Panel on Climate Change*, Cambridge, United Kingdom and New York, USA, Cambridge University Press.
- STANLEY, G. D. 1981. Early history of scleractinian corals and its geological consequences. *Geology*, 9, 507-511.
- STEEMANN NIELSEN, E. 1975. Marine photosynthesis with special emphasis on the ecological aspects. *Elsevier oceanogr Ser*, 13, 1-141.
- STEINACHER, M., JOOS, F., FROELICHER, T. L., PLATTNER, G. K. & DONEY, S. C. 2009. Imminent ocean acidification in the Arctic projected with the NCAR global coupled carbon cycle-climate model. *Biogeosciences*, 6, 515-533.
- STELLER, D. L., RIOSMENA-RODRIGUEZ, R., FOSTER, M. S. & ROBERTS, C. A. 2003. Rhodolith bed diversity in the Gulf of California: the importance of rhodolith structure and consequences of disturbance. *Aquatic Conservation-Marine and Freshwater Ecosystems*, 13, S5-S20.
- STILLMAN, J. H. 2003. Acclimation Capacity Underlies Susceptibility to Climate Change. *Science*, 301, 65.
- STITT, M., GERHARDT, R., WILKE, I. & HELDT, H. W. 1987. THE CONTRIBUTION OF FRUCTOSE 2,6-BISPHOSPHATE TO THE REGULATION OF SUCROSE SYNTHESIS DURING PHOTOSYNTHESIS. *Physiologia Plantarum*, 69, 377-386.
- STONE, L., HUPPERT, A., RAJAGOPALAN, B., BHASIN, H. & LOYA, Y. 1999. Mass coral reef bleaching: A recent outcome of increased El Nino activity? *Ecology Letters*, 2, 325-330.
- STOSCHECK, C. M. 1990. INCREASED UNIFORMITY IN THE RESPONSE OF THE COOMASSIE BLUE G-PROTEIN ASSAY TO DIFFERENT PROTEINS. *Analytical Biochemistry*, 184, 111-116.
- SUGGETT, D. J., LE FLOCH, E., HARRIS, G. N., LEONARDOS, N. & GEIDER, R. J. 2007. Different strategies of photoacclimation by two strains of *Emiliana huxleyi* (Haptophyta). *Journal of Phycology*, 43, 1209-1222.
- TAMBUTTE, S., TAMBUTTE, E., ZOCCOLA, D., CAMINITI, N., LOTTO, S., MOYA, A., ALLEMAND, D. & ADKINS, J. 2007. Characterization and role of carbonic anhydrase in the calcification process of the azooxanthellate coral *Tubastrea aurea*. *Marine Biology*, 151, 71-83.
- TASHIAN, R. E., VENTA, P. J., NICEWANDER, P. H. & HEWETT-EMMETT, D. 1990. EVOLUTION STRUCTURE AND EXPRESSION OF THE CARBONIC ANHYDRASE MULTIGENE FAMILY. *Ogita, Z.-I. And C. L. Markert*.
- TATTERS, A. O., ROLEDA, M. Y., SCHNETZER, A., FU, F., HURD, C. L., BOYD, P. W., CARON, D. A., LIE, A. A. Y., HOFFMANN, L. J. & HUTCHINS, D. A. 2013. Short- and long-term conditioning of a temperate marine diatom community to

- acidification and warming. *Philosophical Transactions of the Royal Society B: Biological Sciences*, 368.
- TAVIANI, M., REMIA, A., CORSELLI, C., FREIWALD, A., MALINVERNO, E., MASTROTOTARO, F., SAVINI, A. & TURSI, A. 2005. First geo-marine survey of living cold-water *Lophelia* reefs in the Ionian Sea (Mediterranean basin). *Facies*, 50, 409-417.
- TEICHERT, S., WOELKERLING, W., RUGGEBERG, A., WISSHAK, M., PIEPENBURG, D., MEYERHOEFER, M., FORM, A., BUEDENBENDER, J. & FREIWALD, A. 2012. Rhodolith beds (Corallinales, Rhodophyta) and their physical and biological environment at 80 degrees 31 ' N in Nordkappbukta (Nordaustlandet, Svalbard Archipelago, Norway). *Phycologia*, 51, 371-390.
- THOMPSON, T. G. & BONNAR, R. U. 1931. The buffer capacity of sea water. *Industrial and Engineering Chemistry-Analytical Edition*, 3, 0393-0395.
- THRESHER, R., RINTOUL, S. R., KOSLOW, J. A., WEIDMAN, C., ADKINS, J. & PROCTOR, C. 2004. Oceanic evidence of climate change in southern Australia over the last three centuries. *Geophysical Research Letters*, 31.
- TIERNEY, P. & JOHNSON, M. 2012. Stabilization Role of Crustose Coralline Algae During Late Pleistocene Reef Development on Isla Cerralvo, Baja California Sur (Mexico). *J Coast Res*, 28, 244 - 254.
- TRENBERTH, K. E., DAI, A., RASMUSSEN, R. M. & PARSONS, D. B. 2003. The Changing Character of Precipitation. *Bulletin of the American Meteorological Society*, 84, 1205-1217.
- TRENBERTH, K. E. & JONES, P. D. 2007. *Observations: Surface and Atmospheric Climate Change*.
- TUYA, F., CACABELOS, E., DUARTE, P., JACINTO, D., CASTRO, J. J., SILVA, T., BERTOCCI, I., FRANCO, J. N., ARENAS, F., COCA, J. & WERNBERG, T. 2012. Patterns of landscape and assemblage structure along a latitudinal gradient in ocean climate. *Marine Ecology Progress Series*, 466, 9-+.
- VAN WEERING, T. C. E., DE HAAS, H., DE STIGTER, H. C., LYKKE-ANDERSEN, H. & KOUVAEV, I. 2003. Structure and development of giant carbonate mounds at the SW and SE Rockall Trough margins, NE Atlantic Ocean. *Marine Geology*, 198, 67-81.
- VENN, A. A., TAMBUTTÉ, E., HOLCOMB, M., LAURENT, J., ALLEMAND, D. & TAMBUTTÉ, S. 2013. Impact of seawater acidification on pH at the tissue-skeleton interface and calcification in reef corals. *Proceedings of the National Academy of Sciences*, 110, 1634-1639.
- VIEROD, A. D. T., GUINOTTE, J. M. & DAVIES, A. J. 2014. Predicting the distribution of vulnerable marine ecosystems in the deep sea using presence-background models. *Deep-Sea Research Part II-Topical Studies in Oceanography*, 99, 6-18.
- VONCAEMMERER, S. & FARQUHAR, G. D. 1981. SOME RELATIONSHIPS BETWEEN THE BIOCHEMISTRY OF PHOTOSYNTHESIS AND THE GAS-EXCHANGE OF LEAVES. *Planta*, 153, 376-387.
- VU, J. C. V., ALLEN JR, L. H., BOOTE, K. J. & BOWES, G. 1997. Effects of elevated CO₂ and temperature on photosynthesis and Rubisco in rice and soybean. *Plant Cell and Environment*, 20, 68-76.
- WALZ 2014. http://www.walz.com/products/chl_p700/diving-pam/red_blue_version.html. Accessed 06 June 2014.
- WANDERS, J. B. W. 1976. The role of benthic algae in the shallow reef of Curaçao (Netherlands antilles). I: Primary productivity in the coral reef. *Aquatic Botany*, 2, 235-270.
- WASSMANN, P., DUARTE, C. M., AGUSTÍ, S. & SEJR, M. K. 2011. Footprints of climate change in the Arctic marine ecosystem. *Global Change Biology*, 17, 1235-1249.

- WEISS, I. M. & SCHONITZER, V. 2006. The distribution of chitin in larval shells of the bivalve mollusk *Mytilus galloprovincialis*. *Journal of Structural Biology*, 153, 264-277.
- WERNBERG, T., SMALE, D. A. & THOMSEN, M. S. 2012. A decade of climate change experiments on marine organisms: procedures, patterns and problems. *Global Change Biology*, 18, 1491-1498.
- WERNBERG, T., THOMSEN, M. S., CONNELL, S. D., RUSSELL, B. D., WATERS, J. M., ZUCCARELLO, G. C., KRAFT, G. T., SANDERSON, C., WEST, J. A. & GURGEL, C. F. D. 2013. The Footprint of Continental-Scale Ocean Currents on the Biogeography of Seaweeds. *Plos One*, 8.
- WHALAN, S., WEBSTER, N. S. & NEGRI, A. P. 2012. Crustose coralline algae and cnidarian neuropeptide trigger larval settlement in two coral reef sponges. *Plos One*, 7, e30386. doi:10.1371/journal.pone.0030386.
- WHITE, A. J. & CRITCHLEY, C. 1999. Rapid light curves: A new fluorescence method to assess the state of the photosynthetic apparatus. *Photosynthesis Research*, 59, 63-72.
- WHITMARSH, J. & GOVINDJEE 1999. The photosynthetic process. In: Concepts in Photobiology: Photosynthesis and Photomorphogenesis, (Eds) GS Singhal, G Renger, SK Sopory, K-D Irrgang and Govindjee, Narosa Publishers/New Delhi; and Kluwer Academic/Dordrecht., 11-51.
- WICKS, L. C. & ROBERTS, J. M. 2012. Benthic invertebrates in a high-CO₂ world. In: GIBSON, R. N., ATKINSON, R. J. A. & GORDON, J. D. M. (eds.) *Oceanography and Marine Biology*. CRC Press.
- WIDDICOMBE, S. & NEEDHAM, H. R. 2007. Impact of CO₂-induced seawater acidification on the burrowing activity of *Nereis virens* and sediment nutrient flux. *Marine Ecology Progress Series*, 341, 111-122.
- WIEBE, W. J., JOHANNES, R. E. & WEBB, K. L. 1975. Nitrogen Fixation in a Coral Reef Community. *Science*, 188, 257-259.
- WILSON, J. B. 1979. PATCH DEVELOPMENT OF THE DEEP-WATER CORAL *LOPHELIA-PERTUSA* (L) ON ROCKALL BANK. *Journal of the Marine Biological Association of the United Kingdom*, 59, 165-&.
- WILSON, S., BLAKE, C., BERGES, J. A. & MAGGS, C. A. 2004. Environmental tolerances of free-living coralline algae (maerl): implications for European marine conservation. *Biological Conservation*, 120, 279-289.
- WOOD, H. L., SPICER, J. I. & WIDDICOMBE, S. 2008. Ocean acidification may increase calcification rates, but at a cost. *Proceedings of the Royal Society B-Biological Sciences*, 275, 1767-1773.
- YAO, W. & BYRNE, R. H. 1998a. Simplified seawater alkalinity analysis - application to the potentiometric titration of the total alkalinity and carbonate content in sea water. *Deep Sea Research Part I: Oceanographic Research Papers*, 45, 1383-1392.
- YAO, W. S. & BYRNE, R. H. 1998b. Simplified seawater alkalinity analysis: Use of linear array spectrometers. *Deep-Sea Research Part I-Oceanographic Research Papers*, 45, 1383-1392.
- ZHANG, Z., FALTER, J., LOWE, R., IVEY, G. & MCCULLOCH, M. 2013. Atmospheric forcing intensifies the effects of regional ocean warming on reef-scale temperature anomalies during a coral bleaching event. *Journal of Geophysical Research-Oceans*, 118, 4600-4616.
- ZOU, D. H. 2005. Effects of elevated atmospheric CO₂ on growth, photosynthesis and nitrogen metabolism in the economic brown seaweed, *Hizikia fusiforme* (Sargassaceae, Phaeophyta). *Aquaculture*, 250, 726-735.